NBS MONOGRAPH 164

U.S. DEPARTMENT OF COMMERCE / National Bureau of Standards

Electromagnetic Boundary-Value Problems Based Upon a Modification of Residue Calculus and Function Theoretic Techniques

NATIONAL BUREAU OF STANDARDS

The National Bureau of Standards[1] was established by an act of Congress March 3, 1901. The Bureau's overall goal is to strengthen and advance the Nation's science and technology and facilitate their effective application for public benefit. To this end, the Bureau conducts research and provides: (1) a basis for the Nation's physical measurement system, (2) scientific and technological services for industry and government, (3) a technical basis for equity in trade, and (4) technical services to promote public safety. The Bureau's technical work is performed by the National Measurement Laboratory, the National Engineering Laboratory,. and the Institute for Computer Sciences and Technology.

THE NATIONAL MEASUREMENT LABORATORY provides the national system of physical and chemical and materials measurement; coordinates the system with measurement systems of other nations and furnishes essential services leading to accurate and uniform physical and chemical measurement throughout the Nation's scientific community, industry, and commerce; conducts materials research leading to improved methods of measurement, standards, and data on the properties of materials needed by industry, commerce, educational institutions, and Government; provides advisory and research services to other Government Agencies; develops, produces, and distributes Standard Reference Materials; and provides calibration services. The Laboratory consists of the following centers:

Absolute Physical Quantities[2] — Radiation Research — Thermodynamics and Molecular Science — Analytical Chemistry — Materials Science.

THE NATIONAL ENGINEERING LABORATORY provides technology and technical services to users in the public and private sectors to address national needs and to solve national problems in the public interest; conducts research in engineering and applied science in support of objectives in these efforts; builds and maintains competence in the necessary disciplines required to carry out this research and technical service; develops engineering data and measurement capabilities; provides engineering measurement traceability services; develops test methods and proposes engineering standards and code changes; develops and proposes new engineering practices; and develops and improves mechanisms to transfer results of its research to the utlimate user. The Laboratory consists of the following centers:

Applied Mathematics — Electronics and Electrical Engineering[2] — Mechanical Engineering and Process Technology[2] — Building Technology — Fire Research — Consumer Product Technology — Field Methods.

THE INSTITUTE FOR COMPUTER SCIENCES AND TECHNOLOGY conducts research and provides scientific and technical services to aid Federal Agencies in the selection, acquisition, application, and use of computer technology to improve effectiveness and economy in Government operations in accordance with Public Law 89-306 (40 U.S.C. 759), relevant Executive Orders, and other directives; carries out this mission by managing the Federal Information Processing Standards Program, developing Federal ADP standards guidelines, and managing Federal participation in ADP voluntary standardization activities; provides scientific and technological advisory services and assistance to Federal Agencies; and provides the technical foundation for computer-related policies of the Federal Government. The Institute consists of the following divisions:

Systems and Software — Computer Systems Engineering — Information Technology.

[1]Headquarters and Laboratories at Gaithersburg, Maryland, unless otherwise noted;
mailing address Washington,D.C. 20234.
[2]Some divisions within the center are located at Boulder, Colorado, 80303.

The National Bureau of Standards was reorganized, effective April 9, 1978.

Electromagnetic Boundary-Value Problems Based Upon a Modification of Residue Calculus and Function Theoretic Techniques

James Patrick Montgomery
David C. Chang

Center for Electronics
  and Electrical Engineering
National Engineering Laboratory
National Bureau of Standards
Boulder, Colorado 80302

PREFACE

The work reported in this monograph is the result of an intensive collaborative effort between the authors and NBS scientists. The contract to the University of Colorado was initiated because of the need for an accurate, well-defined in-situ method of measuring the complex dielectric properties of the earth in the frequency range of 0.1 to 12.4 GHz. The work is part of a larger National Bureau of Standards project that is systematically determining the measurement capability (accuracy and precision) of selected measurement techniques presently used in high frequency and microwave remote sensing, as well as developing well defined data bases and new measurement techniques for particular application of high national need.

The particular approach presented in this monograph was chosen primarily because of the availability of TEM type antennas that have a very large bandwidth, and because of the desirability of making the measurements with the antennas very close (in the near field) to the material being measured.

The needed open region mathematical techniques are systematically developed through the solution of selected closed region problems before extension to the open region problems.

The work presents powerful new tools that can be applied to either open or closed region problems and, hopefully, lays the basic theoretical ground work for the development of the needed well-defined, accurate techniques of in-situ measurement of earth type materials.

The application of the presented theoretical ideas to experimental measurement systems is currently being actively pursued.

W.E. Little
National Engineering Laboratory
National Bureau of Standards
Boulder, Colorado 80302

CONTENTS

PART I

SOLUTION OF CLOSED REGION PROBLEMS

PART II

SOLUTION OF OPEN REGION PROBLEMS

ELECTROMAGNETIC BOUNDARY-VALUE PROBLEMS BASED UPON
A MODIFICATION OF RESIDUE CALCULUS AND FUNCTION THEORETIC TECHNIQUES

James Patrick Montgomery*
David C. Chang**

ABSTRACT

The solution of a number of electromagnetic problems, in both closed and open systems, using the modified residue calculus and functional theoretic techniques is presented.

The solutions start with known closed region problems and then are extended to new closed region problems and finally to several open region problems.

Specific problems considered for the closed region are: 1) the trifurcated waveguide; 2) the dielectrically loaded trifurcated waveguide; 3) the N-furcated waveguide; 4) the dielectrically loaded N-furcated waveguide; 5) determination of the Eigenvalues of ridged waveguide; and 6) scattering by a dielectric stop.

Open region problems considered are: 1) a parallel plate radiating into a homogeneous half-space; 2) a finite phased array; 3) remote sensing of the earth using parallel plate waveguides; 4) a flanged waveguide radiating into a half-space; 5) scattering by a thick, semi-infinite plane; and 6) radiation from a slot in a waveguide wall.

Some suggested extension of the techniques to other types of problems is also included.

Key words: Closed systems; electromagnetic problems; functional theoretic techniques; modified residue calculus; open systems; remote sensing.

PART I

SOLUTION OF CLOSED REGION PROBLEMS

CHAPTER 1. INTRODUCTION

The first part of this monograph is concerned with the analysis of closed region waveguide junction problems. This allows simplification of the techniques to be used since no branch cuts are involved in the spectral representation of the fields. However, the analysis can be extended to open region problems in a logical manner. This is the subject of the second part of this monograph.

The problems of interest will be confined to two-dimensional geometries for which a strictly TE or TM solution is possible.

Generally speaking, direct mode matching could be employed as a method of solution of the problems to be presented. However, direct mode matching has several disadvantages which often outweigh the simplicity of the method. One of the disadvantages is that many problems have been shown to exhibit a relative convergence phenomena with regard to the truncation of the modal representations of the various regions. For the bifurcated waveguide the solution is known (Mittra and Lee, 1971) to converge to the correct result only when the ratio of the number of modes is chosen equal to the ratio of the heights of the waveguides. This choice ensures the satisfaction of the edge condition of the problem and

*Montgomery is with Texas Instrument Corporation, Dallas, Texas.
**Chang is Professor of Electrical Engineering, University of Colorado, Boulder, Colorado.

hence the uniqueness of the solution. However, for more complicated structures the solution is not generally known. Accurate solutions are still possible; however, this is often at the expense of including an excessively large number of modes in the larger waveguide region. For the most efficient solution one must have some guidelines in the choice of the number of modes of the various regions. For many problems this is not possible without an extensive numerical convergence study. Even with this disadvantage, mode matching is often used because of its simplicity or generality. However, direct mode matching has another disadvantage that is often overlooked. Direct mode matching does not use a priori information regarding the geometry. For example, the bifurcated waveguide solution is known exactly; yet, a direct mode matching solution is of the same order of difficulty as a nonsoluble geometry.

For many problems there are two analysis techniques which appear to be superior to direct mode matching: the generalized scattering matrix technique (GSMT) and the modified residue calculus technique (MRCT). Both of these techniques recognize that many problems are composed of a combination of soluble problems. The GSMT and the MRCT are used to solve problems by efficiently combining these known solutions.

The basic soluble problem used in the solution of two dimensional waveguide disconti-nuity problems is the bifurcated waveguide. It is well known that the solution of the bi- furcated waveguide can be obtained either by the Wiener-Hopf method or the residue calculus technique (Mittra and Lee, 1971). Pace and Mittra (1964) originally used these known solu-tions in conjunction with the generalized scattering matrix technique (GSMT) to arrive at the solution of composite problems. These composite problems were obtained by identifying an auxiliary problem such that it was clear that the solution of the problem was a modifi-cation of the bifurcated junction. As distances and material parameters approached limiting values, the solution to the original problem was obtained.

The GSMT, although a numerically efficient scheme, has one particular weakness. Since the GSMT uses truncated matrix representations of junctions, it is difficult to show that the edge conditions of composite problems are either changed or added to the edge conditions of the soluble problems. Since the edge conditions of the composite problem may not be satisfied, one may not be assured of the uniqueness of the solution. However, it is fre-quently the case that these effects are small when calculating quantities such as dominant mode reflection coefficients. Van Blaricum and Mittra (1969) remedied this for a certain class of problems. They made use of the same auxiliary problem used in the GSMT; however, they formulated the problem in a manner where a modified residue calculus technique (MRCT) was used. The MRCT solution was obtained by recognizing that the solution to the problem is obtained by shifting zeroes of the original residue calculus solution of the bifurcated waveguide. These shifted zeroes could be found asymptotically by using the edge condition of the problem. Iterative and matrix techniques were used (Mittra and Lee, 1971) to find a finite set of shifted zeroes or the equivalent Lagrangian interpolating polynomial repre-sentation. Only a small number of these zeroes were needed to accurately find such quanti-ties as the reflection coefficients of the dominant modes. Additionally, because the solu-tion explicitly satisfied the edge condition, the convergence of the results was better than the GSMT solution.

Recently, Royer and Mittra (1972) examined a dielectric step in a parallel plate waveguide. Since there was interest in high dielectric constants, the solution was formulated using an extension of the MRCT. However, the asymptotic shift of zeroes could not be found. Thus an infinite form of a Lagrangian interpolating polynomial was used instead of a shifted zero representation. Consequently, the asymptotic form of the coefficients of the expansion were found from an application of the edge condition. This enabled the infinite equations to be truncated and solved in an efficient manner.

This part of the monograph studies a canonical problem of a bifurcated waveguide with infinitely many known modes incident from all guides. The solution of the problem can be expressed advantageously using an infinite form of the Lagrangian interpolating polynomial. This solution can then be used to solve various composite problems. In particular, the E-plane step is solved using this representation as opposed to a shifted zero representation.

The canonical solution is then applied to junctions which have not been solved using the MRCT previously. Solutions are given for the trifurcated waveguide as well as the modification of the junction due to dielectric loading. The trifurcated waveguide for arbitrary spacing of the plates has been solved by Pace and Mittra (1966) using the GSMT.

The solution of the trifurcated waveguide is then generalized to the N-furcated waveguide with arbitrary spacing of the conducting plates. The general solution of an arbitrary number of plates has been given formally by Heins (1948). Heins' solution, however, has little practical value. More recently, Igarashi (1964) used a diagonalization procedure in conjunction with the simultaneous Wiener-Hopf equations and obtained explicit expressions for the fields in the various waveguides. A necessary condition for the diagonalization of the equations was equal spacing of the conducting plates. No such restriction is necessary for the MRCT solution of the N-furcated waveguide. The solution is also given for a particular dielectric loading of the N-furcated waveguide.

One interesting point of the MRCT solution of these problems is that multiple edge conditions are explicitly satisfied, thus enhancing the convergence of the solution over those which have been (or might be) obtained using the GSMT.

Chapter 5 serves as a forum for discussing solutions of other closed region problems. Among these are: the eigenvalue solution of ridged waveguide and the dielectric step in a waveguide. Additionally, further numerical results are presented for the N-furcated waveguide.

It should be noted that these concepts can be used to solve many problems which are modifications of soluble Wiener-Hopf problems other than just the bifurcated waveguide.

CHAPTER 2. FOUNDATION OF THE MODIFIED RESIDUE CALCULUS TECHNIQUE

1. Introduction

It is the purpose of this chapter to show that the modified residue calculus technique can be approached in a direct manner by considering the canonical problem of a bifurcated waveguide with infinitely many modes incident from all waveguides. The general solution can be conveniently written in the form of a perturbation expansion. It is then shown that this solution can be applied to composite problems such as the E-plane waveguide step.

2. The Canonical Problem

Geometry of the canonical problem is shown in figure 2.2.1. It consists of three air-filled parallel-plate waveguide sections with the width of the larger section equal to the sum of widths of the two smaller sections; i.e., $a = b+c$. The solution to this problem has been known for a number of years for a single mode incident from one of the three waveguides. These solutions have been found either the Wiener-Hopf technique or the residue calculus technique (Mittra and Lee, 1971). We shall discuss in this section the generalization of this solution to the case involving infinitely many modes incident from all directions.

Let us consider the TM solution of the problem. The TE solution follows in the same manner and will not be given.

The TM fields are derivable from a scaler function $\phi = H_y$ and the fields in each region are given by [Mittra and Lee, 1971]

$$\phi_A = \sum_{n=0}^{\infty} \left[A_n^{(o)} e^{\gamma_{na} z} + A_n e^{-\gamma_{na} z} \right] \cos \frac{n\pi}{a} (x-x_0)$$

$$\phi_B = \sum_{n=0}^{\infty} \left[B_n^{(o)} e^{-\gamma_{nb} z} + B_n e^{\gamma_{nb} z} \right] \cos \frac{n\pi}{b} (x-x_0)$$

$$\phi_C = \sum_{n=0}^{\infty} \left[C_n^{(o)} e^{-\gamma_{nc} z} + C_n e^{\gamma_{nc} z} \right] \cos \frac{n\pi}{c} (x-x_1)$$

where the superscript (o) indicates an incident field and

$$\gamma_{nh} = \begin{cases} \sqrt{(n\pi/h)^2 - k_o^2} \,, & n\pi/h > k_o \\ \\ j\sqrt{k_o^2 - \left(\frac{n\pi}{h}\right)^2} \,, & n\pi/h < k_o \end{cases}$$

and a time convention, $e^{j\omega t}$, is assumed and suppressed. We further define $k_o = \omega(\mu_o \epsilon_o)^{\frac{1}{2}}$ as the wave number in air, and η_o as the intrinsic impedance of a plane wave in air.

Matching the tangential magnetic field $H_y (=\phi)$ and the tangential electric field E_z, i.e., $-jk_o^{-1}\eta_o (\partial/\partial x)\phi$, at $z = z_o$ we can arrive at the equations

4
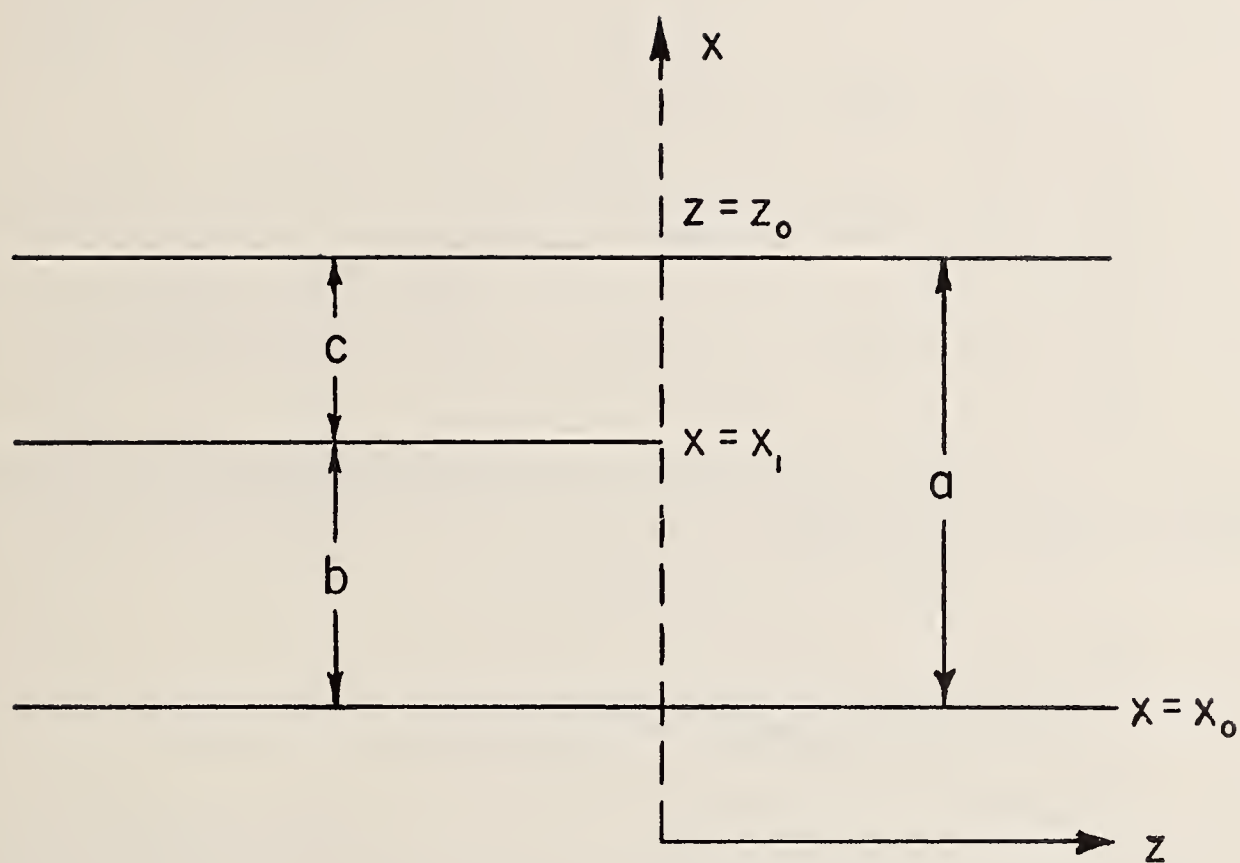
Fig. 2.2.1:   The Canonical Problem: The Bifurcated
Waveguide.

$$\sum_{n=0}^{\infty} \left[A_n^{(o)} \, e^{\gamma_{na}z_o} + A_n \, e^{-\gamma_{na}z_o} \right] \cos \frac{n\pi}{a}(x-x_0) =$$

$$\begin{cases} \sum_{n=0}^{\infty} \left[C_n^{(o)} \, e^{-\gamma_{nc}z_o} + C_n \, e^{\gamma_{nc}z_o} \right] \cos \frac{n\pi}{c}(x-x_1); & x_1 \le x \le x_1 + c, \\[2em] \sum_{n=0}^{\infty} \left[B_n^{(o)} \, e^{-\gamma_{nb}z_o} + B_n \, e^{\gamma_{nb}z_o} \right] \cos \frac{n\pi}{b}(x-x_0); & x_o \le x \le x_0 + b \end{cases}$$

and

$$\sum_{n=0}^{\infty} \gamma_{na} \left[A_n^{(o)} \, e^{\gamma_{na}z_o} - A_n \, e^{-\gamma_{na}z_o} \right] \cos \frac{n\pi}{a}(x-x_0) =$$

$$\begin{cases} -\sum_{n=0}^{\infty} \gamma_{nc} \left[C_n^{(o)} \, e^{-\gamma_{nc}z_o} - C_n \, e^{\gamma_{nc}z_o} \right] \cos \frac{n\pi}{c}(x-x_1); & x_1 \le x \le x_1 + c, \\[2em] -\sum_{n=0}^{\infty} \gamma_{nb} \left[B_n^{(o)} \, e^{-\gamma_{nb}z_o} - B_n \, e^{\gamma_{nb}z_o} \right] \cos \frac{n\pi}{b}(x-x_0); & x_0 \le x \le x_0 + b \end{cases}$$

We may use the orthogonality of the eigenfunction expansions and eliminate coefficients to obtain the following four equations.

$$\gamma_{mb} B_m \, b \, \varepsilon_m \, e^{\gamma_{mb}z_o} = 2jk_o b \, A_o^{(o)} \, e^{jk_o z_o} \, \delta_{mo}$$

$$+ \, (-1)^{m+1} \sum_{n=1}^{\infty} \frac{A_n^{(o)} \frac{n\pi}{a} \sin \frac{n\pi b}{a} \, e^{\gamma_{na}z_o}}{\gamma_{mb} - \gamma_{na}}$$

$$+ \, (-1)^{m+1} \sum_{n=1}^{\infty} \frac{A_n \frac{n\pi}{a} \sin \frac{n\pi b}{a} \, e^{-\gamma_{na}z_o}}{\gamma_{mb} + \gamma_{na}}; \qquad m = 0,1,2,\cdots . \tag{2.1}$$

$$\gamma_{mb} \, B_m^{(o)} \, b \, \varepsilon_m \, e^{-\gamma_{mb}z_o} = 2jk_o \, b \, A_o \, e^{-jk_o z_o} \, \delta_{mo}$$

$$+ \, (-1)^{m+1} \sum_{n=1}^{\infty} \frac{A_n^{(o)} \frac{n\pi}{a} \sin \frac{n\pi b}{a} \, e^{\gamma_{na}z_o}}{\gamma_{mb} + \gamma_{na}}$$

$$+ \, (-1)^{m+1} \sum_{n=1}^{\infty} \frac{A_n \frac{n\pi}{a} \sin \frac{n\pi b}{a} \, e^{-\gamma_{na}z_o}}{\gamma_{mb} - \gamma_{na}}; \qquad m = 0,1,2,\cdots . \tag{2.2}$$

$$\gamma_{mc} \, C_m \, c \, \varepsilon_m \, e^{\gamma_{mc} z_o} = 2 j k_o \, c \, A_o^{(o)} \, e^{j k_o z_o} \, \delta_{mo}$$

$$+ \sum_{n=1}^{\infty} \frac{A_n^{(o)} \frac{n\pi}{a} \sin \frac{n\pi b}{a} e^{\gamma_{na} z_o}}{\gamma_{mc} - \gamma_{na}}$$

$$+ \sum_{n=1}^{\infty} \frac{A_n \frac{n\pi}{a} \sin \frac{n\pi b}{a} e^{-\gamma_{na} z_o}}{\gamma_{mc} + \gamma_{na}}; \qquad m = 0, 1, 2, \cdots, \qquad (2.3)$$

$$\gamma_{mc} \, C_m^{(o)} \, c \, \varepsilon_m \, e^{-\gamma_{mc} z_o} = {}^{\cdot} 2 j k_o \, c \, A_o \, e^{-j k_o z_o} \, \delta_{mo}$$

$$+ \sum_{n=1}^{\infty} \frac{A_n^{(o)} \frac{n\pi}{a} \sin \frac{n\pi b}{a} e^{\gamma_{na} z_o}}{\gamma_{mc} + \gamma_{na}}$$

$$+ \sum_{n=1}^{\infty} \frac{A_n \frac{n\pi}{a} \sin \frac{n\pi b}{a} e^{-\gamma_{na} z_o}}{\gamma_{mc} - \gamma_{na}}; \qquad m = 0, 1, 2, \cdots. \qquad (2.4)$$

where

$$\varepsilon_m = \begin{cases} 2, & m = 0 \\ 1, & m \geq 1 \end{cases}$$

and δ_{mn} is the Kronecker delta.

Equations (2.2) and (2.4) relate the unknown modal amplitudes A_n and the incident fields $A_n^{(o)}$, $B_n^{(o)}$, and $C_n^{(o)}$, while (2.1) and (2.3) relate the unknown modal amplitudes A_n to B_n and C_n.

For m=0, (2.2) and (2.4) become identical in form since $\gamma_{ob} = \gamma_{oc} \, j k_o$, allowing one to eliminate the summations and find

$$A_o = \frac{c}{a} \, C_o^{(o)} + \frac{b}{a} \, B_o^{(o)} \qquad (2.5)$$

which is a unique feature of the TM solution.

The key to the residue calculus technique is to __construct__ a complete solution to the problem according to the matching equation (2.2) to (2.4), rather than solving them directly. Thus, let us now consider the following integral,

$$\frac{(-1)^{m+1}}{2\pi j} \oint \frac{T(\omega) d\omega}{\omega - \gamma_{mb}}, \qquad \frac{1}{2\pi j} \oint \frac{T(\omega) d\omega}{\omega - \gamma_{mc}} \qquad (2.6)$$

7

where m = 0,1,2,$\cdots$ and $T(\omega)$ is to be constructed uniquely with the residue series of these integrals identical with equations (2.2) and (2.4). The contour of integration is the infinite circle in the complex ω plane. We assume that $T(\omega)$ behaves appropriately at infinity so that the integrals exist and are zero.

Let us further assume that $T(\omega)$ has simple poles at γ_{na}, $-\gamma_{na}$, n = 1,2,$\cdots$. Then

$$\frac{1}{2\pi j} \oint \frac{T(\omega)d\omega}{\omega - \gamma_{mc}} = \sum_{n=1}^{\infty} \frac{\text{RES}[T,\gamma_{na}]}{\gamma_{na} - \gamma_{mc}} - \sum_{n=1}^{\infty} \frac{\text{RES}[T,-\gamma_{na}]}{\gamma_{na} + \gamma_{mc}} + T(\gamma_{mc}) = 0. \tag{2.7}$$

and

$$\frac{(-1)^{m+1}}{2\pi j} \oint \frac{T(\omega)d\omega}{\omega - \gamma_{mb}} = (-1)^{m+1} \sum_{n=1}^{\infty} \frac{\text{RES}[T,\gamma_{na}]}{\gamma_{na} - \gamma_{mb}}$$

$$- (-1)^{m+1} \sum_{n=1}^{\infty} \frac{\text{RES}[T,-\gamma_{na}]}{\gamma_{na} + \gamma_{mb}}$$

$$+ (-1)^{m+1} T(\gamma_{mb}) = 0. \tag{2.8}$$

where m = 0,1,2$\cdots$. Comparing (2.7) and (2.8) with (2.4) and (2.2) we find these two sets of equations are identical provided that

(i) $\quad \text{RES}[T,-\gamma_{ma}] = -A_m^{(o)} \frac{m\pi}{a} \sin \frac{m\pi b}{a} e^{\gamma_{ma} z_o} \qquad$ m = 1,2,$\cdots$

(ii) $\quad \text{RES}[T,\gamma_{ma}] = -A_m \frac{m\pi}{a} \sin \frac{m\pi b}{a} e^{-\gamma_{ma} z_o} \qquad$ m = 1,2,$\cdots$

(iii) $\quad T(\gamma_{mc}) = -C_m^{(o)} \gamma_{mc} c\, e^{-\gamma_{mc} z_o} \qquad$ m = 1,2,$\cdots$

(iv) $\quad T(\gamma_{mb}) = (-1)^m B_m^{(o)} \gamma_{mb} b\, e^{-\gamma_{mb} z_o} \qquad$ m = 1,2 $\cdots$

(v) $\quad T(jk_o) = 2jk_o c\, e^{-jk_o z_o} (A_o - C_o^{(o)})$

We can also consider the integrals

$$\frac{(-1)^{m+1}}{2\pi j} \oint \frac{T(\omega)d\omega}{\omega + \gamma_{mb}} \quad \frac{1}{2\pi j} \oint \frac{T(\omega)d\omega}{\omega + \gamma_{mc}} \tag{2.9}$$

where m = 0,1,2,$\cdots$. Using the above properties we find the following by comparing with (2.1) and (2.3)

(vi) $\quad T(-\gamma_{mc}) = C_m \gamma_{mc} c\, e^{\gamma_{mc} z_o} \qquad$ m = 1,2,$\cdots$

(vii) $\quad T(-\gamma_{mb}) = (-1)^{m+1} \gamma_{mb} b\, B_m\, e^{\gamma_{mb} z_o} \qquad$ m = 1,2,$\cdots$

8

(viii)　$T(-jk_o) = 2jk_o c [C_o - A_o^{(o)}] \ e^{jk_o z_o}$

(ix)　　$T(-jk_o) = -2jk_o b [B_o - A_o^{(o)}] \ e^{jk_o z_o}$

Alternatively, (ix) can be replaced by $A_o^{(o)} = \dfrac{c}{a} C_o + \dfrac{b}{a} B_o$ which is then analogous to the relationship given in (2.5). From Appendix A it is shown that the edge condition implies $T(\omega) = 0(\omega^{-1/2})$ as $|\omega| \to \infty$ and hence the assumption regarding the convergence of the integrals is justified. Because of its importance let us also consider this in our list of properties of $T(\omega)$ (for the bifurcated case only)

(x)　　$T(\omega) = 0(\omega^{-1/2})$, $|\omega| \to \infty$

　　Thus, the question now becomes one of constructing the function $T(\omega)$ uniquely from some of the properties listed above. Upon finding $T(\omega)$ the complete solution to the problem is given by (ii), (vi), (vii), (viii) and (ix).

　　The clue to the construction is found by considering the solution with only a single mode incident on the junction. For simplicity say the incident mode is $B_o^{(o)} = 1$. Then (i) implies that $T(\omega)$ has no poles at $-\gamma_{na}$; (iii) implies that $T(\omega)$ has simple zeroes at γ_{mc}; and (iv) implies that $T(\omega)$ has simple zeroes at γ_{mb}. Hence

$$T(\omega) = K \ H(\omega) \ \frac{\Pi(\omega, \gamma_b) \ \Pi(\omega, \gamma_c)}{\Pi(\omega, \gamma_a)} \tag{2.10}$$

where

$$\Pi(\omega, \gamma_h) = \prod_{n=1}^{\infty} \left(1 - \frac{\omega}{\gamma_{nh}} \right) e^{\omega h / n\pi}$$

and $H(\omega)$ is an entire function with no zeroes. The exponential factor has been introduced into the infinite product in order to insure uniform convergence. However, when the products are grouped as in (2.10) the exponential is not needed. From Mittra and Lee (page 13, 1971) we find the asymptotic expansion of the following infinite produce

$$T(\omega) = K \ H(\omega) \ \omega^{-1/2} \ e^{\omega/\pi [b \ln \frac{b}{a} + c \ln \frac{c}{a}]}, \ \omega \neq |\omega|$$

In order for condition (x) to be met we must have

$$H(\omega) = e^{-\omega/\pi [b \ln(b/a) + c \ln(c/a)]} \tag{2.11}$$

where K is a constant. However, K can be determined from (v) and (2.5),

$$T(jk_o) = k \ H(jk_o) \ \frac{\Pi(jk_o, \gamma_b) \ \Pi(jk_o, \gamma_c)}{\Pi(jk_o, \gamma_a)}$$

$$= 2jk_o \ c \ e^{-jk_o z_o} \left(\frac{b}{a} \right)$$

9

Hence, the solution is

$$T(\omega) = 2jk_o \frac{bc}{a} e^{-jk_o z_o} \frac{H(\omega) \, F(\omega)}{H(jk_o) \, F(jk_o)} \qquad (2.12)$$

where $F(\omega) = \dfrac{\Pi(\omega, \gamma_b) \Pi(\omega, \gamma_c)}{\Pi(\omega, \gamma_a)}$. The reflection coefficient is given by (ix)

$$B_o = \frac{-c}{a} e^{-j2k_o z_o} \frac{H(-jk_o) \, F(-jk_o)}{H(jk_o) \, F(jk_o)} \qquad (2.13)$$

When the waveguides are single moded structures, we obtain $|B_o| = c/a$, a well-known result (Marcuvitz, 1964).

Let us now consider how (2.12) can be modified to reflect the general solution. From (i) we see that if $A_m^{(o)} \neq 0$ we must introduce simple poles at $-\gamma_{na}$. Similarly, from (iii) and (iv) we see that we must introduce simple poles at γ_{mb} and γ_{mc} in order to remove the zeroes of $F(\omega)$. This leads us to consider a function of the form

$$T(\omega) = H(\omega) \, F(\omega) \left[K_o - (\omega - jk_o) \left\{ \sum_{n=1}^{\infty} \frac{g_n^{(b)}}{\omega - \gamma_{nb}} \right. \right.$$

$$\left. \left. + \sum_{n=1}^{\infty} \frac{g_n^{(c)}}{\omega - \gamma_{nc}} + \sum_{n=1}^{\infty} \frac{g_n^{(a)}}{\omega + \gamma_{na}} \right\} \right] \qquad (2.14)$$

where

$$H(\omega) = e^{-\omega/\pi [\pm b \ln b/a + c \ln c/a]}$$

K_o, $g_n^{(a)}$, $g_n^{(b)}$ and $g_n^{(c)}$ can be obtained by using (i), (iii), (iv), and (v).

$$K_o H(jk_o) F(jk_o) = 2jk_o \, c \, e^{-jk_o z_o} (A_o - C_o^{(o)}) \qquad (2.15)$$

$$H(-\gamma_{na}) F(-\gamma_{na}) (\gamma_{na} + jk_o) \, g_n^{(a)}$$

$$= -A_n^{(o)} \frac{n\pi}{a} \sin \frac{n\pi b}{a} e^{\gamma_{na} z_o} \qquad n = 1, 2, \cdots \qquad (2.16)$$

$$H(\gamma_{nc}) F^{(n)}(\gamma_{nc}) \frac{(\gamma_{nc} - jk_o)}{\gamma_{nc}} g_n^{(c)}$$

$$= -C_n^{(o)} \gamma_{nc} \, c \, e^{-\gamma_{nc} z_o} \qquad n = 1, 2, \cdots \qquad (2.17)$$

$$H(\gamma_{nb}) F^{(n)}(\gamma_{nb}) \frac{(\gamma_{nb} - jk_o)}{\gamma_{nb}} g_n^{(b)}$$

$$= (-1)^n B_n^{(o)} \gamma_{nb} \, b \, e^{-\gamma_{nb} z_o} \qquad n = 1, 2, \cdots \qquad (2.18)$$

10

where $F^{(n)}(\gamma_{nc})$ and $F^{(n)}(\gamma_{nb})$ are to be interpreted as omitting the nth zero at either γ_{nc} or γ_{nb}, and A_o is related to the incident field $B_o^{(o)}$ and $C_o^{(o)}$ according to (25).

This represents the complete general solution to the bifurcated waveguide problem.

3. Formulation and Solution of Composite Problems

The key to the MRCT is the identification of an auxiliary problem. The auxiliary problem is such that the solution may be identified in terms of soluble problems. For example, the auxiliary problem may clearly indicate that the desired solution is a perturbation of a bifurcated waveguide or a parallel plate in a homogeneous space. Mittra and Lee (1970) have indicated a number of such problems.

Before proceeding let us illustrate the above process with a problem which has been solved using the MRCT using the concept of shifted zeroes (Mittra, Lee, Van Blaricum; 1968). We will solve the E-plane step using the canonical solution of section 2.

Figure 2.3.1 illustrates the E-plane step and the auxiliary geometry. Notice that the auxiliary geometry has a recessed dielectric of finite permittivity. When $\delta =$ and $\varepsilon = \infty$, the auxiliary problem coincides with the original E-plane step. Notice that this recession has identified two soluble problems: (1) a bifurcated waveguide junction at z=0, and (2) a dielectric junction within a parallel plate waveguide at z=−δ. This auxiliary problem allows us to perturb the bifurcated solution advantageously.

For simplicity let us consider the case of TEM incidence from the smaller guide. Extension to higher order incidence or a TE solution is straightforward. The dielectric creates reflections of any scattered modes from the junction at z=0. This may be thought of as an incident field upon the junction. From the canonical solution we recognize that if we knew these modal amplitudes, $T(\omega)$ would be given by (2.14) with $g_n^{(a)} \equiv g_n^{(b)} \equiv 0$ and say $g_n^{(c)} = g_n$. It is still convenient to use this form even with g_n unknown. In this case g_n represents a perturbation of the bifurcated solution due to the dielectric loading. From (2.14) we have

$$T(\omega) = H(\omega)F(\omega)\left[K_o - (\omega - jk_o) \sum_{n=1}^{\infty} \frac{g_n}{\omega - \gamma_{nc}} \right] \tag{3.1}$$

where the notation is similar to section 2. This will be referred to as a perturbation type expansion. Using (2.17) we have that

$$g_n = K_n C_n^{(o)} \tag{3.2}$$

where K_n is found from (2.17) as $K_n = - (\gamma_{nc}c)(1-jk_o/\gamma_{nc})^{-1}[H(\gamma_{nc})F^{(n)}(\gamma_{nc})]^{-1}$ and involves only simple calculable functions. If we represent the H_y component of the field in the dielectric as

$$\phi_y = \sum_{n=0}^{\infty} D_n e^{\Gamma_{nc} z} \cos \frac{n\pi}{c} (x-b) \tag{3.3}$$

11
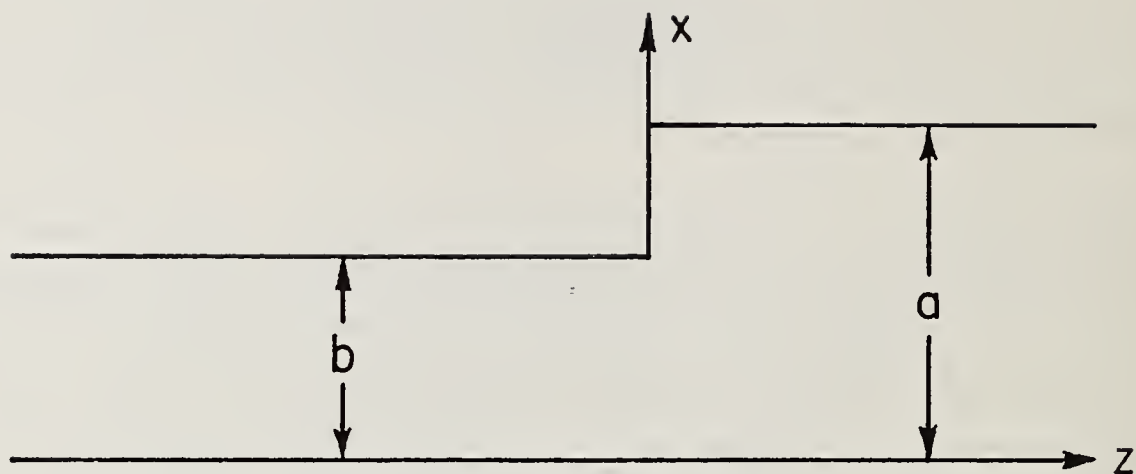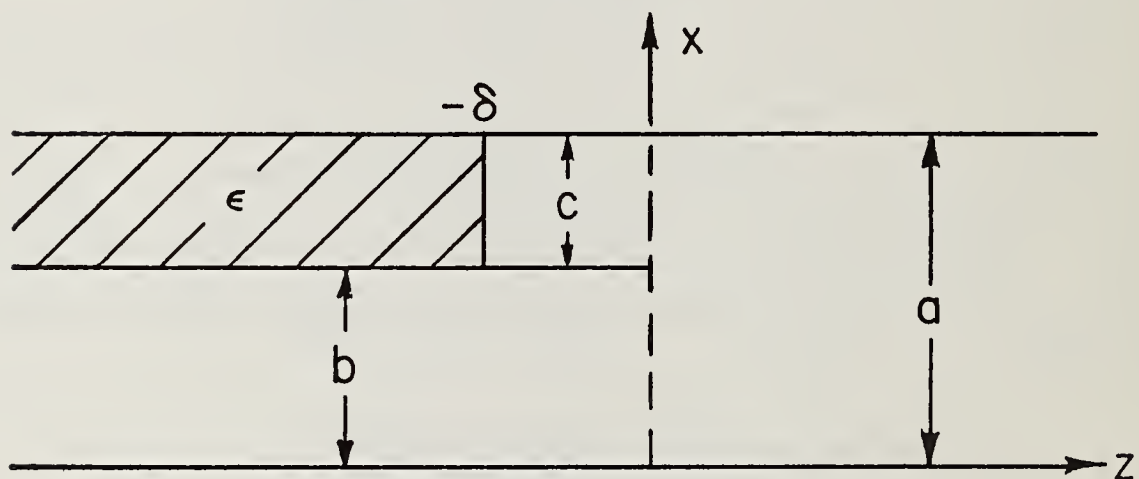
(a) E-Plane Step

(b) Auxiliary Geometry

Fig. 2.3.1: The E-Plane Step and the Auxiliary
Problem.

where

$$\Gamma_{nc} = \left(\frac{n\pi}{c}\right)^2 - \varepsilon k_o^2$$

we can easily find that

$$C_n^{(o)} = R_n C_n = \left(\frac{\varepsilon \gamma_{nc} - \Gamma_{nc}}{\varepsilon \gamma_{nc} + \Gamma_{nc}}\right) e^{-2\gamma_{nc}\delta} C_n \qquad (3.4)$$

and

$$D_n = e^{\Gamma_{nc}\delta + \gamma_{nc}\delta} \frac{2\varepsilon\gamma_{nc}}{\varepsilon\gamma_{nc} - \Gamma_{nc}} C_n^{(o)} \qquad (3.5)$$

From (210) on p. 14, we have $K_n = 0(n^{1/2})$ as $n \to \infty$, and thus we see from (3.5) and (3.2) that for $\delta = 0$

$$g_n = 0(n^{1/2} D_n), \quad n \to \infty$$

For the $\delta = 0$ case it is also easy to show (Mittra and Lee, page 170, 1971) that

$$D_n = 0(n^{-3/2-\Delta}), \quad n\to\infty \qquad (3.6)$$

where

$$\Delta = \frac{1}{\pi} \sin^{-1}\left(\frac{(\varepsilon-1)}{2(\varepsilon+1)}\right) \qquad (3.7)$$

hence

$$g_n = 0(n^{-1-\Delta}), \quad n\to\infty \qquad (3.8)$$

This allows us to write (3.1) in an approximate form suitable for numerical analysis

$$T(\omega) \simeq H(\omega)F(\omega)\left[K_o - (\omega - jk_o)\left\{\sum_{n=1}^{\infty} \frac{g_n}{\omega - \gamma_{nc}} + \bar{g} \sum_{n=N+1}^{\infty} \frac{n^{-1-\Delta}}{\omega - \gamma_{nc}}\right\}\right] \qquad (3.9)$$

In this particular problem the edge condition has changed from $T(\omega) = 0(\omega^{-1/2})$, $|\omega| \to \infty$, to $T(\omega) = 0(\omega^{-1/2-\Delta})$, $|\omega| \to \infty$. An examination of (3.9) reveals that the multiplying term of $H(\omega)F(\omega)$ must be $0(\omega^{-\Delta})$, $|\omega| \to \infty$. This implies that any constant terms contributed by the perturbation sums must cancel with K_o in order for the higher term of the second sum to dominate. Hence, we must have

$$K_o - \sum_{n=1}^{N} g_n - \bar{g} \sum_{n=N+1}^{\infty} n^{-1-\Delta} = 0. \qquad (3.10)$$

This argument has assumed that

13

$$\sum_{n=N+1}^{\infty} \frac{n^{-1-\Delta}}{\omega-\gamma_{nc}} = O(\omega^{-1}) + O(\omega^{-1-\Delta}) \tag{3.11}$$

as $|\omega| \to \infty$. This is shown in Appendix B.

In order to derive the necessary equations for g_n we consider that

$$T(-\gamma_{mc}) = \gamma_{mc} \ c \ C_m$$

Using (3.2) and (3.4) we have

$$T(-\gamma_{mc}) = \gamma_{mc} \ c \ R_m^{-1} \ K_m^{-1} \ g_m \qquad m = 1,2,\cdots,N$$

which according to (3.1) yields the following set of linear equation for g_n

$$H(-\gamma_{mc})F(-\gamma_{mc})[K_o-(\gamma_{mc}+jk_o)\left\{ \sum_{n=1}^{N} \frac{g_n}{\gamma_{nc}+\gamma_{mc}} + \bar{g} \sum_{n=N+1}^{\infty} \frac{n^{-1-\Delta}}{\gamma_{nc}+\gamma_{mc}} \right\}] = \gamma_{mc} c R_m^{-1} K_m^{-1} g_n \tag{3.12}$$

$$\text{for } m = 1,2,\ldots N,$$

From (v) and (viii) of section 2 we also have an additional equation

$$K_o F(jk_o)H(jk_o) = 2jk_o \frac{bc}{a}\left(B_o^{(o)} - \frac{R_o}{2jk_o c} T(-jk_o)\right) \tag{3.13}$$

Equations (3.10), (3.12), and (3.13) are the necessary linear equations to solve for K_o, g_n, for $n = 1,2,\ldots N$, and $\bar{g}$. The scattered modes in the two regions can then be found by using properties (v) and (iv) of section 2.

It should be noted that the concept of shifted zeroes could have been used to solve this problem. The interested reader is referred to Mittra and Lee (1971). The interesting point of this solution is that the perturbation expansion approach can be used to solve problems that can be solved using the shifted zero technique, but the reverse is not always true (see Royer and Mittra, 1972).

14

1. Introduction

This chapter is concerned with the application of the generalized MRCT to the trifur-
cated waveguide and the dielectrically loaded trifurcated waveguide. This type of problem
has not been solved by the MRCT previously. However, this problem has been previously
solved using the GSMT by Pace and Mittra (1966). It is shown that the satisfaction of the
edge condition at both edges by the MRCT solution improves the convergence over that
obtained using the GSMT. The solution of the trifurcated waveguide then allows one to
proceed to the more complicated case of the N-furcated waveguide with minimal difficulty.

2. Formulation of the Equations

Figure 3.2.1 illustrates the trifurcated waveguide geometry and the associated auxiliary
problem.

With reference to the auxiliary problem we see that we are perturbing two bifurcated
waveguide junctions. This leads us to construct two meromorphic functions as follows:

$$T_1(\omega) = H_1(\omega)F_1(\omega)\left[K_o^{(1)}-(\omega-jk_o)\sum_{n=1}^{\infty}\frac{g_n^{(1)}}{\omega+\gamma_{nc}}\right] \qquad (2.1)$$

$$T_2(\omega) = H_2(\omega)F_2(\omega)\left[K_o^{(2)}-(\omega-jk_o)\sum_{n=1}^{\infty}\frac{g_n^{(2)}}{\omega-\gamma_{nc}}\right] \qquad (2.2)$$

where

$$H_1(\omega) = e^{-\omega/\pi[b_1\ln(b_1/c) + b_2\ln(b_2/c)]}$$

$$H_2(\omega) = e^{-\omega/\pi[b_o\ln(b_o/a) + c\ln(c/a)]}$$

$$F_1(\omega) = \frac{\Pi(\omega,\gamma_{b_1})\ \Pi(\omega,\gamma_{b_2})}{\Pi(\omega,\gamma_c)}$$

$$F_2(\omega) = \frac{\Pi(\omega,\gamma_{b_o})\ \Pi(\omega,\gamma_c)}{\Pi(\omega,\gamma_a)}$$

where TEM mode incidence in any one of the four waveguide sections has been assumed. Ex-
tension to higher order TM mode incidence or TE incidence is straightforward. It may be
recognized that (2.1) and (2.2) are just special cases of the canonical solution. $T_1(\omega)$
is identified with the junction at z = 0. The scattered modes from z = Δ produce an
incident modal spectrum on the junction at z = 0 from the coupling region c. From the
canonical solution we recognize that $g_n^{(b)} \equiv g_n^{(c)} \equiv 0$ and $g_n^{(a)} = g_n^{(1)}$. Similarly for $T_2(\omega)$
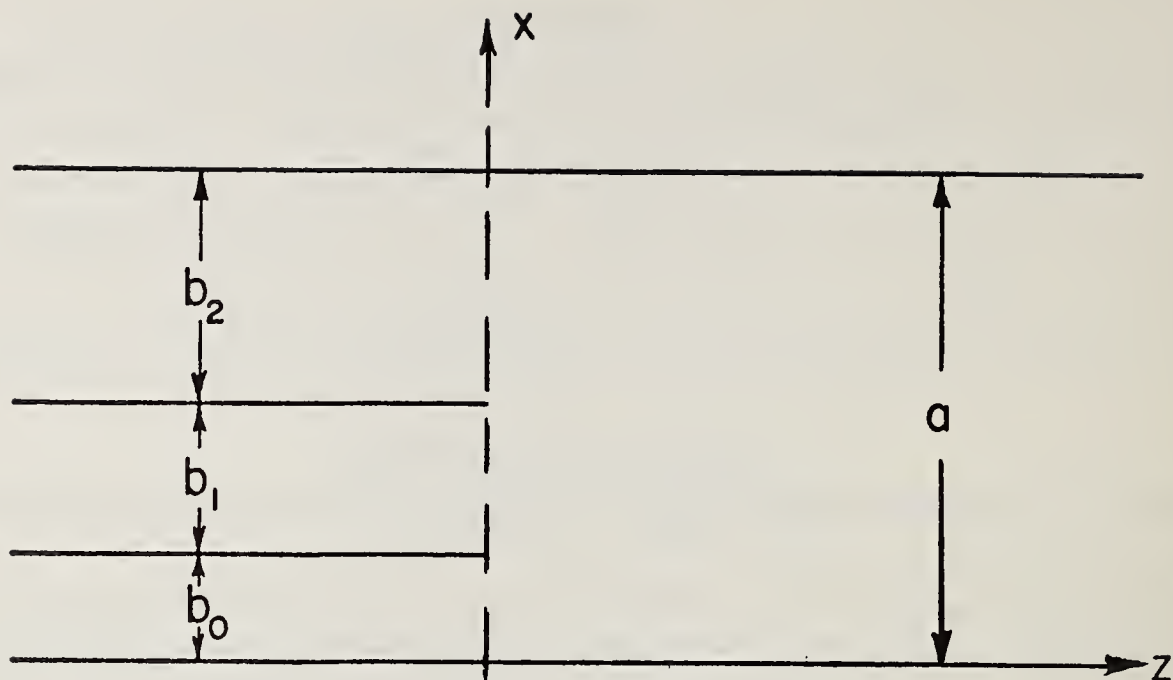
(a)   Trifurcated Waveguide
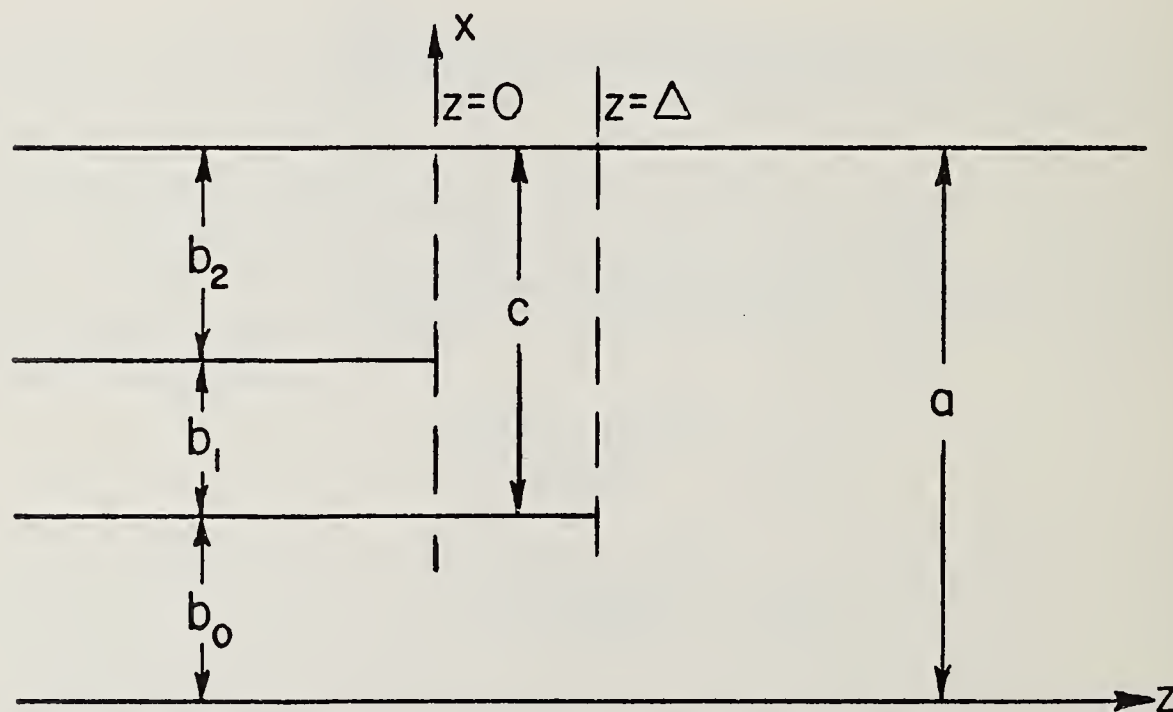
(b) Auxiliary Geometry

Fig. 3.2.1:   The Trifurcated Waveguide and the
Auxiliary Problem.

16

we recognize that the solution is obtained from the canonical solution with $g_n^{(b)} \equiv g_n^{(a)} \equiv 0$ and $g_n^{(c)} = g_n^{(2)}$. Here, the superscripts a, b, c refer to the three different regions in canonical problem (see Fig. 2.2.1).

For this particular problem $K_o^{(1)}$ and $K_o^{(2)}$ are known and are given by property (v) of section 2, Chapter 2 as

$$K_o^{(1)} = 2jk_o b_2 \left[C_o^+ - B_{o,2}^{(o)} \right] / \left[H_1(jk_o)F_1(jk_o) \right] \tag{2.3}$$

$$K_o^{(2)} = 2jk_o \ c \left[A_o - C_o^+ \right] / \left[H_2(jk_o)F_2(jk_o) \right] \tag{2.4}$$

where

$$C_o^+ = b_2/c \ B_{o,2}^{(o)} + b_1/c \ B_{o,1}^{(o)}$$

$$A_o = c/a \ C_o^+ + b_o/a \ B_{o,o}^{(o)}$$

and $B_{o,n}^{(o)}$ (n = 0,1,2) is the amplitude of the TEM mode incident from the b_n region.

The perturbation coefficients may be related to the modal coefficients $C_n^{\pm}$ in the coupling region c of the auxiliary problem using properties (i) and (iii) of section 2, Chapter 2.

$$g_n^{(1)} = K_n^{(1)} \ C_n^-, \qquad n \geq 1 \tag{2.5}$$

$$g_n^{(2)} = K_n^{(2)} \ C_n^+, \qquad n \geq 1 \tag{2.6}$$

where

$$K_n^{(1)} = \frac{-n\pi}{c} \sin \frac{n\pi b_1}{c} / \left[F_1(-\gamma_{nc})H_1(-\gamma_{nc})(\gamma_{nc}+jk_o) \right], \ n \geq 1 \tag{2.7}$$

$$K_n^{(2)} = -\gamma_{nc}^2 \ c / \left[F_2^{(n)}(\gamma_{nc})H_2(\gamma_{nc})(\gamma_{nc}-jk_o) \right], \qquad n \geq 1 \tag{2.8}$$

where $F_2^{(n)}(\gamma_{nc})$ indicates that the nth zero term at γ_{nc} is to be omitted.

The equations for $g_n^{(1)}$ and $g_n^{(2)}$ may be derived by requiring that $T_1(\omega)$ and $T_2(\omega)$ give consistent results for the modal coefficients in the coupling region. Using properties (ii) and (vi) of section 2, Chapter 2 and (2.5) and (2.6) we have for $\Delta = 0$:

$$\text{RES}[T_1, \gamma_{nc}] = \frac{-n\pi}{c} \sin \frac{n\pi b_1}{c} \left[K_n^{(2)} \right]^{-1} g_n^{(2)} \qquad n \geq 1 \tag{2.9}$$

$$T_2(-\gamma_{nc}) = \gamma_{nc} \ c \left[K_n^{(1)} \right]^{-1} g_n^{(1)}, \qquad n \geq 1 \tag{2.10}$$

(2.9) and (2.10), together with the definition of $T_1(\omega)$ and $T_2(\omega)$ in (2.1) and (2.2).

17

Then represent two infinite sets of equations for the perturbation coefficients $g_n^{(1)}$ and $g_n^{(2)}$.

3. Asymptotics

In order to efficiently truncate equations (2.9) and (2.10), we shall use the asymptotic behavior of the perturbation coefficients.

The asymptotic behavior of $g_n^{(1)}$ and $g_n^{(2)}$ for $\Delta = 0$ is found by considering a double limiting procedure. We first consider the asymptotic form for $\Delta \neq 0$. In (ii) and (vi) of section 2, chapter 2, we set $\gamma_{mc} \sim \frac{m\pi}{c} + \varepsilon$ as $m \to \infty$; then let $\varepsilon \to 0$ and $\Delta \to 0$. Using (page 14), this respectively yields

$$C_m^- = 0(m^{-3/2}) \tag{3.1}$$

$$C_m^+ = 0(m^{-3/2} \sin \frac{m\pi b_1}{c}) \tag{3.2}$$

where the notation for the mode coefficients in the coupling region is obvious. (Note also that C_m^+ and C_m^- correspond respectively to A_n in (A.7) and C_m in (A.5) of Appendix A.) The oscillatory portion of C_m^+ is necessary in order that the field be properly singular at $x = b_0 + b_1$.

This is an important point. In general if we have N edges of various types in a large guide of dimension a, then the asymptotic behavior as $n \to \infty$ is

$$A_n = \sum_{m=1}^{N} 0\left\{ n^{-(1+p_m)} \sin \frac{n\pi}{a} x_m \right\} \tag{3.3}$$

where x_m is the location of the mth region and p_m is the power index associated with the edge condition at x_m. This can be more clearly understood if we examine the field in region a

$$H_y = \phi_A = \sum_{n=0}^{\infty} A_n e^{-\gamma_{na} z} \cos \frac{n\pi}{a} x \tag{3.4}$$

Examine E_z which behaves as $z^{p_m - 1}$ as $z \to 0$ and $x = x_m$. Then from Mittra and Lee (page 11, 1971) we have

$$n A_n \sin \frac{n\pi}{a} x_m = 0(n^{-p_m}) \tag{3.5}$$

If we multiply (3.3) by $\sin n\pi x_k/a$ all terms will be oscillatory except the term $m = k$, and we will pick the appropriate edge condition out of the sum. (Note that $\sin^2 \frac{n\pi}{a} x_m = 0(1)$.) With a single edge this oscillatory term is generally implicitly stated. However, when multiple edges exist it is important to give these terms explicitly.

From (page 14) we can find that

$$K_n^{(1)} = 0(n^{1/2} \sin \frac{n\pi b_1}{c}) \tag{3.6}$$

18

$$K_n^{(2)} = O(n^{1/2})$$ (3.7)

Hence from (3.6), (3.7), (2.5) and (2.6) we have

$$g_n^{(1)} = O(n^{-1} \sin \frac{n\pi b_1}{c})$$ (3.8)

$$g_n^{(2)} = O(n^{-1} \sin \frac{n\pi b_1}{c})$$ (3.9)

Using (3.8) and (3.9) we can write (2.1) and (2.2) in a form more tractable for numerical computations.

$$T_1(\omega) = H_1(\omega)F_1(\omega) \left\{ K_o^{(1)} - (\omega - jk_o) \left[\sum_{n=1}^{N_1} \frac{g_n^{(1)}}{\omega + \gamma_{nc}} \right. \right.$$

$$+ \bar{g}^{(1)} \sum_{n=1+N_1}^{\infty} \frac{n^{-1} \sin n\pi b_1/c}{\omega + \gamma_{nc}} \left. \right\}$$ (3.10)

$$T_2(\omega) = H_2(\omega)F_2(\omega) \left\{ K_o^{(2)} - (\omega - jk_o) \left[\sum_{n=1}^{N_2} \frac{g_n^{(2)}}{\omega - \gamma_{nc}} \right. \right.$$

$$+ \bar{g}^{(2)} \sum_{n=1+N_2}^{\infty} \frac{n^{-1} \sin n\pi b_1/c}{\omega - \gamma_{nc}} \left. \right] \right\}$$ (3.11)

where clearly

$$g_n^{(1)} = \bar{g}^{(1)} n^{-1} \sin n\pi b_1/c, \quad n \geq 1+N_1$$

$$g_n^{(2)} = \bar{g}^{(2)} n^{-1} \sin n\pi b_1/c, \quad n \geq 1+N_2$$

Before using (3.10) and (3.11) in (2.9) and (2.10) let us consider the mode coefficients in the regions a and b, in order to insure that the field is properly singular using (3.8) and (3.9) for the asymptotic behavior of $g_n^{(1)}$ and $g_n^{(2)}$. Using properties (ii) and (vii) of section 2, Chapter 2 we respectively have that

$$T_1(-\gamma_{mb_1}) = (-1)^{m+1} \gamma_{mb_1} b_1 B_{m,1}$$ (3.12)

and

$$RES[T_2, \gamma_{na}] = -A_n \frac{n\pi}{a} \sin \frac{n\pi b_o}{a}$$ (3.13)

where $B_{m,1}$ is the mth reflected modal coefficient in the waveguide with dimension b_1.

19

This leads to an examination of the sums

$$S_1 = \sum_{n=N_1+1}^{\infty} \frac{n^{-1} \sin n\pi b_1/c}{n - \dfrac{cm}{b_1}}, \quad m \to \infty$$

and

$$S_2 = \sum_{n=N_2+1}^{\infty} \frac{n^{-1} \sin n\pi b_1/c}{n - \dfrac{cm}{a}}, \quad m \to \infty$$

Thus let us examine the universal sum

$$S = \sum_{n=N}^{\infty} \frac{n^{-1} \sin n\theta}{n - \omega}, \quad \omega \to \infty \tag{3.14}$$

In Appendix C it is shown that

$$S = O(\omega^{-1}) + O\left(\omega^{-1} \frac{\sin (\pi-\theta)}{\sin \omega\pi}\right)$$

hence from (3.12)

$$T_1(-\gamma_{mb_1}) = O(m^{-1/2}) + O(m^{-1/2}(-1)^m)$$

and thus (3.12) yields

$$B_{m,1} = O(m^{-3/2}) + O(m^{-3/2}(-1)^m)$$

The first term therefore can be used to satisfy the edge condition at the lower edge $x = b_o$ while the second term for the upper edge at $x = (b_o+b_1)$. This result is then in agreement with the concept of (3.3). Similarly,

$$RES[T_2, \gamma_{na}] = n^{-1/2} \sin \frac{n\pi b_o}{a} \left[O\left(\sin \frac{n\pi b_o}{a}\right)\right.$$

$$\left. + O\left(\sin \frac{n\pi(b_o+b_1)}{a}\right)\right]$$

and thus from (3.13)

$$A_n = O\left(n^{-3/2} \sin \frac{n\pi b_o}{a}\right) + O\left(n^{-3/2} \sin \frac{n\pi(b_o+b_1)}{a}\right)$$

Again, the first term then explicitly satisfies the edge condition at $x = b_o$, while the second term satisfies the edge condition at $x = (b_o+b_1)$. Hence the asymptotic results (3.8), (3.9) allow both edge conditions to be satisfied.

20

4. Truncation of the Equations

We are now in a position to use the knowledge of the asymptotic behavior of the perturbation coefficients in truncating equations (2.9) and (2.10). This section examines two ways of truncating the equations using the asymptotic behavior of the perturbation coefficients.

The first kind of truncation is what has commonly been used (Royer and Mittra, 1972). This consists of merely choosing extra equations by letting the free index of (2.9) and (2.10) take on one additional value. This yields the following simultaneous linear equations

$$
\sum_{m=1}^{N_1} \frac{g_m^{(1)}}{\gamma_{nc} + \gamma_{mc}} + \bar{g}^{(1)} \sum_{m=N_1+1}^{\infty} \frac{m^{-1} \sin m\pi b_1/c}{\gamma_{nc} + \gamma_{mc}} - \lambda_n^{(1)} g_n^{(2)}
$$

$$
= \frac{K_o^{(1)}}{\gamma_{nc} - jk_o} \qquad n = 1,2,\cdots,1+N_2 \tag{4.1}
$$

$$
\lambda_n^{(2)} g_n^{(1)} + \sum_{m=1}^{N_2} \frac{g_m^{(2)}}{\gamma_{nc} + \gamma_{mc}} + \bar{g}^{(2)} \sum_{m=N_2+1}^{\infty} \frac{m^{-1} \sin m\pi b_1/c}{\gamma_{nc} + \gamma_{mc}}
$$

$$
= \frac{K_o^{(2)}}{\gamma_{nc} + jk_o} \qquad n = 1,2,\cdots,1+N_1 \tag{4.2}
$$

where

$$
\lambda_n^{(1)} = \frac{\dfrac{n\pi}{c} \sin \dfrac{n\pi b_1}{c}}{H_1(\gamma_{nc})\mathrm{RES}[F_1,\gamma_{nc}](\gamma_{nc}-jk_o)K_n^{(2)}} \tag{4.3}
$$

$$
\lambda_n^{(2)} = \frac{\gamma_{nc} \; c}{H_2(-\gamma_{nc})F_2(-\gamma_{nc})(\gamma_{nc}+jk_o) K_n^{(1)}} \tag{4.4}
$$

Note that since we are not changing an edge condition but <u>adding</u> an edge condition, an equation comparable to (3.10) in Chapter 2 is not needed.

It should be noted that with any truncation there are an infinite number of equations which remain. As in other MRCT solutions these remaining equations can be used as a check on accuracy of the solution.

Of course, the above choice is not the only manner of truncation. For example one can equate the leading asymptotic terms of equations (2.9) and (2.10). This results in two equations independent of a free index. Using the asymptotic expressions for the infinite product in Mittra and Lee (1971) we find from (2.9)

$$
\sum_{n=1}^{N_1} g_n^{(1)} + \bar{g}^{(1)} \sum_{n=1+N_1}^{\infty} n^{-1} \sin n\pi b_1/c + \frac{\pi}{c} P_1 \bar{g}^{(2)} = K_o^{(1)} \tag{4.5}
$$

$$
\sum_{n=1}^{N_2} g_n^{(2)} + \bar{g}^{(2)} \sum_{n=1+N_2}^{\infty} n^{-1} \sin n\pi b_1/c - \pi P_2 \bar{g}^{(1)} = K_o^{(2)} \tag{4.6}
$$

21

where

$$P_1 = \sqrt{\frac{b_1 \, c \, a}{b_o}}$$

and

$$P_2 = \sqrt{\frac{b_o \, c^2}{a \, b_1 \, b_2}}$$

The remaining equations are chosen as in the previous truncation.

There is yet another possible choice. This is the direct truncation of the original equations. However, because of the arguments given in section 3, this solution will not explicitly satisfy both of the edge conditions of the problem.

5. Dielectric Loading

Figure 3.5.1 illustrates a trifurcated waveguide with a dielectric loading in the largest waveguide. The auxiliary problem is similar to the normal trifurcated waveguide.

With reference to the auxiliary problem we see that we can identify a function $T_1(\omega)$ with the junction at $z = -\Delta$.

$$T_1(\omega) = H_1(\omega)F_1(\omega)\left[K_o^{(1)} - (\omega - jk_o) \sum_{n=1}^{\infty} \frac{g_n^{(1)}}{\omega + \gamma_{nc}}\right] \tag{5.1}$$

This equation is identical to (2.1). However, the function (2.2) for the junction at $z = 0$ is modified to be

$$T_2(\omega) = H_2(\omega)F_2(\omega)\left[K_o^{(2)} - (\omega - jk_o)\left\{\sum_{n=1}^{\infty} \frac{g_n^{(2)}}{\omega - \gamma_{nc}} + \sum_{n=1}^{\infty} \frac{g_n^{(3)}}{\omega + \gamma_{na}}\right\}\right] \tag{5.2}$$

where $g_n^{(3)}$ corresponds to $g_n^{(a)}$ of the canonical solution, due to the presence of the dielectric.

Equations (2.3) – (2.10) apply to the dielectrically loaded case if the expression for $T_2(\omega)$ given in (5.2) is used.

Similarly we still have

$$g_n^{(1)}, \; g_n^{(2)} = O\left(n^{-1} \sin \frac{n\pi b_1}{c}\right)$$

since for $d \neq 0$ we are not changing or adding an edge condition.

In order to account for the dielectric consider the following. In the region between the trifurcated junction and the dielectric, the field is given by

$$\phi = H_y = \sum_{n=0}^{\infty} \left(A_n^{(o)} e^{\gamma_{na} z} + A_n e^{-\gamma_{na} z}\right) \cos \frac{n\pi}{a} z \tag{5.3}$$

22
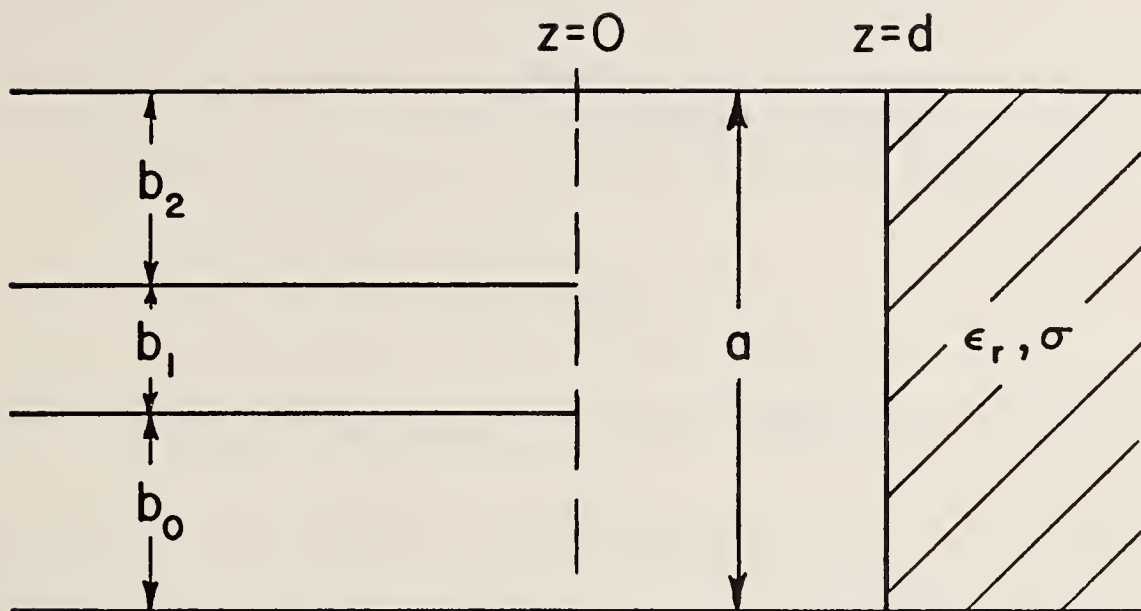
(a) Dielectrically Loaded Trifurcated Waveguide
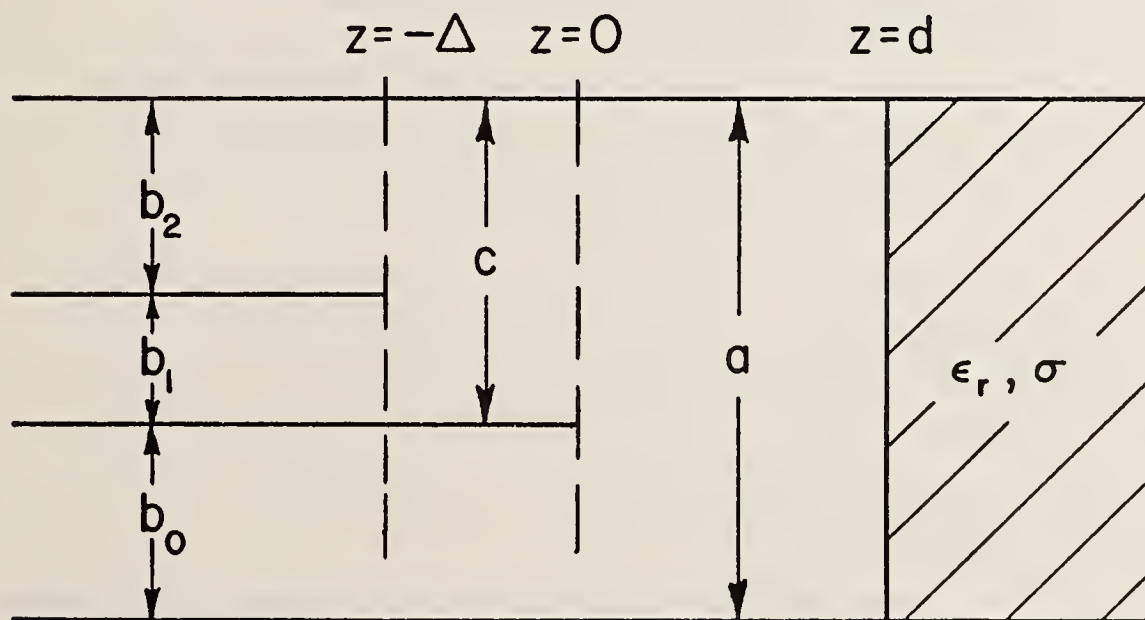
(b) Auxiliary Geometry

Fig. 3.5.1: Dielectrically Loaded Trifurcated
             Waveguide and the Auxiliary Problem.

23

and it is easily shown that

$$A_n^{(o)} = R_n A_n \tag{5.4}$$

where

$$R_n = \frac{\epsilon \gamma_{na} - \Gamma_{na}}{\epsilon \gamma_{na} + \Gamma_{na}} e^{-2\gamma_{na}d} \tag{5.5}$$

and where

$$\Gamma_{na} = \sqrt{\left(\frac{n\pi}{a}\right)^2 - \epsilon k_o^2} $$

We will consider the case of conduction losses in the dielectric by using the complex permittivity

$$\epsilon = \epsilon_r - j \frac{120 \pi \sigma}{k_o} \tag{5.6}$$

From property (i) of section 2, Chapter 2 we have that

$$g_n^{(3)} = K_n^{(3)} A_n^{(o)} \tag{5.7}$$

where

$$K_n^{(3)} = \frac{-n\pi}{a} \sin \frac{n\pi b_o}{a} / [F_2(-\gamma_{na})H_2(-\gamma_{na})(\gamma_{na}+jk_o)] \tag{5.8}$$

The asymptotic behavior of $g_n^{(3)}$ can be found using (5.7) and (5.4) to be

$$g_n^{(3)} = 0(n^{-1} e^{-2n\pi d/a}) \tag{5.9}$$

Because of the exponential behavior of $g_n^{(3)}$ the series appearing in (5.2) can be truncated at a finite value, say $n = N_3$.

An equation for $g_n^{(3)}$ can now be derived using property (ii) of section 2, Chapter 2 and (5.4), (5.7) and (5.9)

$$RES[T_2, \gamma_{na}] = \frac{-n\pi}{a} \sin \frac{n\pi b_o}{a} A_n$$

$$= \frac{-n\pi}{a} \sin \frac{n\pi b_o}{a} R_n^{-1} \left[K_n^{(3)}\right]^{-1} g_n^{(3)} \qquad n = 1, 2, \cdots, 1+N_3 \tag{5.10}$$

Equations (5.10) together with the appropriately modified forms of (2.9) and (2.10) represent the necessary simultaneous equations for $g_n^{(1)}$, $g_n^{(2)}$ and $g_n^{(3)}$.

Note that we are considering only the conventional method of truncation.

6. The Scattered Fields

The previous sections have dealt with the formulation and solution of the MRCT equations for the perturbation coefficients. Upon finding the perturbation coefficients, we are able to evaluate the constructed meromorphic functions at the appropriate points in the complex plane and determine the scattered fields. This is done with the aid of the auxiliary geometry. Using the properties (viii) and (ix) of section 2, Chapter 2, we find the following TEM coefficients of the scattered fields for the unloaded trifurcated waveguide

$$B_{o,o} = -T_2(-jk_o)/(2jk_o b_o) \tag{6.1}$$

$$B_{o,1} = -T_1(-jk_o)/(2jk_o b_1) + T_2(-jk_o)/(2jk_o c) \tag{6.2}$$

$$B_{o,2} = T_1(-jk_o)/(2jk_o b_2) + T_2(-jk_o)/(2jk_o c) \tag{6.3}$$

where $B_{o,n}$ (n = 0,1,2) is the amplitude of the reflected TEM mode in the waveguide of dimension b_n.

When only a single waveguide is excited with a TEM mode with an amplitude of unity, (6.1)-(6.3) represent either (current) reflection coefficients or (current) coupling coefficients. The reader is reminded that for TEM incidence from the largest guide the TEM solution is immediate, the solution being given by properties (viii) and (ix) of section 2, Chapter 2. Also, the TEM transmission coefficient to the larger waveguide is found immediately from repeated use of equation (2.5).

The complete scattered fields can be found with the aid of the auxiliary problem and the properties given in section 2, Chapter 2. For this monograph, only the TEM modal amplitudes are of immediate interest.

For the case of the dielectric loaded trifurcated waveguide, the results are essentially the same as those already given except that we must add in the reflected TEM field from the dielectric. This yields

$$B_{o,o} = -T_2(-jk_o)/(2jk_o b_o) + R_o A_o \tag{6.4}$$

$$B_{o,1} = -T_1(-jk_o)/(2jk_o b_1) + T_2(-jk_o)/(2jk_o c) + R_o A_o \tag{6.5}$$

$$B_{o,2} = T_1(-jk_o)/(2jk_o b_2) + T_2(-jk_o)/(2jk_o c) + R_o A_o \tag{6.6}$$

where R_o is given by (5.5) and

$$A_o = \frac{c}{a} C_o^+ + \frac{b_o}{a} B_{o,o}^{(o)}$$

and

$$C_o^+ = \frac{b_2}{c} B_{o,2}^{(o)} + \frac{b_1}{c} B_{o,1}^{(o)}$$

25

The remainder of this chapter concerns only TEM incidence. Other incident modes may be included in a direct manner using the properties discussed in section 2, Chapter 2.

7. Numerical Results

7.1 Introduction

This section presents the numerical solution of the trifurcated waveguide as well as the dielectric loaded trifurcated waveguide.

One interesting aspect of the numerical solution of the problems is the method used to evaluate the infinite product form $H(\omega)F(\omega)$ appearing in (2.14) of Chapter 2. The method is capable of giving results accurate to an arbitrary accuracy using only a small number of terms in the product plus some correction terms. For the data computed in this report, 50 terms were used in the evaluation of the infinite product for 5 place accuracy. The technique used is given in Appendix D.

The infinite oscillatory summations used in the construction of the meromorphic functions (see (3.10) and (3.11), for example) were summed numerically using a moving average. Less than 50 terms were generally necessary to yield 5 place accuracy.

7.2 The Trifurcated Waveguide

The practical solution of the trifurcated waveguide using the truncated equations required two numerical considerations. We must decide how to choose the ratio of N_1/N_2, and we must decide how large N_1 and N_2 must be for acceptable accuracy of the results.

A numerical study of the ratio, N_1/N_2, revealed that the final result was independent of the ratio (as opposed to direct mode matching where the solution does depend on such ratios). It was thus convenient to choose $N_1 = N_2$.

The choice of how large $N_p = N_1 = N_2$ must be for a given accuracy, depends on the geometry of the problem. Even for a given trifurcated waveguide we must decide how b_o and b_2 are chosen, since switching b_o and b_2 merely turns the waveguide upside down. Table 3.7.2.1 illustrates the TEM current reflection coefficient of an edge waveguide as a function of $N_p = N_1 = N_2$. The column $B_{o,o}$ is the reflection coefficient of an incident current mode of unity in waveguide section "0", while $B_{o,2}$ in the next column is the reflection coefficient when the current mode is incident from section "2". Since the geometry of the two cases is identical, one expects the two coefficients to converge to the same value as N_p increases. This geometry was also considered by Pace and Mittra (1966) and their data is shown with N_p corresponding to the size of the scattering matrix used.

26

Table 3.7.2.1 Convergence Results for the Reflection Coefficient
in the Outer Section of a Trifurcated Waveguide.

N_p	$B_{o,o}^{*}$		$B_{o,2}^{\dagger}$		$B_{o,o}$ (Pace)	
1	0.32424	131.91°	0.32427	131.91°	0.326	133.1°
2	0.32425	131.91°	0.32424	131.93°	0.327	132.0°
3	0.32425	131.91°	0.32424	131.92°	0.324	132.5°
4	0.32425	131.91°	0.32425	131.91°	0.324	132.5°
6	0.32425	131.91°	0.32425	131.91°	0.324	132.6°
8	0.32425	131.91°	0.32425	131.91°	--	

$*k_o b_o = 1.27046$, $k_o b_1 = 0.41417$, $k_o b_2 = 0.20033$

$\dagger k_o b_2 = 1.27046$, $k_o b_1 = 0.41417$, $k_o b_o = 0.20033$

The above MRCT data was computed using the conventional method of truncation. Note that 5 place accuracy is achieved almost immediately. This is a definite improvement over the GSMT, although for many engineering applications the GSMT results are still quite acceptable. It is interesting to note that the reflection coefficient without the adjacent conducting plate is found from (2.13) in Chapter 2 to be 0.326 exp(132.6°). Note that $B_{o,o}$ converges faster than $B_{o,2}$. This later case corresponds to a larger coupling region dimension, c.

The reflection coefficient of the central waveguide of the above case is given in Table 3.7.2.2.

Table 3.7.2.2 Convergence Results for the Reflection Coefficient
in the Center Section of a Trifurcated Waveguide.

N_p	$B_{o,1}^{*}$	
1	0.74244	152.38°
2	0.74244	152.37°
3	0.74244	152.37°
4	0.74244	152.37°

$*k_o b_o = 1.27046$, $k_o b_1 = 0.41417$, $k_o b_2 = 0.20033$

Again the convergence is extremely fast.

The above data was computed using the conventional method of truncation of the equations. The same data was computed using the asymptotic choice of the extra equations. This is shown in Table 3.7.2.3.

Table 3.7.2.3 Effect of the Choice of Truncation on the Convergence of the Reflection Coefficients $B_{o,o}$, $B_{o,2}$ and the Coupling Coefficient $B_{o,1}$.

N_p	$B_{o,o}$*		$B_{o,2}$†		$B_{o,1}$*	
1	0.32418	131.93°	0.32308	132.35°	0.74296	152.54°
2	0.32426	131.91°	0.32406	131.95°	0.74241	152.36°
3	0.32426	131.91°	0.32436	131.90°	0.74242	152.36°
4	0.32425	131.91°	0.32438	131.90°	0.74246	152.38°
6	0.32425	131.91°	0.32426	131.91°	0.74244	152.37°
8	0.32425	131.91°	0.32424	131.91°	0.74244	152.37°

*$k_o b_o = 1.27046$, $k_o b_1 = 0.41417$, $k_o b_2 = 0.20033$

†$k_o b_2 = 1.27046$, $k_o b_1 = 0.41417$, $k_o b_o = 0.20033$

Five place accuracy is again achieved; however, this choice of the truncated equations does not appear to be quite as good as the conventional truncation choice. This is logical since we are truncating the equations at such small indices that the asymptotic value of the equations has not been reached.

As a further comparison with the above data, Table 3.7.2.4 gives the results of using direct truncation (i.e., no asymptotics).

Table 3.7.2.4 Convergence of Direct Truncation.

N_p	$B_{o,o}$*		$B_{o,2}$†		$B_{o,1}$*	
1	0.3233	131.4°	0.3257	135.3°	0.7394	153.8°
2	0.3244	132.0°	0.3245	132.3°	0.7429	152.1°
3	0.3244	132.0°	0.3237	131.5°	0.7428	152.2°
4	0.3241	131.8°	0.3237	131.4°	0.7420	152.6°
6	0.3243	131.9°	0.3243	131.9°	0.7425	152.3°
8	0.3243	131.9°	0.3244	132.1°	0.7425	152.3°

*$k_o b_o = 1.27046$, $k_o b_1 = 0.41417$, $k_o b_2 = 0.20033$

†$k_o b_2 = 1.27046$, $k_o b_1 = 0.41417$, $k_o b_o - 0.20033$

This solution does not explicitly satisfy both of the edge conditions; however, it does converge to the correct result just as the computations made by Pace and Mittra (1966) using the GSMT did. However, the convergence of both of these methods is much slower than either of the methods described which satisfy both edge conditions explicitly. It is also interesting to note that the direct truncation appears to converge faster than the GSMT solution. This is important to note since the MRCT solution without asymptotics can be applied as easily as the GSMT.

The data presented thus far has been for a waveguide junction which propagates only the TEM mode in any waveguide region. It is instructive to solve multimoded waveguide problems using the MRCT. Table 3.7.2.5 presents data for a case where two of the waveguides support the TM_1 mode in addition to the TEM mode.

Table 3.7.2.5 Effect of Multimoding on the Convergence Results of the
Reflection Coefficients $B_{o,2}$, $B_{o,o}$ in the Outer Section
of the Trifurcated Waveguide and the Coupling Coefficient
$B_{o,1}$ in the Center Section.

N_p	$B_{o,2}$*		$B_{o,o}$†		$B_{o,1}$*	
1	0.38296	74.68°	0.31798	75.03°	0.85180	156.01°
2	0.38287	74.75°	0.37277	74.79°	0.85159	155.99°
3	0.38287	74.70°	0.38013	74.72°	0.85160	156.01°
4	0.38289	74.67°	0.38226	74.68°	0.85164	156.02°
6	0.38290	74.66°	0.38321	74.65°	0.85166	156.02°
8	0.38289	74.66°	0.38320	74.65°	0.85165	156.02°
10	0.38289	74.66°	0.38306	74.65°	0.85165	156.02°
12	0.38289	74.66°	0.38296	74.66°	0.85165	156.02°

*$k_o b_2 = 1.27046$, $k_o b_1 = 0.41417$, $k_o b_o = 4.41205$

†$k_o b_o = 1.27046$, $k_o b_1 = 0.41417$, $k_o b_2 = 4.41205$

The convergence is again quite fast and five place accuracy can be achieved. The convergence
of the recession with the larger coupling dimension, c, is somewhat slower than in the
single moded case because of the multimoding in the coupling region. Also the overmoded
data represents more of a perturbation to the bifurcated solution since the magnitude of
the reflection coefficient without the adjacent conducting plate is 0.4452 (from (2.13),
Chapter 2).

Table 3.7.2.6 illustrates this same data using the asymptotic choice of the last
equations.

Table 3.7.2.6 Effect of Multimoding on the Convergence Results of
the Trifurcated Waveguide (Asymptotic Truncation)

N_p	$B_{o,2}$*		$B_{o,2}$†		$B_{o,1}$*	
1	0.38695	75.92°	0.43375	74.52°	0.83744	156.62°
2	0.38310	74.83°	0.40086	72.97°	0.84925	156.15°
3	0.38327	74.68°	0.39194	71.82°	0.85304	155.77°
4	0.38329	74.67°	0.38780	73.65°	0.85317	155.75°
6	0.38288	74.66°	0.38433	74.34°	0.85172	156.02°
8	0.38282	74.62°	0.38317	74.77°	0.85144	156.08°
10	0.38290	74.67°	0.38284	74.96°	0.85165	156.02°
12	0.38296	74.68°	0.38283	74.96°	0.85173	155.99°

*$k_o b_2 = 1.27046$, $k_o b_1 = 0.41417$, $k_o b_o = 4.41205$

†$k_o b_o = 1.27046$, $k_o b_1 = 0.41417$, $k_o b_2 = 4.41205$

From the data it is clear that for larger waveguides the differences of the conventional
and asymptotic truncation methods are amplified with the conventional truncation method
apparently being better.

For a complete comparison of methods it is instructive to compute the multimoded data
with direct truncation. This is shown in Table 3.7.2.7.

Table 3.7.2.7 Effect of Multimoding on the Convergence Results of the
Trifurcated Waveguide (Direct Truncation)

N_p	$B_{o,2}^{*}$		$B_{o,o}^{\dagger}$		$B_{o,1}^{*}$	
1	0.3888	82.3°	0.4447	79.1°	0.8482	150.8°
2	0.3835	75.5°	0.4330	78.8°	0.8514	155.4°
3	0.3807	73.6°	0.4167	78.3°	0.8518	157.0°
4	0.3806	73.5°	0.4042	77.4°	0.8518	157.1°
6	0.3829	74.7°	0.3889	75.6°	0.8517	156.0°
8	0.3836	75.0°	0.3821	74.3°	0.8516	155.7°
10	0.3829	74.7°	0.3797	73.8°	0.8517	156.0°
12	0.3825	74.5°	0.3796	73.7°	0.8517	156.2°

$*k_o b_2 = 1.27046$, $k_o b_1 = 0.41417$, $k_o b_o = 4.41205$

$\dagger k_o b_o = 1.27046$, $k_o b_1 = 0.41417$, $k_o b_2 = 4.41205$

Again the convergence of the direct truncation method is slower than either the conventional or asymptotic truncation methods.

The choice of recession giving the larger coupling region serves as a convenient comparison of all the truncation methods since the effects are magnified. Figure 3.7.2.1 illustrates graphically the convergence of the magnitude of the·reflection coefficient $B_{o,o}$ given in Tables 3.7.2.5 - 3.7.2.7. It is clear that both of the methods which satisfy both of the edge conditions explicitly are superior to the direct truncation method, particularly for extremely accurate results. For some engineering applications, however, the direct truncation method is acceptable and will yield results more efficient than many more conventional methods. Figure 3.7.2.1 also illustrates that the conventional choice of the truncation method converges faster than the asymptotic choice of the truncation.

The discussion thus far has been limited to the convergence of various reflection coefficients. It is also interesting to examine some typical perturbation coefficients. Figure 3.7.2.2 illustrates the behavior of $g_n^{(1)}$ for the data of Table 3.7.2.1 for $N_p = 8$ and the calculation of $B_{o,o}$. It is quite clear that the asymptotic behavior given in (3.8) and (3.9) is quickly achieved.

7.3 The Dielectrically Loaded Trifurcated Waveguide

The dielectric loading of the trifurcated waveguide adds an additional numerical parameter, N_3. It was generally convenient to choose $N_p = N_1 = N_2 = N_3$. However, since the perturbation coefficients due to the dielectric decay exponentially, N_3 can generally be chosen smaller than N_1 and N_2.

Since there is no existing data for the dielectrically loaded trifurcated waveguide the following steps were taken to check the programming: (1) The dielectric was combined with the unloaded trifurcated waveguide using only a TEM mode interaction. This was a particularly good check for large d or small ϵ_r. The data computed agreed with this data. (2) The results of interchanging b_o and b_2 yielded the same results. This is an independent check of the new programming.
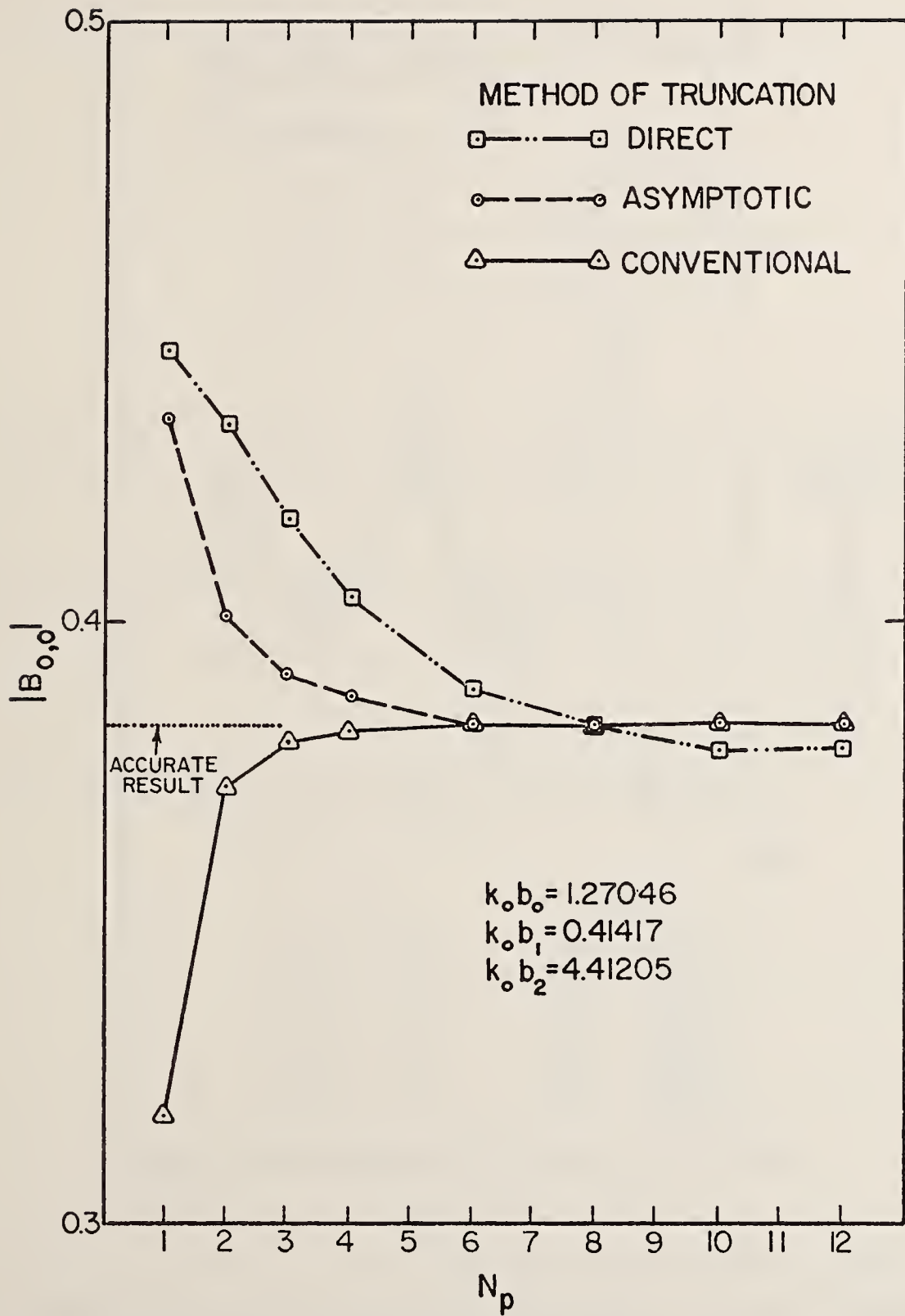
Fig. 3.7.2.1:   Comparison of Methods of Truncation
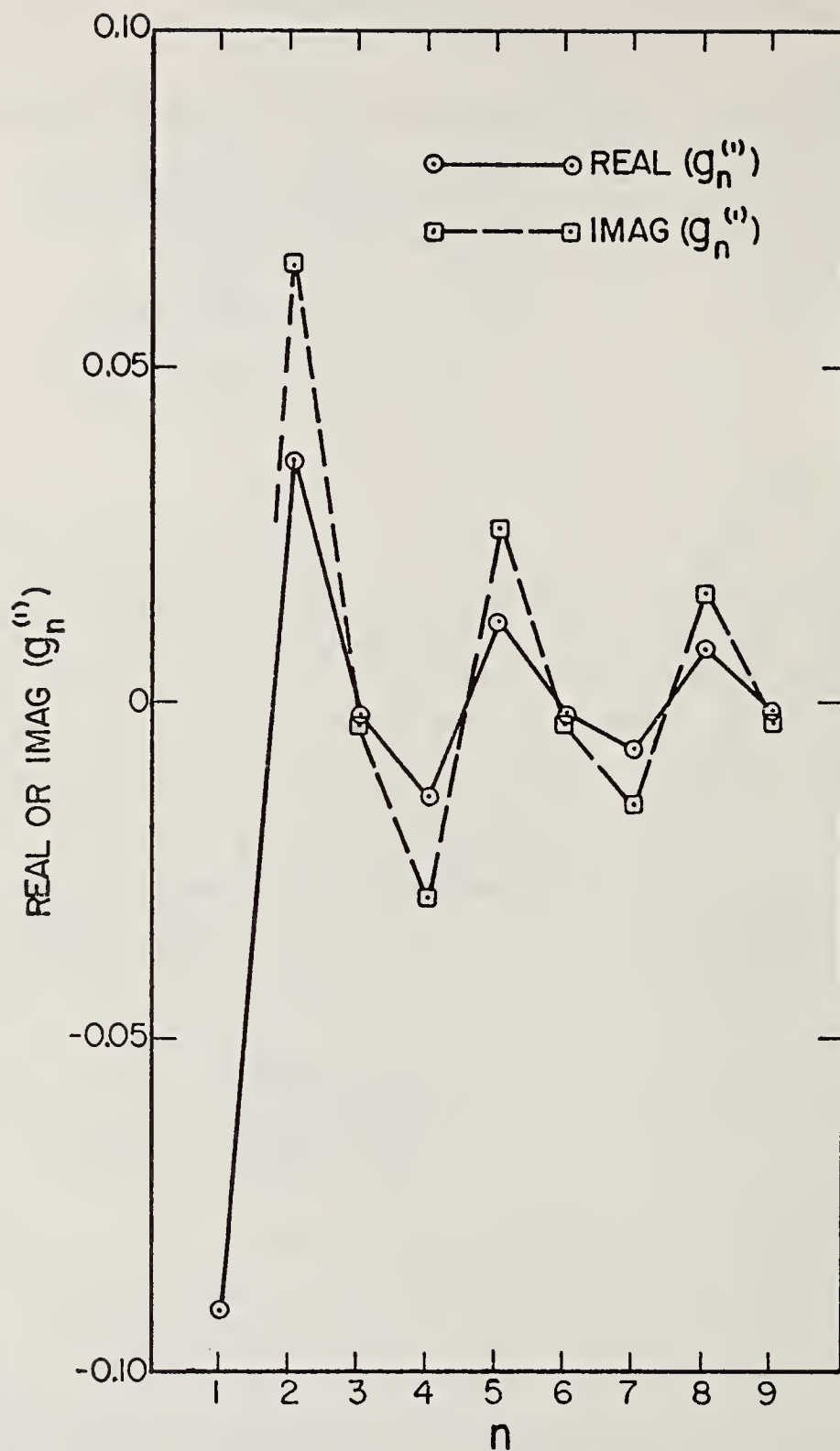for the Trifurcated Waveguide.

31

Fig. 3.7.2.2: Typical Perturbation Coefficients for the Trifurcated Waveguide.

32

Table 3.7.3.1 illustrates the change of the data of Table 3.7.2.1 and 3.7.2.2 with the dielectric parameters: $k_o d = 1.256$, $\varepsilon_r = 10$, and $\sigma/k_o = 0.01$.

Table 3.7.3.1 Convergence Results for the Reflection Coefficient in the Outer Section of a Dielectrically Loaded Trifurcated Waveguide.

N_p	$B^*_{o,o}$		$B^*_{o,1}$	
1	0.52772	172.64°	0.80422	158.83°
2	0.52773	172.64°	0.80421	158.82°
3	0.52773	172.64°	0.80420	158.82°
4	0.52773	172.64°	0.80420	158.82°
6	0.52773	172.64°	0.80420	158.82°

$^*k_o b_o = 1.27046$, $k_o b_1 = 0.41417$, $k_o b_2 = 0.20033$

The above data was computed using the conventional truncation method. The convergence is comparable to the trifurcated waveguide without dielectric loading. The recession corresponding to the larger coupling region yielded results comparable to the non-loaded waveguide junction.

The waveguides in the above example are single moded except for the dielectric region which supports two modes. Table 3.7.3.2 illustrates the change of the multimoded data of Table 3.7.2.5 due to the addition of dielectric material with the parameters $k_o d = 1.256$, $\varepsilon_r = 10$, $\sigma/k_o = 0.01$.

Table 3.7.3.2 Effect of Multimoding on the Convergence Results for the Dielectrically Loaded Trifurcated Waveguide (Conventional Truncation).

N_p	$B^*_{o,2}$		$B^*_{o,1}$	
1	0.15261	168.61°	0.88923	160.27°
2	0.14271	159.59°	0.88667	160.10°
3	0.14187	159.49°	0.88517	159.95°
4	0.14168	159.51°	0.88521	159.96°
6	0.14161	159.51°	0.88523	159.96°
8†	0.14164	159.51°	0.88522	159.96°
10†	0.14165	159.51°	0.88521	159.96°

$^*k_o b_o = 4.41205$, $k_o b_1 = 0.41417$, $k_o b_2 = 1.27046$
$†N_3 = 6$

Again the convergence was comparable to the trifurcated waveguide without dielectric loading.

A comparison of the above data with that of section 7.2 illustrates the dramatic effect that dielectric loading can have on the reflection coefficients.

1. Introduction

This chapter presents the extension of the results of Chapter 3 to the more complicated case of the N-furcated waveguide and its modification due to dielectric loading. The N-furcated waveguide is a waveguide junction which has received little theoretical attention. The N-furcated waveguide junction can be used in the synthesis of desired ratios of higher order modes in multimoded waveguides. Also the N-furcated waveguide can be used as a closed region approximation to the reflection and coupling coefficients of a finite array of parallel plate waveguides.

2. Formulation of the Equations

Figure 4.2.1 illustrates the N-furcated waveguide and its auxiliary geometry.

The solution to this problem is found by construction N-1 meromorphic functions. The function associated with the first plate and the (N-1)th plate will only have a single perturbation sum, while the remaining plates will have functions with two perturbation sums. From the canonical solution these functions are readily written.

$$T_{N-1}(\omega) = H_{N-1}(\omega)F_{N-1}(\omega)\left[K_o^{N-1}-(\omega-jk_o)\sum_{n=1}^{\infty}\frac{g_n^{N-1,R}}{\omega+\gamma_{n,c_{N-2}}}\right] \qquad (2.1)$$

where it is understood that the appropriate geometrical factors for the (N-1)th junction are used in the canonical solution. It is convenient to introduce an additional superscript R to g_n which refers to the location of the perturbation, in this case to the right of the (N-1)th junction. Similarly,

$$T_1(\omega) = H_1(\omega)F_1(\omega)\left[K_o^1-(\omega-jk_o)\sum_{n=1}^{\infty}\frac{g_n^{1,L}}{\omega-\gamma_{n,c_1}}\right] \qquad (2.2)$$

where the superscript L of g_n indicates the perturbation is to the left of the 1st junction. For the Mth junction between 1 and N-1 we have

$$T_M(\omega) = H_M(\omega)F_M(\omega)\left[K_o^M-(\omega-jk_o)\left\{\sum_{n=1}^{\infty}\frac{g_n^{M,R}}{\omega+\gamma_{n,c_{M-1}}}+\sum_{n=1}^{\infty}\frac{g_n^{M,L}}{\omega-\gamma_{n,c_M}}\right\}\right] \qquad (2.3)$$

Note that there are 2N-4 sets of unknown g_n's.

The TEM normalization constants are given according to property (V) of section 2 of Chapter 2 by

$$K_o^{N-1} H_{N-1}(jk_o)F_{N-1}(jk_o) = -2jk_o \, b_{N-1}\left[U_o^{N-2}-B_{o,N-1}^{(o)}\right] \qquad (2.4)$$

$$K_o^1 H_1(jk_o)F_1(jk_o) = -2jk_o \, b_1\left[U_o^o-B_{o,1}^{(o)}\right] \qquad (2.5)$$
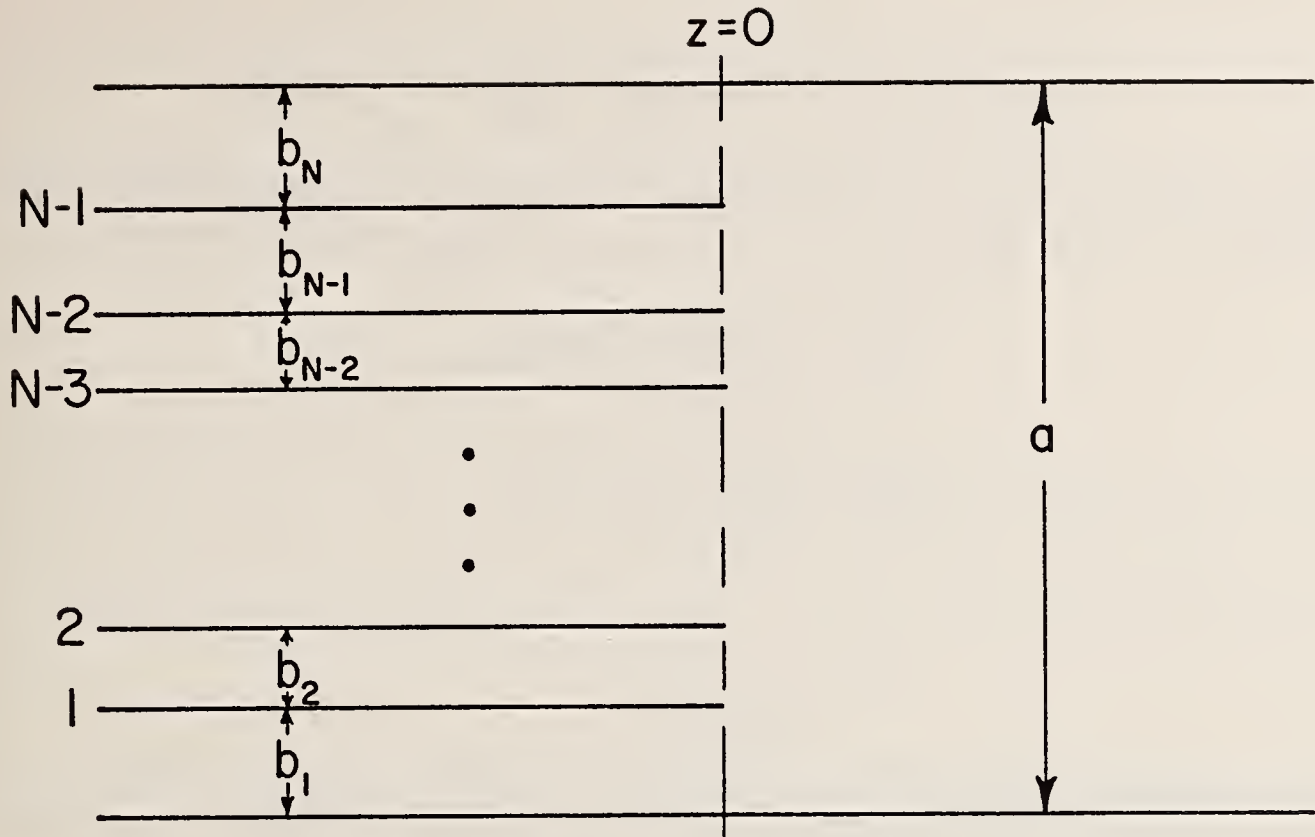
(a)   N-Furcated Waveguide
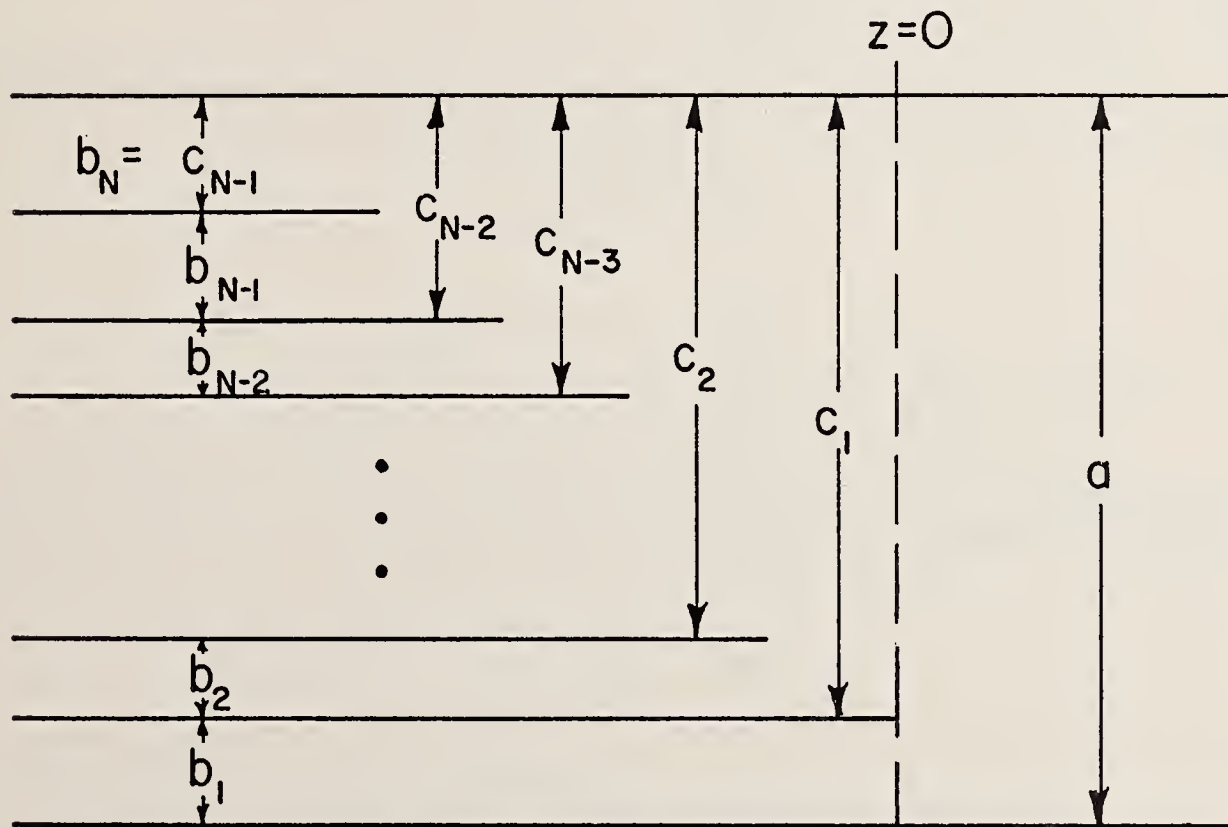
(b) Auxiliary Geometry

Fig. 4.2.1:   The N-Furcated Waveguide and the
Auxiliary Problem.

35

$$K_o^M H_M(jk_o)F_M(jk_o) = -2jk_o \ b_M\left[U_o^{M-1} - B_{o,M}^{(o)}\right] \qquad (2.6)$$

where U_o^m is the amplitude of the TEM mode incident from the left in the mth junction (refer to Figure 4.2.1 and the subscript of the c's). The U_o's are given by the equations

$$U_o^{N-2} = \frac{b_N}{c_{N-2}} B_{o,N}^{(o)} + \frac{b_{N-1}}{c_{N-2}} B_{o,N-1}^{(o)} \qquad (2.7)$$

$$U_o^{M-1} = \frac{c_M}{c_{M-1}} U_o^M + \frac{b_M}{c_{M-1}} B_{o,M}^{(o)} \qquad (2.8)$$

and

$$U_o^o = \frac{c_1}{a} U_o^1 + \frac{b_1}{a} B_{o,1}^{(o)} \qquad (2.9)$$

We have assumed TEM incidence from the waveguides to the left of the junction. The solution for the TEM scattered fields for TEM incidence from the largest waveguide is direct since no higher order modes are excited.

In order to derive equations for the perturbation coefficients, we again make use of the auxiliary geometry and insist that the expressions for the modal coefficients in the various coupling regions be consistent.

For the Mth plate we have in general coupling regions to the left and right of the plate truncation. From property (i) of section 2, Chapter 2, we have

$$g_n^{M,R} = K_n^{M,R} \ c_{n,M-1}^- \qquad (2.10)$$

where

$$K_n^{M,R} = \frac{-n\pi}{c_{M-1}} \sin \frac{n\pi b_M}{c_{M-1}} \ /[F_M(-\gamma_{n,c_{M-1}})H_M(-\gamma_{n,c_{M-1}}) \cdot (\gamma_{n,c_{M-1}} + jk_o)] \qquad (2.11)$$

Equations (2.10) and (2.11) are valid for $M = 2, \cdots N-1$.

For the left perturbation coefficients we find from property (iii) of section 2, Chapter 2

$$g_n^{M,L} = K_n^{M,L} \ c_{n,M}^+ \qquad (2.12)$$

where

$$K_n^{M,L} = -\gamma_{n,c_M}^2 \ c_M/[F_M^{(n)}(\gamma_{n,c_M})H_M(\gamma_{n,c_M})(\gamma_{n,c_M}-jk_o)] \qquad (2.13)$$

Equations (2.12) and (2.13) are valid for $M = 1, \cdots N-2$.

From property (ii) of section 2, Chapter 2, we have for the Mth plate

$$\text{RES}[T_M, \gamma_{n,c_{M-1}}] = \frac{-n\pi}{c_{M-1}} \sin \frac{n\pi b_M}{c_{M-1}} [K_n^{M-1,L}]^{-1} g_n^{M-1,L} \tag{2.14}$$

where we have used (2.12). This equation is valid for $M = 2, \cdots, N-1$. Similarly, we use property (vi) of section 2, Chapter 2, and find

$$T_M(-\gamma_{n,c_M}) = \gamma_{n,c_M} c_M [K_n^{M+1,R}]^{-1} g_n^{M+1,R} \tag{2.15}$$

Where we have used (2.10). This equation is valid for $M = 1, \cdots, N-2$.

Equations (2.14) and (2.15) represent the desired simultaneous equations for the perturbation coefficients. Note that the end plates each contribute only one kind of equation, while the central plates each contribute both kinds of equations. Hence, we have 2N-4 sets of infinite equations for the 2N-4 sets of unknown right and left perturbation coefficients.

3. Asymptotics

In order to effectively truncate the equations for the N-furcated waveguide, we shall find the asymptotic behavior of the perturbation coefficients.

Using (page 14) we can easily find the asymptotic behavior of $K_n^{M,R}$ to be

$$K_n^{M,R} = 0\left(n^{1/2} \sin \frac{n\pi b_M}{c_{M-1}}\right) \tag{3.1}$$

We can also find that similar to C_n^- in (3.1), Chapter 3, the expression

$$C_{n,M-1}^- = 0(n^{-3/2}) \tag{3.2}$$

Hence

$$g_n^{M,R} = 0\left(n^{-1} \sin \frac{n\pi b_M}{c_{M-1}}\right) \tag{3.3}$$

This is in agreement with the results found for the trifurcated waveguide.

The results begin to deviate from the trifurcated waveguide at this point when finding the asymptotic behavior of the left perturbation coefficients. In order to illustrate this consider the case of $M = 1$. From (ii) of section 2, Chapter 2, we have

$$-A_n \frac{n\pi}{a} \sin \frac{n\pi b_1}{a} = \text{RES}[T_1, \gamma_{na}] \qquad n = 1, 2, \cdots \tag{3.4}$$

Because of the concept of (3.3), the summation,

$$\sum_{n=1}^{\infty} \frac{g_n^{1,L}}{\omega - \gamma_{n,c_1}}$$

of $T_1(\omega)$ must contribute more than one oscillatory term asymototically in order to meet all of the edge conditions. In particular, this sum must contribute the necessary terms to

37

satisfy the edge condition of the plates: $2,3,\cdots N-1$. This result can be arrived at by considering a sequential collapse of the recessed junctions. Figure 4.3.1 illustrates this concept. For the mth junction, we need to satisfy the edge condition for all edges, from n to $N-1$. Hence

$$c_{n,M}^{+} = 0\left(n^{-3/2} \sin \frac{n\pi b_{M+1}}{c_M}\right) + 0\left(n^{-3/2} \sin \frac{n\pi(b_{M+1} + b_{M+2})}{c_M}\right) + \cdots$$

$$+ 0\left(n^{-3/2} \sin \frac{n\pi(b_{M+1} + b_{M+2} + \cdots + b_{N-1})}{c_M}\right) \qquad (3.5)$$

Using (2.12), (2.13), and the asymptotic expansion $K_n^{M,L} = 0(n^{\frac{1}{2}})$, we obtain

$$g_n^{M,L} = \sum_{p=1}^{N-M-1} 0\left\{n^{-1} \sin\left(\frac{n\pi}{c_M} \sum_{M=M+1}^{M+p} b_m\right)\right\} \qquad (3.6)$$

for $M = 1,2,\cdots,N-2$. These multi term asymptotic forms are necessary so that <u>all</u> the edge conditions are satisfied explicitly.

The argument presented above for the multiterm asymptotic expansions of the left perturbation coefficients is not totally rigorous. This is because we are really only in a position to argue the multiterm expansion of $g_n^{1,L}$. The remaining expansions do not necessarily follow, although they do appeal to the intuition.

A rigorous justification of the remaining multiterm asymptotic expansions can, however, be presented. In order to do this, let us assume the existence of the expansions and then show that they are necessary to satisfy all of the edge conditions. The procedure is to examine the leading asymptotic terms of (2.14). However, we must first consider the approximate forms of (2.1)-(2.3). Using (3.3) and (3.6) we have

$$T_{N-1}(\omega) \simeq H_{N-1}(\omega)F_{N-1}(\omega)\left[K_0^{N-1} - (\omega-jk_0)\left\{ \sum_{n=1}^{N^{N-1,R}} \frac{g_n^{N-1,R}}{\omega+\gamma_{n,c_{N-2}}} \right.\right.$$

$$\left.\left. + \overline{g}^{N-1,R} \sum_{n=1+N^{N-1,R}}^{\infty} \frac{n^{-1} \sin n\pi b_{N-1}/c_{N-2}}{\omega+\gamma_{n,c_{N-2}}} \right\}\right] \qquad (3.7)$$

and
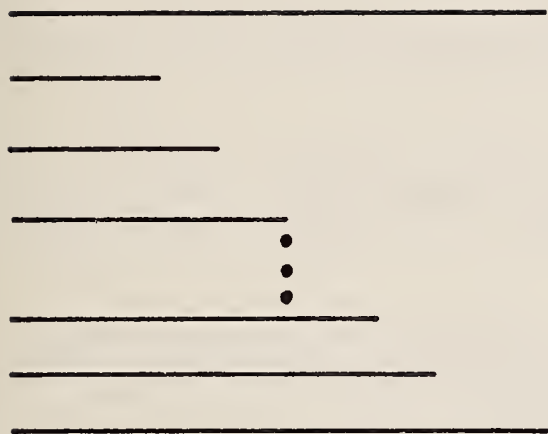
Step 1
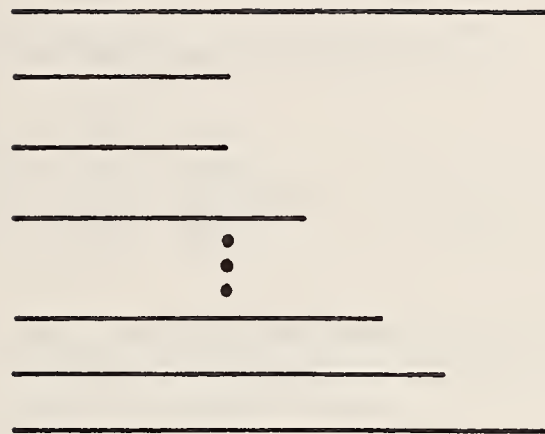
Step 2

Step N-2

Step N-1

Fig. 4.3.1: The Sequential Collapse of the
N-Furcated Waveguide Junction.

39

$$T_1(\omega) \simeq H_1(\omega)F_1(\omega)\left[K_o^1-(\omega-jk_o)\left\{\sum_{n=1}^{N^{1,L}}\frac{g_n^{1,L}}{\omega-\gamma_{n,c_1}}\right.\right.$$

$$+\bar{g}_1^{1,L}\sum_{n=1+N^{1,L}}^{\infty}\frac{n^{-1}\sin n\pi b_2/c_1}{\omega-\gamma_{n,c_1}}$$

$$+\bar{g}_2^{1,L}\sum_{n=1+N^{1,L}}^{\infty}\frac{n^{-1}\sin n\pi(b_2+b_3)/c_1}{\omega-\gamma_{n,c_1}}$$

$$\left.\left.+\cdots+\bar{g}_{N-2}^{1,L}\sum_{n=1+N^{1,L}}^{\infty}\frac{n^{-1}\sin n\pi(b_2+b_3+\cdots+b_{N-1})/c_1}{\omega-\gamma_{n,c_1}}\right\}\right] \tag{3.8}$$

and for the central plates

$$T_M(\omega) \simeq H_M(\omega)F_M(\omega)\left[K_o^M-(\omega-jk_o)\left\{\sum_{n=1}^{N^{M,R}}\frac{g_n^{M,R}}{\omega-\gamma_{n,c_{M-1}}}\right.\right.$$

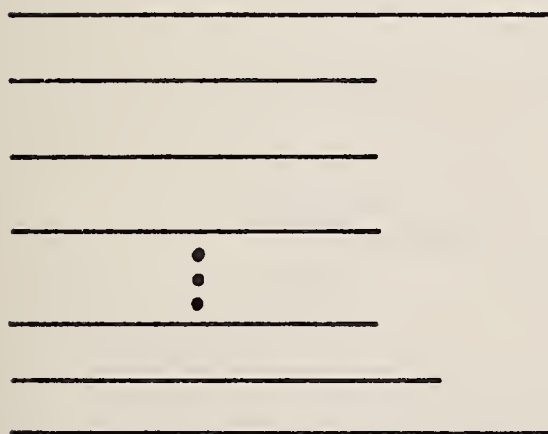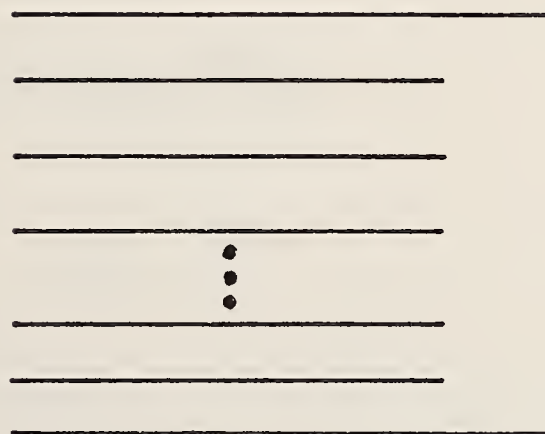$$+\bar{g}^{M,R}\sum_{n=1+N^{M,R}}^{\infty}\frac{n^{-1}\sin n\pi b_M/c_{M-1}}{\omega+\gamma_{n,c_{M-1}}}+\sum_{n=1}^{N^{M,L}}\frac{g_n^{M,L}}{\omega-\gamma_{n,c_M}}$$

$$+\bar{g}_1^{M,L}\sum_{n=1+N^{M,L}}^{\infty}\frac{n^{-1}\sin b_{M+1}/c_M}{\omega-\gamma_{n,c_M}}+\cdots \tag{3.9}$$

$$\left.\left.+\bar{g}_{N-M-1}^{M,L}\sum_{n=1+N^{M,L}}^{\infty}\frac{n^{-1}\sin n\pi(b_{M+1}+\cdots+b_{N-1})/c_M}{\omega-\gamma_{n,c_M}}\right\}\right]$$

where N indicates the number of perturbation coefficients and the superscript refers to the appropriate coefficient. The notation for the asymptotic perturbation coefficients is obvious. However, note that since there is more than one left asymptotic perturbation coefficient in general there is a subscript to distinguish the various asymptotic terms of the same perturbation coefficient. Since there is always only one right perturbation coefficient, no subscript is necessary.

When examining the asymptotic expansions we will keep the constants associated with the expansions for reasons which will become obvious. Using (page 14) and the results of Appendix C we have the asymptotic expansion

$$\mathrm{RES}[T_{M,\gamma n,c_{M-1}}]_{n\to\infty} \sim -\sqrt{\frac{2}{n\pi b_M C_M}}\sin^2\frac{n\pi b_M}{C_{M-1}}\times\left\{\left(K_o-\sum_{m=1}^{N^{M,R}}g_m^{M,R}-\bar{g}^{M,R}\sum_{m=N^{M,R}+1}^{\infty}m^{-1}\sin m\pi\frac{b_M}{C_{M-1}}\right.\right.$$

$$\left. - \sum_{m=1}^{N^{M,L}} g_m^{M,L} - \sum_{k=1}^{N-M-1} \left(\overline{g}_k^{M,L} \sum_{m=N^{M,L}+1}^{\infty} m^{-1} \sin\left(\frac{m\pi}{C_M} \sum_{\ell=1}^{k} b_{M+\ell} \right) \right) \right]$$

$$\left. + \pi \sum_{k=1}^{N-M-1} \overline{g}_k^{M,L} \frac{\sin \frac{n\pi}{C_{M-1}} (C_M - \sum_{\ell=1}^{k} b_{M+\ell})}{\sin \frac{n\pi}{C_{M-1}} (C_{M-1} - b_M)} \right\} .$$

Also, using the asymptotic expansion (3.6) the right-hand side of (2.14) becomes

$$\left. \frac{-n\pi}{C_{M-1}} \sin \frac{n\pi b_M}{C_{M-1}} \times \pm K_n^{M-i,L_1-1} g_n^{M-1,L} \right|_{n\to\infty} \sim - \sqrt{\frac{2\pi C_{M-2}}{n \, b_{M-1}}} \frac{\sin\frac{n\pi b_M}{C_{M-1}}}{C_{M-1}} \sum_{k=0}^{N-M-1} \overline{g}_{k+1}^{M-1,L} \sin\left(\frac{n\pi}{C_{M-1}} \sum_{\ell=0}^{k} b_{M+\ell} \right)$$

We thus find that (2.14 oscillatory terms of different arguments times the large parameter n. The first equation is of the form

$$P_M \left(K_o^M - \sum_{m=1}^{N^{M,R}} g_m^{M,R} - \overline{g}^{M,R} \sum_{m=1+N^{M,R}}^{\infty} m^{-1} \sin m\pi b_M/c_{M-1} \right.$$

$$- \sum_{m=1}^{N^{M,L}} g_m^{M,L} - \overline{g}_1^{M,L} \sum_{m=1+N^{M,L}}^{\infty} m^{-1} \sin m\pi b_{M+1}/c_M$$

$$\left. - \cdots - \overline{g}_{N-M-1}^{M,L} \sum_{m=1+N^{M,L}}^{\infty} m^{-1} \sin m\pi (b_{M+1}+\cdots+b_{N-1})/c_M \right)$$

$$= \frac{\pi}{c_{M-1}} \overline{g}_1^{M-1,L}$$

(3.10)

where

$$P_M = \frac{b_{M-1}}{b_M c_M c_{M-2}}$$

The remaining equations are all similar in form and are given by

$$P_M \overline{g}_1^{M,L} = \overline{g}_2^{M-1,L}/c_{M-1}$$

$$\vdots$$

(3.11)

$$P_M \overline{g}_{N-M-1}^{M,L} = \overline{g}_{N-M}^{M-1,L}/c_{M-1}$$

Equations (3.11) prove that multiterm asymptotic expansions are necessary for every left perturbation coefficient. If any of these coefficients are set to zero we see that (3.11) imply that other perturbation coefficients (which we know must be non-zero because of an

edge condition) must be zero. Hence, the existence of the multiterm asymptotic expansions of the left perturbation coefficients is proved by contradiction.

Using (3.7)-(3.9) and Appendix C we can easily show that _all_ of the edge conditions are explicitly satisfied just as was the case for the trifurcated waveguide.

4. Truncation of the Equations

The truncation of the equations for the N-furcated waveguide is more difficult than the trifurcated waveguide because of the asymptotic degeneracy of equation (2.14). Two basic choices of the truncation method are considered in this section.

The basic difference between methods is the choice of the extra equations for the asymptotic perturbation coefficients. Both of the methods use the following equations, which are obtained by using (3.7)-(3.9) in (2.14) and (2.15). For the first plate we obtain

$$
\sum_{m=1}^{N^{1,L}} \frac{g_m^{1,L}}{\gamma_{m,c_1} + \gamma_{n,c_1}} + \bar{g}_1^{-1,L} \sum_{m=1+N^{1,L}}^{\infty} \frac{m^{-1} \sin m\pi b_2/c_1}{\gamma_{m,c_1} + \gamma_{n,c_1}}
$$

$$
+ \bar{g}_2^{-1,L} \sum_{m=1+N^{1,L}}^{\infty} \frac{m^{-1} \sin m\pi (b_2+b_3)/c_1}{\gamma_{m,c_1} + \gamma_{n,c_1}}
$$

$$
+ \cdots + \bar{g}_{N-2}^{-1,L} \sum_{m=1+N^{1,L}}^{\infty} \frac{m^{-1} \sin m\pi (b_2+b_3+\cdots+b_{N-1})/c_1}{\gamma_{m,c_1} + \gamma_{n,c_1}}
$$

(4.1)

$$
+ (\lambda_n^{1,R})^{-1} \gamma_{n,c_1} c_1 g_n^{2,R} = K_o^1/(\gamma_{n,c_1} + jk_o) \qquad n = 1,2,\cdots,N^{2,R}
$$

And for the central plates we obtain the following two sets of equations

42

$$(\lambda_n^{M,L})^{-1} \frac{n\pi}{c_{M-1}} \sin \frac{n\pi b_M}{c_{M-1}} g_n^{M-1,L} - \sum_{m=1}^{N^{M,R}} \frac{g_m^{M,R}}{\gamma_{m,c_{M-1}} + \gamma_{n,c_{M-1}}}$$

$$- \bar{g}^{M,R} \sum_{m=1+N^{M,R}}^{\infty} \frac{m^{-1} \sin m\pi b_M / c_{M-1}}{\gamma_{m,c_{M-1}} + \gamma_{n,c_{M-1}}} + \sum_{m=1}^{N^{M,L}} \frac{g_m^{M,L}}{\gamma_{m,c_M} - \gamma_{n,c_{M-1}}}$$

$$+ \bar{g}_1^{M,L} \sum_{m=1+N^{M,L}}^{\infty} \frac{m^{-1} \sin m\pi b_{M+1} / c_M}{\gamma_{m,c_M} - \gamma_{n,c_{M-1}}}$$

$$+ \bar{g}_2^{M,L} \sum_{m=1+N^{M,L}}^{\infty} \frac{m^{-1} \sin m\pi (b_{M+1} + b_{M+2}) / c_M}{\gamma_{m,c_M} - \gamma_{n,c_{M-1}}} \qquad (4.2)$$

$$+ \cdots + \bar{g}_{N-M-1}^{M,L} \sum_{m=1+N^{M,L}}^{\infty} \frac{m^{-1} \sin m\pi (b_{M+1} + b_{M+2} + \cdots + b_{N-1}) / c_M}{\gamma_{n,c_M} - \gamma_{n,c_{M-1}}}$$

$$= -K_o^M (\gamma_{n,c_{M-1}} - jk_o) \qquad n = 1,2,\cdots,N^{M-1,L}$$

And

$$\sum_{m=1}^{N^{M,R}} \frac{g_m^{M,R}}{\gamma_{m,c_{M-1}} - \gamma_{n,c_M}} + \bar{g}_2^{M,R} \sum_{m=1+N^{M,R}}^{\infty} \frac{m^{-1} \sin m\pi b_M / c_{M-1}}{\gamma_{m,c_{M-1}} - \gamma_{n,c_M}}$$

$$- \sum_{m=1}^{N^{M,L}} \frac{g_m^{M,L}}{\gamma_{m,c_M} + \gamma_{n,c_M}} + \bar{g}_1^{M,L} \sum_{m=1+N^{M,L}}^{\infty} \frac{m^{-1} \sin m\pi b_{M+1} / c_M}{\gamma_{m,c_M} + \gamma_{n,c_M}}$$

$$- \bar{g}_2^{M,L} \sum_{m=1+N^{M,L}}^{\infty} \frac{m^{-1} \sin m\pi (b_{M+1} b_{M+2}) / c_M}{\gamma_{m,c_M} + \gamma_{n,c_M}} \qquad (4.3)$$

$$- \cdots - \bar{g}_{N-M-1}^{M,L} \sum_{m=1+N^{M,L}}^{\infty} \frac{m^{-1} \sin m\pi (b_{M+1} + b_{M+2} + \cdots + b_{N-1}) / c_M}{\gamma_{m,c_M} + \gamma_{n,c_M}}$$

$$- (\lambda_n^{M,R})^{-1} \gamma_{n,c_M} c_M g_n^{M+1,R} = -K_o^M / (\gamma_{n,c_M} + jk_o) \qquad n = 1,2,\cdots,N^{M+1,R}$$

Similarly, for the (N-1)th plate we obtain

$$(\lambda_n^{N-1,L})^{-1} \frac{n\pi}{c_{N-2}} \sin \frac{n\pi b_{N-1}}{c_{N-2}} g_n^{N-2,L}$$

$$-\sum_{m=1}^{N^{N-1,R}} \frac{g_m^{N-1,R}}{\gamma_{m,c_{N-2}}+\gamma_{n,c_{N-2}}} - \bar{g}^{N-1,R} \sum_{m=1+N^{N-1,R}}^{\infty} \frac{m^{-1}\sin m\pi b_{N-1}/c_{N-2}}{\gamma_{m,c_{N-2}}+\gamma_{n,c_{N-2}}}$$

$$= -\frac{K_o^{N-1}}{(\gamma_{n,c_{N-2}}-jk_o)} \qquad n = 1,2,\cdots,N^{N-2,L} \tag{4.4}$$

where

$$\lambda_n^{M,L} = -\gamma_{n,c_{M-1}}^2 \; c_{M-1} \frac{RES[F_M,\gamma_{n,c_{M-1}}]H_M(\gamma_{n,c_{M-1}})}{F_{M-1}^{(n)}(\gamma_{n,c_{M-1}})H_{M-1}(\gamma_{n,c_{M-1}})} \tag{4.5}$$

$$\lambda_n^{M,R} = \frac{-n\pi}{c_M} \sin \frac{n\pi b_{M+1}}{c_M} \frac{F_M(-\gamma_{n,c_M})H_M(-\gamma_{n,c_M})}{F_{M+1}(-\gamma_{n,c_M})H_{M+1}(-\gamma_{n,c_M})} \tag{4.6}$$

The asymptotic choice of the last equations can be logically extended to the N-furcated waveguide. Proceeding in a similar manner to the trifurcated waveguide, we find the following asymptotic form for equation (4.1)

$$\sum_{m=1}^{N^{1,L}} g_m^{1,L} + \bar{g}_1^{-1,L} \sum_{m=1+N^{1,L}}^{\infty} m^{-1} \sin m\pi b_2/c_1 + \cdots +$$

$$\bar{g}_{N-2}^{-1,L} \sum_{m=1+N^{1,L}}^{\infty} m^{-1} \sin m\pi(b_2+b_3+\cdots+b_{N-1})/c_1$$

$$+ \pi Q_1 \bar{g}^{-2,R} = K_o^1 \tag{4.7}$$

where

$$Q_M = -\sqrt{\frac{b_M \, c_M^2}{b_{M+1} \, c_{M-1} \, c_{M+1}}}$$

The asymptotic form of (4.2) has already been given in equations (3.10) and (3.11).

The asymptotic form of (4.3) is

$$\sum_{m=1}^{N^{M,R}} g_m^{M,R} + \bar{g}^{M,R} \sum_{m=1+N^{M,R}}^{\infty} m^{-1} \sin m\pi b_M / c_{M-1}$$

$$+ \sum_{m=1}^{N^{M,L}} g_m^{M,L} + \bar{g}_1^{M,L} \sum_{m=1+N^{M,L}}^{\infty} m^{-1} \sin m\pi b_{M+1} / c_M$$

$$+ \cdots + \bar{g}_{N-M-1}^{M,L} \sum_{m=1+N^{M,L}}^{\infty} m^{-1} \sin m\pi (b_{M+1} + \cdots + b_{N-1}) / c_M$$

$$+ \pi Q_M \bar{g}^{M+1,R} = K_o^M$$

(4.8)

Similarly, the asymptotic form of (4.4) is

$$\sum_{m=1}^{N^{N-1,R}} g_m^{N-1,R} + \bar{g}^{N-1,R} \sum_{m=1+N^{N-1,R}}^{\infty} m^{-1} \sin m\pi b_{N-1} / c_{N-2}$$

$$+ \frac{\pi}{c_{N-2}} P_{N-1} \bar{g}_1^{N-2,L} = K_o^{N-1}$$

(4.9)

and P_{N-1} was given in conjunction with (3.10).

The conventional choice of the truncation as mentioned for the trifurcated waveguide is apparently not possible in the case of the N-furcated waveguide because of the asymptotic degeneracy of (2.14). Any choice other than the asymptotic choice for the extra equations associated with (2.14) will apparently lead to numerical instabilities. Hence, we will use a hybrid choice. That is, we will use the asymptotic equations for the extra equations associated with (4.2), that is, eq. 11, and we will use the equations obtained by using the next index for (4.1), (4.3) and (4.4). In the case of N=3, we will have the conventional truncation scheme. However, for N greater than 3 we will have a true hybrid choice.

Of course, one other truncation is also possible -- direct truncation. As in the case of the trifurcated waveguide, this solution will not explicitly satisfy all of the edge conditions. However, for many applications the solution may be adequate and even better than many other more conventional methods of solution.

5.   Dielectric Loading

The dielectrically loaded N-furcated waveguide is shown in Figure 4.5.1. The modification of the N-furcated solution to account for the dielectric is similar to the modification of the trifurcated waveguide given in Chapter 3. Only the results will be givin. $T_1(\omega)$ becomes

$$T_1(\omega) = H_1(\omega) F_1(\omega) \left[K_o^1 - (\omega - jk_o) \left\{ \sum_{n=1}^{\infty} \frac{g_n^{1,R}}{\omega + \gamma_{n,a}} + \sum_{n=1}^{\infty} \frac{g_n^{1,L}}{\omega - \gamma_{n,c_1}} \right\} \right]$$
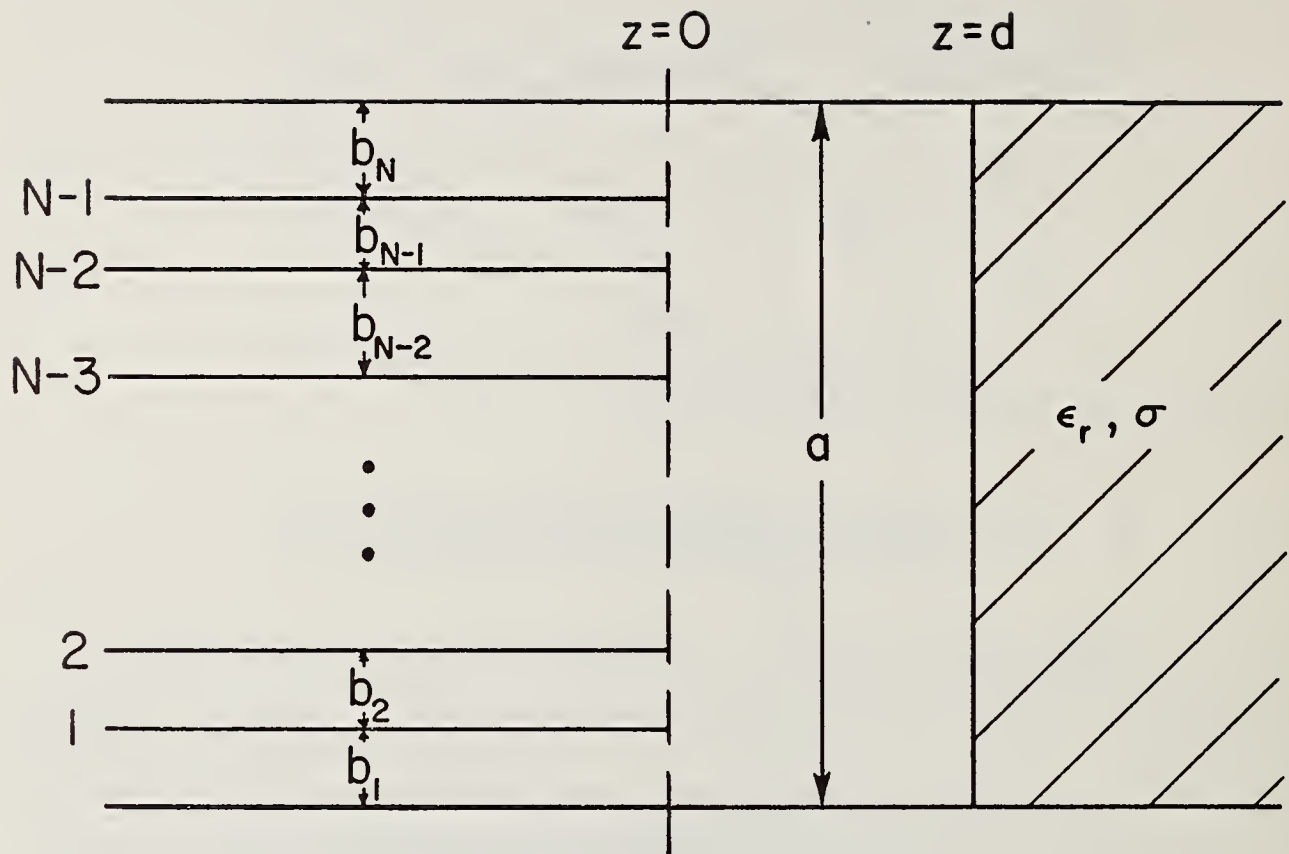
(5.1)

45

Fig. 4.5.1: Dielectrically Loaded N-Furcated
Waveguide.

Again $g_n^{1,R}$ is asymptotically given by

$$g_n^{1,R} = 0(n^{-1} e^{-2\pi nd/a})$$ (5.2)

Using the truncated form of (5.1), (4.1) is modified to be

$$-\sum_{m=1}^{N^{1,R}} \frac{g_m^{1,R}}{\gamma_{m,a}-\gamma_{n,c_1}} - \overline{g}^{1,R} \sum_{m=1+N^{1,R}}^{\infty} \frac{m^{-1} e^{-2m\pi d/a}}{\gamma_{m,a}-\gamma_{n,c_1}}$$

$$+\sum_{m=1}^{N^{1,L}} \frac{g_m^{1,L}}{\gamma_{m,c_1}+\gamma_{n,c_1}} + \overline{g}_1^{1,L} \sum_{m=1+N^{1,L}}^{\infty} \frac{m^{-1} \sin m\pi b_2/c_1}{\gamma_{m,c_1}+\gamma_{n,c_1}}$$

$$+\cdots+ \overline{g}_{N-2}^{1,L} \sum_{m=1+N^{1,L}}^{\infty} \frac{m^{-1} \sin m\pi(b_2+b_3+\cdots+b_{N-1})/c_1}{\gamma_{m,c_1}+\gamma_{n,c_1}}$$

$$+ (\lambda_n^{1,R})^{-1} \gamma_{n,c_1} c_1 g_n^{2,R} = K_o^1/(\gamma_{n,c_1}+jk_o) \quad n = 1,2,\cdots,N^{2,R}$$ (5.3)

Due to the introduction of $g_n^{1,R}$, the following equations must be included in the solution

$$\sum_{m=1}^{N^{1,R}} \frac{g_m^{1,R}}{\gamma_{m,a}+\gamma_{n,a}} + \overline{g}^{1,R} \sum_{m=1+N^{1,R}}^{\infty} \frac{m^{-1} e^{-2m\pi d/a}}{\gamma_{m,a}+\gamma_{n,a}}$$

$$+ \lambda_n^a g_n^{1,R} - \sum_{m=1}^{N^{1,L}} \frac{g_m^{1,L}}{\gamma_{m,c_1}-\gamma_{n,a}} - \overline{g}_1^{1,L} \sum_{m=1+N^{1,L}}^{\infty} \frac{m^{-1} \sin m\pi b_2/c_1}{\gamma_{m,c_1}-\gamma_{n,a}}$$

$$-\cdots- \overline{g}_{N-2}^{1,L} \sum_{m=1+N^{1,L}}^{\infty} \frac{m^{-1} \sin m\pi(b_2+\cdots+b_{N-1})/c_1}{\gamma_{m,c_1}-\gamma_{n,a}} = \frac{K_o^1}{(\gamma_{n,a}-jk_o)}$$

$$n = 1,2,\cdots,N^{1,R}$$ (5.4)

where

$$\lambda_n^a = \frac{R_n^{-1} F_1(-\gamma_{n,a}) H_1(-\gamma_{n,a})}{RES[F_1,\gamma_{n,a}] H_1(\gamma_{n,a})} \frac{(\gamma_{n,a}+jk_o)}{(\gamma_{n,a}-jk_o)}$$ (5.5)

It should be noted that the infinite sum involving the asymptotic form of $g_n^{1,R}$ makes an insignificant contribution and could be omitted.

For the dielectrically loaded N-furcated waveguide we are only considering the case of the hybrid choice of the truncation.

6. The Scattered Fields

The previous sections have dealt with the formulation and solution of the MRCT equations for the perturbation coefficients. Upon finding the perturbation coefficients, we are able to evaluate the constructed meromorphic functions at the appropriate points in the complex plane and determine the scattered fields. This is done with the aid of the auxiliary geometry.

Using the properties of section 2, Chapter 2, we find the following TEM modal coefficients of the scattered fields for the N-furcated waveguide.

$$B_{o,1} = \frac{-T_1(-jk_o)}{2jk_o b_1} \tag{6.1}$$

$$B_{o,M} = \frac{-T_m(-jk_o)}{2jk_o b_M} + \sum_{n=1}^{M-1} \frac{T_n(-jk_o)}{2jk_o c_n} \qquad M = 2, \cdots, N-1 \tag{6.2}$$

and

$$B_{o,N} = \frac{T_{N-1}(-jk_o)}{2jk_o c_{N-1}} + \sum_{n=1}^{N-2} \frac{T_n(-jk_o)}{2jk_o c_n} \tag{6.3}$$

When only a single waveguide is excited with an amplitude of unity, (6.1)-(6.3) represent either (current) reflection coefficients or (current) coupling coefficients. The reader is reminded that for TEM incidence from the largest waveguide the TEM solution is immediate.

For the purpose of this monograph, only the TEM modal coefficients are desired. Other higher order modal coefficients can be calculated using the auxiliary geometry and the properties of section 2, Chapter 2.

For the case of the dielectrically loaded N-furcated waveguide, the results are essentially the same as those given above, except we must add in the TEM reflected field from the dielectric. This yields

$$B_{o,1} = \frac{-T_1(-jk_o)}{2jk_o b_1} + U_o^o R_o \tag{6.4}$$

$$B_{o,M} = \frac{-T_M(-jk_o)}{2jk_o b_M} + \sum_{n=1}^{M-1} \frac{T_n(-jk_o)}{2jk_o c_n} + U_o^o R_o; \quad M = 2, \cdots, N-1 \tag{6.5}$$

$$B_{o,N} = \frac{T_{N-1}(-jk_o)}{2jk_o c_{N-1}} + \sum_{n=1}^{N-2} \frac{T_n(-jk_o)}{2jk_o c_n} + U_o^o R_o \tag{6.6}$$

where U_o^o is given by (2.9).

7. Numerical Results

7.1 Introduction

This section presents the numerical solution of the N-furcated waveguide as well as the dielectrically loaded N-furcated waveguide.

7.2 The N-Furcated Waveguide

Since there is no existing data for an N-furcated waveguide, the following steps were indicative of the validity of the results: (1) The results agreed with the trifurcated waveguide for N = 3. (2) Reversing the order of b_1, b_2, $\cdots$, b_N, yielded the same results. (3) The bifurcated waveguide with a magnetic wall was solved similar to the solution given in section 2, Chapter 2. This solution is given in Appendix E. This canonical solution was used to solve a trifurcated waveguide with a magnetic wall (ref. Appendix F). This solution was then combined with the solution given in Chapter 3 to yield results for a symmetric N-furcated waveguide with N = 5. These results were then in agreement giving a simultaneous check of the magnetic wall trifurcated waveguide program and the N-furcated waveguide program. (4) By feeding more than one waveguide simultaneously, we can simulate a trifurcated waveguide with a magnetic or electric wall. These results also agreed.

Table 4.7.2.1 illustrates the convergence for a case with N=5. In this example a convenient choice of the number of perturbation coefficients was $N^{R,M} \equiv N^{L,M} \equiv N_p$.

Table 4.7.2.1 Convergence Results for the N-furcated Waveguide
(Hybrid Truncation)

N_p	$B_{o,2}^*$		$B_{o,4}^*$		$T_{2-4}^\dagger$		$T_{4-2}^\dagger$	
3	0.830	155°	0.832	155°	0.101	−5°	0.111	7°
4	0.838	155°	0.832	155°	0.099	−5°	0.105	−5°
5	0.842	155°	0.835	155°	0.098	−4°	0.098	−10°
6	0.842	155°	0.836	155°	0.097	−4°	0.098	−10°
7	0.840	155°	0.835	155°	0.098	−4°	0.102	−5°
8	0.838	155°	0.834	155°	0.098	−4°	0.103	−2°
9	0.836	155°	0.834	155°	0.099	−5°	0.100	−4°
10	0.834	155°	0.835	155°	0.099	−5°	0.098	−5°

$^*k_o b_1 = k_o b_5 = 1.27046$, $k_o b_2 = k_o b_4 = 0.41417$, $k_o b_3 = 0.40066$.

$^\dagger T_{2-4} = B_{o,4}$ with $B_{o,2}^{(o)} = 1$, $T_{4-2} = B_{o,2}$ with $B_{o,4}^{(o)} = 1$.

By the symmetry of the geometry $B_{o,2} = B_{o,4}$ and $T_{2-4} = T_{4-2}$. However, because of the larger coupling region associated with the second plate, the calculations are more accurate for the fourth plate and hence $B_{o,4}$ and T_{2-4} are more accurate. This difference is more evident from an examination of the coupling coefficients. For inaccuracies less than a percent, convergence is essentially achieved for N_p greater than 5. In order to calculate all of the TEM scattering parameters to the same accuracy, one can choose the number of the perturbation coefficients to have a gradient, with the larger coupling region having more coefficients. As an example for $N^{1,L} = N^{2,R} = 10$, $N^{2,L} = N^{3,R} = 6$, and $N^{3,L} = N^{4,R} = 3$, we calculate the following results for the example given in Table 4.7.2.1.

$$B_{o,2} = 0.833 \quad 155°, \quad B_{o,4} = 0.835 \quad 155°, \quad T_{2-4} = 0.099 \quad -5°$$

$$T_{4-2} = 0.099 \quad -5°$$

The symmetry is obvious.

The above data is for the hybrid truncation method. Table 4.7.2.2 illustrates this same data for the asymptotic choice of the truncation.

Table 4.7.2.2 Convergence Results for the N-furcated Waveguide
(Asymptotic Truncation)

N_p	$B^*_{o,2}$		$B^*_{o,4}$		$T^\dagger_{2-4}$		$T^\dagger_{4-2}$	
3	0.838	154°	0.831	155°	0.094	3°	0.113	8°
4	0.835	155°	0.830	155°	0.093	6°	0.105	0°
5	0.834	156°	0.835	155°	0.100	-4°	0.098	-11°
6	0.834	156°	0.835	155°	0.102	-7°	0.098	-11°
7	0.834	156°	0.834	155°	0.098	-3°	0.101	-5°
8	0.834	155°	0.833	155°	0.097	-1°	0.102	-3°
9	0.835	155°	0.834	155°	0.098	-4°	0.100	-4°
10	0.835	155°	0.835	155°	0.100	-6°	0.098	-5°

$^*k_ob_1 = k_ob_5 = 1.27046, \ k_ob_2 = k_ob_4 = 0.41417, \ k_ob_3 = 0.40066.$

$^\dagger T_{2-4} = B_{o,4}$ with $B^{(o)}_{o,2} = 1, \ T_{4-2} = B_{o,2}$ with $B^{(o)}_{o,4} = 1.$

A comparison of the coupling coefficients with those of Table 4.7.2.1 clearly shows that the hybrid choice is again superior.

As a final comparison, let us compute this same data using direct truncation. This is shown in Table 4.7.2.3.

Table 4.7.2.3 Convergence Results for the N-Furcated Waveguide
(Direct Truncation)

N_p	$B^*_{o,2}$		$B^*_{o,4}$		$T^\dagger_{2-4}$		$T^\dagger_{4-2}$	
3	0.836	154°	0.832	156°	0.111	9°	0.111	9°
4	0.832	155°	0.827	156°	0.102	0°	0.102	0°
5	0.832	156°	0.831	155°	0.097	-11°	0.097	-11°
6	0.832	156°	0.834	155°	0.096	-11°	0.096	-11°
7	0.833	156°	0.835	155°	0.099	-5°	0.099	-5°
8	0.834	155°	0.834	155°	0.101	-2°	0.101	-2°
9	0.836	155°	0.835	155°	0.100	-3°	0.100	-3°
10	0.836	155°	0.835	155°	0.099	-5°	0.099	-5°
11	0.835	155°	0.835	155°	0.100	-4°	0.100	-4°

$^*k_ob_1 = k_ob_5 = 1.27046, \ k_ob_2 = k_ob_4 = 0.41417, \ k_ob_3 = 0.40066.$

$^\dagger T_{2-4} = B_{o,4}$ with $B^{(o)}_{o,2} = 1, \ T_{4-2} = B_{o,2}$ with $B^{(o)}_{o,4} = 1.$

It is interesting to note the symmetry of the coupling coefficients in the above table. This is apparently due to the symmetry of the equations. A comparison of the direct

truncation method with the asymptotic method of truncation shows that the convergence of the data computed from the larger coupling region function is about the same. However, a comparison of the data computed from the smaller coupling region shows that we can apparently order the methods of truncation (with the best method first) as follows: (1) hybrid, (2) asymptotic, and (3) direct. This is the same conclusion arrived at for the trifurcated waveguide.

It should be noted that the above example is the same as the first trifurcated example treated in Chapter 3, except the waveguide has been folded about a symmetry plane. This allows us to ascertain the accuracy of the N-furcated results by exciting the waveguides in a symmetrical manner so as to simulate an electric symmetry wall and hence a trifurcated waveguide. Exciting the 2nd and 4th waveguide with unit amplitude we find

$$B_{o,4} = 0.835 \exp(155°) + 0.099 \exp(-5°)$$

$$B_{o,4} = 0.743 \exp(152°)$$

This is compared with the value of $0.742 \exp(152°)$ given in Chapter 3, which is very good indeed.

Similarly, exciting the 1st and 5th waveguides with unit amplitude we find

$$B_{o,5} = 0.168 \exp(92°) + 0.223 \exp(161°)$$

$$B_{o,5} = 0.324 \exp(132°)$$

This is compared with the value $0.324 \exp(132°)$ given in Chapter 3. Hence, three place accuracy is clearly obtained.

7.3 The Dielectrically Loaded N-Furcated Waveguide

Since no existing data is available for the dielectrically loaded N-furcated waveguide, checks similar to those described for the N-furcated waveguide were performed.

Table 4.7.3.1 illustrates the change of the data of Table 4.7.2.1 with the inclusion of dielectric loading with the parameters: $k_o d = 1.256$, $\varepsilon_r = 10$, $\sigma/k_o = 0.01$.

Table 4.7.3.1 Convergence Results for the Dielectrically Loaded N-Furcated Waveguide (Hybrid Truncation)

N_p	$B_{o,2}^*$		$B_{o,4}^*$		T_{2-4}^+		T_{4-2}^+	
1	0.815	153°	0.875	158°	0.098	-23°	0.061	-122°
2	0.839	156°	0.870	159°	0.066	-28°	0.043	-19°
3	0.857	158°	0.860	158°	0.061	-27°	0.064	-4°
4	0.866	159°	0.859	158°	0.059	-27°	0.062	-18°
5	0.870	159°	0.863	158°	0.057	-27°	0.062	-36°
6	0.870	159°	0.864	158°	0.057	-27°	0.062	-36°
7†	0.868	159°	0.863	158°	0.057	-27°	0.061	-26°
8†	0.866	159°	0.862	158°	0.058	-27°	0.061	-22°
9†	0.864	158°	0.862	158°	0.059	-27°	0.059	-26°
10†	0.862	158°	0.863	158°	0.059	-27°	0.058	-29°

$^*k_o b_1 = k_o b_5 = 1.27046$, $k_o b_2 = k_o b_4 = 0.41417$, $k_o b_3 = 0.40066$.
$N^{1,R} = 6$.

$^+T_{2-4} = B_{o,4}$ with $B_{o,2}^{(o)} = 1$, $T_{4-2} = B_{o,2}$ with $B_{o,4}^{(o)} = 1$.

As with the unloaded N-furcated waveguide, the results for the smaller coupling region again exhibit better convergence. In order to ascertain the accuracy of the results, we can again simulate an electric symmetry wall at $x = a/2$ by exciting the waveguides appropriately. Exciting the 2nd and 4th waveguides with unit amplitude we have

$$B_{o,4} = 0.863 \exp(158°) + 0.059 \exp(-27°)$$

$$= 0.804 \exp(159°)$$

This compares with the value $0.804 \exp(159°)$ obtained in Chapter 3.

Similarly, exciting the 1st and 5th waveguides with unit amplitude we have

$$B_{o,5} = 0.149 \exp(-158°) + 0.404 \exp(162°)$$

$$= 0.527 \exp(173°)$$

This compares to the value $0.528 \exp(173°)$ obtained in Chapter 3. Thus three place accuracy is again obtained.

1. Introduction

This chapter considers the application of the MRCT to four additional problems in order to illustrate the ease of applying the method to various kinds of problems. For example, the problem of finding the eigenvalues of a single ridged waveguide is outlined.

Another problem discussed is the scattering by a dielectric step. This problem has been solved by Royer and Mittra (1972). However, it is believed the solution outlined would be easier to derive than Royer's.

Another problem considered is the variation of the reflection coefficient of a rectangular waveguide with a change in the permittivity and conductivity of the dielectric loading. Numerical results are given.

2. TE Eigenvalues of Ridged Waveguide

Figure 5.2.1 illustrates a cross sectional view of a single ridged waveguide as well as the associated auxiliary problem. (The dimensions have been changed from those of Chapter 2 in order to conform with standard notation used with ridged waveguide.) The basic difference of this problem in comparison with the problems solved previously is that there are no sources. The problem is homogeneous.

Montgomery (1971) illustrates how the transverse resonance argument is applied to the ridged waveguide eigenvalue problem. In order to find the dominant TE_{10} mode eigenvalue, we must make the boundary condition at the symmetry wall of the magnetic type. In this formulation, we must then make the reflection coefficient at the first dielectric -1. This implies $\mu_1 \to \infty$. For the boundaries at $x = a/2$ and $x = s/2$ to be electric conductors the reflection coefficients must be $+1$ in the limit for the auxiliary problem solution to approach the desired solutions.

The solution essentially proceeds as that of the E-plane step given in Chapter 2, except that $T(\omega)$ must have two additional terms. From Chapter 2, we have

$$T(\omega) = H(\omega)F(\omega)\left[K_o - (\omega-jk_o)\left\{\sum_{n=1}^{\infty}\frac{g_n^{c}}{\omega-\gamma_{nc}} + \sum_{n=1}^{\infty}\frac{g_n^{b}}{\omega+\gamma_{nb}} + \sum_{n=1}^{\infty}\frac{g_n^{d}}{\omega-\gamma_{nd}}\right\}\right] \qquad (2.1)$$

From Chapter 2, section 3, we can easily find that for a right-angle corner,

$$g_n^{c} = 0(n^{-7/6})$$

in the limit as $\varepsilon_2 \to \infty$. Since g_n^{b} and g_n^{d} decay exponentially we can truncate these series without any loss of generality. Hence we can write

$$T(\omega) \simeq H(\omega)F(\omega)\left[K_o - (\omega-jk_o)\left\{\sum_{n=1}^{N_c}\frac{g_n^{c}}{\omega-\gamma_{nc}}\right.\right.$$

$$\left.\left. + \bar{g}^{c}\sum_{n=1+N_c}^{\infty}\frac{n^{-7/6}}{\omega-\gamma_{nc}} + \sum_{n=1}^{N_b}\frac{g_n^{b}}{\omega+\gamma_{nb}} + \sum_{n=1}^{N_d}\frac{g_n^{d}}{\omega-\gamma_{nd}}\right\}\right] \qquad (2.2)$$
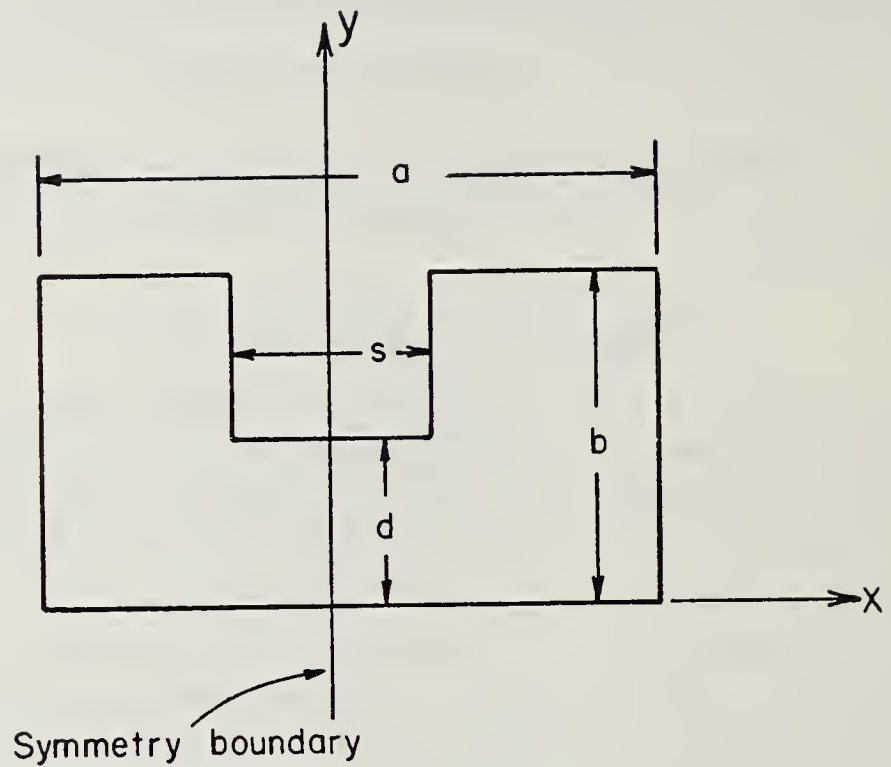
(a)   Ridged Waveguide Geometry
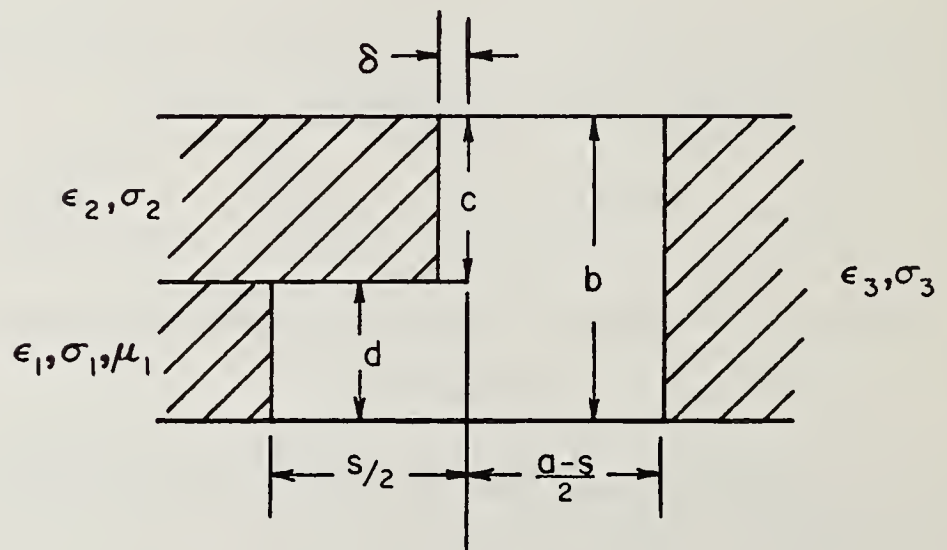
(b)   Auxiliary Problem

Fig. 5.2.1:   Ridged Waveguide

Again from Chapter 2, section 3 we find that

$$K_o - \sum_{n=1}^{N_c} g_n^c - \bar{g}^c \sum_{n=1+N_c}^{\infty} n^{-7/6} - \sum_{n=1}^{N_b} g_n^b - \sum_{n=1}^{N_d} g_n^d = 0. \qquad (2.3)$$

In order to arrive at the additional equations, we require that the modal coefficients be consistent in the various region. From properties (i) and (ii) in section 2 Chapter 2, we have the following equations,

$$\text{RES}[T, -\gamma_{nb}] = -B_n^{(o)} \frac{n\pi}{b} \sin \frac{n\pi d}{b} \, e^{\gamma_{nb} s/2} \qquad (2.4a)$$

$$\text{RES}[T, \gamma_{nb}] = -B_n \frac{n\pi}{b} \sin \frac{n\pi d}{b} \, e^{-\gamma_{nb} s/2} \qquad (2.4b)$$

where $n = 1, 2, 3, \cdots N_b$, and where $B_n^{(o)}$ is the coefficient of the nth mode incident on the junction from the region with dimension, b. B_n is similarly the nth modal coefficient away from the junction in the region with dimension, b. But from the boundary condition at $x = \frac{a-s}{2}$ we must have

$$\frac{B_n^{(o)}}{B_n} = e^{-(a-s)\gamma_{nb}} \qquad (2.5)$$

Combining (2.4) and (2.5) we have that

$$\text{RES}[T, -\gamma_{nb}] = e^{-(a-2s)\gamma_{nb}} \, \text{RES}[T, \gamma_{nb}] \qquad (2.6)$$

Similarly for the region with dimension, d, we have

$$T(\gamma_{nd}) = (-1)^n \gamma_{nd} \, d \, D_n^{(o)} \, e^{-\gamma_{nd} \, s/2} \qquad (2.7a)$$

$$T(-\gamma_{nd}) = (-1)^{n+1} \gamma_{nd} \, d \, D_n \, e^{\gamma_{nd} \, s/2} \qquad (2.7b)$$

where $n = 1, 2, \cdots, N_d$. But from the magnetic symmetry condition at $x = o$ we have that

$$\frac{D_n^{(o)}}{D_n} = -e^{-s\gamma_{nd}} \qquad (2.8)$$

Hence, combining (2.7) and (2.8) we have that

$$T(\gamma_{nd}) = e^{-2s\gamma_{nd}} \, T(-\gamma_{nd}) \qquad (2.9)$$

Equations (2.6) and (2.9) express the interaction of the higher order modes with the boundaries at $x = a/2$ and $s/2$.

Similarly, we can easily find

$$T(\gamma_{nc}) = -C_n^{(o)} \gamma_{nc} \ C \ e^{-\gamma_{nc} \ s/2} \tag{2.10a}$$

$$T(-\gamma_{nc}) = C_n \ \gamma_{nc} \ C \ e^{\gamma_{nc} \ s/2} \tag{2.10b}$$

but from the boundary condition at the conductor we have

$$C_n = C_n^{(o)} \tag{2.11}$$

Hence,

$$T(\gamma_{nc}) = -T(-\gamma_{nc}) \ e^{-\gamma_{nc} \ s} \tag{2.12}$$

One should note that this equation has the most pronounced effect on the solution since this equation accounts for the change in the edge condition. Equations (2.6) and (2.9) account for higher order mode interaction with the edge conductor and the ridge symmetry plane. But since these modes decay exponentially, the effect is not generally great. This can also be seen from (2.6) and (2.9). As $n \to \infty$, we have that g_n^d, $g_n^b \to 0$, exponentially. However these coefficients do become important in the calculation of higher order mode eigenvalues.

For the first few eigenvalues, generally all the higher order modes are cut off except for the TEM to x mode. Hence, let us concentrate on the TEM equations.

From Chapter 2, we have

$$B_o = \frac{c}{b} C_o^{(o)} + \frac{d}{b} D_o^{(o)} \tag{2.13a}$$

$$T(jk_o) = 2jk_o c \ (B_o - C_o^{(o)}) \tag{2.13b}$$

$$T(-jk_o) = 2jk_o c \ (C_o - B_o^{(o)}) \tag{2.13c}$$

$$T(-jk_o) = -2jk_o d \ (D_o - B_o^{(o)}) \tag{2.13d}$$

From these equations, we can arrive at the following equations

$$B_o = 0 + \frac{d}{b} D_o^{(o)} + \frac{c}{b} C_o^{(o)} \tag{2.14a}$$

$$D_o = B_o^{(o)} - \frac{c}{b} \frac{T(-jk_o)}{T(jk_o)} \ D_o^{(o)} + \frac{c}{b} \frac{T(-jk_o)}{T(jk_o)} \ C_o^{(o)} \tag{2.14b}$$

$$C_o = B_o^{(o)} + \frac{d}{b} \frac{T(-jk_o)}{T(jk_o)} \ D_o^{(o)} - \frac{d}{b} \frac{T(-jk_o)}{T(jk_o)} \ C_o^{(o)} \tag{2.14c}$$

These equations can also be written in matrix form

$$
\begin{pmatrix} B_o \\ D_o \\ C_o \end{pmatrix} = [Q] \begin{pmatrix} B_o^{(o)} \\ D_o^{(o)} \\ C_o^{(o)} \end{pmatrix}
\tag{2.15}
$$

However, from the boundary conditions we have

$$
\begin{pmatrix} B_o^{(o)} \\ D_o^{(o)} \\ C_o^{(o)} \end{pmatrix} = \begin{pmatrix} e^{-jk_o(a-s)} & 0 & 0 \\ 0 & -e^{-jk_o s} & 0 \\ 0 & 0 & 1 \end{pmatrix} \begin{pmatrix} B_o \\ D_o \\ C_o \end{pmatrix}
$$

$$
\begin{pmatrix} B_o^{(o)} \\ D_o^{(o)} \\ C_o^{(o)} \end{pmatrix} = [W] \begin{pmatrix} B_o \\ D_o \\ C_o \end{pmatrix}
\tag{2.16}
$$

Thus using (2.16) in (2.15)

$$
\left\{ [I] - [Q][W] \right\} \begin{pmatrix} B_o \\ D_o \\ C_o \end{pmatrix} = [0]
\tag{2.17}
$$

where $[I]$ is the unit diagonal matrix. For a solution to exist, we must have

$$
\det = \{[I] - [Q][W]\} = 0.
\tag{2.18}
$$

In essence, this is the equation for k_o. The complete solution to the problem is then found from equations (2.18), (2.12), (2.9) and (2.6). Note that all of these equations are homogenous. Hence, a solution exists only if the determinant of the associated matrix of coefficients is zero. The eigenvalues are found by finding the values of k_o for which this is true. The associated eigenvectors (arbitrarily normalized) are found by recourse to (2.4), (2.7), (2.10) and (2.14).

This section has thus outlined the solution of an eigenvalue problem using the MRCT. This solution should prove to be beneficial when accurate higher order eigenvalues are desired. Additionally, the dominant eigenvalues can be found from the zeroes of the determinant of a small matrix because of the efficient truncation due to the use of the asymptotics of the unknowns.

3.   Scattering by a Dielectric Step

Royer and Mittra (1972) have considered the solution of the scattering by a dielectric step using the MRCT. A MRCT solution was used because of interest in high permittivity dielectric materials. However, the method of obtaining the equations does not appear to be straight forward. It is the purpose of this section to outline how the extension of the MRCT can be applied to obtain the equation in a straight forward manner.

Figure 5.3.1 illustrates the dielectric step and the associated auxiliary problem. Note that the auxiliary problem is different from that of Royer and Mittra (1972).

With reference to the auxiliary geometry, we see that we have three distinct junctions. The first at $z = -\Delta_1$, is just a bifurcated waveguide. The second is the junction at $z = 0$, which is just a junction between air and a dielectric filling the waveguide. The third is the junction at $z = \Delta_2$. This junction is just a bifurcated waveguide with slab loading. This junction can be solved in a manner similar to the way the normal bifurcated waveguide was solved in Chapter 2. The main difference is that the modal propagation constants in the partial slab loaded guide must be found numerically, whereas they are known in closed form with no dielectric loading. Hence the solution is obtained by construction two holomorphic functions. Each function will be of a doubly modified form. The four infinite sets of equations are found from the consistency of modal coefficients in the regions $0 \leq x \leq b$ and $b \leq x \leq a$ where $-\Delta_1 \leq z \leq \Delta_2$. The asymptotic behavior of the perturbation coefficients must be such that when Δ_1, $\Delta_2 \to 0$ that the edge condition at the dielectric is satisfied. Royer and Mittra solved the case of TE incidence and thus the edge condition is

$$
\left.
\begin{aligned}
E_y &= 0(\rho^{\Delta}) \\[4pt]
H_x &= 0(\rho^{\Delta-1}) \\[4pt]
H_z &= 0(\rho^{\Delta-1})
\end{aligned}
\right\} \quad \rho \to 0
$$

where

$$
\Delta = \frac{2}{\pi} \cos^{-1}\left(\frac{1}{2} \left(\frac{\varepsilon - 1}{\varepsilon + 1} \right) \right)
$$

where ρ is the radial distance from the dielectric edge.

4.   Dielectric Loaded N-Furcated Waveguide

This section serves as a forum to present some numerical data for the problem already considered in Chapter 4, section 5. In particular, we consider the case of $N = 5$, the junction being symmetrical about the center. This particular solution can be considered as an approximation of the coupling of two waveguides above a homogeneous earth. However, as shown in part 2 of this monograph this is not generally very accurate. If, however, a sample can be obtained and placed in a waveguide, this analysis applies provided one replaces the free space wavelength by the guide wavelength.

(a)   Dielectric Step Geometry

(b)   Auxiliary Geometry

Fig. 5.3.1:   The Dielectric Step
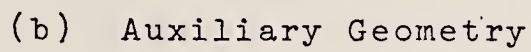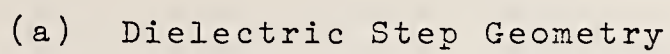
From this discussion, it is logical to compute argand diagrams for the reflection and transmission coefficients as a function of the earth's parameters. Figure 5.4.1 illustrates the change of the coupling coefficient, i.e., T_{2-4} in magnitude (dB) and phase versus the parameters ϵ_r and σ. Note that the data is normalized to the case of no dielectric (a subscript w indicates the dielectric is present, a subscript w/o indicates the dielectric is not present). The resolution for nominal measurement accuracies is quite acceptable. The resolution for nominal measurement accuracies is quite acceptable. The resolution is better for the lower permittivity and conductivity cases. However, since there is a larger range in the magnitude than phase, the vertical resolution will not be as great as the horizontal resolution of the figure. Note that the constant ϵ_r curves tend to be vertical lines for the lower conductivities and hence the main resolution is in ϵ_r. This can be somewhat remedied by considering the reflection coefficient argand diagram for figure 5.4.2. Notice that the range of the phase is about a third of that of figure 5.4.1. However, the range of the magnitude change is greater. These diagrams can be used simultaneously to obtain increased accuracy. One interesting combination of figures 5.4.1 and 5.4.2 is shown in figure 5.4.3. This argand diagram uses only the amplitude data of the transmission and reflection coefficients. No phase data is used. For nominal accuracies of the amplitudes the resolution is again acceptable and no phase data is required. However, use of phase data will in general allow increased resolution.

This data tends to indicate that remote sensing of the earth with waveguide horns is reasonable at frequencies where the horns are not excessively large.

The data presented has been for dimensions rather small compared to a wavelength. This is due to the limitation of the closed region analysis. A broader range of dimensions is more feasible for the associated open region problem. This is the subject of part 2 of this monograph.

CHAPTER 6.   CONCLUSIONS (PART I)

This part of the monograph has presented the MRCT solution of a new class of closed region problems. The approach has been to solve a canonical problem of a bifurcated waveguide with known incident fields. The solution of a composite problem is readily found from an associated auxiliary problem.

The particular class of problems solved are problems associated with the N-furcated waveguide junction. The convergence of the MRCT solutions is rapid requiring only a few perturbation terms for any particular meromorphic function constructed.

Data computed using the closed region analysis tends to indicate the usefulness of waveguide horns in remote sensing of the parameters of a homogeneous earth.

It should be noted that the approach used in this report is straight forward to apply to most problems which can be solved using the GSMT. The advantage of the MRCT is that the edge condition of a particular problem can be either underlined changed or edge conditions underlined added explicitly. This enhances the convergence of the solution over the GSMT.

Fig. 5.4.1:   Variation of the Coupling Coefficient
of Two Parallel Plate Waveguides with
the Earth's Parameters ($k_o b_1 = k_o b_5 = 1.0708$,
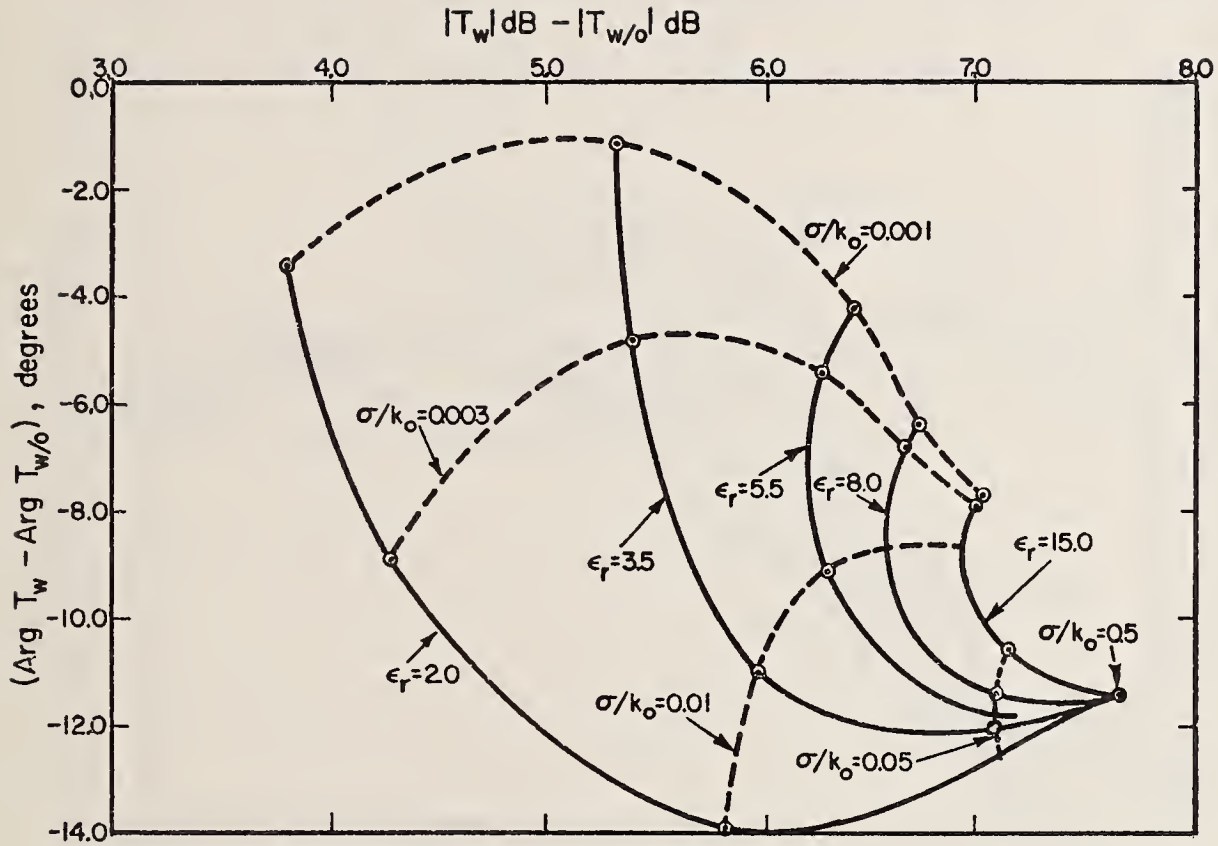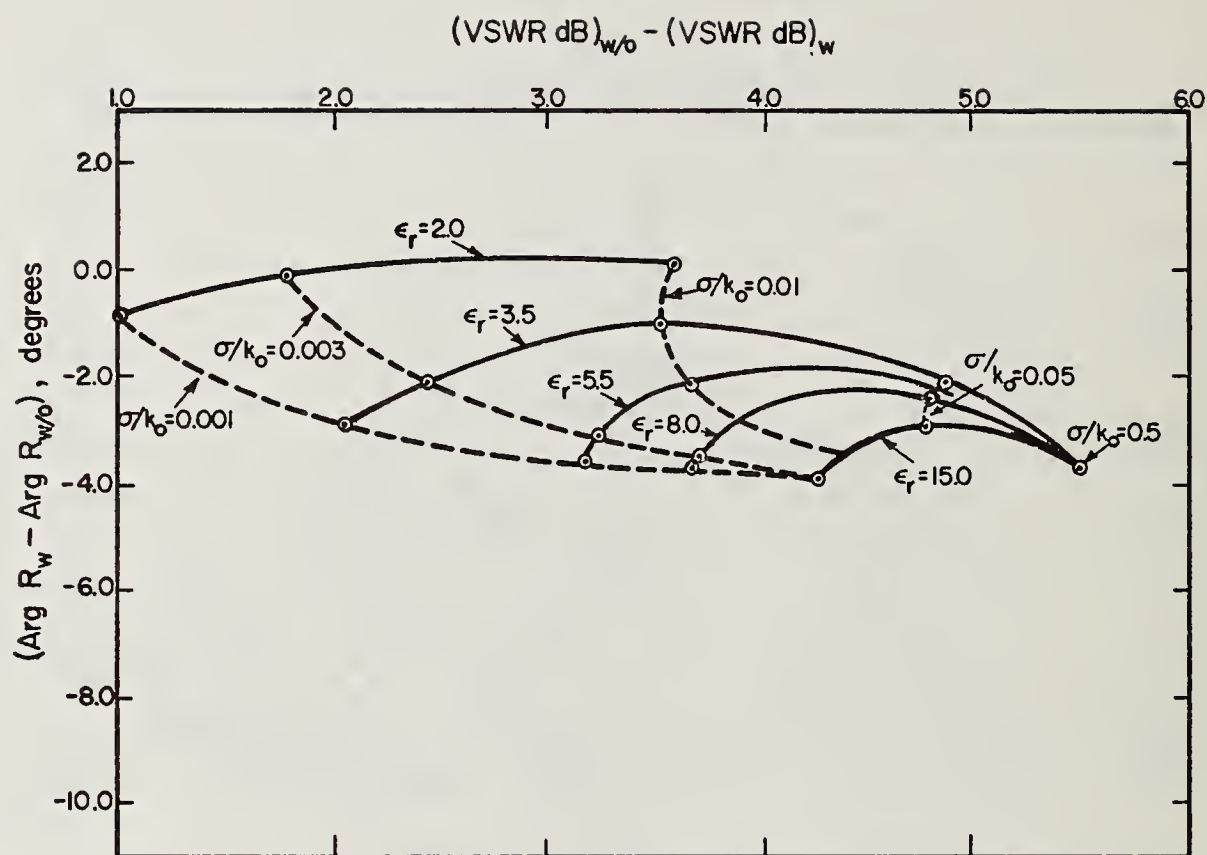$k_o b_2 = k_o b_4 = 0.4$, $k_o b_3 = 0.2$, $k_o d = 0.31416$).

Fig. 5.4.2: Variation of the Reflection Coefficient of Two Parallel Plate Waveguides with the Earth's Parameters ($k_o b_1 = k_o b_5 = 1.0708$, $k_o b_2 = k_o b_4 = 0.4$, $k_o b_3 = 0.2$, $k_o d = 0.31416$).
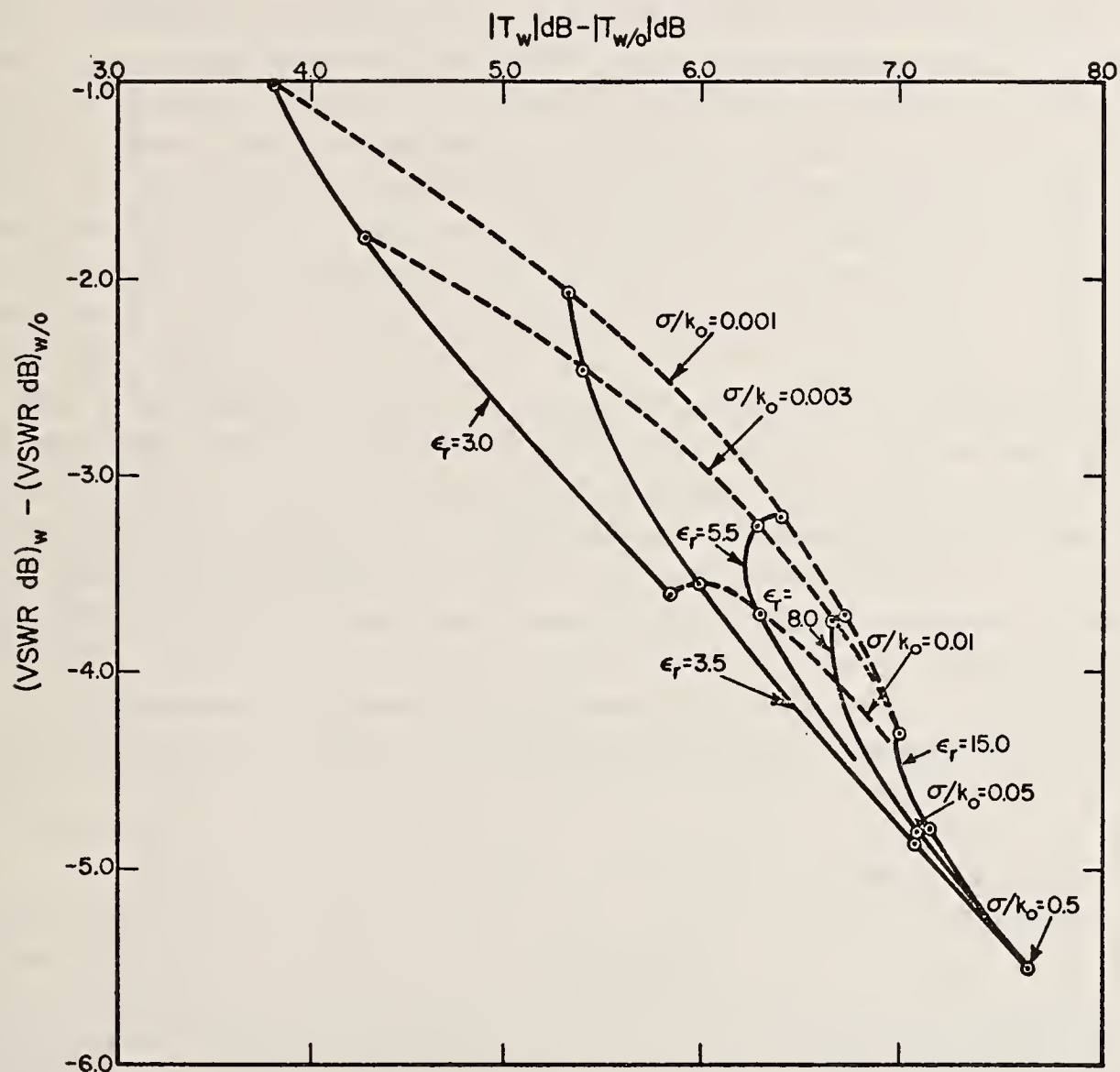
Fig. 5.4.3:   The Combined Argand Diagram $(k_o b_1 = k_o b_5 = 1.0708, \ k_o b_2 = k_o b_4 = 0.4, \ k_o b_3 = 0.2, \ k_o d = 0.31416)$.

PART II

SOLUTION OF OPEN REGION PROBLEMS

CHAPTER 7. INTRODUCTION

This part of the monograph is concerned with the analysis of open region waveguide problems. Up until now, we have confined our discussion to closed region problems. This allowed testing of the techniques expected to be employed on open region problems as well as solving some interesting closed region problems. The basic analysis was simpler since branch points were not encountered. In addition to strictly open region problems, we shall discuss composite problems containing both open and closed region parts.

Historically, semi-infinite waveguide problems like those to be discussed have been solved using the Wiener-Hopf technique or modifications of the Wiener-Hopf technique (Mittra and Lee, 1971). However, we have chosen to exploit the techniques developed in the first part and extend the MRCT to the open region case. Actually, one still has to solve the same equations; however, it is believed that the solution is more straightforward using the modified function theoretic technique (MFTT). The first use of this method was reported by Kostenicek and Mittra (1971). They solved the problem of radiation of a parallel-plate waveguide into a dielectric slab. It is interesting to note that in Kostelnicek's original technical report (Kostelnicek and Mittra, 1969) that the solution of this problem was obtained by limiting arguments applied to the associated closed region problem which was solved using the MRCT.

In what follows we shall complete the derivation of the technique suggested by Kostelnicek and Mittra (1971) and bring it full circle by uniting it with the MRCT. In this process, the open region analogue of the GSMT is in essence used. However, all edge conditions are satisfied explicitly in order to enhance the convergence of the solution over that which would normally be obtained.

The vehicle which allows one to solve a certain class of modified open region problems is the canonical problem of a semi-infinite parallel plate waveguide. An infinite number of known discrete modes are assumed to be incident from the interior of the waveguide, as well as assuming fields with known arbitrary spectra incident on the waveguide junction from the exterior. This solution (given in Chapter 8) is just the superposition of solutions which are given in many texts (for example: Mittra and Lee, 1971). However, the combined solution has never been given and is important in the solution of modified semi-infinite problems.

The problem of radiation from a flanged waveguide is given as a first example of the technique in Chapter 8. This particular problem was solved using the MFTT by Itoh and Mittra (1971). However, the techniques of this monograph allow a simpler derivation of the solution.

In Chapter 9, the MFTT is applied to the problem of radiation of a semi-infinite parallel plate waveguide into a homogeneous half space. This problem is in many respects similar to the problem solved by Kostelnicek and Mittra (1971); however, there are important differences. First, the problem of singularities is extensively studied and efficient numerical schemes to

solve the integral equation are derived. Kostelnicek used the most basic form of point matching and subsequently had to invert a much larger matrix than necessary. Secondly, the problem of radiation into a half space is interesting in itself because of the physical results. Thirdly, Kostelnicek used an incorrect form for his infinite products and hence apparently did not satisfy the edge condition (Montgomery, 1973).

The problem of a finite phased array is solved in Chapter 10. The importance of this solution is that it is not necessary to assume the array is flushed-mounted to an infinite ground plane in order to obtain a solution. Also it is interesting to note that the solution only involves the solution of simultaneous linear equations as opposed to an integral equation. This particular solution is extremely important to the array designer because it corresponds more closely to actual practice than the assumption of an infinite ground plane. It is also possible to·solve the problem of a finite array with a finite ground plane; however, the solution will not be given. Comparison with the results obtained by Lee (1967) for the case of a finite array with an infinite ground plane yields some interesting results.

Chapter 11 combines the results of Chapters 9 and 10 to give the solution of a finite array of waveguides radiating into a homogeneous half space (in this case considered to be a model of the earth's surface). Argand diagrams for the variation of the reflection coefficient and coupling coefficient of a two element array as a function of the earth's permittivity and conductivity are given.

Chapter 12 outlines the solution of several other open region problems. Among these problems is the radiation of a flanged waveguide into a half space. It is interesting to note that Kostelnicek and Mittra (1971) indicated that such a solution was <u>not</u> possible using the MFTT, indicating that a complete understanding of the method did not exist at that time.

CHAPTER 8. FOUNDATION OF THE MODIFIED FUNCTION THEORETIC TECHNIQUE

1. Introduction

It is the purpose of this chapter to show that the modified function theoretic techniques can be approached in a direct manner by considering the canonical problem of a semi-infinite parallel plate waveguide with an infinite number of waveguide modes incident from the exterior. The general solution is obtained from a non-homogeneous Hilbert problem and can be written in a manner similar to the perturbation expansion discussed in Chapter 1. In order to illustrate the method, the solution of a flanged parallel plate waveguide radiating into free space is given.

2. The Canonical Problem

2.1 Introduction

Because of their importance, we will consider two canonical problems: (1) a semi-infinite parallel plate waveguide with an electric symmetry boundary (ref. Figure 8.2.1),
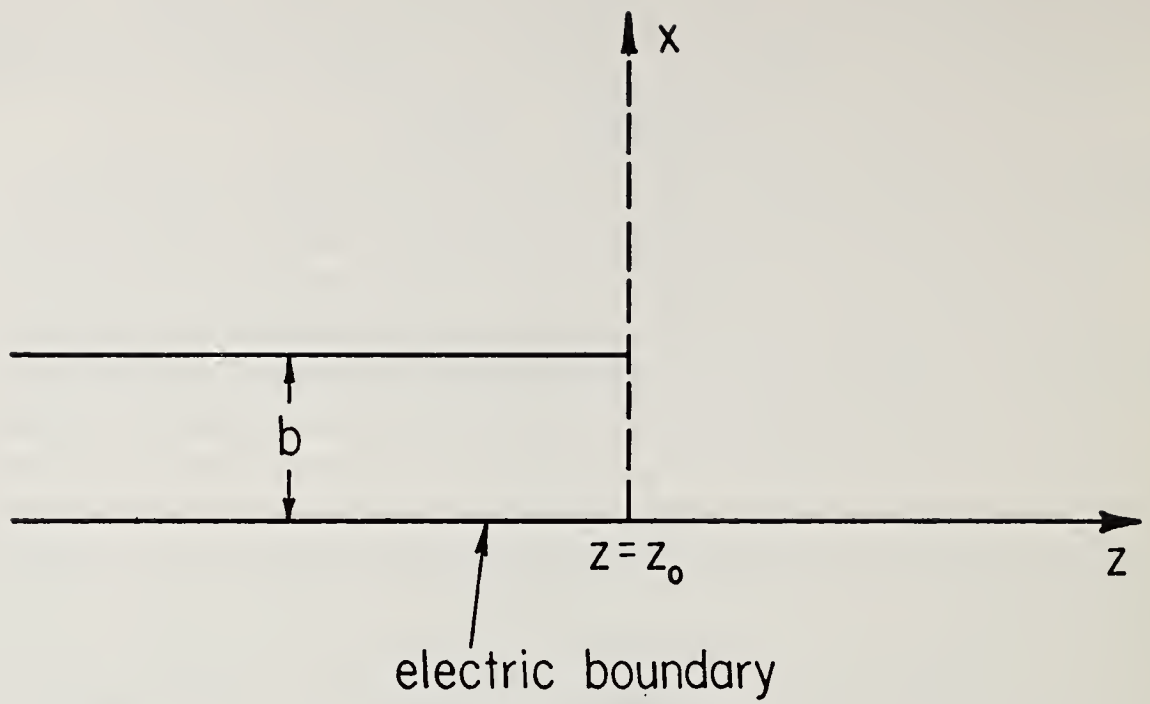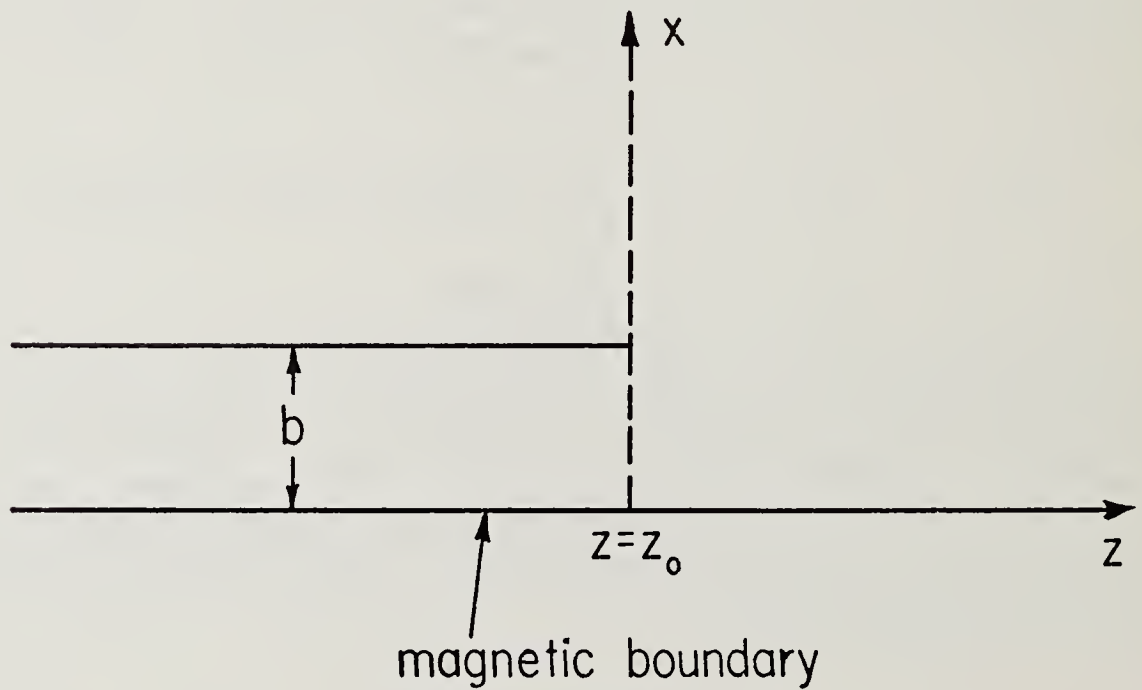
Fig. 8.2.1: Parallel Plate Waveguide

Fig. 8.2.2: Parallel Plate Waveguide

66

and (2) a semi-infinite parallel plate waveguide with a magnetic symmetry wall (ref. Figure 8.2.2). Both of these problems have been solved for the case of a single incident waveguide mode or plane wave incidence from the exterior. The solution to be given here represents a general superposition of these solutions. The form of the solution is of particular advantage when solving composite problems.

2.2 The Electric Wall Case

Let us consider the TM solution of the geometry shown in Figure 8.2.1. The TE solution follows in a similar manner and will not be given.

The TM fields are derivable from $\phi = H_y$ and the fields in each region are given by

$$\phi_B = \sum_{n=0}^{\infty} \left(B_n^{(o)} e^{-\gamma_{nb} z} + B_n e^{\gamma_{nb} z} \right) \cos \frac{n\pi x}{b} \qquad z \leq 0; \ 0 \leq x \leq b \qquad (2.2.1)$$

$$\phi_C = \int_0^{\infty} \left[C^o(\lambda) e^{-\gamma z} + C(\lambda) e^{\gamma z} \right] \cos \lambda(x-b) \, d\lambda \qquad z \leq z_o, \ x \geq b \qquad (2.2.2)$$

$$\phi_A = \int_0^{\infty} \left[A^o(\lambda) e^{\gamma z} + A(\lambda) e^{-\gamma z} \right] \cos \lambda x \, d\lambda \qquad z \geq z_o, \ x \geq 0 \qquad (2.2.3)$$

where the superscript (o) indicates an incident field and

$$\gamma_{nb} = \sqrt{(n\pi/b)^2 - k_o^2}$$

and

$$\gamma = \sqrt{\lambda^2 - k_o^2}$$

A time convention of $e^{j\omega t}$ has been assumed and suppressed.

The branch of γ is chosen as shown in Figure 8.2.3 so that $\text{Re}(\gamma) > 0$. The inverse function $\lambda = \sqrt{\gamma^2 + k_o^2}$ corresponding to the upper half of the λ-plane is defined as shown in Figure 8.2.4.

Matching the tangential fields at $z = z_o$ we can arrive at the equations

$$\int_0^{\infty} \left[A^o(\lambda) e^{\gamma z_o} + A(\lambda) e^{-\gamma z_o} \right] \cos \lambda x \, d\lambda = \qquad (2.2.4)$$

$$\begin{cases} \int_0^{\infty} \left[C^o(\lambda) e^{-\gamma z_o} + C(\lambda) e^{\gamma z_o} \right] \cos \lambda(x-b) \, d\lambda; \ x \geq b, \\[2em] \sum_{n=0}^{\infty} \left(B_n^{(o)} e^{-\gamma_{nb} z_o} + B_n e^{\gamma_{nb} z_o} \right) \cos \frac{n\pi x}{b}; \ 0 \leq x \leq b. \end{cases}$$
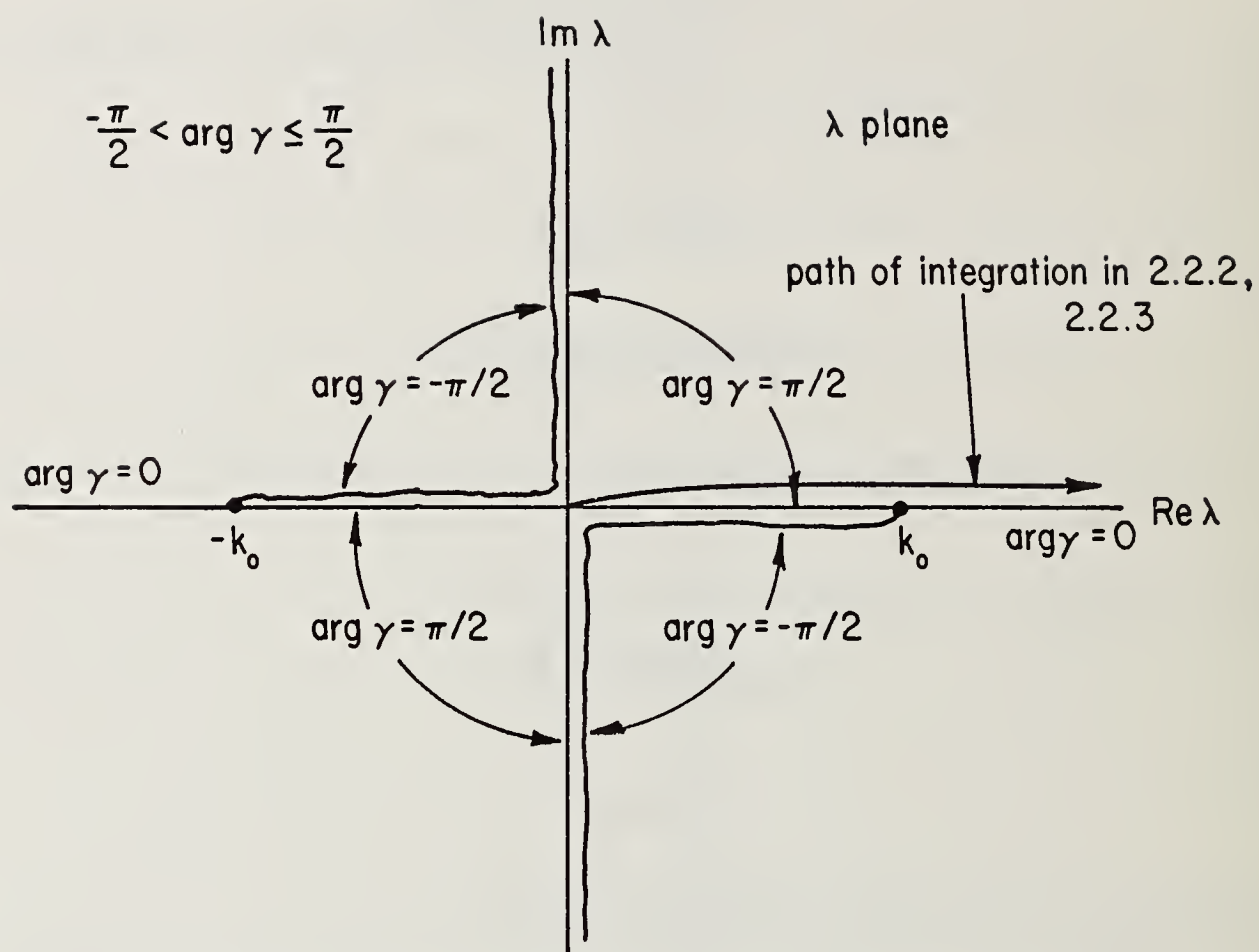
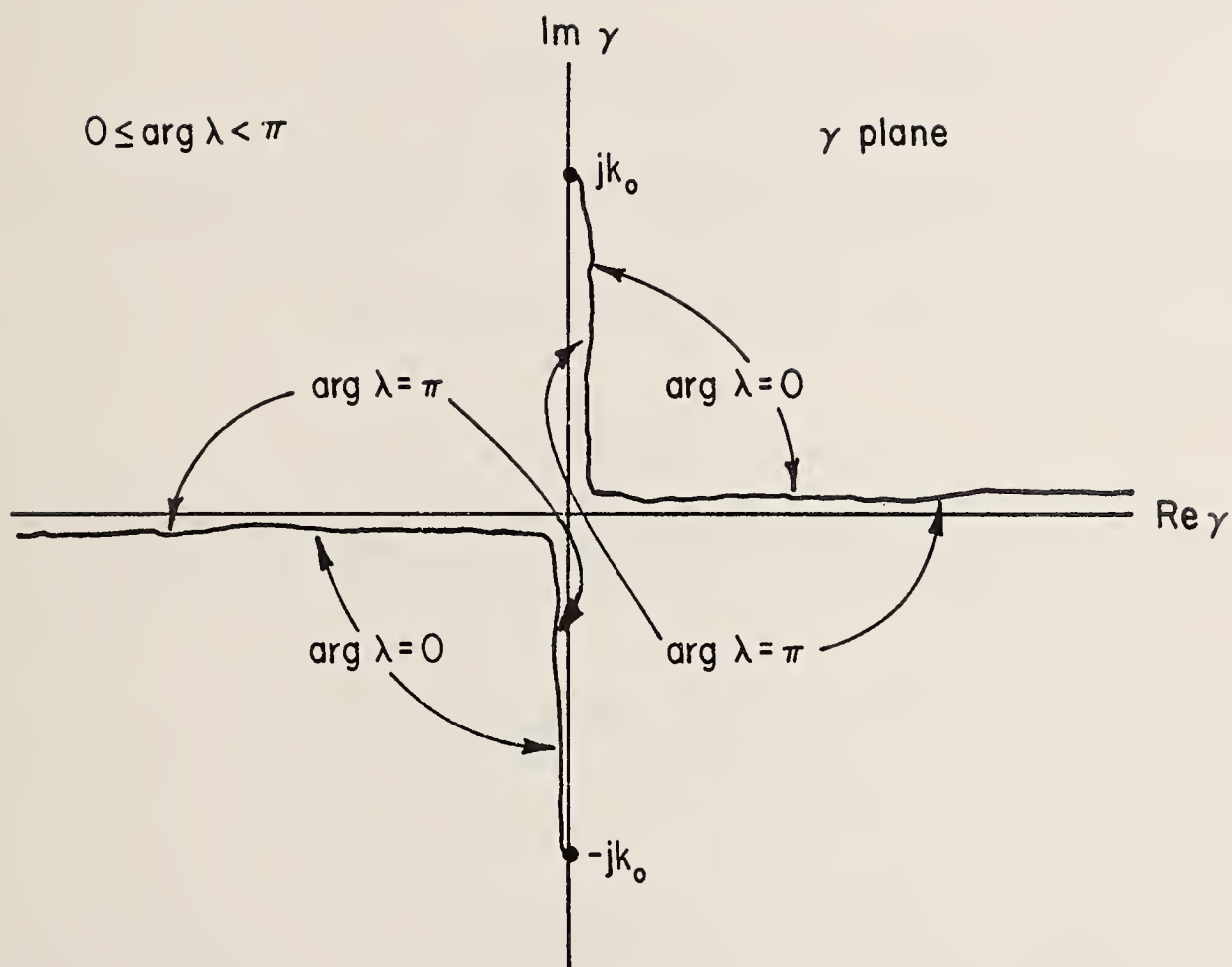Fig. 8.2.3: Branch Cut Selection of $\gamma = \sqrt{\lambda^2 - k_o^2}$

Fig. 8.2.4: Branch Cut Selection of $\lambda = \sqrt{\gamma^2 + k_o{}^2}$

and

$$\int_0^\infty \left[A^o(\lambda)e^{\gamma z_o} - A(\lambda)e^{-\gamma z_o} \right] \gamma \cos \lambda x \, d\lambda =$$

$$\begin{cases} -\int_0^\infty \left[C^o(\lambda)e^{-\gamma z_o} - C(\lambda)e^{\gamma z_o} \right] \gamma \cos \lambda(x-b) \, d\lambda; \quad x \geq b, \\[3mm] -\sum_{n=0}^\infty \gamma_{nb} \left[B_n^{(o)} e^{-\gamma_{nb} z_o} - B_n e^{\gamma_{nb} z_o} \right] \cos \dfrac{n\pi x}{b}; \quad 0 \leq x \leq b. \end{cases} \tag{2.2.5}$$

We may use the orthogonality of $\cos n\pi x/b$ and eliminate coefficients to find the following two equations in B_m, $B_m^{(o)}$, $A(\lambda)$, $A^o(\lambda)$.

$$\gamma_{mb} b \, \varepsilon_m \, B_m e^{\gamma_{mb} z_o} = (-1)^{m+1} \int_0^\infty \frac{A^o(\lambda)\lambda \sin \lambda b \, e^{\gamma z_o}}{\gamma_{mb} - \gamma} \, d\lambda$$

$$+ (-1)^{m+1} \int_0^\infty \frac{A(\lambda)\lambda \sin \lambda b \, e^{-\gamma z_o}}{\gamma_{mb} + \gamma} \, d\lambda \tag{2.2.6}$$

$$\gamma_{mb} b \, \varepsilon_m \, B_m^{(o)} e^{-\gamma_{mb} z_o} = (-1)^{m+1} \int_0^\infty \frac{A^o(\lambda)\lambda \sin \lambda b \, e^{\gamma z_o}}{\gamma_{mb} + \gamma} \, d\lambda$$

$$+ (-1)^{m+1} \int_0^\infty \frac{A(\lambda)\lambda \sin \lambda b \, e^{-\gamma z_o}}{\gamma_{mb} - \gamma} \, d\lambda \tag{2.2.7}$$

where

$$\varepsilon_m = \begin{cases} 2, & m = 0 \\ 1, & m \geq 1 \end{cases}$$

and $m = 0, 1, 2, \ldots$. It should be noted that the integrals are not Cauchy principal values since the apparent pole is actually a removable singularity.

The equations involving $C(\lambda)$, $C^o(\lambda)$, $A(\lambda)$, and $A^o(\lambda)$ are more difficult to obtain because of singularities.

Consider multiplying (2.2.4) and (2.2.5) by $\cos \alpha(x-b)$ and integrating x from b to ∞. From the orthogonality of the eigenfunctions in region c we have

$$\int_b^\infty \cos \alpha(x-b) \cos \lambda(x-b) \, dx = \frac{\pi}{2} \delta(\lambda-\alpha) \tag{2.2.8}$$

Using Gel'fand and Shilov (1964), we can also find

$$\int_b^\infty \cos \alpha(x-b) \cos \lambda x \, dx = \frac{\pi}{2} \cos \lambda b \, \delta(\lambda-\alpha) - \frac{\lambda \sin \lambda b}{\lambda^2 - \alpha^2} \tag{2.2.9}$$

In both (2.2.8) and (2.2.9), $\delta(\cdot)$ is the Dirac delta function. Using these results we may find

$$\pi\, C(\alpha)\, \Gamma\, e^{\Gamma z_0} = \pi\, \Gamma\, \cos\, \alpha b\; A^0(\alpha) e^{\Gamma z_0}$$

$$- PV \int_0^\infty \frac{A^0(\lambda)\lambda\, \sin\, \lambda b\; e^{\gamma z_0}}{\gamma - \Gamma}\, d\lambda + \int_0^\infty \frac{A(\lambda)\lambda\, \sin\, \lambda b\; e^{-\gamma z_0}}{\gamma + \Gamma}\, d\lambda \qquad (2.2.10)$$

and

$$\pi\, C^0(\alpha)\, \Gamma\, e^{-\Gamma z_0} = \pi\, \Gamma\, \cos\, \alpha b\; A(\alpha) e^{-\Gamma z_0}$$

$$+ \int_0^\infty \frac{A^0(\lambda)\lambda\, \sin\, \lambda b\; e^{\gamma z_0}}{\gamma + \Gamma}\, d\lambda - PV \int_0^\infty \frac{A(\lambda)\lambda\, \sin\, \lambda b\; e^{-\gamma z_0}}{\gamma - \Gamma}\, d\lambda \qquad (2.2.11)$$

where

$$\Gamma = \sqrt{\alpha^2 - k_0^2}$$

Again, $-\pi/2 \le \arg(\Gamma) \le \pi/2$. Note that the Cauchy principal value is used in (2.2.10) and (2.2.11). This interpretation of the meaning of the integrals may be found by considering the transform pair

$$F(\alpha) = \int_b^\infty \cos\, \alpha(x-b)\; f(x)\; dx \qquad (2.2.12a)$$

$$f(x) = \frac{2}{\pi} \int_0^\infty \cos\, \alpha(x-b)\; F(\alpha)\; d\alpha \qquad (2.2.12b)$$

We may consider that $f(x)$ is our original equation, either (2.2.4) or (2.2.5). Then the integrations involved in (2.2.10) and (2.2.11) must be interpreted in a manner such that (2.2.12b) will yield the original result. In doing this we use the following integral (Erdelyi; 1954)

$$PV \int_0^\infty \frac{\cos\, \lambda(x-b)\; d\lambda}{\alpha^2 - \lambda^2} = \frac{\pi}{2\alpha} \sin\, \alpha(x-b)$$

Equations (2.2.7) and (2.2.11) relate the incident fields and the unknown spectrum $A(\lambda)$. Equations (2.2.6) and (2.2.10) relate B_n and $C(\lambda)$ in terms of $A(\lambda)$.

The solution of these equations is found in a manner similar to Itoh and Mittra (1971).

Consider a function $T(1)$ with branch cuts L_1 and L_2 as shown in Figure 8.2.5. Then consider the integrals

$$\frac{(-1)^{m+1}}{2\pi j} \int_\Sigma \frac{T(\omega)\; d\omega}{\omega - \gamma_{mb}}, \qquad \frac{1}{2\pi j} \int_\Sigma \frac{T(\omega)\; d\omega}{\omega - \Gamma}$$

71

where m = 0,1,2, ... ; and Σ is the contour shown in Figure 8.2.5. Then

$$\frac{(-1)^{m+1}}{2\pi j} \int_{\Sigma} \frac{T(\omega)\, d\omega}{\omega - \gamma_{mb}} = \frac{(-1)^{m+1}}{2\pi j} \int_{0}^{\infty} \frac{T^-(\omega) - T^+(\omega)}{\omega - \gamma_{mb}} \frac{\lambda d\lambda}{\omega}$$

$$+ \frac{(-1)^{m+1}}{2\pi j} \int_{0}^{\infty} \frac{T^+(-\omega) - T^-(-\omega)}{\omega + \gamma_{mb}} \frac{\lambda d\lambda}{\omega}$$

$$- (-1)^{m+1} T(\gamma_{mb}) = 0 \qquad (2.2.13)$$

where we have used $T^-(\gamma_{mb}) = T^+(\gamma_{mb}) = T(\gamma_{mb})$ in order to insure that we don't have principal value integrals. Also we have transformed variables from ω to λ via $\lambda d\lambda = \omega d\omega$, i.e., $\lambda = \sqrt{\omega^2 + k_o^2}$. We note that on L_1 and L_2 the value of λ is chosen as a positive and real number according to the path of integration given in (2.2.13).

Similarly

$$\frac{1}{2\pi j} \int_{\Sigma} \frac{T(\omega)\, d\omega}{\omega - \Gamma} = \frac{PV}{2\pi j} \int_{0}^{\infty} \frac{T^-(\omega) - T^+(\omega)}{\omega - \Gamma} \frac{\lambda d\lambda}{\omega}$$

$$+ \frac{1}{2\pi j} \int_{0}^{\infty} \frac{T^+(-\omega) - T^-(-\omega)}{\omega + \Gamma} \frac{\lambda d\lambda}{\omega}$$

$$- \frac{1}{2} [T^+(\Gamma) + T^-(\Gamma)] = 0 \qquad (2.2.14)$$

Comparing (2.2.13) and (2.2.14) with (2.2.7) and (2.2.11) we find

(i) $(-1)^{m+1} T(\gamma_{mb}) = \gamma_{mb}\, b\, \epsilon_m\, B_m^{(o)} e^{-\gamma_{mb} z_o}$, m = 0,1,2,...

(ii) $T^+(-\omega) - T^-(-\omega) = 2\pi j\, \omega \sin \lambda b\, A^o(\lambda) e^{\omega z_o}$, $\omega \epsilon L_1$

((iii) $T^-(\omega) - T^+(\omega) = -2\pi j\, \omega \sin \lambda b\, A(\lambda) e^{-\omega z_o}$, $\omega \epsilon L_1$

(iv) $T^+(\omega) + T^-(\omega) = -2\pi \omega \cos \lambda b\, A(\lambda) e^{-\omega z_o}$

$$+ 2\pi \omega\, C^o(\lambda) e^{-\omega z_o}, \qquad \omega \epsilon L_1$$

We can also consider the integrals

$$\frac{(-1)^{m+1}}{2\pi j} \int_{\Sigma} \frac{T(\omega)\, d\omega}{\omega + \gamma_{mb}}, \quad \frac{1}{2\pi j} \int_{\Sigma} \frac{T(\omega)\, d\omega}{\omega + \Gamma}$$

Using the above properties and comparing the results obtained from these integrals we find upon comparing with (2.2.6) and (2.2.10) the following properties
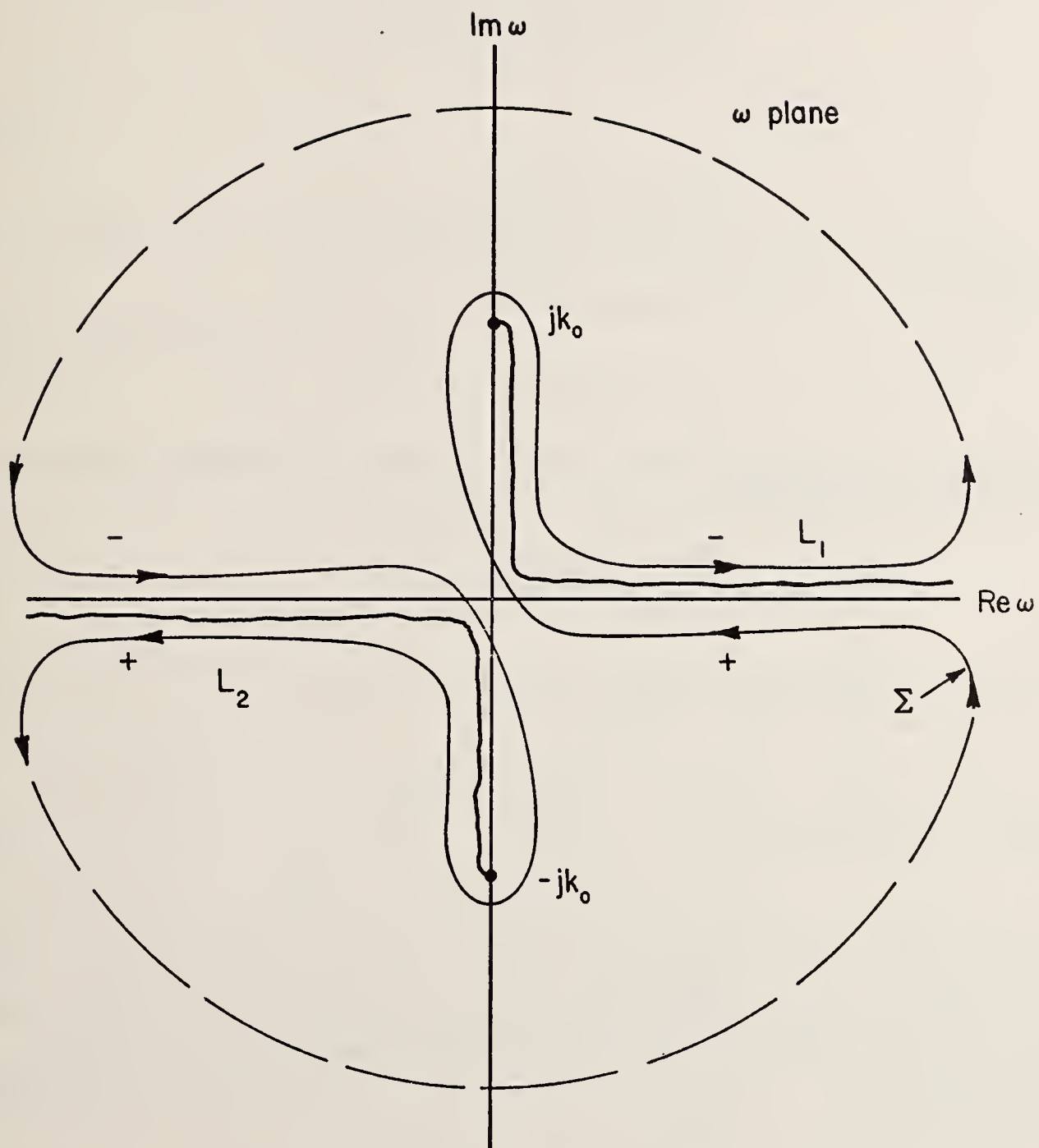
Fig. 8.2.5: The Integration Contour, Σ

(v) $\qquad (-1)^{m+1} T(-\gamma_{mb}) = -\gamma_{mb} \ b \ \epsilon_m \ B_m \ e^{\gamma_{mb} z_o}, \ m = 0,1,2, \ \ldots$

(vi) $\qquad T^+(-\omega) + T^-(-\omega) = 2\pi\omega \ \cos \lambda b \ A^o(\lambda) e^{\omega z_o} - 2\pi\omega \ C(\lambda) e^{\omega z_o}, \quad \omega\epsilon L_1$

Applying the edge condition (Mittra and Lee, 1971) we can easily show that

$$B_m (-1)^m = O(m^{-3/2}), \ m \to \infty$$

Hence from (v) it follows that

(vii) $\qquad T(\omega) = O(\omega^{-1/2}), \ |\omega| \to \infty$

The original problem of solving the integral equation is now reduced to that of constructing a function $T(\omega)$ satisfying the properties given above.

Using (iv) and (iii) we can easily find that

$$T^-(\omega) = T^+(\omega) \ e^{j2\lambda b} - 2\pi j \ \omega \ \sin \lambda b \ e^{j\lambda b} \ e^{-\omega z_o} \ C^o(\lambda), \quad \omega\epsilon L_1 \qquad (2.2.15)$$

This relates the discontinuity across L_1 to just the known incident field. We may then combine (2.2.15) and (ii) to give

$$T^-(\omega) = T^+(\omega) \ G(\omega) + g(\omega) \qquad (2.2.16)$$

where

$$G(\omega) = \begin{cases} e^{j2\lambda b}, & \omega\epsilon L_1 \\ 1, & \omega\epsilon L_2 \end{cases}$$

$$g(\omega) = \begin{cases} -2\pi j \ \omega \ \sin \lambda b \ e^{j\lambda b} \ e^{-\omega z_o} \ C^o(\lambda), & \omega\epsilon L_1 \\ +2\pi j \ \omega \ \sin \lambda b \ e^{\omega z_o} \ A^o(\lambda), & \omega\epsilon L_2 \end{cases}$$

where we recall $\lambda = (\omega^2 + k^2)^{\frac{1}{2}}$ has to take a positive value on L_1 and L_2 according to the integrals defined in (2.2.13) and (2.2.14). Equation (2.2.16) is a non-homogeneous Hilbert problem whose solution may be found using the theory of singular integral equations (Muskhelishveli, 1953). The solution is facilitated by first considering the associated homogeneous problem

$$X^-(\omega) = X^+(\omega) \ e^{j2\lambda b}, \quad \omega\epsilon L_1^-; \quad X^-(\omega) = X^+(\omega), \quad \omega\epsilon L_2 \qquad (2.2.17)$$

in the absence of any incident field, i.e., $A^{(o)}(\lambda) = C^{(o)}(\lambda) = B_m^{(o)} \equiv 0$. The solution of (2.2.17) is found from a direct application of the Plemelj formulas (Muskhelishveli, 1953).

$$\frac{\ln\ X(\omega)}{\omega^2 + k_o^2} = \frac{b}{\pi}\int_{L_1^-}\frac{dt}{\sqrt{t^2+ k_o^2}\,(t-\omega)} \tag{2.2.18}$$

Here, the sign L_1^- denotes the integration path from jk_o to ∞ along the $(-)$ side of L_1. The details of this integration may be found in Appendix G with the result being

$$\frac{\ln\ X(\omega)}{\omega^2 + k_o^2} = \frac{b}{\pi}\ \frac{1}{\sqrt{\omega^2+k_o^2}}\ \text{Ln}\ \left[\frac{\omega\ -\ \sqrt{\omega^2+k_o^2}}{-jk_o}\right]$$

hence

$$X(\omega)\ =\ H(\omega)\exp\left[\frac{b\sqrt{\omega^2+k_o^2}}{\pi}\ \text{Ln}\left(\frac{\omega-\sqrt{\omega^2+k_o^2}}{-jk_o}\right)\right] \tag{2.2.19}$$

where $H(\omega)$ is an unknown entire function found from (i) with $B_m^{(o)} \equiv 0$. Note that $X(\omega)$ has only a branch cut singularity. Hence

$$H(\omega)\ =\ H_1(\omega)\ \Pi(\omega,\gamma_b)(\omega-jk_o)$$

where $H_1(\omega)$ is an entire function which can be found from condition (vii). Before proceeding with the solution it is worth discussing the meaning of the multivalued function

$$\sqrt{\omega^2+k_o^2}\ \text{Ln}\left[\frac{\omega\ -\ \sqrt{\omega^2+k_o^2}}{-jk_o}\right]$$

appearing in (2.2.19) (Abramowitz and Stegun, p. 67, 1965). This function must be interpreted so that it only has a branch cut L_1 with a discontinuity as given by (2.2.17) as well as being continuous across L_2.

Consider the phase of the argument of the log as we traverse L_1 and L_2 as shown in Figure 8.2.6. Figure 8.2.7 illustrates the associated variation of the phase of argument of the logarithm.

Recalling the definition of the branch cut of $(\omega^2 + k_o^2)^{\frac{1}{2}}$ given in Figure 8.2.4, we can write the following explicit forms for $X(\omega)$ on the top and bottom of L_1 and L_2. For $\omega\varepsilon L_1$,

$$X^-(\omega)\ =\ H(\omega)\exp\left\{\frac{b}{\pi}\ \left|\sqrt{\omega^2+k_o^2}\right|\left(\ln\ \left|\frac{\omega-\sqrt{\omega^2+k_o^2}}{-jk_o}\right|\ +\ j\phi_c\right)\right\}$$

$$\tag{2.2.20}$$

$$X^+(\omega)\ =\ H(\omega)\exp\left\{\frac{-b}{\pi}\ \left|\sqrt{\omega^2+k_o^2}\right|\left(\ln\ \left|\frac{\omega+\sqrt{\omega^2+k_o^2}}{-jk_o}\right|\ +\ j\phi_a\right)\right\}$$

where
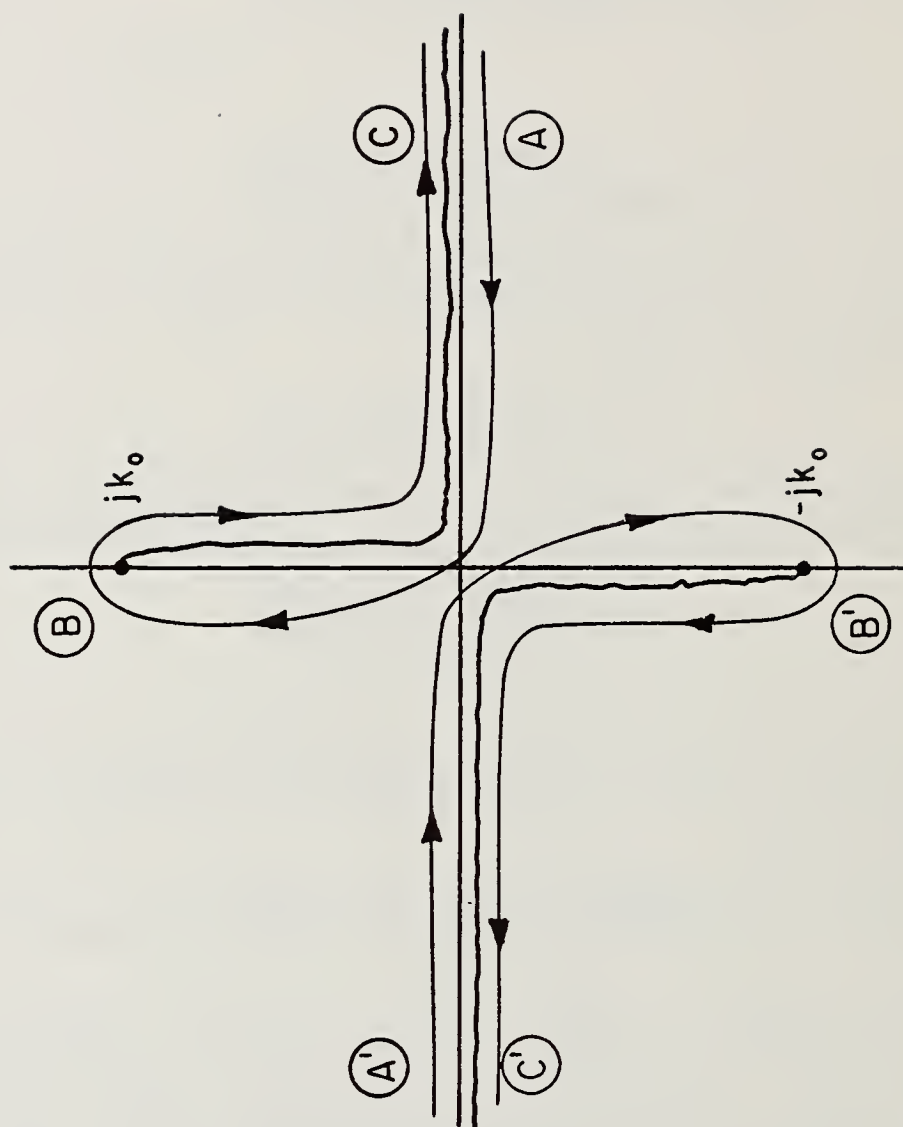
Fig. 8.2.6: Path Location for Use with Fig. 8.2.7

76

$$\arg\left(\omega - \frac{\sqrt{\omega^2 + k_0^2}}{-jk_0}\right)$$

ω plane

Fig. 8.2.7: Phase of the Argument of the Logarithm

$$\phi_c = \arg \left[\frac{\omega - \sqrt{\omega^2 + k_o^2}}{-jk_o} \right] \quad \text{along } L_1^- \quad \text{and}$$

$$\phi_a = \arg \left[\frac{\omega - \sqrt{\omega^2 + k_o^2}}{-jk_o} \right] \quad \text{along } L_1^+ \tag{2.2.21}$$

Hence

$$\frac{X^-(\omega)}{X^+(\omega)} \exp \left[j \frac{b}{\pi} |\sqrt{\omega^2 + k_o^2}| \; (\phi_c + \phi_a) \right] \quad , \qquad \omega \varepsilon L_1 \tag{2.2.22}$$

Similarly, for $\omega \varepsilon L_2$

$$X^-(\omega) = H(\omega) \; \exp \left\{ \frac{-b}{\pi} |\sqrt{\omega^2 + k_o^2}| \left(\ln \left| \frac{\omega + \sqrt{\omega^2 + k_o^2}}{jk_o} \right| + j\phi_a' \right) \right\}$$
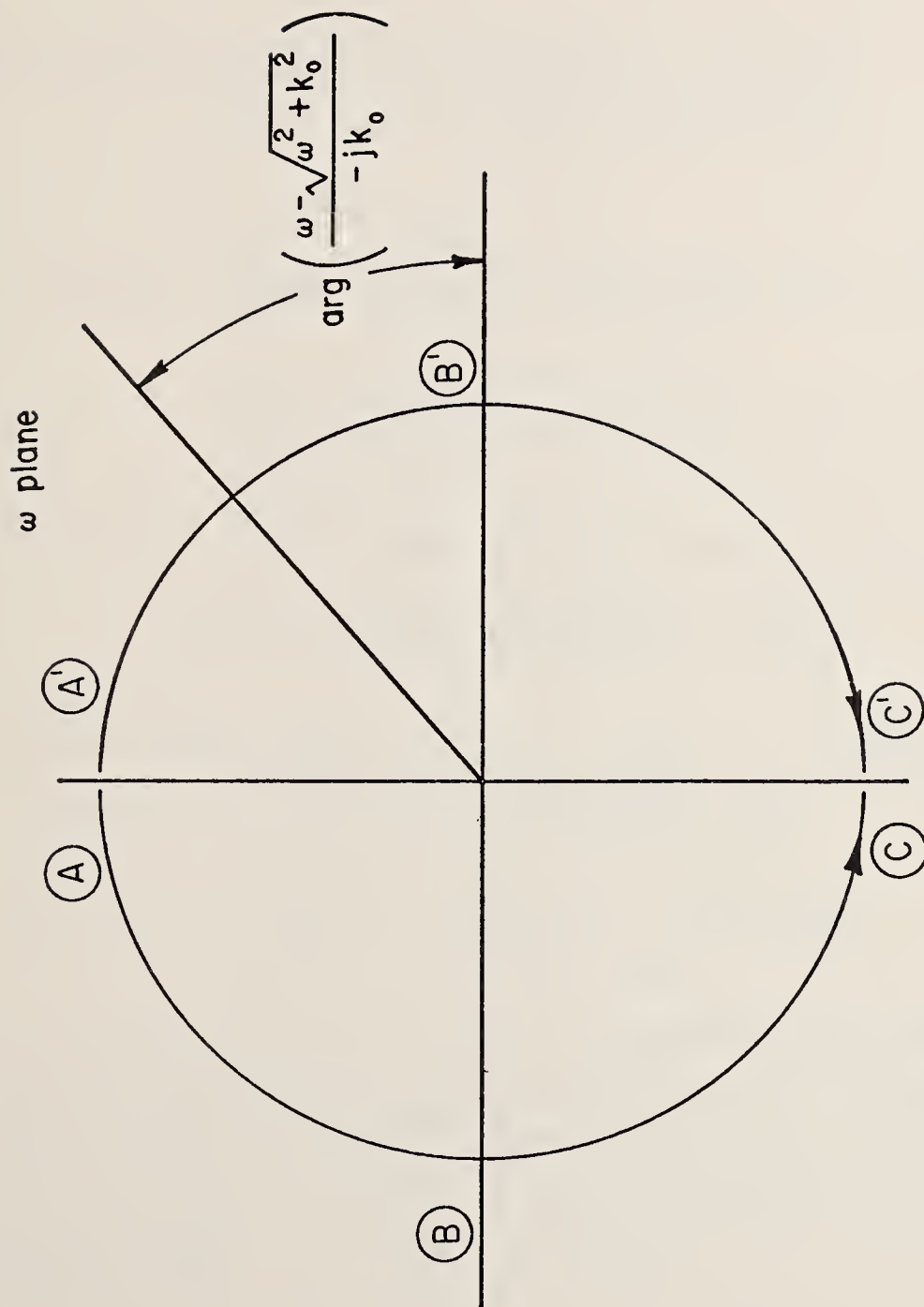
$$X^+(\omega) = H(\omega) \; \exp \left\{ \frac{b}{\pi} |\sqrt{\omega^2 + k_o^2}| \left(\ln \left| \frac{\omega + \sqrt{\omega^2 + k_o^2}}{jk_o} \right| + j\phi_c' \right) \right\} \tag{2.2.23}$$

where ϕ_a' and ϕ_c' are defined similar to ϕ_a and ϕ_c. Thus

$$\frac{X^-(\omega)}{X^+(\omega)} = \exp \left[\frac{-jb}{\pi} |\sqrt{\omega^2 + k_o^2}| \; (\phi_a' + \phi_c') \right] \quad , \qquad \omega \varepsilon L_2 \tag{2.2.24}$$

Clearly then we must have

$$\phi_c + \phi_a = 2\pi$$

and

$$\phi_a' + \phi_c' = 0$$

for (2.2.17) to hold. Hence we must have

$$\phi_a = \frac{\pi}{2}, \qquad \phi_c = \frac{3\pi}{2}$$

and

$$\phi_a' = \frac{\pi}{2}, \qquad \phi_c' = \frac{-\pi}{2}$$

Thus in order for $X(\omega)$ to be the solution to (2.2.17) we must choose a branch cut along the negative imaginary axis with the argument of the logarithm taking on either $3\pi/2$ or $-\pi/2$ along the cut depending on the direction of approach.

We can now rewrite (2.2.16) using (2.2.17) as follows

78

$$\frac{T^-(\omega)}{X^-(\omega)} = \frac{T^+(\omega)}{X^+(\omega)} + \frac{g(\omega)}{X^-(\omega)} \qquad (2.2.25)$$

This can be solved using the Plemelj formulas

$$T(\omega) = X(\omega)\left\{P(\omega) + \int_{L_1} \frac{g^{(1)}(t)\ dt}{X^-(t)(t-\omega)} - \int_{L_2} \frac{g^{(2)}(t)\ dt}{X^-(t)(t-\omega)}\right\} \qquad (2.2.26)$$

where L_1^- and L_2^+ are defined in Figure 8.2.5, and

$$g^{(1)}(\omega) = -\omega\,\sin\lambda b\ e^{j\lambda b}\ e^{-\omega z_o}\ C^o(\lambda)$$

$$\qquad (2.2.27)$$

$$g^{(2)}(\omega) = \omega\,\sin\lambda b\ e^{-\omega z_o}\ A^o(\lambda)$$

where $P(\omega)$ is to be found. Using condition (i)

$$T(\gamma_{mb}) = (-1)^{m+1}\ \gamma_{mb}\ b\ \varepsilon_m B_m^{(o)}\ e^{-\gamma_{mb} z_o}$$

$$\qquad (2.2.28)$$

$$= X(\gamma_{mb})\ P(\gamma_{mb})$$

Clearly then $P(\omega)$ is just a perturbation sum of the form

$$P(\omega) = \frac{K_o}{\omega - jk_o} + \sum_{n=1}^{\infty} \frac{g_n}{\omega - \gamma_{nb}}$$

where K_o and g_n can be related to $B_m^{(o)}$ using (2.2.28). Hence

$$T(\omega) = H_1(\omega)\ \Pi(\omega,\gamma_b)\exp\left\{\frac{b\sqrt{\omega^2+k_o^2}}{\pi}\left[\ln\left(\frac{\omega-\sqrt{\omega^2+k_o^2}}{k_o}\right) + \frac{j\pi}{2}\right]\right\} \cdot$$

$$\left[K_o + (\omega-jk_o)\left\{\sum_{n=1}^{\infty}\frac{g_n}{\omega-\gamma_{nb}} + \int_{L_1^-}\frac{g^{(1)}(t)\ dt}{X^-(t)(t-\omega)} - \int_{L_2^+}\frac{g^{(2)}(t)\ dt}{X(t)\ (t-\omega)}\right\}\right] \qquad (2.2.29)$$

where we have used the fact that on L_2 we have $X^+(\omega) = X^-(\omega) = X(\omega)$. We note that the term $(-j)$ in (2.2.19) for the expression of $X(\omega)$ has been removed from the logarithmic sign in (12.2.29). Consequently, the log function now takes a principle value between $-\rho$ and ρ. It is seen that the singularities of the integrands are of two types: a simple pole at $\omega=t$ and a branch cut in $X(t)$ along L_1. This will be important in later chapters when choosing an efficient numerical scheme.

From condition (vii) we can easily find

$$H_1(\omega) = \exp\left\{\frac{\omega b}{\pi}\left[1-C_e-\ln\left(\frac{k_o b}{2\pi}\right)\right] - \frac{j\omega b}{2}\right\}$$

where $C_e = 0.577216\ldots$ is Euler's constant.

Equation (2.2.29) is very reminiscent to the perturbation expansion used in connection with modification of the bifurcated waveguide. There are two primary differences: (1) the homogeneous solution has changed form to reflect the removal of a conductor to infinity, and (2) the summations associated with the regions which become infinite become integrals. Equation (2.2.29) represents the complete general solution of a semi-infinite parallel plate waveguide.

2.3 The Magnetic Wall Case

Let us now consider the TM solution of the geometry shown in Figure 8.2.2. Since many of the details are similar to that of the dielectric wall case, only the distinctive results will be presented.

The TM fields are derivable from $\phi = H_y$ and the fields in each region are given by

$$\phi_B = \sum_{n=1}^{\infty} \left[B_n^{(o)} e^{-\gamma_{2n-1,2b} z} + B_n e^{\gamma_{2n-1,2b} z} \right] \sin k_{nb} x \qquad z \leq z_o,\ 0 \leq x \leq b \qquad (2.3.1)$$

$$\phi_C = \int_0^{\infty} \left[C^o(\lambda) e^{-\gamma z} + C(\lambda) e^{\gamma z} \right] \cos \lambda(x-b)\ d\lambda \qquad z \leq z_o,\ x \geq b \qquad (2.3.2)$$

$$\phi_A = \int_0^{\infty} \left[A^o(\lambda) e^{\gamma z} + A(\lambda) e^{-\gamma z} \right] \sin \lambda x\ d\lambda, \qquad z \geq z_o,\ x \geq 0 \qquad (2.3.3)$$

where

$$k_{nb} = \frac{(2n-1)\pi}{2b}$$

In a manner similar to the electric wall case we can find the following integral equations:

$$b\, \gamma_{2m-1,2b}\, B_m\, e^{\gamma_{2m-1,2b} z_o} = (-1)^{m+1} \int_0^{\infty} \frac{A^o(\lambda)\lambda \cos \lambda b\ e^{\gamma z_o}}{\gamma_{2m-1,2b} - \gamma} d\lambda$$

$$+ (-1)^{m+1} \int_0^{\infty} \frac{A(\lambda)\lambda \cos \lambda b\ e^{-\gamma z_o}}{\gamma_{2m-1,2b} + \gamma} d\lambda \qquad (2.3.4)$$

$$b\, \gamma_{2m-1,2b}\, B_m^{'(o)}\, e^{-\gamma_{2m-1,2b} z_o} = (-1)^{m+1} \int_0^{\infty} \frac{A^o(\lambda)\lambda \cos \lambda b\ e^{\gamma z_o}}{\gamma_{2m-1,2b} + \gamma} d\lambda$$

$$+ (-1)^{m+1} \int_0^{\infty} \frac{A(\lambda)\lambda \cos \lambda b\ e^{-\gamma z_o}}{\gamma_{2m-1,2b} - \gamma} d\lambda \qquad (2.3.5)$$

where $m = 1, 2, \ldots$. Note that as in the electric wall case the Cauchy principal value is not required for (2.3.4) and (2.3.5). Also

$$\pi \, C(\alpha)\Gamma \, e^{\Gamma z_o} = \pi \, \Gamma \, \sin \alpha b \, A^o(\alpha) \, e^{\Gamma z_o}$$

$$+ \, PV \int_0^\infty \frac{A^o(\lambda)\lambda \, \cos \lambda b \, e^{\gamma z_o}}{\gamma - \Gamma} \, d\lambda - \int_0^\infty \frac{A(\lambda)\lambda \, \cos \lambda b \, e^{-\gamma z_o}}{\gamma + \Gamma} \, d\lambda \qquad (2.3.6)$$

$$\pi \, C^o(\alpha)\Gamma \, e^{-\Gamma z_o} = \pi \, \Gamma \, \sin \alpha b \, A(\alpha) \, e^{-\Gamma z_o}$$

$$- \int_0^\infty \frac{A^o(\lambda)\lambda \, \cos \lambda b \, e^{\gamma z_o}}{\gamma + \Gamma} \, d\lambda + \, PV \int_0^\infty \frac{A(\lambda)\lambda \, \cos \lambda b \, e^{-\gamma z_o}}{\gamma - \Gamma} \, d\lambda \qquad (2.3.7)$$

Note that the principal value is again required for the equations associated with both of the open regions.

The solution to equations (2.3.4) – (2.3.7) is found by considering the following integrals

$$\frac{(-1)^{m+1}}{2\pi j} \int_\Sigma \frac{T(\omega) \, d\omega}{\omega \pm \gamma_{2m-1,2b}} , \qquad \frac{1}{2\pi j} \int_\Sigma \frac{T(\omega) \, d\omega}{\omega \pm \Gamma}$$

where $T(\omega)$ has branch cuts L_1 and L_2 as shown in Figure 8.2.5, and $m = 1,2,3,\ldots$. Σ is the same contour as the electric wall case. Then comparing the results of the above integrals with (2.3.4) – (2.3.7) we can find

(i) $\qquad (-1)^{m+1}T(\gamma_{2m-1,2b}) = \gamma_{2m-1,2b} \, b \, B_m^{(o)} e^{-\gamma_{2m-1,2b}z_o}, \qquad m = 1,2,3,\ldots$

(ii) $\qquad T^+(-\omega) - T^-(-\omega) = -2\pi j \, \omega \, \cos \lambda b \, A^o(\lambda) e^{\omega z_o}, \qquad\qquad \omega\epsilon L_1$

(iii) $\qquad T^-(\omega) - T^+(\omega) = -2\pi j \, \omega \, \cos \lambda b \, A(\lambda) e^{-\omega z_o}, \qquad\qquad \omega\epsilon L_1$

(iv) $\qquad T^+(\omega) + T^-(\omega) = 2\pi \, \omega \, \sin \lambda b \, A(\lambda) e^{-\omega z_o}$

$$-2\pi \, \omega \, C^o(\lambda) e^{-\omega z_o}, \qquad\qquad \omega\epsilon L_1$$

(v) $\qquad (-1)^{m+1}T(-\gamma_{2m-1,2b}) = -\gamma_{2m-1,2b} \, b \, B_m e^{\gamma_{2m-1,2b}z_o}, \qquad m = 1,2,\ldots$

(vi) $\qquad T^+(-\omega) + T^-(-\omega) = -2\pi \, \omega \, \sin \lambda b \, A^o(\lambda) e^{\omega z_o}$

$$+2\pi \, \omega \, C(\lambda) e^{\omega z_o}, \qquad\qquad \omega\epsilon L_1$$

Also the edge condition requires

(vii) $\qquad T(\omega) = 0(\omega^{-1/2}), \; |\omega| \to \infty$

Using (iii) and (iv) we can easily find

81

$$T^-(\omega) = -e^{j2\lambda b}T^+(\omega) - 2\pi\omega \ C^o(\lambda)e^{-\omega z_o} e^{j\lambda b} \cos \lambda b, \quad \omega\epsilon L_1 \qquad (2.3.8)$$

This relates the discontinuity across L_1 to the known incident field. We may then combine (2.3.8) with (ii) to give

$$T^-(\omega) = T^+(\omega) \ G(\omega) + g(\omega) \qquad (2.3.9)$$

where

$$G(\omega) = \begin{cases} -e^{j2\lambda b}, & \omega\epsilon L_1 \\ 1, & \omega\epsilon L_2 \end{cases}$$

$$g(\omega) = \begin{cases} -2\pi\omega \ \cos \lambda b \ e^{j\lambda b} \ C^o(\lambda)e^{-\omega z_o}, & \omega\epsilon L_1 \\ +2\pi j\omega \ \cos \lambda b \ A^o(\lambda)e^{-\omega z_o}, & \omega\epsilon L_2 \end{cases}$$

Equation (2.3.9) is a non-homogeneous Hilbert problem similar to the electric wall case. The primary difference with the electric wall case is the presence of a minus sign in the homogeneous problem.

$$X^-(\omega) = -X^+(\omega) \ e^{j2\lambda b}, \quad \omega\epsilon L_1$$

$$X^-(\omega) = X^+(\omega), \quad \omega\epsilon L_2 \qquad (2.3.10)$$

The solution to (2.3.10) clearly involves the factorization of $\exp(j2\lambda b)$ as in the electric wall case. However, we must also have a minus sign discontinuity. Such a function is by inspection $\sqrt{\omega - jk_o}$. Hence

$$X(\omega) = H_2(\omega) \prod_{odd} (\omega, \gamma_{2b}) \ \sqrt{\omega - jk_o} \qquad (2.3.11)$$

$$\exp\left\{\frac{b\sqrt{\omega^2 + k_o^2}}{\pi} \left[\ln\left(\frac{\omega - \sqrt{\omega^2 + k_o^2}}{k_o}\right) + \frac{j\pi}{2}\right]\right\}$$

The general solution is now easily shown to be

$$T(\omega) = H_2(\omega) \prod_{odd} (\omega, \gamma_{2b})\sqrt{\omega - jk_o} \ \exp\left\{\frac{b\sqrt{\omega^2 + k_o^2}}{\pi} \left[\ln\left(\frac{\omega - \sqrt{\omega^2 + k_o^2}}{k_o}\right) + \frac{j\pi}{2}\right]\right\}$$

$$\cdot \left[\sum_{n=1}^{\infty} \frac{g_n}{\omega - \gamma_{2n-1,2b}} + \int_{L_1^-} \frac{g^{(1)}(t) \ dt}{X^-(t)(t-\omega)} - \int_{L_2^+} \frac{g^{(2)}(t) \ dt}{X(t)(t-\omega)}\right] \qquad (2.3.12)$$

$H_2(\omega)$ is found from (vii) to be

$$H_2(\omega) = \exp\left\{\frac{\omega b}{\pi} \left[1 - C_e - \ln\left(\frac{2k_o b}{\pi}\right)\right] - \frac{j\omega b}{2}\right\}$$

This choice of $H_2(\omega)$ is the correct one in order for condition (vii) to hold. Note that the asymptotic behavior of the odd infinite product is quite different from the complete infinite product. This combined with the behavior of the term $\sqrt{\omega - jk_o}$ and the perturbation sum ensures that $T(\omega) = O(\omega^{-1/2})$, $|\omega| \to \infty$.

Using (i) we can relate g_n to $B_n^{(o)}$

$$(-1)^{m+1} T(\gamma_{2m-1,2b}) = (-1)^m H_2(\gamma_{2m-1,2b}) \prod_{\text{odd}}^{(m)} (\gamma_{2m-1,2b}, \gamma_{2b})$$

$$\cdot \sqrt{\gamma_{2m-1,2b} - jk_o} \exp\left\{ \frac{2m-1}{2} \left[\ln\left(\frac{\gamma_{2m-1,2b} - (2m-1)\pi/2b}{k_o} \right) + \frac{j\pi}{2} \right] \right\}$$

$$\cdot \left(\frac{1}{\gamma_{2m-1,2b}} \right) g_m = \gamma_{2m-1,2b} \, b \, B_m^{(o)} \, e^{-\gamma_{2m-1,2b} z_o} \tag{2.3.13}$$

Similarly using (2.3.9) we can find

$$g^{(1)}(\omega) = j\omega \cos \lambda b \, e^{j\lambda b} \, C^o(\lambda) e^{-\omega z_o}, \qquad \omega \varepsilon L_1$$

$$g^{(2)}(\omega) = +\omega \cos \lambda b \, A^o(\lambda) e^{-\omega z_o}, \qquad \omega \varepsilon L_2$$

3. Formulation and Solution of Composite Problems

The key to the modified function theoretic technique is the identification of an auxiliary problem. The auxiliary problem is such that the solution may be identified in terms of soluble problems.

Before proceeding to other problems let us illustrate this process with the open region analogue of an E-plane step -- a flanged parallel plate waveguide. This problem has been solved by Itoh and Mittra (1971) using this same technique, but it is believed that a derivation based on the concepts of this work are perhaps clearer. Also Kostelnicek and Mittra (1969) indicated that a solution was possible as well as sketching the equations.
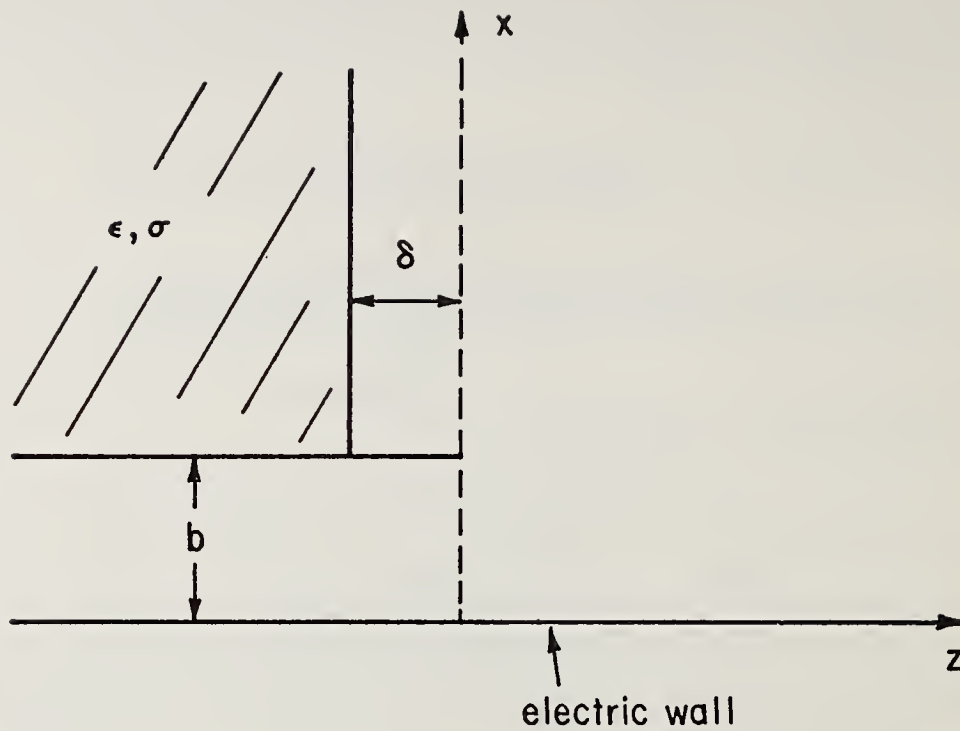
Figure 8.3.1 illustrates the flanged waveguide and the associated geometry. Notice that the associated geometry has a recessed dielectric of finite permittivity. As $\delta \to 0$ and $\varepsilon \to \infty$, the auxiliary problem coincides with the original flanged problem. This auxiliary problem allows us to perturb the parallel plate solution effectively.

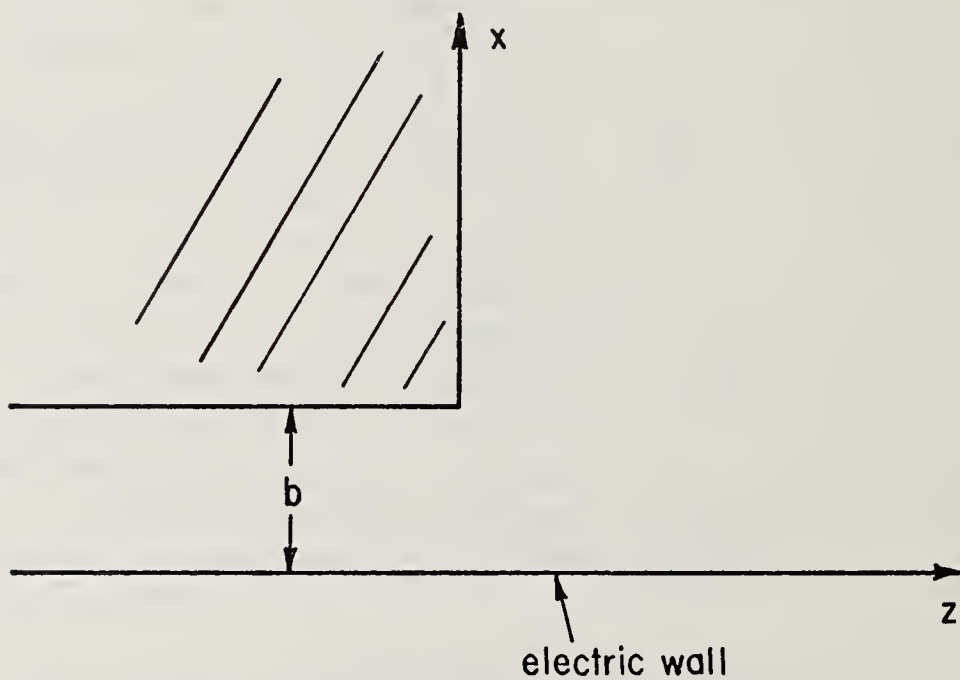Consider the case of a TEM waveguide mode incident on the junction, then from (2.2.29) we can write

$$T(\omega) = X(\omega) \left[\frac{K_o}{\omega - jk_o} + \int_{L_1} \frac{g^{(1)}(t) \, dt}{X^-(t)(t-\omega)} \right] \tag{3.1}$$

where

$$X(\omega) = H_1(\omega)(\omega - jk_o)\Pi(\omega, \gamma_b)\exp\left\{ \frac{b\sqrt{\omega^2 + k_o^2}}{\pi} \left[\ln\left(\frac{\omega - \sqrt{\omega^2 + k_o^2}}{k_o} \right) + \frac{j\pi}{2} \right] \right\}$$

83

(a) Auxiliary Problem

(b) The Flanged Waveguide Geometry

Fig. 8.3.1: The Flanged Parallel Plate Waveguide

where

$$H_1(\omega) = \exp\left\{\frac{\omega b}{\pi}\left[1-C_e-\ln\left(\frac{k_ob}{2\pi}\right)\right] - \frac{j\omega b}{2}\right\}$$

Clearly the other terms are not necessary since $B_m^{(o)} \equiv 0$, $m > 0$ and $A^o(\lambda) \equiv 0$ imply that $g_m \equiv 0$, $m > 0$ and $g^{(2)}(t) \equiv 0$.

K_o is known from (i) of section 2.2 to be given by

$$T(jk_o) = -2jk_ob = K_o\left(\frac{X(\omega)}{\omega-jk_o}\right)_{\omega = jk_o}$$

where $B_o^{(o)} = 1$.

From (vi) of section 2.2 we have

$$T(-\omega) = -\omega\pi \; C(\lambda), \quad \omega\varepsilon L_1 \tag{3.2}$$

where $T^+(-\omega) = T^-(-\omega) = T(-\omega)$ for $\omega\varepsilon L_1$, since (3.1) only has a branch cut L_1. Also from (2.2.27)

$$g^{(1)}(\omega) = -\omega \sin \lambda b \; e^{j\lambda b} \; C^o(\lambda) \tag{3.3}$$

where $\lambda = \sqrt{\omega^2+k_o^2}$ with $\text{Im}\lambda \geq 0$. However, the junction at $z = -\delta$ can be solved to give an additional relation between $C^o(\gamma)$ and $C(\gamma)$, namely

$$C^o(\lambda) = C(\lambda) \; R(\lambda) \tag{3.4}$$

where

$$R(\lambda) = \frac{\varepsilon\omega - \Gamma}{\varepsilon\omega + \Gamma} \; e^{-2\omega\delta}$$

where

$$\Gamma = \sqrt{\lambda^2 - \varepsilon k_o^2}$$

Hence we may combine (3.2) - (3.4) to give the following integral equation for $g^{(1)}(\omega)$

$$g^{(1)}(\omega) = \frac{-\sin \lambda b}{\pi} e^{j\lambda b}R(\lambda)X(-\omega)\left(\frac{K_o}{\omega+jk_o} - \int_{L_1^-} \frac{g^{(1)}(t) \; dt}{X^-(t)(t+\omega)}\right), \quad \omega\varepsilon L_1 \tag{3.5}$$

Consider the change of variable

$$g^{(1)}(\omega) = \frac{-\sin \lambda b \; e^{j\lambda b}R(\lambda)X(-\omega)G(\omega)}{\pi(\omega+jk_o)} \tag{3.6}$$

Then (3.5) becomes, for $\omega\varepsilon L_1$,

85

$$G(\omega) = K_o + (\omega + jk_o) \int_{L_1} \frac{Q(t)\ G(t)\ dt}{t + \omega}$$

(3.7)

where

$$Q(\omega) = \frac{+\sin\ \lambda b\ e^{j\lambda b} R(\lambda) X(-\omega)}{\pi(\omega + jk_o)\ X^-(\omega)}$$

(3.8)

Equation (3.7) is identical (with a slight change of notation) to the equation derived by Kostelnicek and Mittra (1969) and later solved by Itoh and Mittra (1971).

In order to solve (3.7) effectively we should use the asymptotic behavior of $G(\omega)$. To this end consider the field in the dielectric.

$$\phi_D = \int_0^\infty D(\lambda)\ e^{\Gamma z}\ \cos\ \lambda(x-b)\ d\lambda$$

Using the other field relations we can easily find

$$D(\lambda) = e^{(\Gamma+\omega)\delta}\ \frac{2\varepsilon\omega}{\varepsilon\omega-\Gamma}\ C^o(\lambda)$$

(3.9)

And from Mittra and Lee (1971) we can easily show for $\delta = 0$

$$D(\lambda) = O(\lambda^{-3/2-\Delta}),\quad |\lambda| \to \infty$$

(3.10)

where

$$\Delta = \frac{1}{\pi}\ \sin^{-1}\left(\frac{(\varepsilon-1)}{2(\varepsilon+1)}\right)$$

For the case of $\varepsilon \to \infty$, $\Delta = 1/6$. Then from (3.3), (3.6), (3.9) and (3.10) we have

$$G(t) = O(t^{-\Delta})$$

(3.11a)

and from (3.8)

$$Q(t) = O(t^{-1})$$

(3.11b)

This is in agreement with Itoh (1972). Using Stieltges transforms we can show

$$\int_{L_1} \frac{Q(t)\ G(t)\ dt}{t + \omega} = O(\omega^{-1}) + O(\omega^{-1-\Delta})$$

(3.12)

as $|\omega| \to \infty$. Hence we see that the constant terms in (3.7) must cancel as $|\omega| \to \infty$, or

$$K_o + \int_{L_1} Q(t)G(t)\ dt = 0$$

or if we write $Q(t)G(t) = \bar{G}\ t^{-1-\Delta}$ for $t > t_o\ \varepsilon L_1$ we have

86

$$K_o + \int_{L_1}^{(t_o)} Q(t)G(t) \, dt + \overline{G} \int_{t_o}^{\infty} t^{-1-\Delta} \, dt = 0 \qquad (3.13)$$

This equation is similar to (3.10) of chapter 2 derived for the E-plane step. Equation (3.13) in conjunction with (3.7) is the solution to the problem since all the modal coefficients and plane wave spectra are readily found from $T(\omega)$ with $G(\omega)$ determined. The method of solution of the integral equation will be discussed in the next chapter in conjunction with another problem.

1. Introduction

This chapter is directed to the solution of a parallel plate waveguide radiating into a homogeneous half space. This problem has been solved for the case of a dielectric slab by Kostelnicek and Mittra (1969), (1971). The solution as given here has three significant areas of research which warrant the inclusion of the problem: (1) it is believed that the method of formulation and solution is more systematic and simpler to understand than Kostelnicek; (2) the details of solving the integral equation efficiently are looked into carefully; and (3) the results are physically interesting and have not been obtained before this work.

2. Formulation of the Equations

Consider the TM solution of the geometry shown in Figure 9.2.1. For simplicity we will assume TEM incidence, the general TM solution follows directly.

From Chapter 8 we see that $T(\omega)$ is given by

$$T(\omega) = X(\omega) \left\{ \frac{K_o}{\omega - jk_o} - \int_{L_2^+} \frac{g^{(2)}(t) \, dt}{X(t)(t-\omega)} \right\} \tag{2.1}$$

where

$$X(\omega) = H_1(\omega)(\omega - jk_o)\Pi(\omega,\gamma_n)\exp\left\{ \frac{b\sqrt{\omega^2+k_o^2}}{\pi} \left[\ln\left(\frac{\omega - \sqrt{\omega^2+k_o^2}}{k_o} \right) + \frac{j\pi}{2} \right] \right\}$$

and

$$H_1(\omega) = \exp\left\{ \frac{\omega b}{\pi} \left[1 - C_e - \ln\left(\frac{k_o b}{2\pi} \right) \right] - \frac{j\omega b}{2} \right\}$$

where $B_m^{(o)} = 1$.

From (iii) of section 2.2 of Chapter 8 we have

$$T^-(\omega) - T^+(\omega) = -2\pi j \, \omega \sin \lambda b \, A(\lambda), \quad \omega \varepsilon L_1$$

but for $\omega \varepsilon L_1$ and (2.2.16) of Chapter 8 we have

$$T^-(\omega) = T^+(\omega) \, e^{j2\lambda b}$$

thus

$$T^-(\omega) = -\pi \omega e^{j\lambda b} \, A(\lambda), \quad \omega \varepsilon L_1^- \tag{2.2}$$

Also from (2.2.27) of Chapter 8 we have

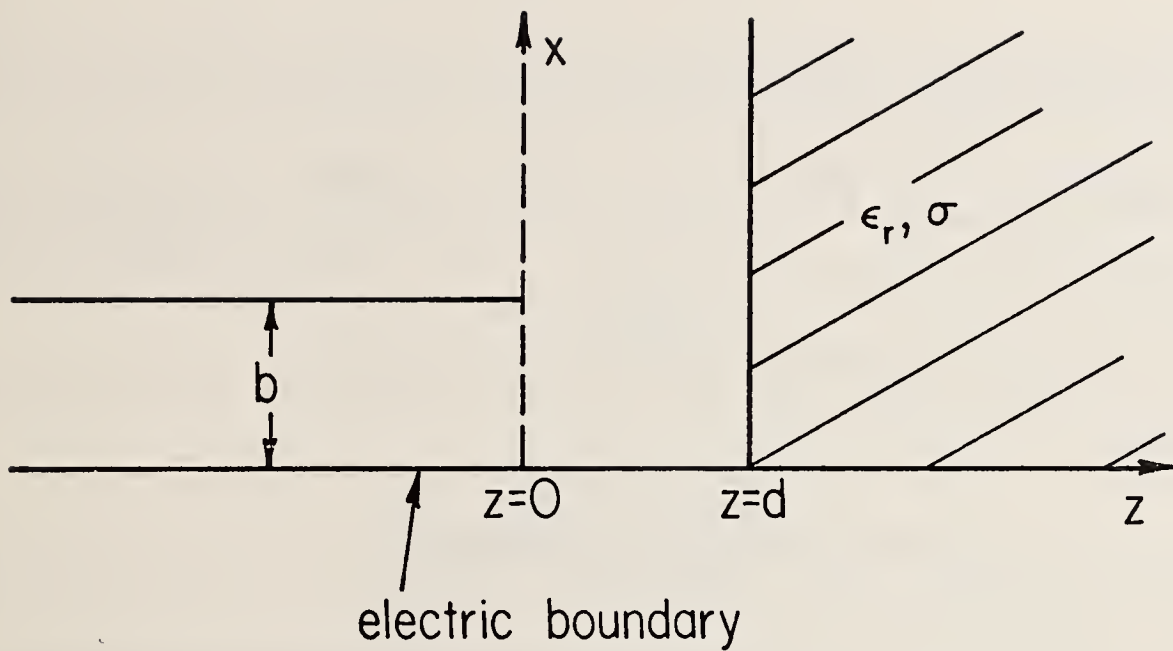$$g^{(2)}(\omega) = \omega \sin \lambda b \, A^o(\lambda), \quad \omega \varepsilon L_2 \tag{2.3}$$

Fig. 9.2.1:   Parallel Plate Waveguide Radiating into
a Homogeneous Half Space

But the spectral densities $A^o(\lambda)$ and $A(\lambda)$ are related by the reflection coefficient

$$A^o(\lambda) = A(\lambda) \ R(\lambda) \tag{2.4}$$

where

$$\Gamma = \sqrt{\lambda^2 - \epsilon k_o^2}$$

where the branch of Γ is chosen such that $\mathrm{Re}\Gamma \geq 0$. Conduction losses in the dielectric are considered by using the complex permittivity

$$\epsilon = \epsilon_r - j \ 120\pi\sigma/k_o \tag{2.4}$$

It should be noted that any layered media can be taken care of by replacing $R(\lambda)$ by its appropriate value. However, care should be taken that any new singularities introduced (i.e., poles of $R(\lambda)$) are properly taken into account. For example, when Kostelnicek and Mittra (1969) solved the case of a slab they found it necessary to shift the path of integration from L_1 to a horizontal path from jk_o to $\infty + jk_o$. A detailed study of the variation of the half space solution in the first quadrant revealed that the original path, L_1, was the best choice, since it apparently gave the smoothest solution.

Before proceeding it will prove to be convenient to change ω to $-\omega$ in the integral of (2.1) giving

$$T(\omega) = X(\omega) \left[\frac{K_o}{\omega - jk_o} - \int_{L_1^-} \frac{g^{(2)}(-t) \ dt}{X(-t)(t+\omega)} \right]$$

Now we may combine (2.2), (2.3) and (2.4) to give the following integral equation for $g^{(2)}(-\omega)$, $\omega\epsilon L_1$.

$$g^{(2)}(-\omega) = \frac{\sin \lambda b}{\pi} R(\lambda) \ e^{-j\lambda b} \ X^-(\omega)$$

$$\cdot \left[\frac{K_o}{\omega - jk_o} - \int_{L_1^-} \frac{g^{(2)}(-t) \ dt}{X(-t)(t+\omega)} \right] , \quad \omega\epsilon L_1^- \tag{2.5}$$

Considering the change of variable

$$g^{(2)}(-\omega) = \frac{K_o \ \sin \lambda b \ R(\lambda)}{\pi(\omega - jk_o)} \ e^{-j\lambda b} \ X^-(\omega) \ G(\omega)$$

we transform (2.5) to

$$G(\omega) = 1 + (\omega - jk_o) \int_{L_1^-} \frac{Q(t)G(t) \ dt}{t + \omega} , \quad \omega\epsilon L_1 \tag{2.6}$$

where

$$Q(\omega) = \frac{1}{\pi} \ \frac{\sin \lambda \ b \ R(\lambda)e^{-j\lambda b}}{(\omega - jk_o)} \ \frac{X^-(\omega)}{X(-\omega)}$$

This is the equation derived by Kostelnicek and Mittra (1971) except for a slight change in notation.

The asymptotic behavior of $G(t)$ is found by examining (2.3) and (2.4). It is easily shown that

$$Q(\omega) = 0\left[\frac{e^{-2\omega d}}{\omega}\right], \qquad |\omega| \to \infty \tag{2.7}$$

and

$$G(\omega) = 0(1), \qquad |\omega| \to \infty \tag{2.8}$$

Because of the exponential behavior of (2.7) it is not necessary to include the asymptotic behavior of $G(\omega)$ in the solution and the integration limit on L_1 can be truncated at a finite value.

The fields are readily derived from $T(\omega)$ upon having found $G(\omega)$; in particular the TEM reflection coefficient is given by

$$B_o = \frac{-T(-jk_o)}{2jk_o b} \tag{2.9}$$

3. Numerical Solution

The solution of (2.6) requires a careful examination of the integrals which must be approximated numerically. An examination of the kernal of (2.6) reveals the following:

(i) $Q(\omega)$ has zeroes of second order at $\omega = \gamma_{nb}$, $n = 1,2...$.

(ii) $Q(\omega)$ has a zero in the complex plane whenever $R(\lambda) = 0$. For a half space this occurs at the pseudo-Brewster angle given by:

$$\omega = \gamma \simeq \frac{\epsilon_r' k_o}{2(1+\epsilon_r)^{3/2}} + j \quad \frac{1}{1+\epsilon_r} k_o$$

where $\epsilon = \epsilon_r - j\epsilon_r'$ and we have assumed $\epsilon_r'/\epsilon_r \ll 1$. Note that since $\mathrm{Re}(\gamma)$ must be greater than zero on the top sheet, for $\epsilon_r' \neq 0$, this root is on the improper Riemann sheet (though it is quite close to the branch cut).

(iii)   Due to the term $\sin \lambda b$, $Q(\omega)$ goes to zero as $\sqrt{\omega-jk_o}$ as $\omega \to jk_o$.

Hence equation (2.6) is a "smooth" equation. However, upon finding $G(\omega)$ we desire to calculate the TEM reflection coefficient which in turn involves an evaluation of the integral

$$\int_{L_1^-} \frac{Q(t)G(t)\ dt}{t-jk_o} \tag{3.1}$$

From (iii) we see that as $t \to jk_o$ the integrand will behave as $1/\sqrt{t-jk_o}$. Hence, careful attention should be given to the branch point $t = jk_o$.

91

The integration was broken into a sequence of finite intervals with the end points being the waveguide propagation constants, γ_{nb}. The origin was also included as an end point. Since the first segment included the branch point the following Gaussian quadrature (Abramowitz and Stegnn, 1965) was used:

$$\int_a^b \frac{f(y)\ dy}{\sqrt{b-y}} = \sqrt{b-a} \sum_{i=1}^n \omega_i f(y_i) \qquad (3.2)$$

where

$$y_i = a + (b-a)x_i$$

where $x_i = 1 - \xi_i^2$ and ξ_i is the ith positive zero of $P_{2n}(x)$ and $w_i = 2n_i^{(2n)}$ where $w_i^{(2n)}$ are the Gaussian weights of order $2n$. Equation (3.2) allows the square root singularity to be taken care of quite satisfactorily hence allowing a good approximation of (3.1). Although this effectively increases the order of the integrand of (2.6) slightly, no degradation of convergence was observed.

Between the remaining end points regular Gaussian quadrature was employed.

It should be noted that Itoh and Mittra (1971) used a pulse function basis with the exception of the vicinity of the branch point.

4. Numerical Results

Table 9.4.1 illustrates the convergence of the TEM reflection coefficient as a function of the number of internals, N, and the number of points, M_n, within the nth interval for the case $k_o b = 1.2566$, $k_o d = 3.14159$, $\varepsilon_r = 10$, $\sigma/k_o = 0.001$.

Table 9.4.1 Convergence of Reflection Coefficient for a Parallel Plate
Waveguide Radiating into a Half Space.

N	M_1	M_2	M_3	B_o	
3	2	2	2	0.5397	63.22°
3	4	4	4	0.4366	65.51°
3	8	4	4	0.4385	65.46°
3	8	8	8	0.4379	66.11°
3	16	8	8	0.4385	66.14°
3	16	16	16	0.4386	66.16°
	with no dielectric			0.2846	88.42°

Note that the reflection coefficient converges quite fast and four place accuracy is achieved with as few as 32 matching points. However, quite acceptable accuracy is achieved with as few as 16 points. This appears to be a considerable savings over Kostelnicek and Mittra (1969), although they used an alternate path of integration on which the solution varied greater than on the path L_1, though they did avoid the poles of $R(\lambda)$.

Figure 9.4.1 illustrates the behavior of $G(\omega)$ for the example whose results are given in Table 9.4.1. Note that the asymptotic behavior given by (2.8) is quickly achieved beyond $\omega = 0.6$. The most radical behavior occurs near the origin; however, even this change is less than 10%. Notice that $G(\omega)$ is quite well behaved at $\omega \simeq 0.3$, which is the location of the pseudo-Brewster angle. Note also that $G(\omega)$ is well behaved near $\omega = \gamma_{1b}$. The phase of $G(\omega)$ was a maximum of $8°$ near the origin, with a nominal value of less than a degree.

Since the distance between the half space and the waveguide was a half wavelength, the exponential decay along L_1 was sufficient to restrict matching intervals to no more than three.

Another case is given in Table 9.4.2 where the waveguide width has been increased to $k_o b = 4.7124$, and the distance from the waveguide to half space has been decreased to $k_o d = 0.5$ ($d \simeq 0.08\lambda$). The parameters of the dielectric are still $\epsilon_r = 10$ and $\sigma/k_o = 0.001$.

Table 9.4.2 Convergence of Reflection Coefficient for a Parallel Plate Waveguide Radiating into a Half Space.

N	M_1	M_2	M_3	M_4	M_5	M_6	M_7	B_o	
6	2	2	2	2	2	2	--	0.4333	-49.68°
6	4	4	4	4	4	4	--	0.4410	-50.16°
6	8	8	8	4	4	4	--	0.4408	-50.13°
6	8	8	8	8	8	8	--	0.4408	-50.13°
6	16	8	8	4	4	4	--	0.4408	-50.13°
7	8	8	8	8	8	8	8	0.4408	-50.12°
-------- with no dielectric --------								0.0616	82.62°

More matching intervals are necessary because the waveguide width is greater as well as the distance, d, being smaller. Four place accuracy is again achieved with excellent results being achieved with as few as 24 matching points.

The solution of a related problem of the radiation of a parallel plate waveguide into a perfectly conducting sheet has been solved using wedge diffraction techniques (Ruddack, Tsai, and Burnside, 1969). Figure 9.4.2 illustrates good agreement between this theory (with $R(\lambda) = e^{-2\gamma d}$) and the wedge diffraction results. However, it should be expected that our result should be better when d/λ is less than $0.15\ \lambda$. (It should be noted that Ruddack's data is subject to the error of reading graphical data.)

Figure 9.4.3 shows the variation of the reflection coefficient of a $0.4\ \lambda$ waveguide as a function of distance to the half space for three sets of permittivity and conductivity. Note that quite significant deviations from the free space case are observed, with the deviations becoming larger as the distance, d, is decreased.

Figure 9.4.4 illustrates the variation of the reflection coefficient of a $0.4\ \lambda$ waveguide as a function of the half space parameters at a constant distance, d, of $0.1\ \lambda$. Note that quite significant changes in the reflection coefficient as the permittivity and conductivity vary. In order to more fully understand Figure 9.4.4, Figure 9.4.5 illustrates the variation of the Fresnel reflection coefficient at the half space interface for normal incidence. Figure 9.4.6 shows the data of Figure 9.4.4, after the substraction of a parallel
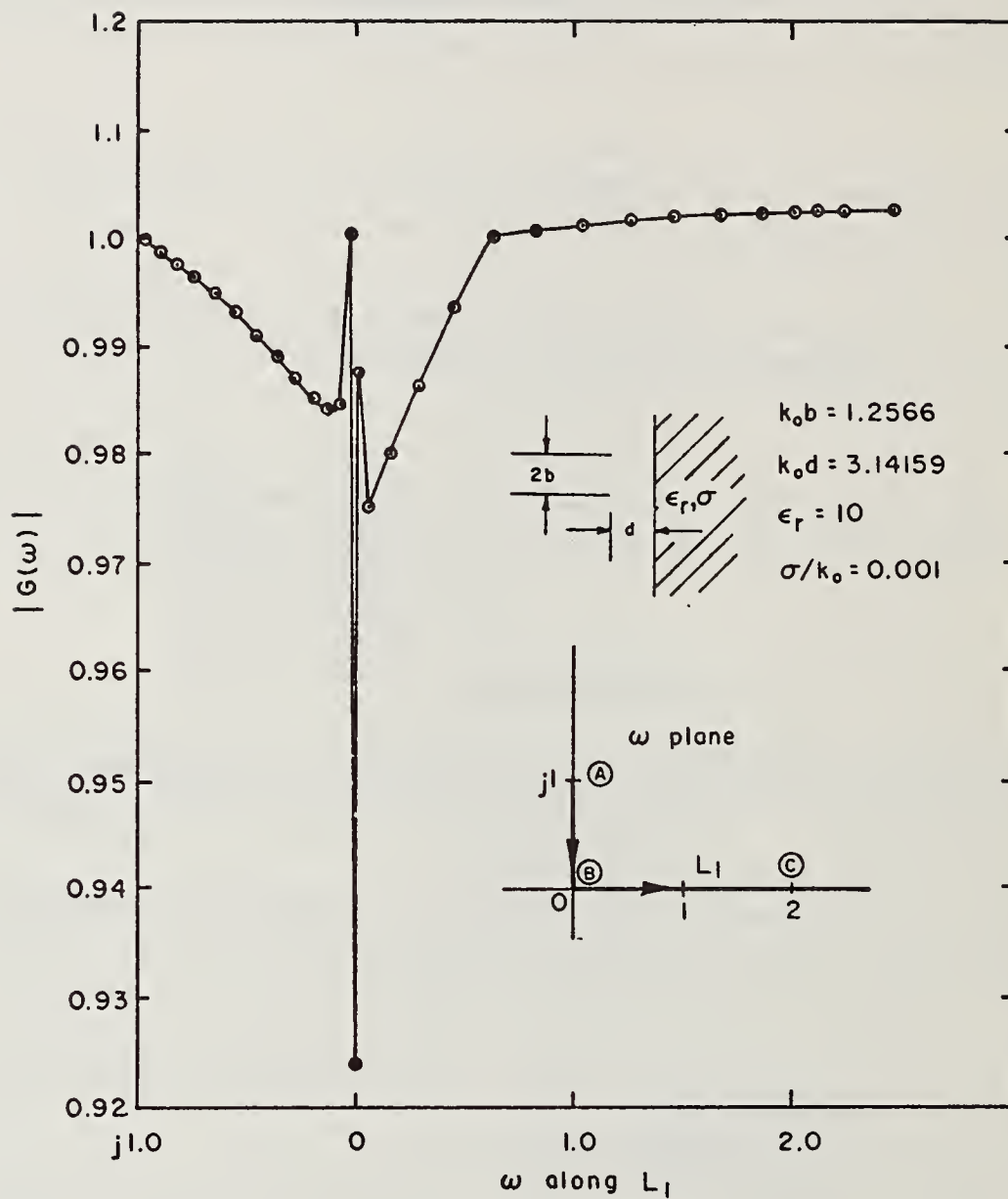
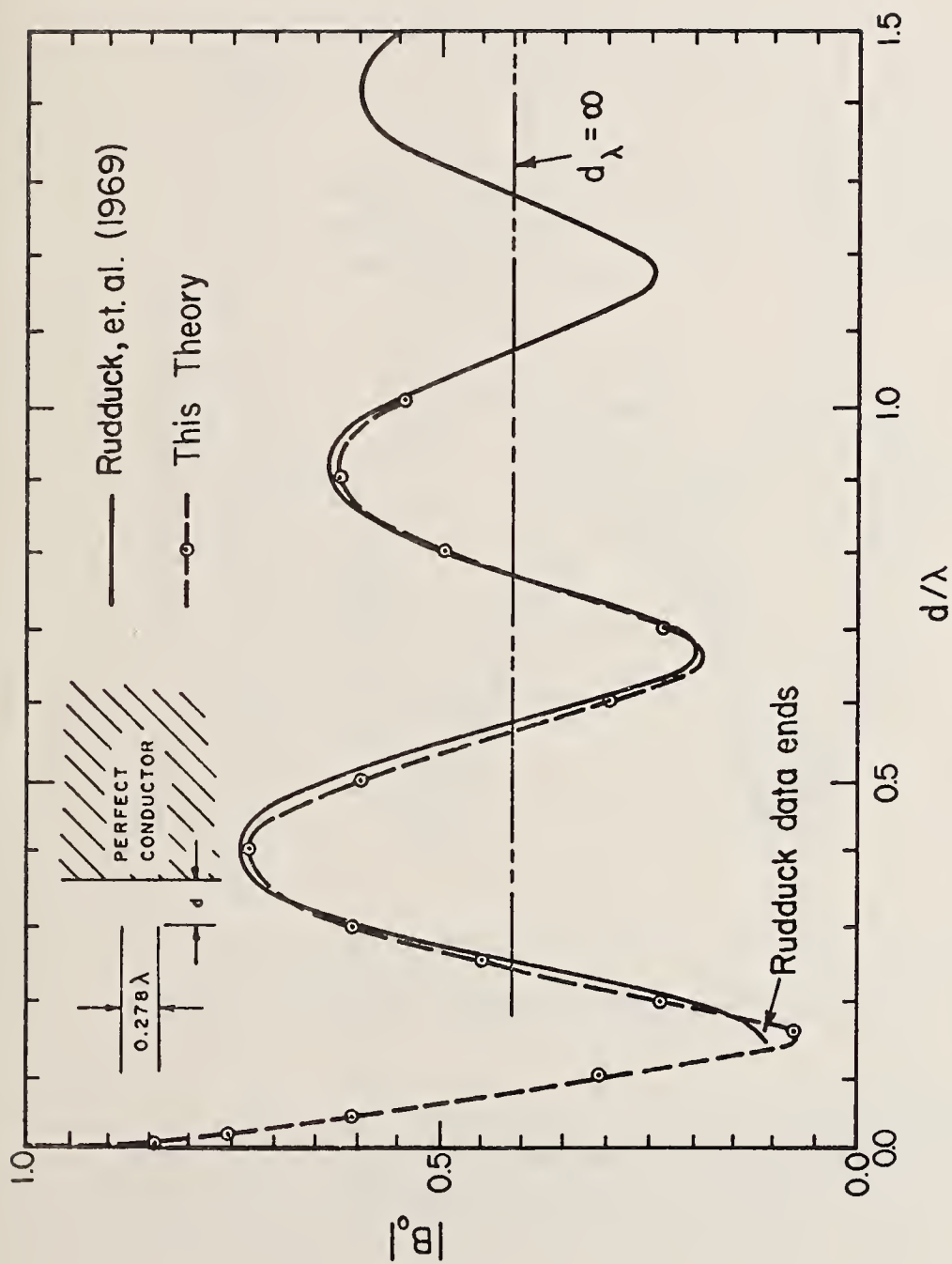Fig. 9.4.1: Variation of the Perturbation Spectrum
along L_1

Fig. 9.4.2: Reflection Coefficient of a Parallel Plate Waveguide Radiating into a Perfectly Conducting Sheet as a Function of the Distance from the Aperture to the Conductor
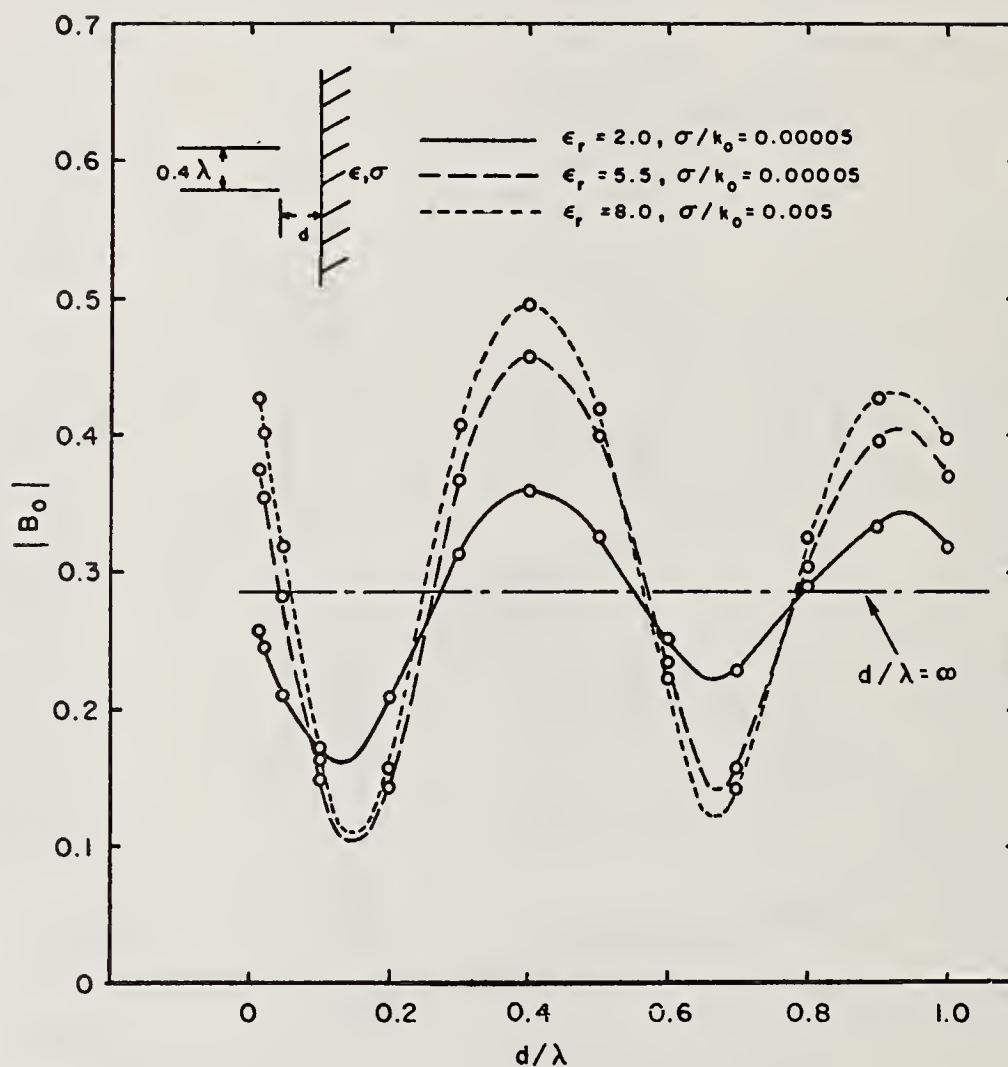
Fig. 9.4.3a: Variation of the Reflection Coefficient of a Parallel Plate Waveguide Radiating into a Dielectric Half Space as a Function of Distance and Dielectric Parameters
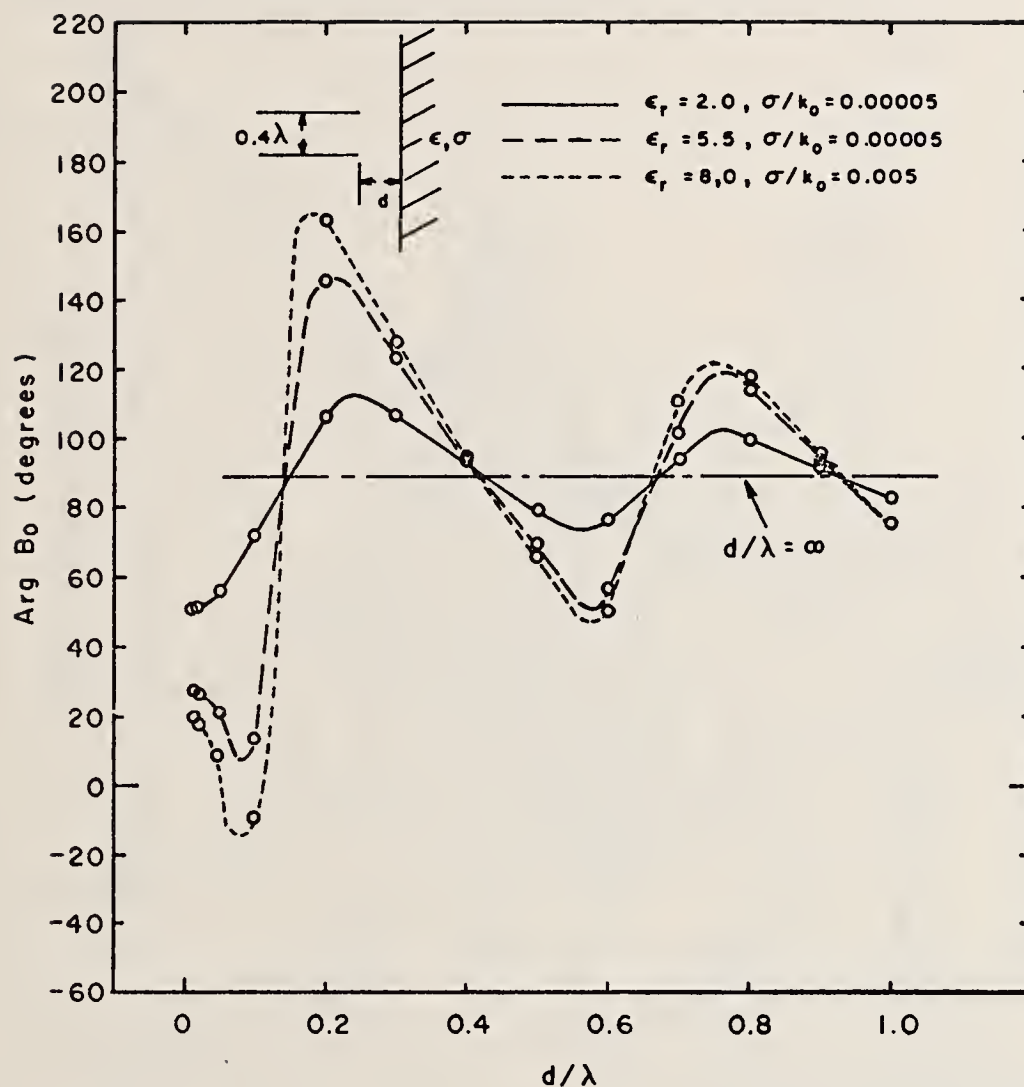
96

Fig. 9.4.3b: Variation of the Reflection Coefficient of a Parallel Plate Waveguide Radiating into a Dielectric Half Space as a Function of Distance and Dielectric Parameters
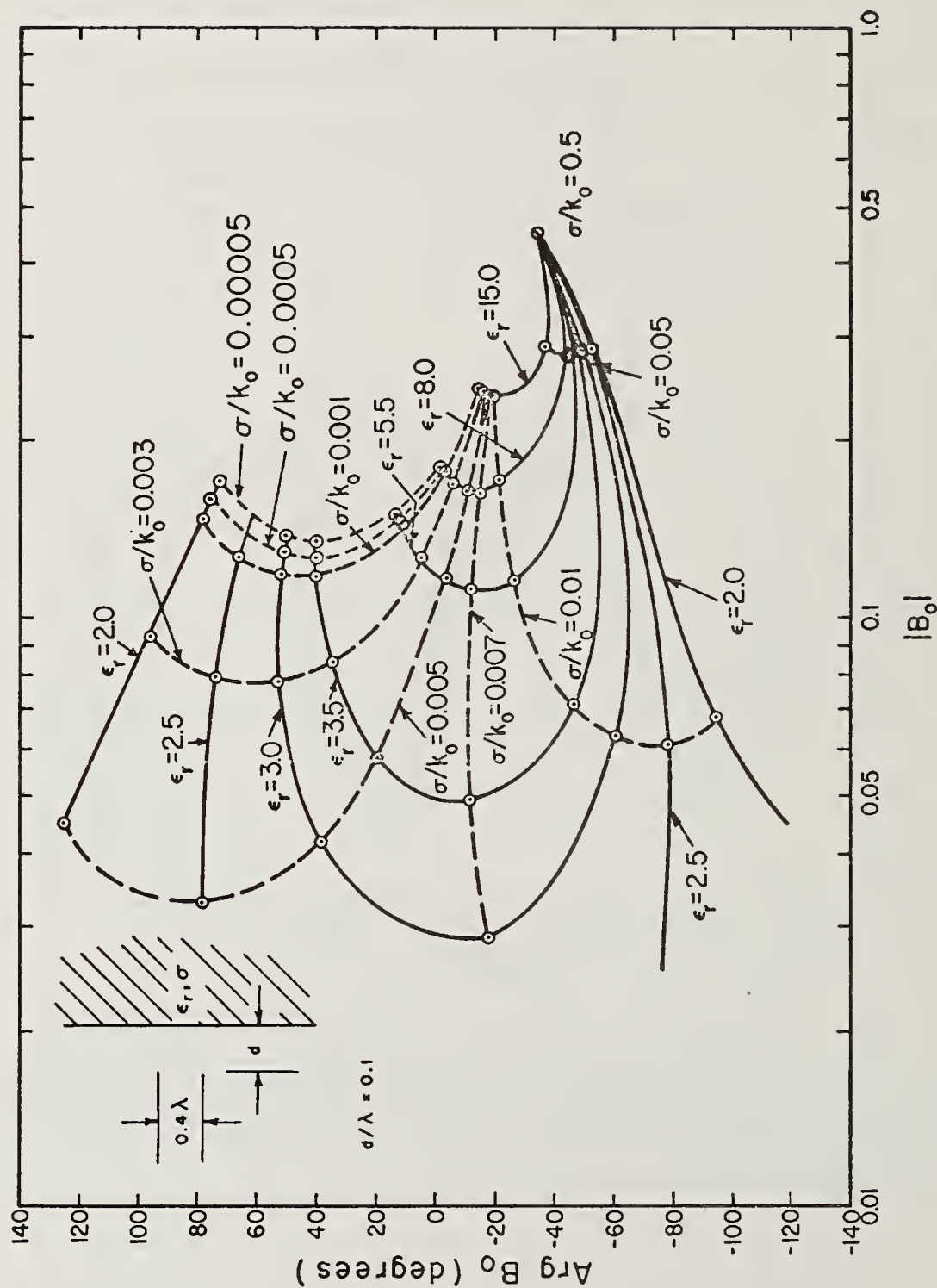
97

Fig. 9.4.4: Reflection Coefficient of a Parallel Plate Waveguide Radiating into a Dielectric Half Space as a Function of the Dielectric Parameters
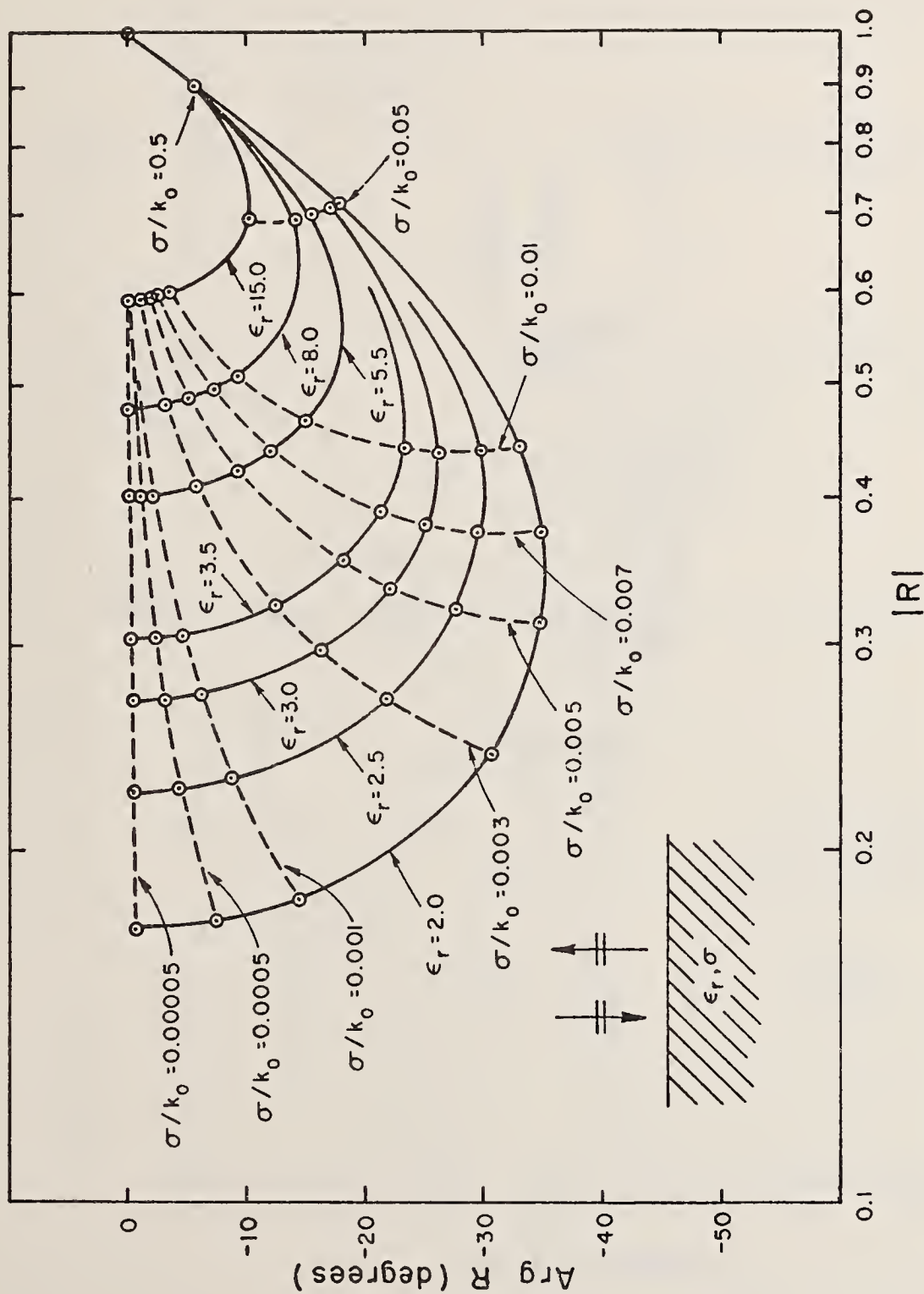
98

Fig. 9.4.5: Fresnel Current Reflection Coefficient as
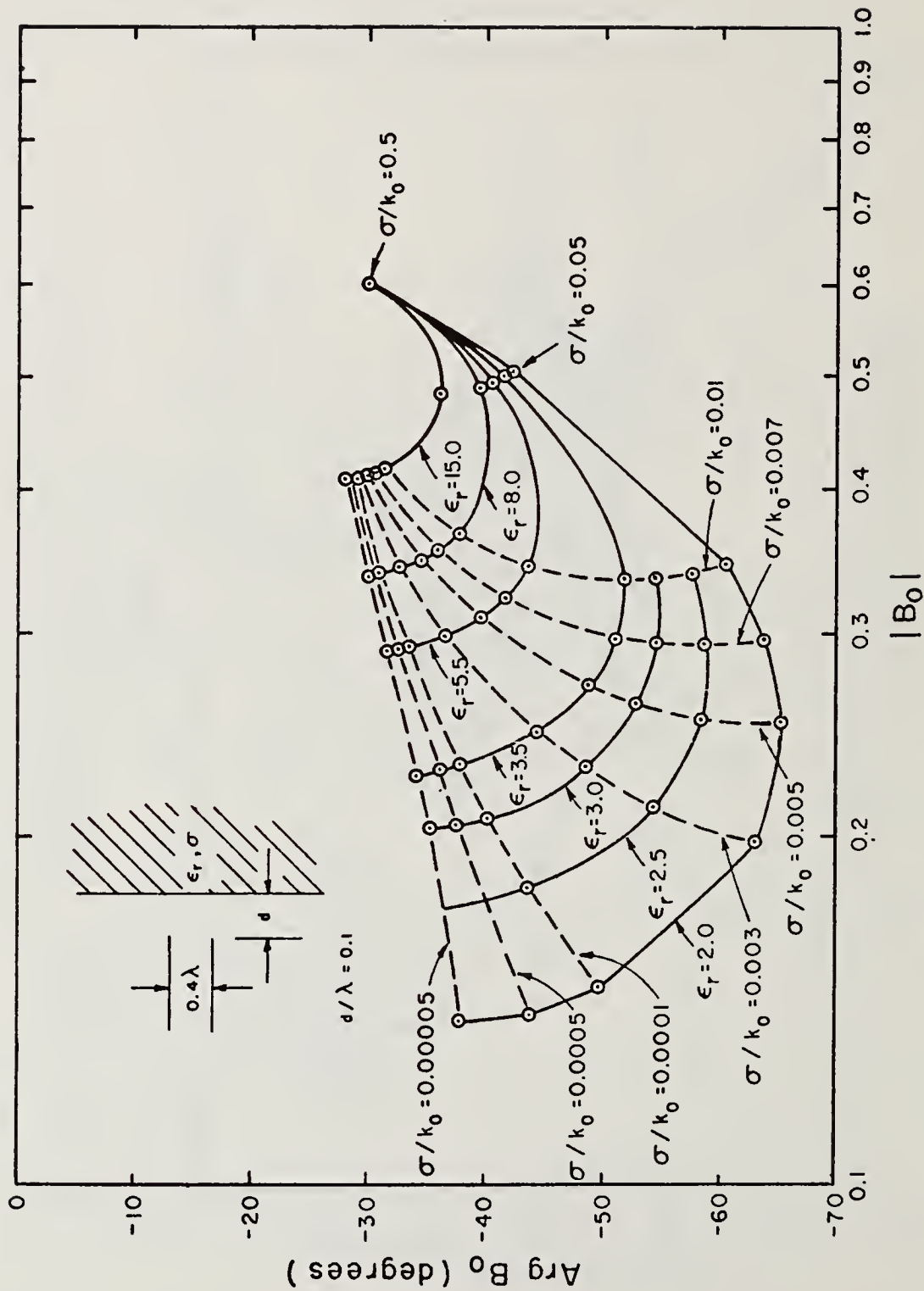a Function of Dielectric Parameters

Fig. 9.4.6: Matched Reflection Coefficient of a Parallel
Plate Waveguide Radiating into a Dielectric
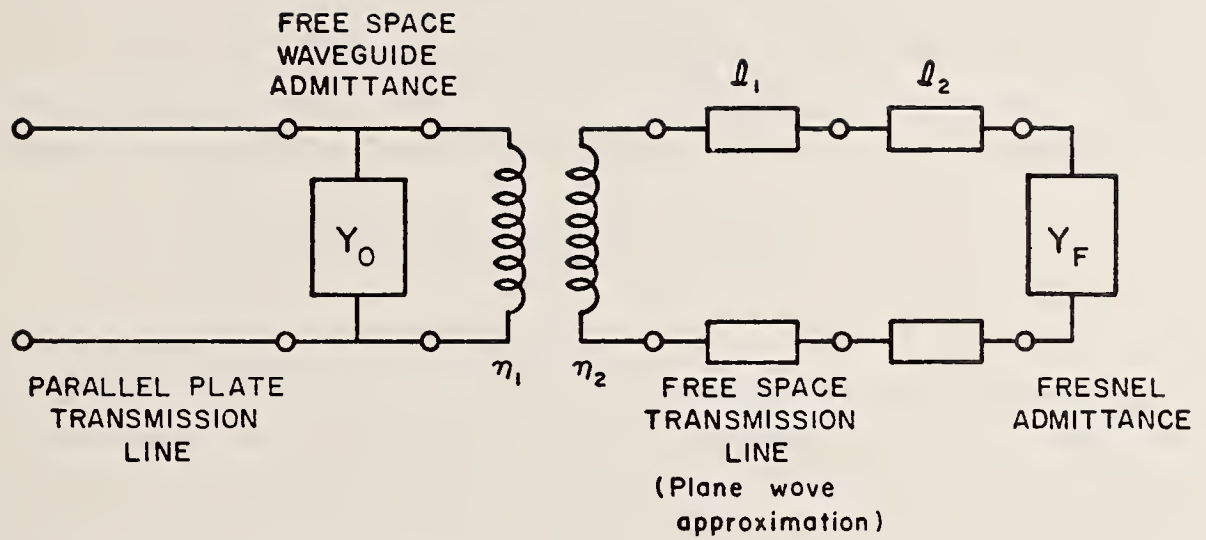Half Space as a Function of the Dielectric
Parameters

100

FREE SPACE
WAVEGUIDE
ADMITTANCE

Y_0

n_1

PARALLEL PLATE
TRANSMISSION
LINE

l_1

l_2

Y_F

n_2

FREE SPACE
TRANSMISSION
LINE
(Plane wove
approximation)

FRESNEL
ADMITTANCE

Fig. 9.4.7: Approximate Equivalent Circuit

101

impedance of a single isolated waveguide radiating into free space. The similarity of the data of Figure 9.4.6 with the Fresnel reflection coefficient is now obvious. Figure 9.4.7 suggests the possibility of establishing an equivalent circuit for a waveguide radiating into a half space. The transformer allows for the scale change and is dependent on the waveguide width 2b and the distance d primarily. The line length, ℓ_1, is just the physical electrical distance $2k_o d$. The second line length, ℓ_2, is a rather complicated function of ϵ, σ, and d. For a given height it is possible to arrive at empirical formulas for the circuit parameters. This would suggest that the more complicated structures such as rectangular and circular waveguides radiating into a half space can be modeled with approximate equivalent circuits, with the parameters of the circuits being determined experimentally.

CHAPTER 10. A FINITE PHASED ARRAY

1. Introduction

Waveguide phased arrays have received much attention in the last few years because of properties such as fast scan capabilities, multimode operation, and reliability. Perhaps the easiest analysis of planar phased arrays has been the application of Floquet's theorem to an infinitely periodic array (Amitay, Galindo, and Wu; 1972). However, many arrays are small enough that such an analysis is not valid. For finite arrays, one common method of analysis has been the moment method. One common approximation in these studies has been the assumption of an infinitely large perfectly conducting ground plane (or some approximation to it). It is the purpose of this chapter to sue the modified function theoretic technique to study a finite phased array with no ground plane. It should be noted that this analysis could also be easily applied to a finite array with a ground plane of finite or infinite extent.

2. Formulation of the Equations

2.1 Introduction

For simplicity in the solution we will assume that the array has a symmetry plane parallel to the waveguide walls. This is not a limitation of theory but is only a convenience. The solution of a completely aperiodic array can be found in a straightforward manner.

Thus we will consider the solution of the two problems illustrated in Figures 10.2.1 and 10.2.2, the only difference being the symmetry wall boundary condition.
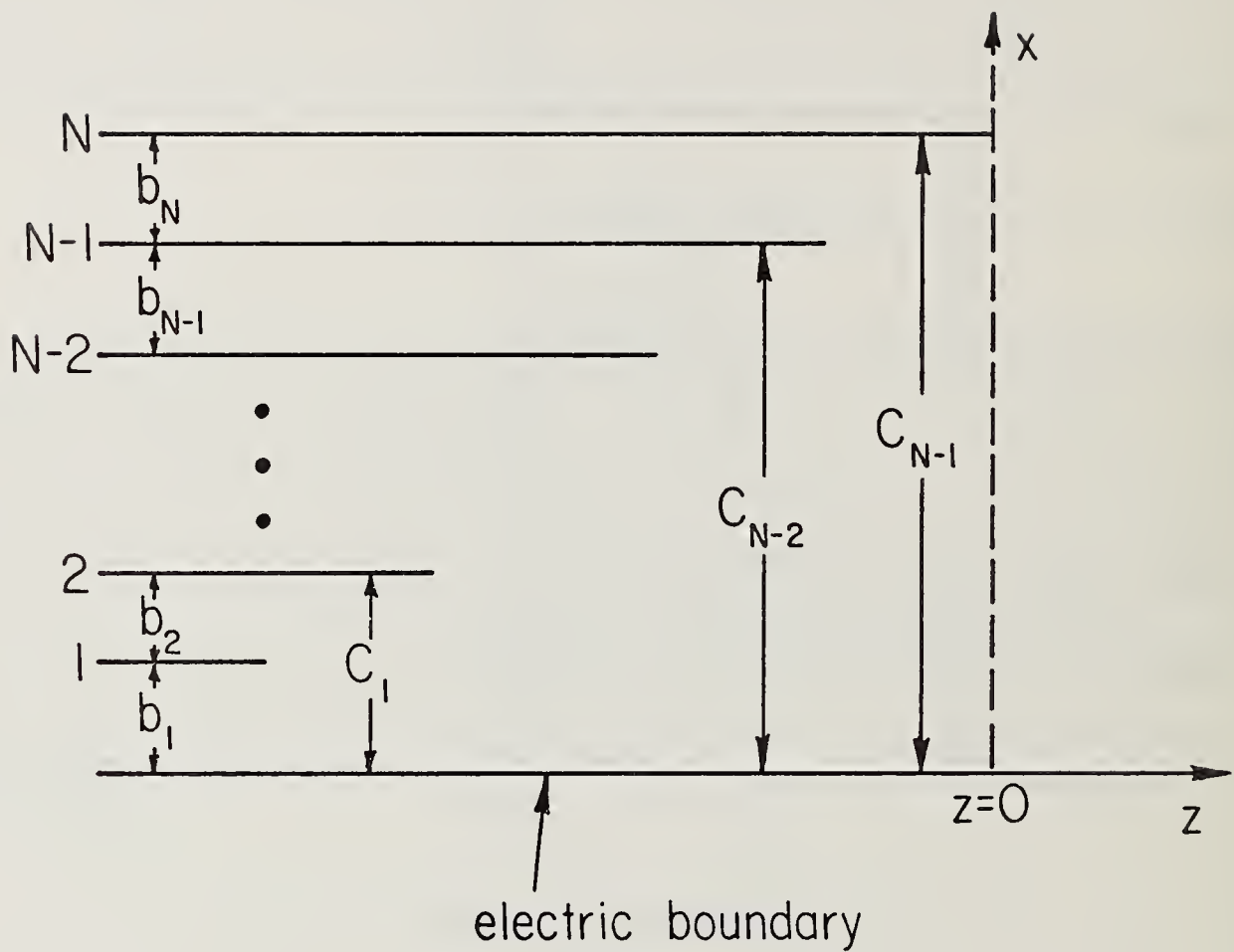
2.2 The Electric Symmetry Wall

Figure 10.2.1b also illustrates the auxiliary problem. Note that the problem can be further separated into two kinds of problems: (1) the interior problem, and (2) the exterior problem. The interior problem is the one associated with the first N-1 plates, and is solved using the theory of Chapter 2 for modifications of the bifurcated waveguide.
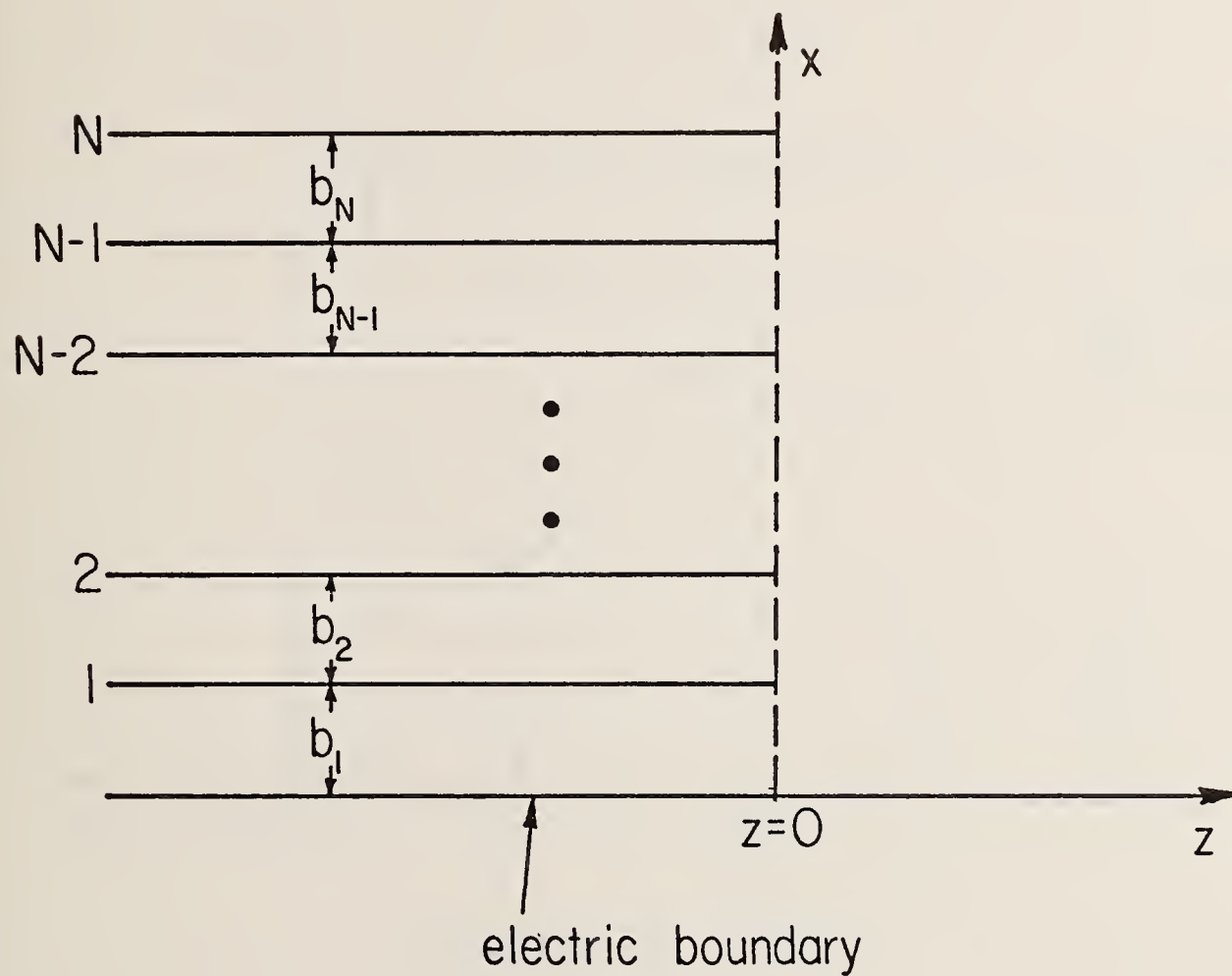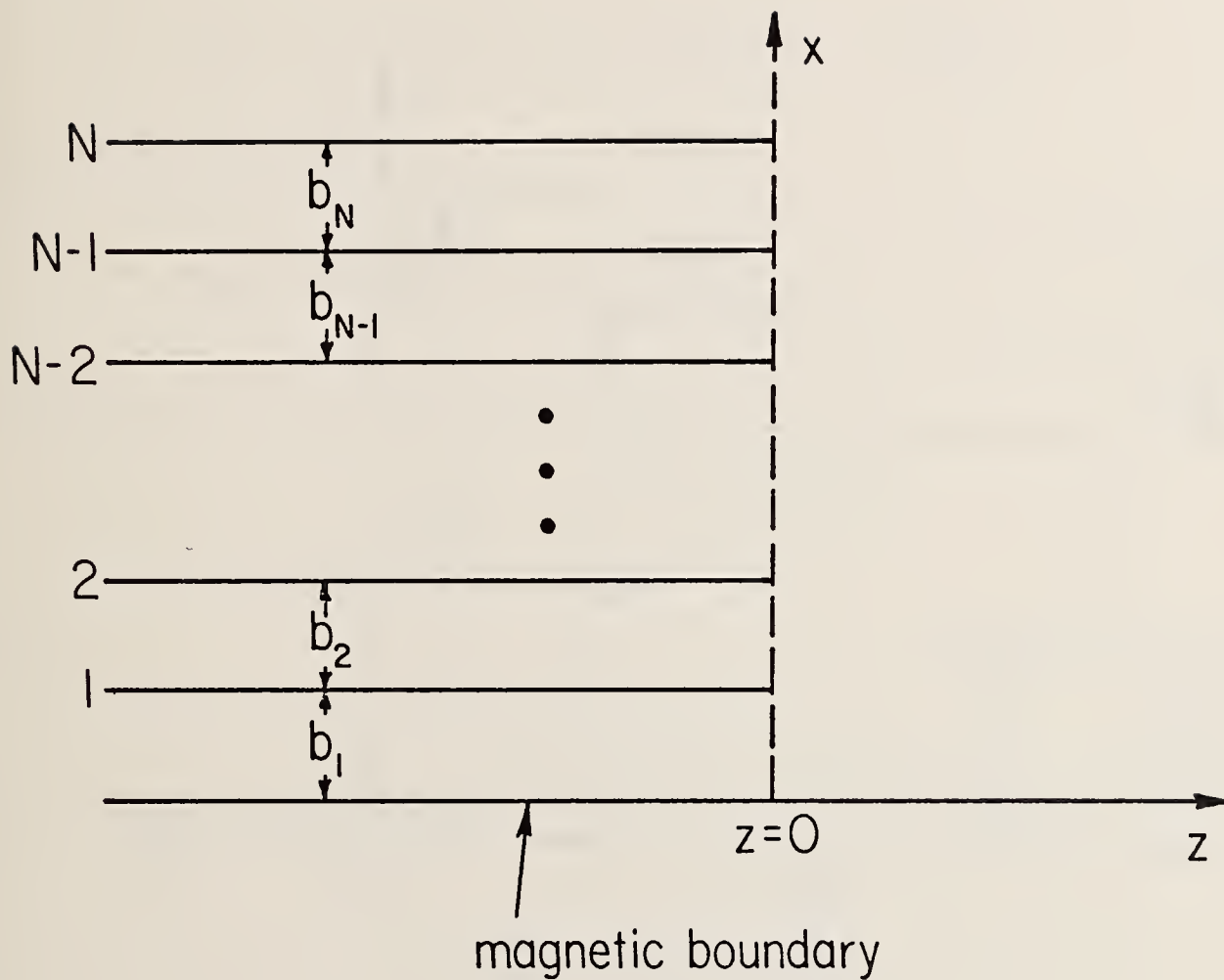
(a) Final Geometry

Fig. 10.2.1: The Finite Array with an Electric Symmetry
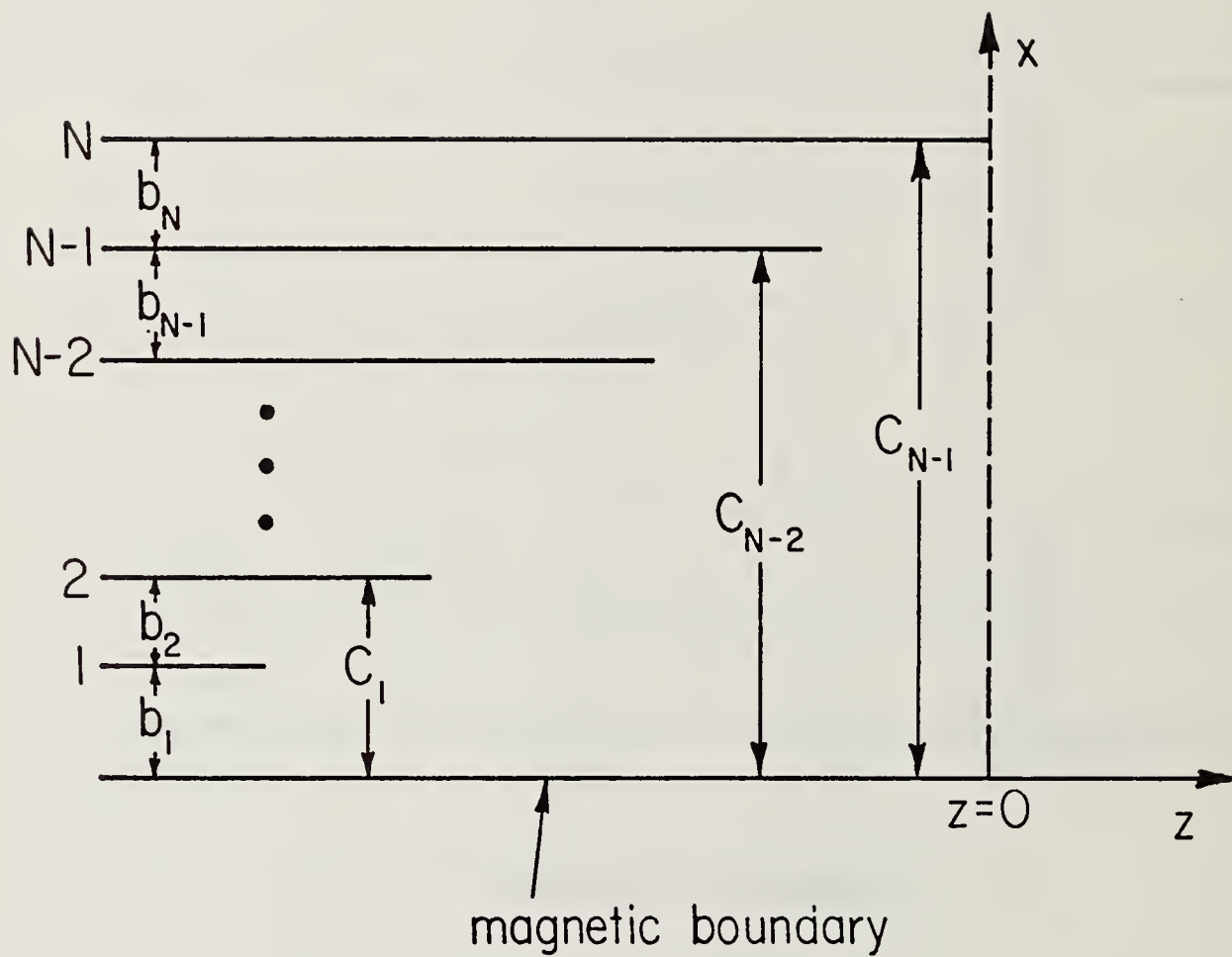Boundary

(b)   Auxiliary Geometry

Fig. 10.2.1:   The Finite Array with an Electric Symmetry
Boundary

(a) Final Geometry

Fig. 10.2.2: The Finite Array with a Magnetic Symmetry Boundary

(b)   Auxiliary Geometry

Fig. 10.2.2:   The Finite Array with a Magnetic Symmetry
Boundary

The exterior problem is the one associated with the Nth plate. This is seen to be just semi-infinite waveguide with an internal modification. With these thoughts in mind we can write the following N holomorphic functions:

$$T_1(\omega) = F_1(\omega)\left[K_o^{(1)} - (\omega - jk_o)\sum_{n=1}^{\infty}\frac{g_n^{1,R}}{\omega + \gamma_{n,c_1}}\right],$$
(2.2.1)

$$T_M(\omega) = F_M(\omega)\left[K_o^{(M)} - (\omega - jk_o)\left\{\sum_{n=1}^{\infty}\frac{g_n^{M,R}}{\omega + \gamma_{n,c_M}} + \sum_{n=1}^{\infty}\frac{g_n^{M,L}}{\omega - \gamma_{n,c_{M-1}}}\right\}\right],$$
(2.2.2)

where $M = 2,3,\ldots,N-1$, and

$$T_N(\omega) = X(\omega)\left[K_o^N + (\omega - jk_o)\sum_{n=1}^{\infty}\frac{g_n^{N,L}}{\omega - \gamma_{n,c_{N-1}}}\right],$$
(2.2.3)

In equations (2.2.1) and (2.2.2), $F(\omega)$ is given by

$$F_1(\omega) = H_1(\omega)\frac{\Pi(\omega,\gamma_{b_1})\Pi(\omega,\gamma_{b_2})}{\Pi(\omega,\gamma_{c_1})}$$

where

$$H_1(\omega) = \exp\left\{\frac{-\omega}{\pi}[b_1\ln b_1/c_1 + b_2\ln b_2/c_1]\right\}$$

and

$$F_M(\omega) = H_M(\omega)\frac{\Pi(\omega,\gamma_{c_{M-1}})\Pi(\omega,\gamma_{b_{M+1}})}{\Pi(\omega,\gamma_{c_M})}$$

where

$$H_M(\omega) = \exp\left\{\frac{-\omega}{\pi}[c_{M-1}\ln c_{M-1}/c_M + b_{M+1}\ln b_{M+1}/c_M]\right\}$$

In equation (2.2.3), $X(\omega)$ is the homogeneous solution given in Chapter 8 for a semi-infinite waveguide with a half height of c_{N-1}, divided by $(\omega - jk_o)$

From Chapter 2, we see that we can write the following equations:

$$(-1)^{n+1}T_M(-\gamma_{n,c_{M-1}}) = \gamma_{n,c_{M-1}}c_{M-1}[K_n^{M-1,R}]^{-1}g_n^{M-1,R},$$
(2.2.4)

where $M = 2, 3, \ldots, N-1$, and

$$K_n^{M,R} = \frac{-n\pi}{c_M} \sin \frac{n\pi \, c_{M-1}}{c_M} \Big/ [F_M(-\gamma_{n,c_M})(\gamma_{n,c_M}+jk_o)]$$

Also for $M = 1, 2, 3, \ldots, N-2$, we have

$$\text{RES}[T_M, \gamma_{n,c_M}] = \frac{-n\pi}{c_M} \sin \frac{n\pi \, c_{M-1}}{c_M} [K_n^{M+1,L}]^{-1} g_n^{M+1,L} \qquad (2.2.5)$$

where

$$K_n^{M,L} = (-1)^n \gamma_{n,c_{M-1}}^2 \, c_{M-1} \Big/ [F_M^{(n)}(\gamma_{n,c_{M-1}})(\gamma_{n,c_{M-1}}-jk_o)] \qquad (2.2.6)$$

where $F_M^{(n)}(\gamma_{n,c_{M-1}})$ implies that the zero at $\gamma_{n,c_{M-1}}$ is omitted from the infinite product.
For the case $M = N-1$, (2.2.5) becomes

$$\text{RES}[T_{N-1}, \gamma_{n,c_{N-1}}] = \frac{-n\pi}{c_{N-1}} \sin \frac{n\pi \, c_{N-2}}{c_{N-1}} [K_n^{N,L(o)}]^{-1} g_n^{N,L} \qquad (2.2.7)$$

where

$$K_n^{N,L(o)} = (-1)^n \gamma_{n,c_{N-1}}^2 \, c_{N-1} \Big/ [X^{(n)}(\gamma_{n,c_{N-1}}) \cdot (\gamma_{n,c_{N-1}}-jk_o)]$$

where $X^{(n)}(\gamma_{n,c_{N-1}})$ implies that the zero at $\gamma_{n,c_{N-1}}$ is omitted from the infinite product.
Equation (2.2.7) is found by using property (i) of Chapter 8 in conjunction with the results
of Chapter 2. From property (v) of Chapter 8 and the results of Chapter 2, we also have that

$$T_N(-\gamma_{n,c_{N-1}}) = (-1)^n \gamma_{n,c_{N-1}} \, c_{N-1} [K_n^{N-1,R}]^{-1} g_n^{N-1,R} \qquad (2.2.8)$$

Equations (2.2.4)-(2.2.8) represent an infinite set of simultaneous equations for the pertur-
bation coefficients, $g_n^{M,L}$ ($M = 2,3,\ldots,N$) and $g_n^{M,R}$ ($M = 1,2,\ldots,N-1$). Note that the recession
of plates in the solution of the closed region case is opposite to the recession chosen in
Chapters 3 and 4. However, this is only a minor change as will be discussed later in this
chapter.

For this particular problem, $K_o^{(M)}$ ($M = 1,2,\ldots N$) are known and can be related to the
incident TEM modal coefficients as follows (ref. Chapter 2):

$$K_o^{(1)} = 2jk_o b_2 [U_1 - B_{o,2}^{(o)}]/F_1(jk_o) \qquad (2.2.9)$$

where

$$U_1 = \frac{b_2}{c_1} B_{o,2}^{(o)} + \frac{b_1}{c_1} B_{o,1}^{(o)}$$

and where $B_{o,n}^{(o)}$ is the incident TEM modal coefficient from the nth waveguide above the sym-metry boundary. Also

$$K_o^{(2)} = 2jk_o b_3 [U_2 - B_{o,3}^{(o)}]/F_2(jk_o)$$

where

$$U_2 = \frac{b_3}{c_2} B_{o,3}^{(o)} + \frac{c_1}{c_2} U_1$$

and in general for M up to N-1, we have

$$K_o^{(M)} = 2jk_o b_{M+1} [U_M - B_{o,M+1}^{(o)}]/F_M(jk_o) \qquad (2.2.10)$$

where

$$U_M = \frac{b_{M+1}}{c_M} B_{o,M+1}^{(o)} + \frac{c_{M-1}}{c_M} U_{M-1}$$

And for the case M=N, we have

$$K_o^{(N)} = -2jk_o c_{N-1} U_{N-1}/X(jk_o) \qquad (2.2.11)$$

where

$$U_{N-1} = \frac{b_N}{c_{N-1}} B_{o,N}^{(o)} + \frac{c_{N-2}}{c_{N-1}} U_{N-2}$$

In order to solve (2.2.4)-(2.2.8) efficiently, we are motivated to investigate the asymptotic behavior of the various perturbation coefficients. This procedure is essentially identical to that discussed in Chapters 3 and 4 and thus only the results will be presented.

As in Chapters 3 and 4, we can find that only a single asymptotic perturbation term is necessary for the right perturbation terms, that is, we will replace $g_n^{M,R}$ by the following for $n > N^{M,R}$.

$$g_n^{M,R} = \overline{g}^{M,R} (-1)^n n^{-1} \sin \frac{n\pi}{c_M} c_{M-1} \qquad (2.2.12)$$

where M = 1,2,...,N-1. Notice that since $c_{M-1} = c_M - b_{M+1}$, (2.2.12) can also be written

$$g_n^{M,R} = -\overline{g}^{M,R} n^{-1} \sin \frac{n\pi}{c_M} b_{M+1}$$

which is in agreement with equation (3.3) of Chapter 4.

We again find that multi-term asymptotic expansions for the left perturbation terms are necessary to satisfy all of the edge conditions explicitly, namely for $n > N^{M,L}$ we will replace $g_n^{M,L}$ by the following:

$$
g_n^{M,L} = \overline{g}_1^{M,L}(-1)^n n^{-1} \sin \frac{n\pi \, b_1}{c_{M-1}}
$$

$$
+ \overline{g}_2^{M,L}(-1)^n n^{-1} \sin n\pi \frac{(b_1+b_2)}{c_{M-1}} + \cdots + \qquad (2.2.13)
$$

$$
+ \overline{g}_{M-1}^{M,L}(-1)^n n^{-1} \sin n\pi \frac{(b_1+b_2+\cdots b_{M-1})}{c_{M-1}}
$$

where $M = 2,3,\ldots,N$.

Upon the substitution of (2.2.12) and (2.2.13) into equations (2.2.1)-(2.2.3) and the subsequent substitution into (2.2.4)-(2.2.8) we arrive at an efficiently truncated linear system of equations for the perturbation coefficients.

However, we must still decide how to choose the additional equations for the asymptotic perturbation coefficients. We may, however, use the results of the truncation study of Chapters 3 and 4, and use what we call the hybrid truncation method. Essentially this choice of truncation chooses the "n+1 equation" of equations (2.2.4), (2.2.6), and (2.2.7). However, (2.2.5) is asymptotically degenerate for reasons outlined in Chapter 4. Hence, the true asymptotic form of (2.2.5) is used, yielding M+1 equations.

For brevity, we will not give the explicit form of the equations. The interested reader is instead referred to Chapter 4.

Upon finding the perturbation coefficients, the waveguide fields as well as the fields in free space are readily found using the properties of the functions as given in Chapters 2 and 8. In particular, the reflected TEM modal coefficients are given by:

$$
B_{o,M} = \frac{-T_1(-jk_o)}{2jk_o \, b_1} + \frac{T_N(-jk_o)}{2jk_o \, c_{N-1}} - \sum_{n=1}^{N-1} \frac{T_n(-jk_o)}{2jk_o \, c_{n-1}} \qquad (2.2.14)
$$

for $M = 2,3,\ldots,N$. The summation is only used for $M \leq N-1$. However, for the case $M=1$ we have

$$
B_{o,1} = \frac{-T_1(-jk_o)}{2jk_o \, b_1} + \frac{T_N(-jk_o)}{2jk_o \, c_{N-1}} - \sum_{n=2}^{N-1} \frac{T_n(-jk_o)}{2jk_o \, c_{n-1}} \qquad (2.2.15)
$$

In both (2.2.14) and (2.2.15), $B_{o,n}$ is the reflected TEM modal coefficient in the nth waveguide above the symmetry plane.

Other waveguide modal quantities can be easily found by recourse to the properties of the canonical function given in Chapters 2 and 8 and the use of the auxiliary geometry.

The far-field radiation pattern is also of interest for a finite array. From equation (2.2.16) of Chapter 8 and property (iii) of the same chapter, we can easily find that the spectral density for $z > 0$ is given by

110

$$A(\lambda) = \frac{-T_N^-(\omega)}{\pi\omega} e^{-j\lambda c_{N-1}}, \quad \omega \epsilon L_1 \tag{2.2.16}$$

Hence,

$$\phi_A(x,z) = \frac{-1}{\pi} \int_0^\infty \frac{T_N^-(\omega)}{\omega} e^{-j\lambda c_{N-1}} e^{-\omega z} \cos \lambda x \, d\lambda \tag{2.2.17}$$

This integral can easily be evaluated asymptotically in the far field using the method of steepest descents (Mittra and Lee, 1971) to give

$$\phi_A(x,z) \simeq \frac{2\pi}{k_o r} e^{-j(k_o r - \pi/4)} \left(\frac{j}{2\pi}\right) \cdot T_N^-(jk_o \cos \theta) e^{-jk_o c_{N-1} \sin \theta} \tag{2.2.18}$$

where θ is the polar angle measured from the z axis. It is interesting to note that the factor $\cos \theta$, which is present for an infinite array problem, is not present in (2.2.18).

2.3 The Magnetic Symmetry Wall

Figure 10.2.2 illustrates the geometry of interest in this section as well as the auxiliary problem. The two basic components of the solution are: (1) the bifurcated waveguide with a magnetic symmetry boundary, and (2) a semi-infinite parallel plate waveguide with a magnetic symmetry wall. The first problem's solution has been given in Appendix E, while the second problem's solution has been given in Chapter 8.

From Appendix E, we can easily find that for the first plate we have

$$T_1(\omega) = F_1(\omega) \left[K_o^{(1)} + (\omega - jk_o) \sum_{n=1}^\infty \frac{g_n^{1,R}}{\omega + \gamma_{2n-1,2c_1}} \right] \tag{2.3.1}$$

where

$$F_1(\omega) = H_1(\omega) \prod_{n=1}^\infty \frac{(1 - \omega/\gamma_{2n-1,2b_1})(1 - \omega/\gamma_{nb_2})}{(1 - \omega/\gamma_{2n-1,2c_1})}$$

where

$$H_1(\omega) = \exp\left\{ \frac{-\omega}{\pi} \left(b_1 \ln \frac{b_1}{c_1} + b_2 \ln \frac{b_2}{c_1} \right) \right\}$$

And in general we have for the Mth plate $(M = 2,3,\ldots,N-1)$

$$T_M(\omega) = F_M(\omega) \left[K_o^{(M)} + (\omega - jk_o) \left\{ \sum_{n=1}^\infty \frac{g_n^{M,R}}{\omega + \gamma_{2n-1,2c_M}} + \sum_{n=1}^\infty \frac{g_n^{M,L}}{\omega - \gamma_{2n-1,2c_{M-1}}} \right\} \right] \tag{2.2.2}$$

where

111

$$F_M(\omega) = H_M(\omega) \prod_{n=1}^{\infty} \frac{(1-\omega/\gamma_{2n-1,2c_{M-1}})(1-\omega/\gamma_{n,b_{M+1}})}{(1-\omega/\gamma_{2n-1,2c_M})}$$

where

$$H_M(\omega) = \exp\left\{\frac{-\omega}{\pi}\left(c_{M-1}\ln\frac{c_{M-1}}{c_M} + b_{M+1}\ln\frac{b_{M+1}}{c_M}\right)\right\}$$

For the Nth semi-infinite plane, we use the results of Chapter 8 and easily find that

$$T_N(\omega) = \dot{X}(\omega) \sum_{n=1}^{\infty} \frac{g_n^{N,L}}{\omega-\gamma_{2n-1,2c_{N-1}}} \qquad (2.3.3)$$

where $X(\omega)$ is the homogeneous solution of the semi-infinite parallel plate waveguide with a magnetic symmetry wall.

We may arrive at simultaneous equations for the perturbation coefficients by a similar manner used in the previous section and in Chapter 2. That is, we require that the expressions for the same modal coefficient in a given region of the auxiliary problem be consistent, whichever holomorphic function is used.

Hence we may find for $M = 1,2,\ldots,N-2$

$$\text{RES}[T_M,\gamma_{2n-1,2c_M}] = k_{n,c_M}\cos(k_{n,c_M}c_{M-1})\,[K_n^{M+1,L}]^{-1}\,g_n^{M+1,L} \qquad (2.3.4)$$

where

$$k_{n,c_M} = \frac{(2n-1)\pi}{2c_M}\,,$$

$$K_n^{M,L} = \frac{(-1)^n\gamma_{2n-1,2c_{M-1}}^2\,c_{M-1}}{F_M^{(n)}(\gamma_{2n-1,2c_{M-1}})(\gamma_{2n-1,2c_{M-1}}-jk_o)}$$

and for $M = 2,3,\ldots,N$

$$(-1)^n T_M(-\gamma_{2n-1,2c_{M-1}}) = \gamma_{2n-1,2c_{M-1}}\,c_{M-1}\,[K_n^{M-1,R}]^{-1}\,g_n^{M-1,R} \qquad (2.3.5)$$

where

$$K_n^{M,R} = \frac{k_{n,c_M}\cos(k_{n,c_M}c_{M-1})}{F_M(-\gamma_{2n-1,2c_M})(\gamma_{2n-1,2c_M}+jk_o)} \qquad (2.3.6)$$

112

And from the open region part of the auxiliary geometry we find

$$\mathrm{RES}[T_{N-1}, \gamma_{2n-1,2c_{N-1}}] = k_{n,c_{N-1}} \cos k_{n,c_{N-1}} c_{N-2} \cdot [K_n^{N,L(o)}]^{-1} g_n^{N,L} \qquad (2.3.7)$$

where

$$K_n^{N,L(o)} = \frac{(-1)^{n+1} \gamma_{2n-1,2c_{N-1}}^2 c_{N-1}}{- X^{(n)}(\gamma_{2n-1,2c_{N-1}})}$$

Note that for this particular problem that $K_o^{(M)}$ is known and given by

$$K_o^{(M)} = -2jk_o b_{M+1} B_{o,M+1}^{(o)}/F_M(jk_o) \qquad (2.3.8)$$

where $M = 1,2,\ldots,N-1$ and where $B_{o,M+1}^{(o)}$ is the incident TEM modal coefficient from the M+1th waveguide. For $M = 1$, we have

$$K_o^{(1)} = -2jk_o b_2 B_{o,2}^{(o)}/F_1(jk_o) \qquad (2.3.9)$$

Note that the equations for these quantities are slightly different from equation (2.2.9) and (2.2.10) for the electric symmetry boundary case. This is due to the fact that the coupling regions of the auxiliary problem cannot support a TEM mode.

Equations (2.3.4)-(2.3.7) constitute an infinite set of linear equations for the perturbation coefficients. In order to solve these equations efficiently, we investigate the asymptotic behavior of the perturbation coefficients. Again the procedure is identical to that discussed in Chapters 3 and 4.

For $n > N^{M,R}$ we will use

$$g_n^{M,R} = \bar{g}^{M,R} n^{-1}(-1)^n \cos k_{n,c_M} c_{M-1} \qquad (2.3.10)$$

for $M = 1,2,\ldots,N-1$. Similarly, for $n > N^{M,L}$ we will use

$$\begin{aligned}
g_n^{M,L} = \bar{g}_{M-1}^{M,L} n^{-1}(-1)^n \cos k_{n,c_{M-1}} b_1, \\
+ \bar{g}_{M-2}^{M,L} n^{-1}(-1)^n \cos k_{n,c_{M-1}} (b_1+b_2) \qquad (2.3.11) \\
+ \cdots + \bar{g}_1^{M,L} n^{-1}(-1)^n \cos k_{n,c_{M-1}} (b_1+b_2+\cdots+b_{M-1})
\end{aligned}$$

With these asymptotic expressions, the proof that all of the edge conditions are satisfied explicitly follows closely to that of the electric wall case.

Upon the substitution of (2.3.10) and (2.3.11) into equation (2.3.1)-(2.3.3) and with the subsequent substitution into (2.3.4)-(2.3.7) we arrive at an efficiently truncated linear system of equations for the perturbation coefficients. The extra equations for the Mth parallel plate region follows by use of *(page 14) and the results of appendix C. We obtain from the left side of (2.3.4)

$$
\mathrm{Res}(T_M, \gamma_{2n-1,2c_M}) \sim \sqrt{\frac{2}{\pi b_{M+1} c_M}} \, (-)^n \, n^{-1/2} \, \cos[(n-\tfrac{1}{2}) \frac{\pi c_{M-1}}{c_M}] \, \sin(n-\tfrac{1}{2}) \frac{\pi b_{M+1}}{c_M} \left\{ \left(K_o + \sum_{M=1}^{N^{M,R}} g_M^{M,R} \right. \right.
$$

$$
+ \bar{g}^{M,R} \sum_{M=N^{M,R}+1}^{\infty} (-)^{M_M-1} \cos k_{M,c_M} c_{M-1} + \sum_{M=1}^{N^{M,L}} g_M^{M,L} + \sum_{j=1}^{M-1} \bar{g}_j^{M,L} \sum_{M=N^{M,L}+1}^{\infty} (-)^{M_M-1} \cos(K_{M,c_{M-1}} c_{M-j-1}) \Big)
$$

$$
+ \pi \sum_{j=2}^{M} \bar{g}_{j-1}^{M,L} \frac{\sin[(n-\tfrac{1}{2})\frac{\pi}{c_M} \sum_{\ell=1}^{j} b_{M+2} - R]}{\sin(n-\tfrac{1}{2}) \frac{\pi b_{M+1}}{c_M}} \right\}
\tag{2.3.12}
$$

from the right side of (2.3.4) we obtain

$$
k_{n,c_M} \cos(k_{n,c_M} c_{M-1})[K_n^{M+1,L}]^{-1} g_n^{M+1,L} \sim \sqrt{\frac{2\pi}{b_{M+2} c_M}} (-)^n \, n^{-\frac{1}{2}} \cos(n-\tfrac{1}{2}) \frac{\pi c_{M-1}}{c_M} \sum_{j=1}^{M} \bar{g}_j^{M+1,L} \sin(k_{n,c_M} \sum_{\ell=1}^{j} b_{M+2-j})
$$

$$
\tag{2.3.13}
$$

Equating (2.3.12) and (2.3.13) produces the extra equations in the same mannaer as in chapter 4. Again, the extra equations arise from the oscillatory terms of different arguments times the large parameter n. Note that equation (2.3.11) can be expressed as a sine sieras, placing the asymptotic result more in conformity with appendix A. The choice of the extra equations for the asymptotic perturbation coefficients is the hybrid truncation method discussed in the previous section.

For brevity, we will not give the explicit form of the extra equations. The interested reader is urged to compare the preceding with equations (3.10) and (3.11) in Chapter 4.

Upon finding the perturbation coefficients, the waveguide fields as well as the fields in free space are readily found using the properties of the functions as given in Chapters 2 and 8. In particular, the reflected TEM modal coefficients are given by:

$$
B_{o,M+1} = \frac{T_M(-jk_o)}{2jk_o b_{M+1}}
\tag{2.3.14}
$$

for M = 1,2,...,N-1, and where $B_{o,M+1}$ is the reflected TEM modal coefficient in the M+1th waveguide.

Other waveguide modal quantities can easily be found be recourse to the properties of the canonical function given in Chapters 2 and 8 and the use of the auxiliary geometry.

114

The far-field radiation pattern is also of interest for a finite array. From equation (2.3.4) of Chapter 8 and property (iii) of the same chapter, we can easily find that the spectral density for $z > 0$ is given by

$$A(\lambda) = \frac{-T_N^-(\omega)\ e^{-j\lambda c_{N-1}}}{\pi j \omega} \qquad (2.3.15)$$

Hence,

$$\phi_A(x,z) = \frac{j}{\pi} \int_0^\infty \frac{1}{\omega}\ T_N^-(\omega) e^{-j\omega c_{N-1}} e^{-\gamma z} \sin \lambda x\ d\lambda \qquad (2.3.16)$$

This integral can easily be evaluated asymptotically in the far field using the method steepest descents (Mittra and Lee, 1971) to give

$$\phi_A(x,z) \simeq \sqrt{\frac{2\pi}{k_o r}}\ e^{-j(k_o r - \pi/4)}\ \frac{j}{4\pi}\ T_N^-(jk_o \cos\theta) \cdot e^{-jk_o c_{N-1}\ \sin\theta} \qquad (2.3.17)$$

3. Numerical Results

3.1 The Electric Wall Case

This section presents the results of two studies. The first study is an examination of how the closed region results of Chapters 3 and 4 converge to the open region results. The second study considers the convergence of the open region results as a function of the number of perturbation coefficients.

Figures 10.3.1 – 10.3.1.3 illustrate the variation of the dominant mode parameters for a trifurcated waveguide with $k_o b_2 = 1.27046$, $k_o b_1 = 0.41417$, and with $k_o b_o$ variable from 0.2 to 20. (Note that the indices of the trifurcated waveguide dimensions must have 1 added to them to correspond to the current notation.) The data calculated using the open region analysis is shown for comparison. Note that of all the parameters that the reflection co-efficient of the waveguide with dimension $k_o b_1 = 0.41417$ converges the fastest. (The phase is not shown but it converged even faster with a maximum deviation of only $4°$ from the open region solution.) However, the reflection coefficient of the waveguide with $k_o b_2 = 1.27046$ converges much slower. The same is true for the coupling coefficient. All of the data is observed to oscillate about the values computed using the open region analysis.

This data reaffirms the conclusions reached by Mittra and Richardson (1970) that the closed region problem generally converges slowly to the open region problem.

Table 10.3.1.1 illustrates the convergence of some dominant mode parameters as a function of the number of perturbation coefficients ($N_p \equiv N^{M,R} \equiv N^{M,L}$) using the open region analysis for the case of $k_o b_1 = 1.27046$, $k_o b_2 = 0.41417$.
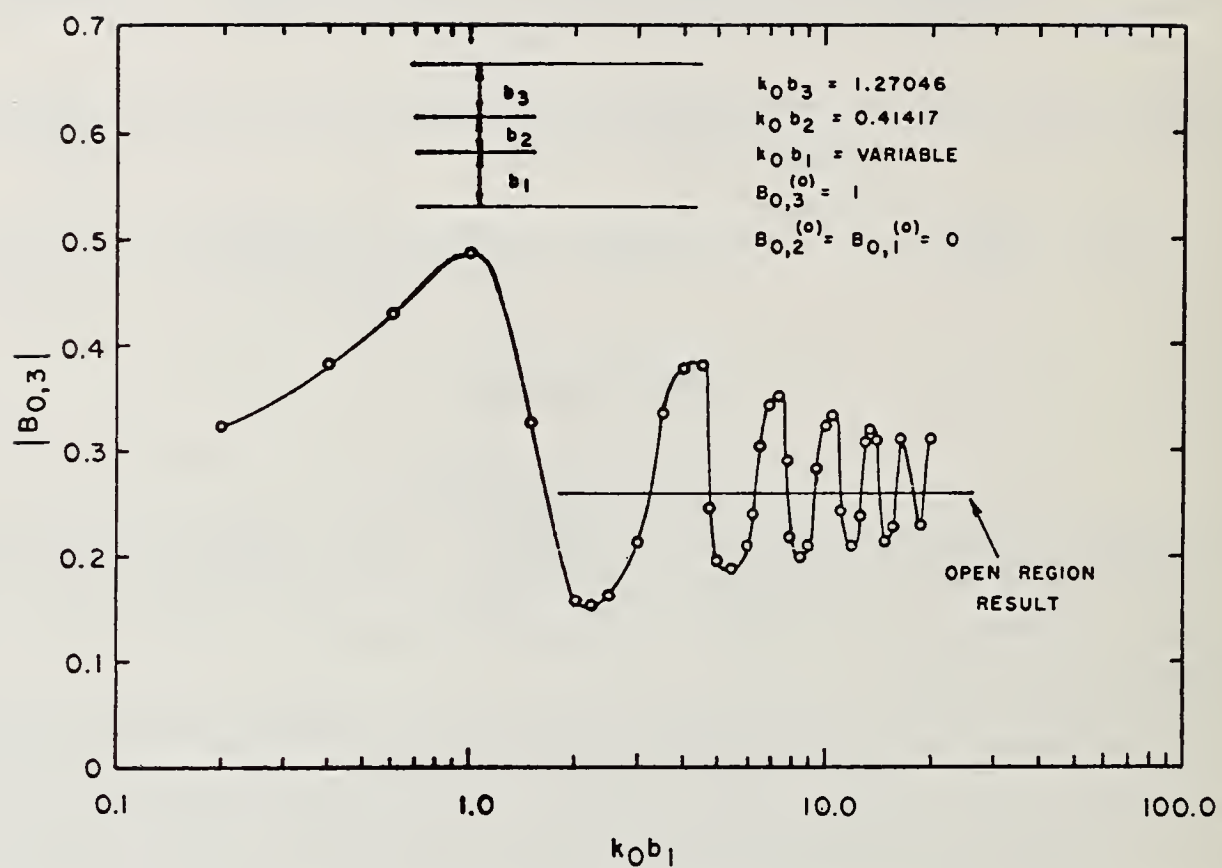
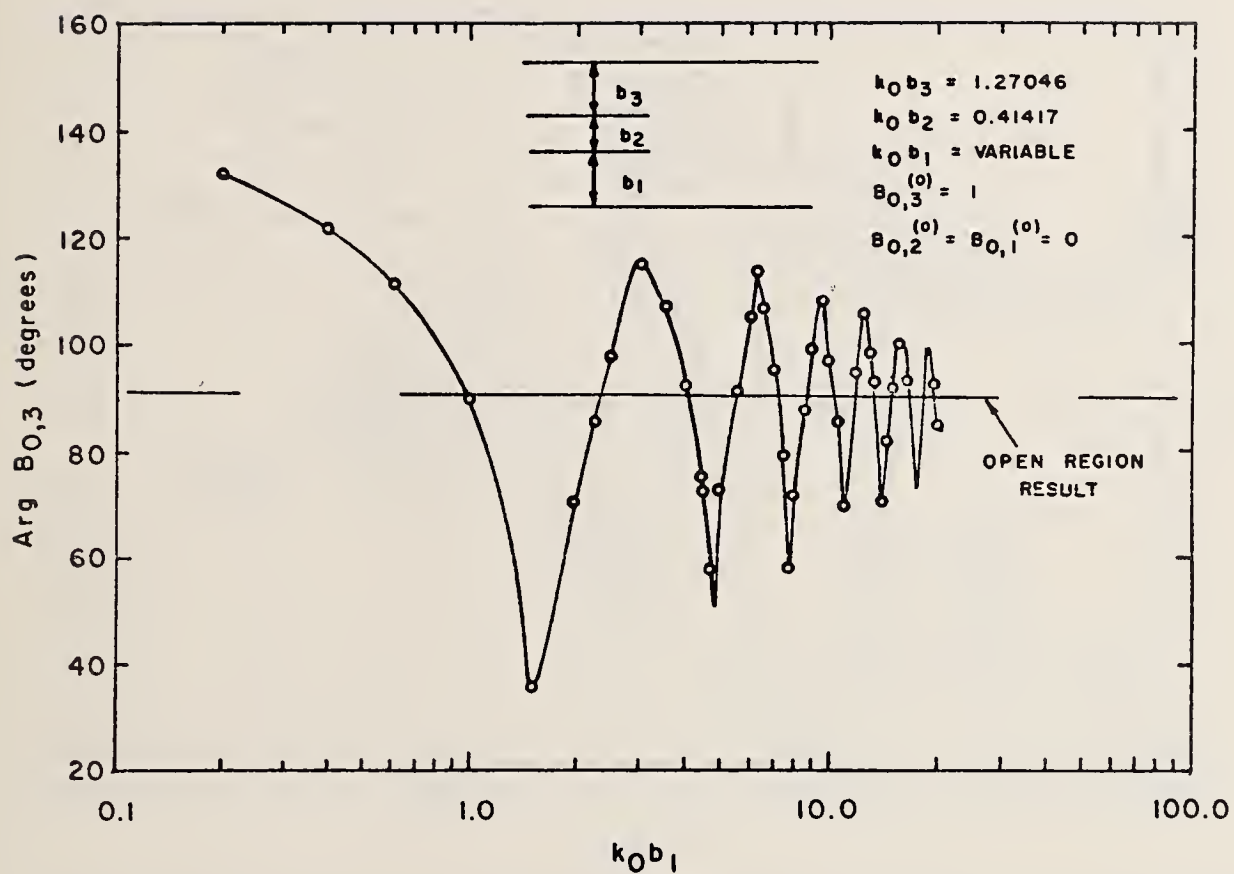Fig. 10.3.2.1a: Reflection Coefficient of Trifurcated Waveguide as a Function of b_1

Fig. 10.3.2.1b: Reflection Coefficient of Trifurcated
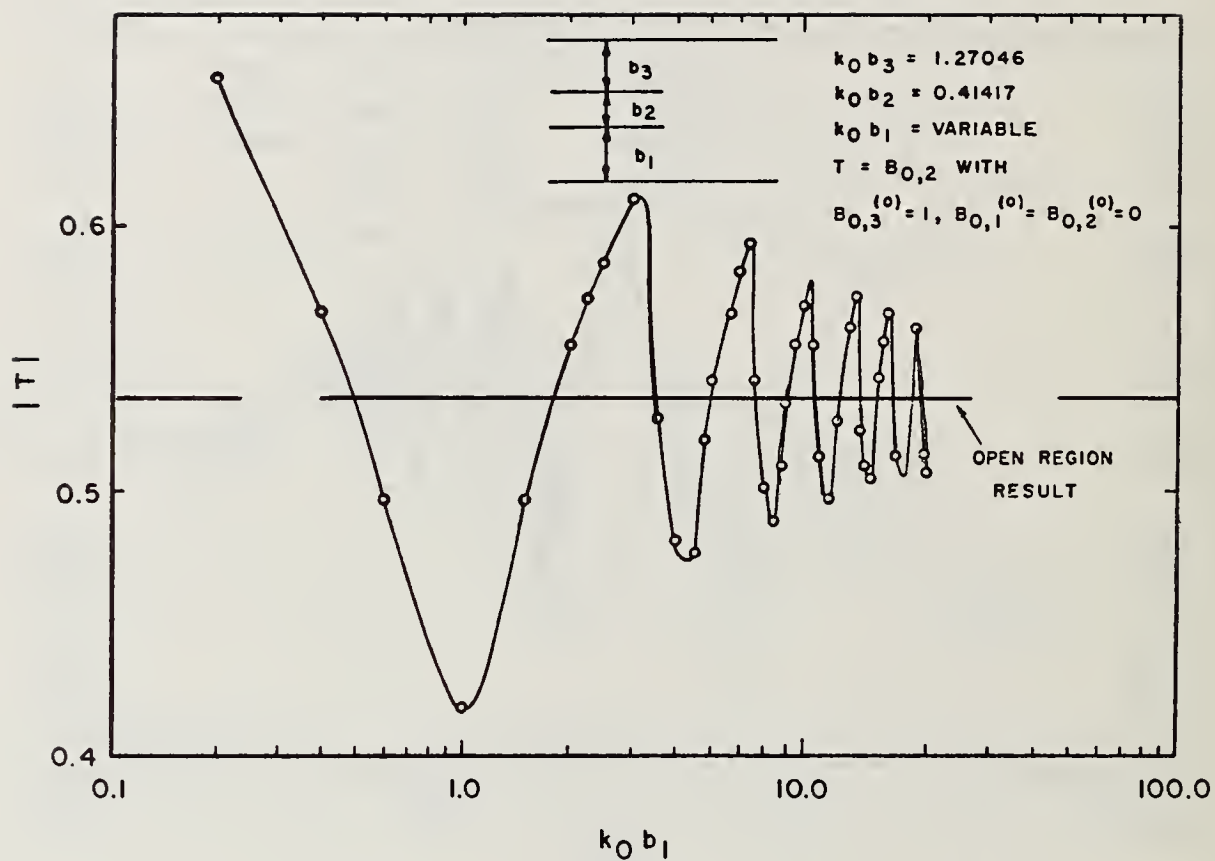Waveguide as a Function of b_1

117

Fig. 10.3.2.2a: Coupling Coefficient of Trifurcated
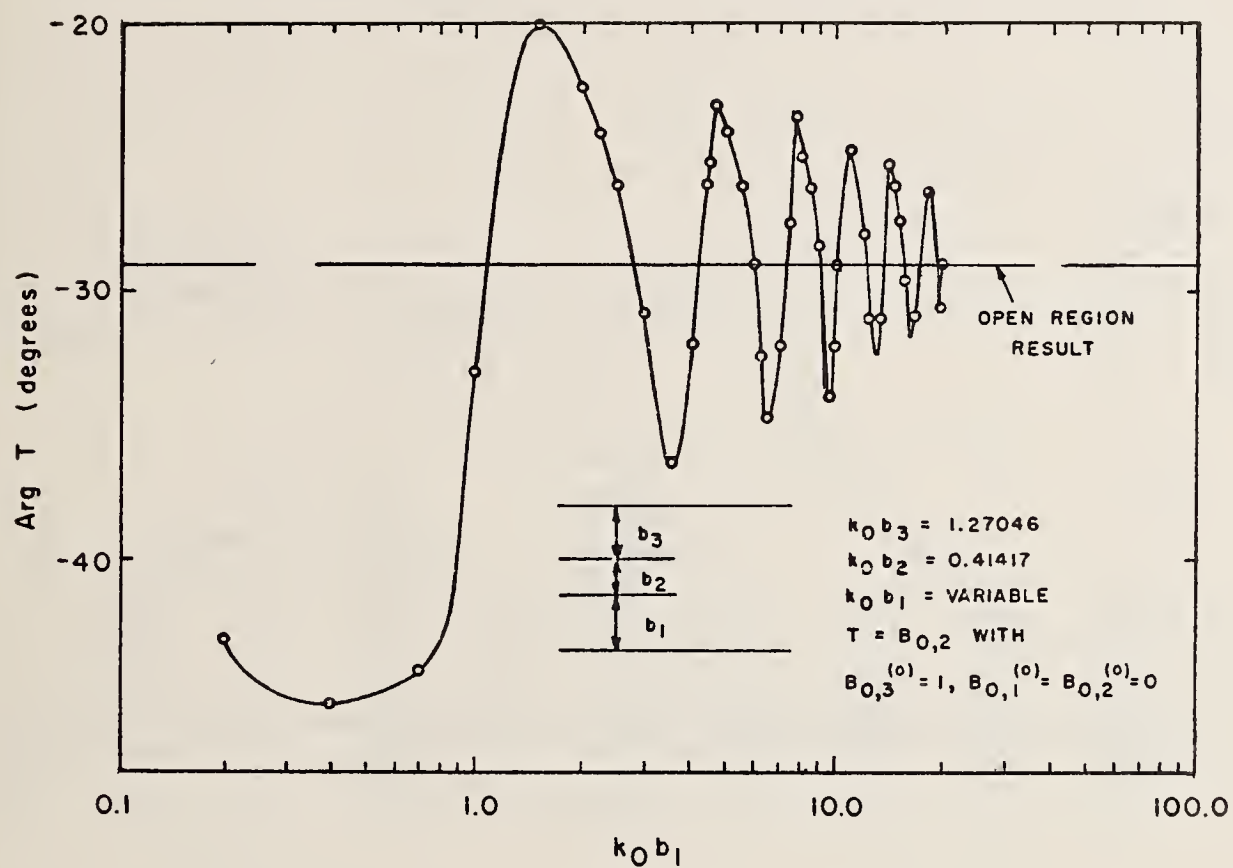Waveguide as a Function of b_1

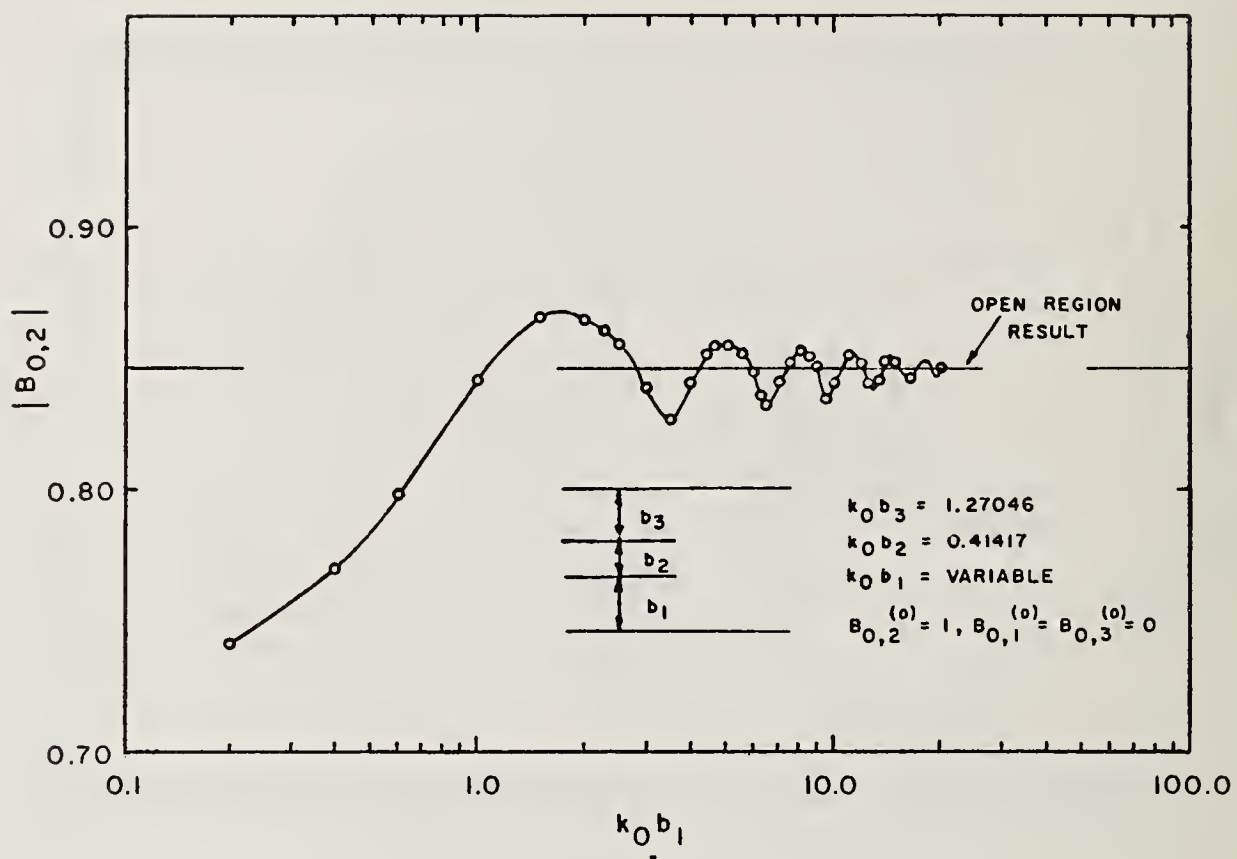Fig. 10.3.2.2b: Coupling Coefficient of Trifurcated
Waveguide as a Function of b_1

Fig. 10.3.2.3: Reflection Coefficient of Trifurcated
Waveguide as a Function of b_1

120

Table 10.3.1.1 Convergence of Open Region Solution

N_p	$B_{o,1}^{*}$		$B_{o,2}^{\dagger}$		$T^{\dagger}$	
5	0.25909	90.222°	0.84558	155.26°	0.53497	−28.770°
7	0.25909	90.226°	0.84557	155.26°	0.53503	−28.771°

$^{\dagger}T = B_{o,2}$ with $B_{o,1}^{(o)} = 1$, * with $B_{o,1}^{(o)} = 1$, $\dagger$ with $B_{o,2}^{(o)} = 1$.

Clearly five place accuracy is achieved with only a few perturbation coefficients for this case. However, the second waveguide has a width of only 0.066λ. Table 10.3.1.2 illustrates the convergence of the dominant mode parameters for the case $k_o b_1 = 1.4137$, $k_o b_2 = 2.82741$, $k_o b_3 = 2.82742$. This particular array was examined by Lee (1967). His data is also shown in the table. Note that the convergence is slower than the previous case where the waveguides were smaller. However, excellent results are still obtained. Also note that the data is in closer agreement to Lee for the central waveguides, which is to be expected since Lee used an approximation to a flush-mounted infinite ground plane while in our analysis no ground plane is assumed.

Table 10.3.1.2 Convergence of Open Region Solution

N_p	$B_{o,1}^{\dagger}$		$B_{o,2}^{\dagger}$		$B_{0.3}^{\ddagger}$		$T_1^{\dagger}$		T_2^{*}	
5	0.2193	73.6°	0.3148	73.6°	0.2766	80.6°	0.1663	−107.8°	0.0918	74.5°
7	0.2181	73.4°	0.3085	74.1°	0.2656	82.9°	0.1649	−107.5°	0.0891	76.5°
9	0.2195	73.7°	0.3126	73.8°	0.2720	81.6°	0.1665	−107.8°	0.0923	74.8°
11	0.2198	73.7°	0.3122	73.8°	0.2702	81.9°	0.1668	−107.8°	0.0932	74.6°
13	0.2197	73.7°	0.3120	73.8°	0.2700	82.0°	0.1667	−107.8°	0.0929	74.7°
15	0.2195	73.7°	0.3122	73.8°	0.2711	81.8°	0.1665	−107.8°	0.0924	74.8°
Lee's Data	0.2160	74.3°	0.3032	75.1°	0.2503	86.2°	0.1625	−106.8°	0.0864	77.7°

$^{\dagger}T_1 = B_{o,2}$ with $B_{o,1}^{(o)} = 1$

$^{*}T_2 = B_{o,3}$ with $B_{o,1}^{(o)} = 1$

$\ddagger$Current reflection coefficients.

Figure 10.3.1.4 illustrates the far field radiation patterns of this same array. Note that the patterns have nulls near the angles expected from separable array theory. However, note that the null at 58° has noticeably filled due to the differences in aperture illumination because of mutual coupling.

3.2 The Magnetic Wall Case

This section presents results similar to section 3.2 for the magnetic wall case.

Figure 10.3.2.1 illustrates the variation of the TEM reflection coefficient of a trifurcated waveguide with a magnetic symmetry wall (ref. Appendix F) with $k_o b_o = 1.27046$, $k_o b_1 = 0.41417$, and $k_o b_2$ variable. The data using the open region analysis is shown for
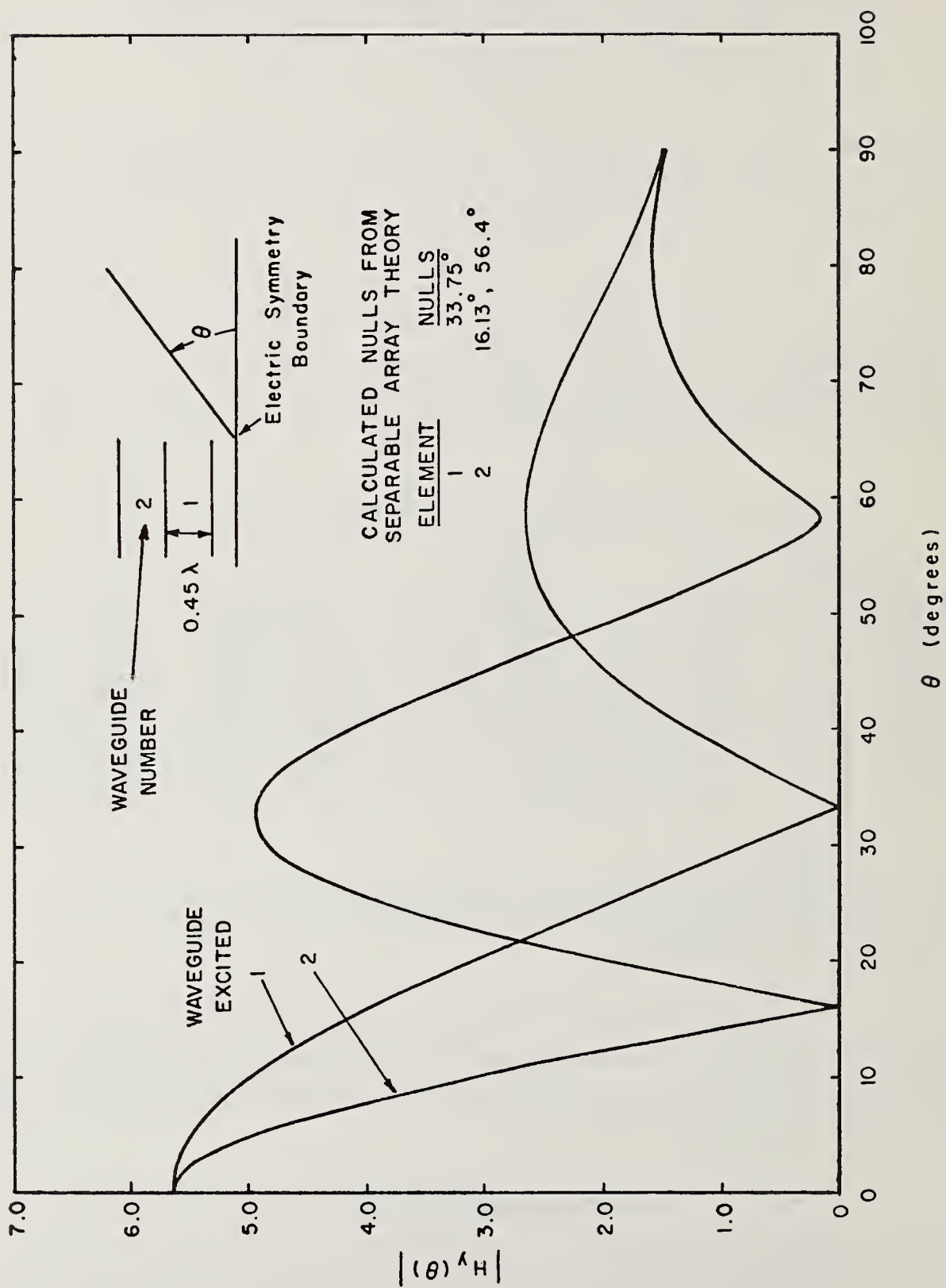
Fig. 10.3.1.4: Element Patterns for Even Excitation of Lee's Array
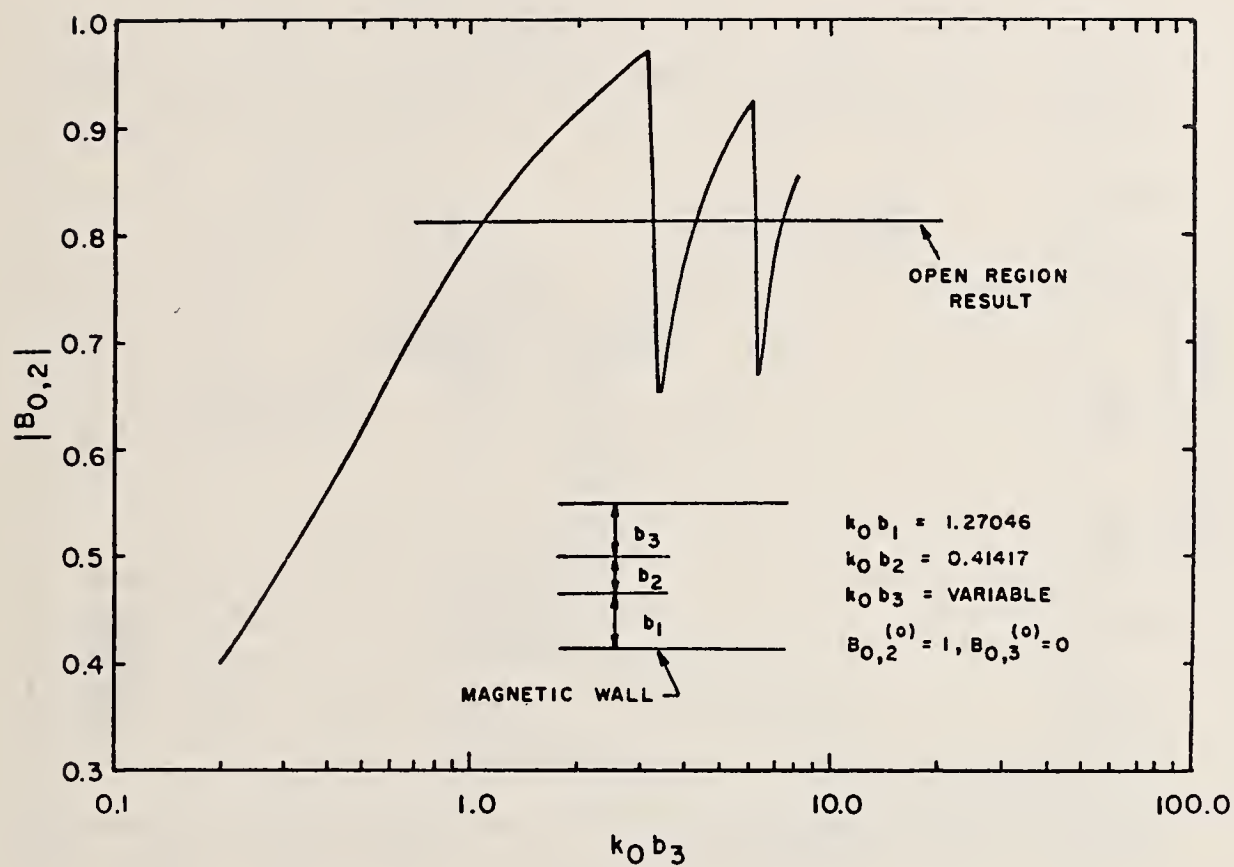
122

Fig. 10.3.2.1a: Reflection Coefficient of Trifurcated Waveguide with Magnetic Wall as a Function of b_3
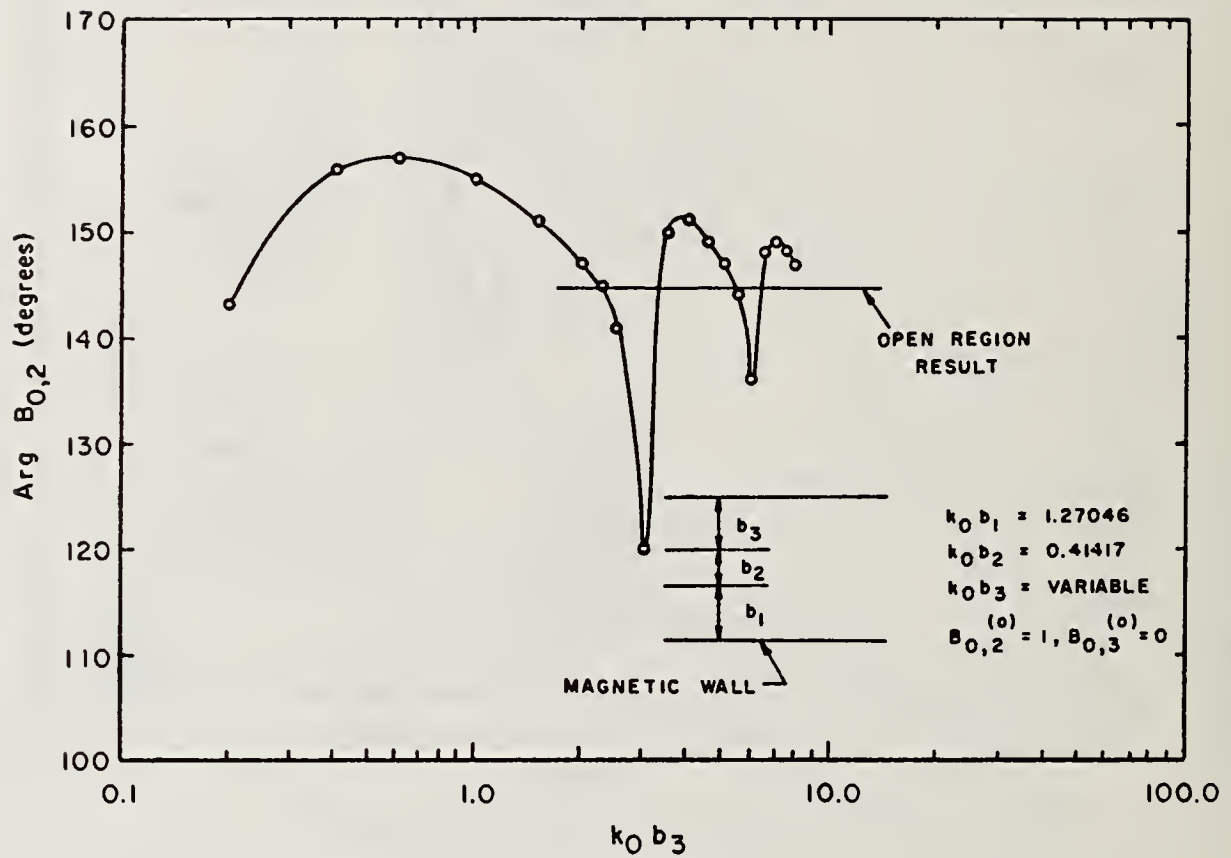
123

Fig. 10.3.2.1b: Reflection Coefficient of Trifurcated
Waveguide with Magnetic Wall as a
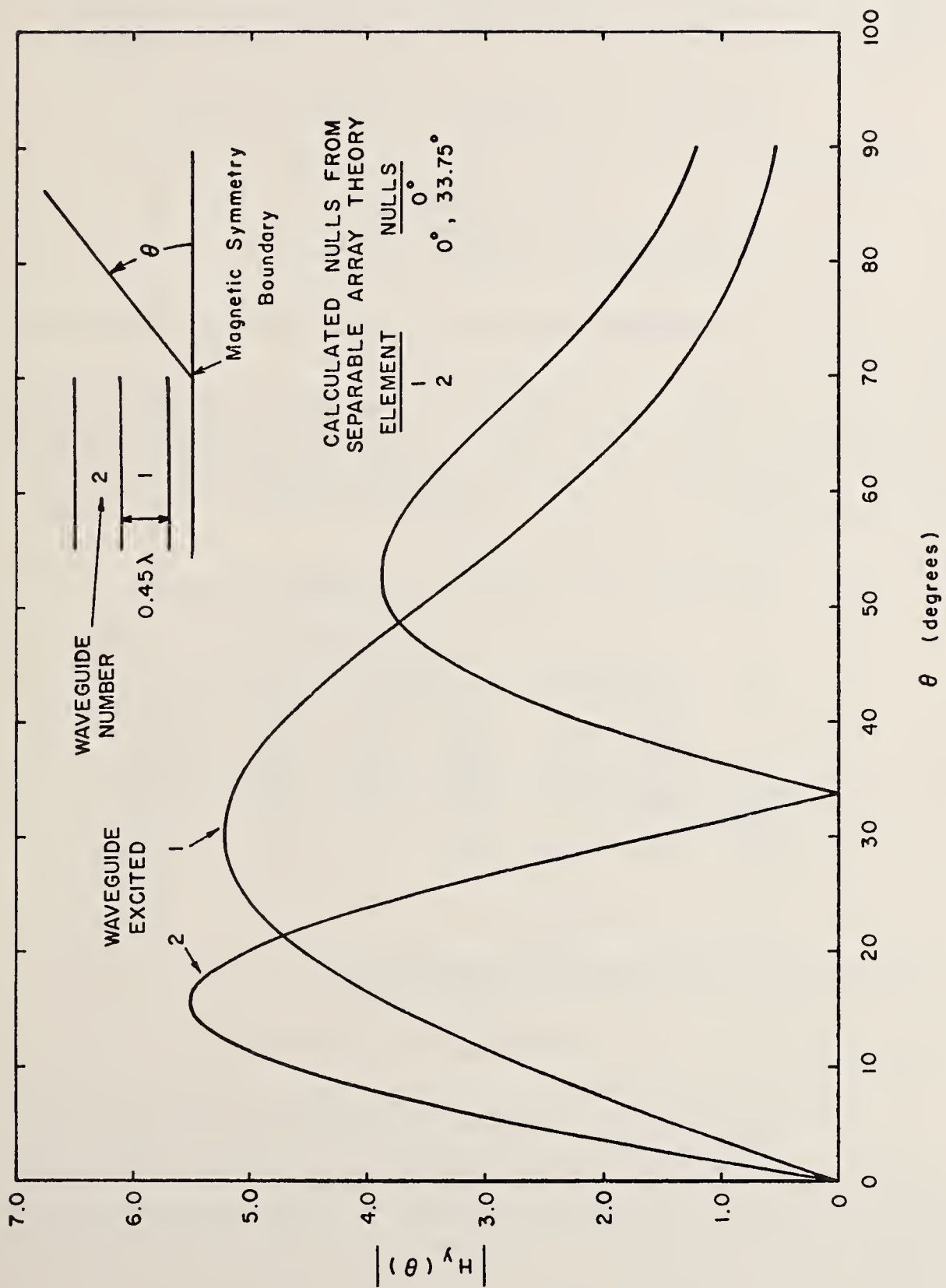Function of b_3

Fig. 10.3.2.2: Element Patterns for Odd Excitation of Lee's Array

comparison. Since the center region does not support a TEM mode only the reflection coefficient of the guide with $k_o b_1 = 0.41417$ is shown. Note that the convergence is slower than the electric wall case for the same geometry (ref. Figure 10.3.1.3). The data also oscillates about the value predicted using open region analysis.

Table 10.3.2.1 illustrates the convergence of this same data as a function of the number of perturbation coefficients ($N_p \equiv N^{M,R} \equiv N^{M,L}$) using the open region analysis.

Table 10.3.2.1 Convergence of Open Region Results

N_p	$B_{o,2}$	
7	0.81226	144.70°
9	0.81227	144.70°

The data illustrates that five place accuracy is achieved with only a few perturbation coefficients.

Table 10.3.2.2 illustrates the convergence of the dominant mode parameters for the case $k_o b_1 = 1.4137$, $k_o b_2 = 2.82741$, $k_o b_3 = 2.82742$. The convergence is quite good. Also, the comparison with Lee's (1967) data is again quite good considering the difference in the presence of a ground plane.

Table 10.3.2.2 Convergence of Open Region Results

N_p	$B_{o,2}$*		$B_{o,3}$*		$T^\dagger$	
5	0.1304	75.7°	0.1981	72.1°	0.1147	-111.5°
7	0.1304	75.7°	0.1970	73.4°	0.1141	-110.2°
9	0.1304	75.7°	0.1972	73.0°	0.1147	-111.2°
11	0.1304	75.9°	0.1972	72.9°	0.1146	-111.1°
13	0.1304	75.9°	0.1971	73.1°	0.1144	-110.6°
Lee's Data	0.1299	76.8°	0.1877	77.5°	0.1146	-107.6°

$\dagger T = B_{o,3}$ with $B_{o,2}^{(o)} = 1$

*Current reflection coefficients

Figure 10.3.2.2 shows the far-field radiation pattern of this same array.

3.3 Superposition of the Results for an Electric and a Magnetic Wall

Little data exists for the coupling of parallel plates without a ground plane. However, Dybdal, Rudduck, and Tsai (1966) solved the problem of coupling between two parallel plates using wedge diffraction techniques. A comparison of their data with that calculated using this theory is shown in Figure 10.3.3.1. Note that the modified function theoretic technique predicts resonant effects whenever the separation is a multiple of 0.5 λ. At these separations, the wedge diffraction techniques used by Dybdal, et al. is inadequate because
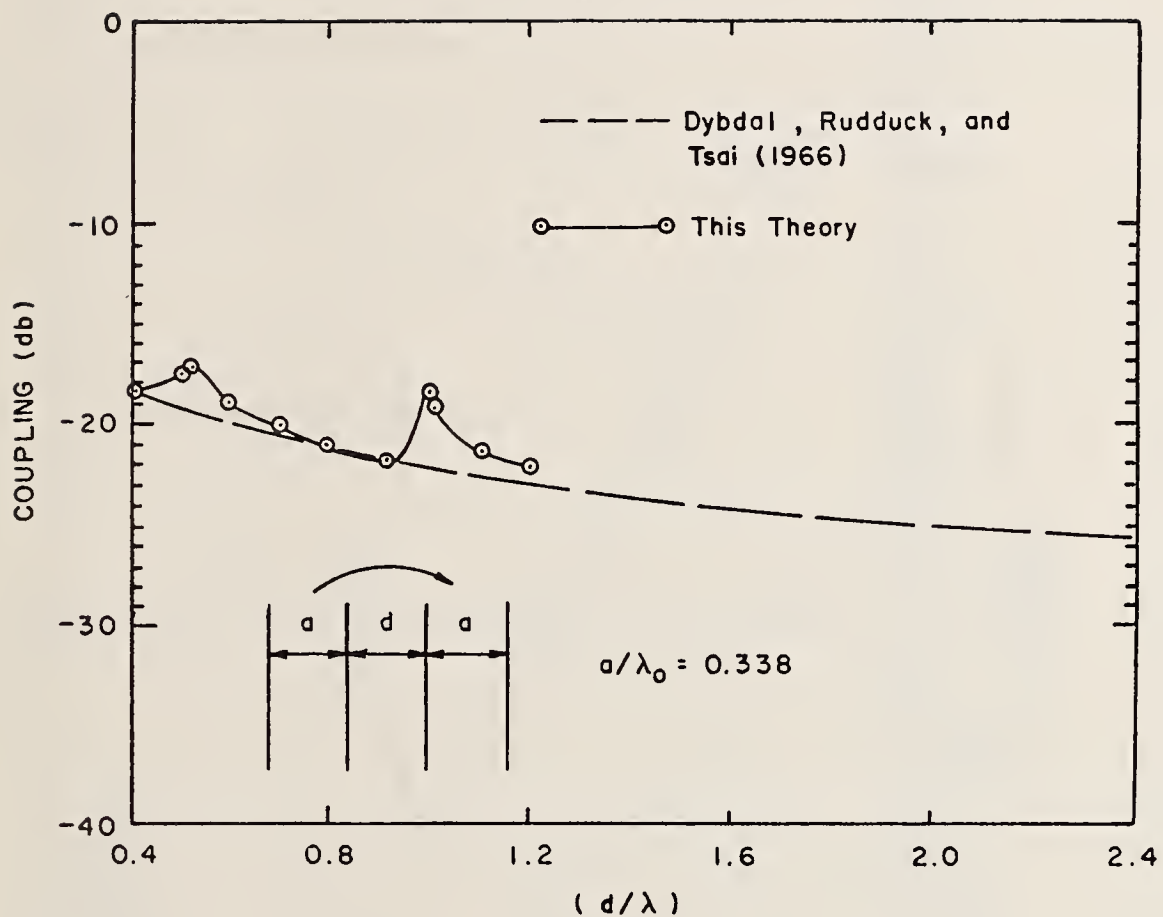
Fig. 10.3.3.1: Mutual Coupling Between Two Parallel
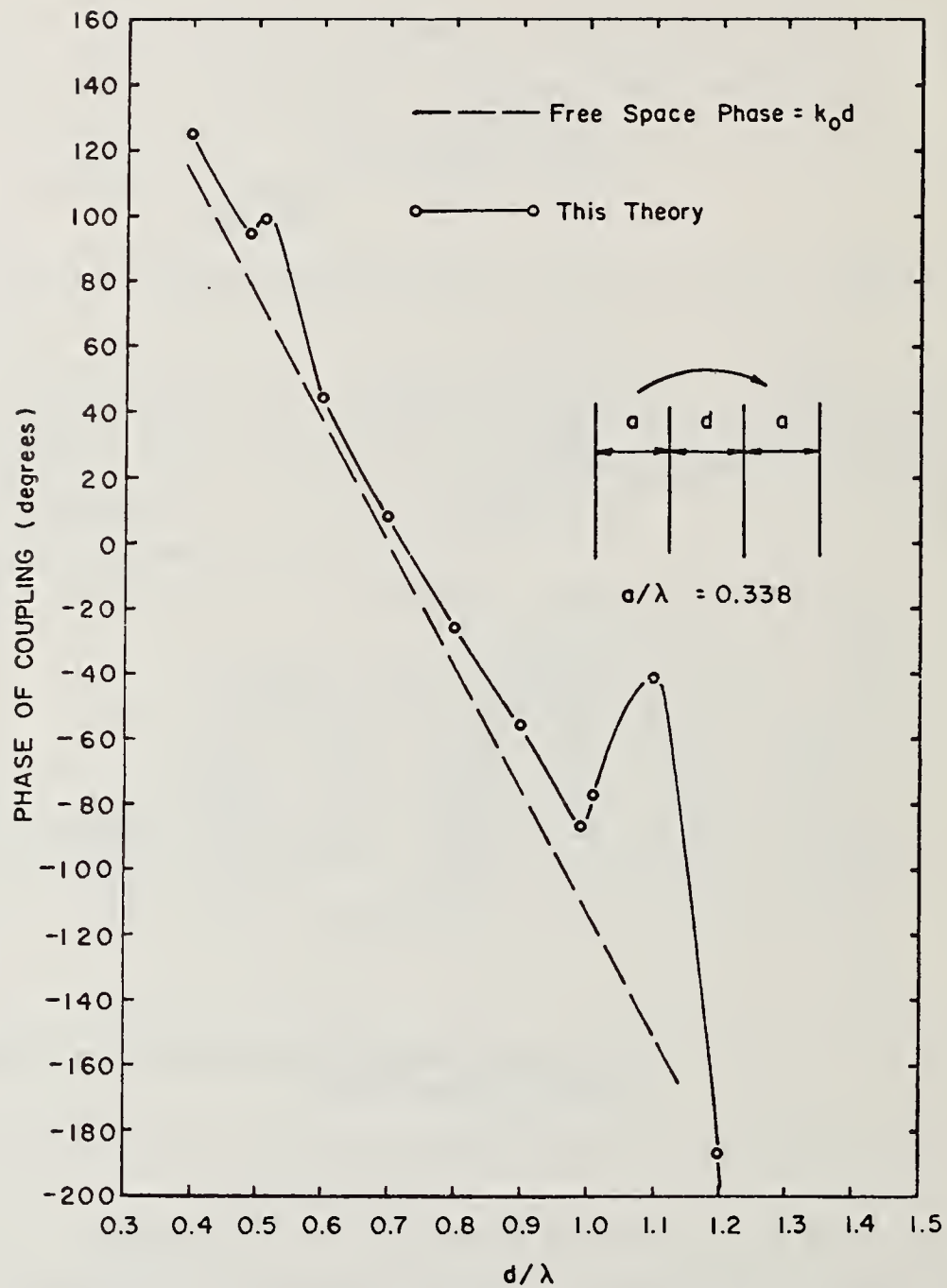Plate Waveguides

Fig. 10.3.3.2:   Phase of Mutual Coupling Between Two
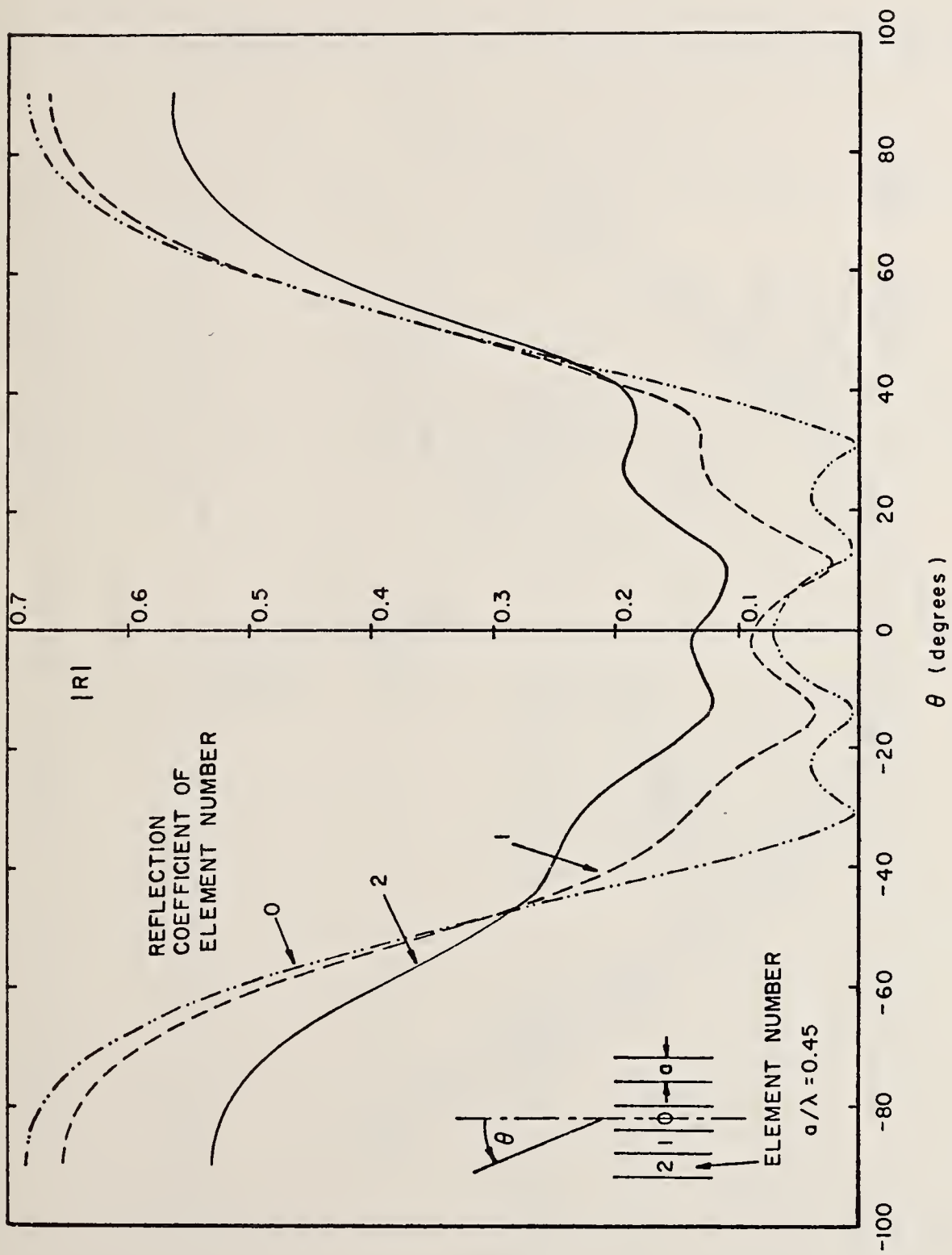   Parallel Plate Waveguides

128

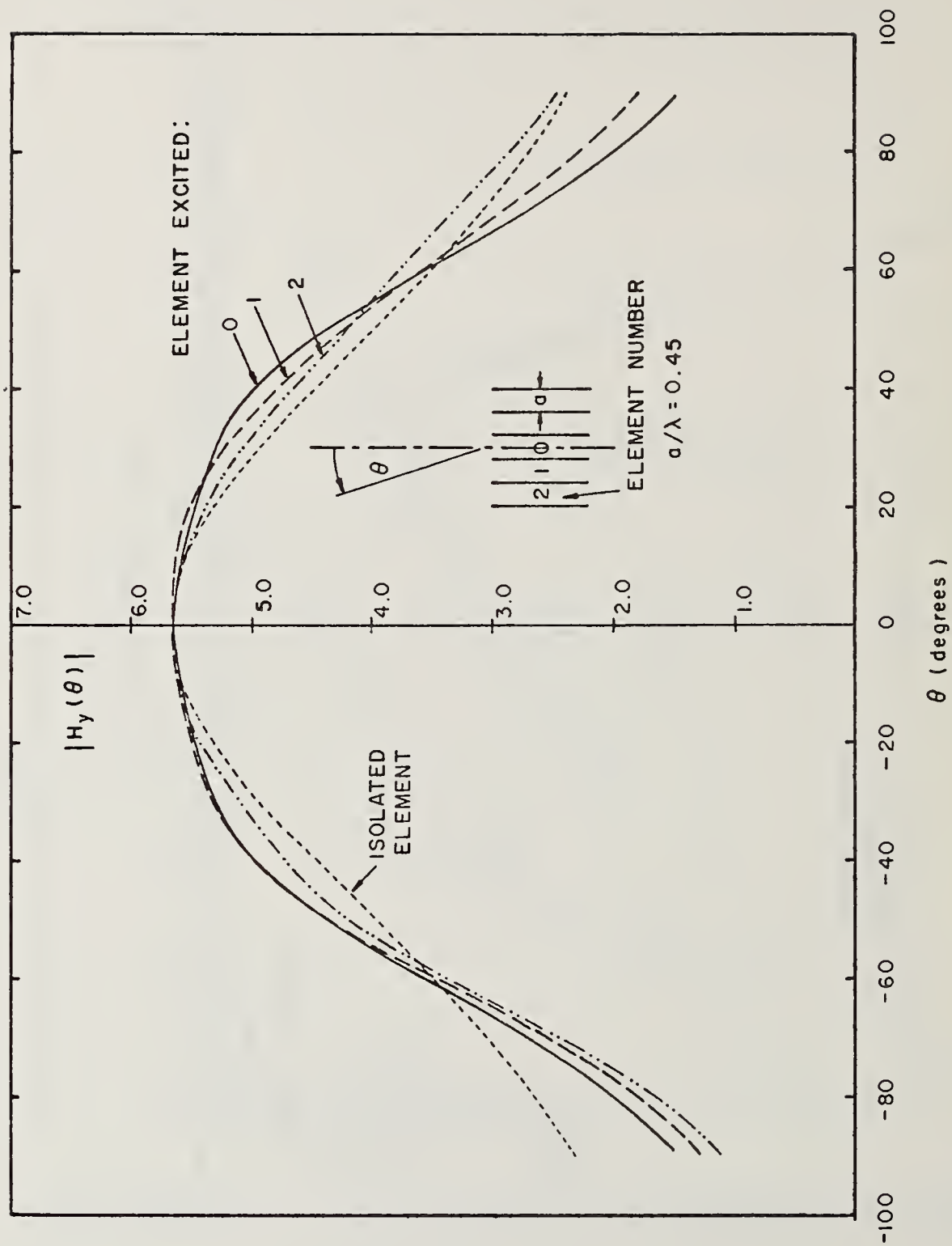Fig. 10.3.3.3: Active Reflection Coefficient of Lee's Array

Fig. 10.3.3.4: Complete Element Patterns of Lee's Array

of the modes at cutoff in the inner region with dimension d. Figure 10.3.3.2 shows the phase of the coupling coefficient for this same case. Note that the phase behaves according to the geometrical distance except near the resonances, where the phase progression is slower than free space.

In section 3.1 and 3.2, we presented data for an array examined by Lee (1967). We shall now consider the superposition of that data to obtain the characteristics of the complete five element array. Table 10.3.3.1 shows the complete comparison of all the scattering coefficients with Lee's data. The waveguide's are numbered 1-5 from the edge. Note that good correlation is obtained with Lee's data even though his data is including the effect of a simulated ground plane. However, there is a trend for the coupling coefficients to decay slower without the presence of the ground plane.

Figure 10.3.3.3 illustrates the variation of the active reflection coefficient of each element as the array is scanned. Note that the reflection coefficient varies from element to element, with the edge element reflection coefficients being asymmetrical.

Figure 10.3.3.4 illustrates the individual patterns of each element of this array as a result of mutual coupling coupling among all elements as well as the isolated element pattern. Note that the edge element patterns are asymmetrical. Note that the element patterns have a

Table 10.3.3.1 Scattering coefficients of Lee's array.

Waveguide Excited	Reflected Mode in Guide No.	This Theory		Lee (1967)	
3	1	0.0924	74.81°	0.0864	77.7°
3	2	0.1665	-107.8°	0.1625	-106.8°
3	3	0.2195	73.67°	0.2160	74.3°
3	4	0.1665	-107.8°	0.1625	-106.8°
3	5	0.0924	74.81°	0.0864	77.7°
2	1	0.1712	-105.2°	0.1630	-102.3°
2	2	0.2212	74.37°	0.2165	75.6°
2	3	0.1713	-105.3°	0.1625	-106.8°
2	4	0.0909	72.4°	0.0867	73.8°
2	5	0.0583	-93.93°	0.0501	-90°
1	1	0.2333	78.1°	0.2184	82.5°
1	2	0.1712	-105.2°	0.1630	-102.3°
1	3	0.0924	74.9°	0.0864	77.7°
1	4	0.0583	-93.9°	0.0502	-90°
1	5	0.0411	103.5°	0.0354	104.8°

finite value at $\theta = \pm 90°$, in contrast to Lee (1967) who predicts zero values. This method of analysis would be particularly powerful in predicting wide angle scan performance of an array in the H plane, where the assumption of an infinite ground plane would produce nulls at $\theta = \pm 90°$. Note that the element grains are greater for angles away from the center elements. Also note that for these values the behavior resembles closely that of an isolated element with no ground plane. Also observe that for angles toward the center of the array that the element patterns tend to be more uniform particularly for large angles of observation.

CHAPTER 11. REMOTE SENSING OF THE EARTH USING PARALLEL PLATE WAVEGUIDES

1. Introduction

The remote sensing of the earth's subsurface properties is commonly done at low frequencies in order to get the desired penetration. At these frequencies loops and dipoles are commonly used. Ward (1967) discusses the application of elementary source theory to this problem.

For the remote sensing of the earth's properties nearer the surface, moderate frequencies are used. Loops and dipoles are still commonly used; however, the antenna dimensions are no longer small compared to a wavelength. Chang (1971) has analyzed many of these problems using the numerical solution of integral equations.

At higher frequencies, waveguides can often be used instead of the more conventional loops and dipoles. Waveguides have been commonly employed at higher frequencies; however, they have been confined to measuring the Fresnel reflection coefficients. Greater sensitivity should be possible if the near fields of the antenna are allowed to interact with the earth. This will cause the characteristics of the antennas themselves to change as a function of the environment. From a theoretical viewpoint, such waveguides are more prone to an exacting analysis than dipoles and loops because waveguides do not have gap corrections and other feed modeling problems. Additionally, one might obtain increased sensitivity by using two waveguides instead of one. The coupling between the waveguides would provide this increased sensitivity.

The analysis presented in the first part of this monograph was confined to closed region problems. If a sample of the earth can be obtained conveniently, then the analysis of part 1 applies directly. In this case if one replaces the free space wavelength by the ~~guide wavelength,~~ the analysis applies to rectangular waveguide. However, generally the determination of the earth's properties must be done remotely.

This chapter considers the problem of a finite array illuminating a homogeneous half space. In essence, this chapter combines the solutions of a waveguide radiating into a half space (Chapter 9) and a finite phased array (Chapter 10). The solution is new and gives physically interesting results for such problems as the coupling of two waveguides above a half space.

2. <u>Formulation of the Equations</u>

2.1 <u>Introduction</u>

As in Chapter 10, we will assume a symmetry boundary parallel to the waveguides. This is not necessary, but is convenient. Hence, we will consider the superposition of the results from two problems: (1) the electric symmetry case and (2) the magnetic symmetry case.

2.2 <u>The Electric Symmetry Case</u>

Figure 11.2.2.1 illustrates the auxiliary problem. As in the case of finite phased array the problem can be further separated into two kinds of problems: (1) the interior problem, and (2) the exterior problem. The interior problem is identical to that of Chapter 10 while the exterior problem is a modification of the results of a single waveguide radiating into a homogeneous half space given in Chapter 9.

Clearly then, the N holomorphic functions are identical to (2.2.1)-(2.2.3) of Chapter 10, with the exception of the function associated with the Nth plate on the open region. This function is appropriately modified to account for the higher order modes incident internally on the junction as well as the scattered field from the half space. From Chapter 8, we can find:

$$T_N(\omega) = X(\omega) \left[\frac{K_o^N}{\omega - jk_o} + \left\{ \sum_{n=1}^{\infty} \frac{g_n^{N,L}}{\omega - \gamma_{n,c_{N-1}}} - \int_{L_2}^{+} \frac{g^{(2)}(t) \, dt}{X(t) \, (t-\omega)} \right\} \right] \tag{2.2.1}$$

where $X(\omega)$ is the homogeneous solution as given in Chapter 8, section 3. Changing t to $-t$ in the integral we have

$$T_N(\omega) = X(\omega) \left[\frac{K_o^N}{\omega - jk_o} + \sum_{n=1}^{\infty} \frac{g_n^{N,L}}{\omega - \gamma_{n,c_{N-1}}} - \int_{L_1}^{-} \frac{g^{(2)}(-t) \, dt}{X(-t) \, (t+\omega)} \right] \tag{2.2.2}$$

From Chapter 9, we can easily derive the integral equation for $g^{(2)}(t)$ by considering the exterior problem. From Chapter 9,

$$T^-(\omega) = -\pi\omega e^{j\lambda c_{N-1}} A(\lambda), \quad \omega\varepsilon L_1^- \tag{2.2.3}$$

and

$$g^{(2)}(\omega) = \omega \sin \lambda c_{N-1} A^o(\lambda), \quad \omega\varepsilon L_2 \tag{2.2.4}$$

But from the boundary condition at the dielectric we can relate $A(\lambda)$ and $A^o(\lambda)$.

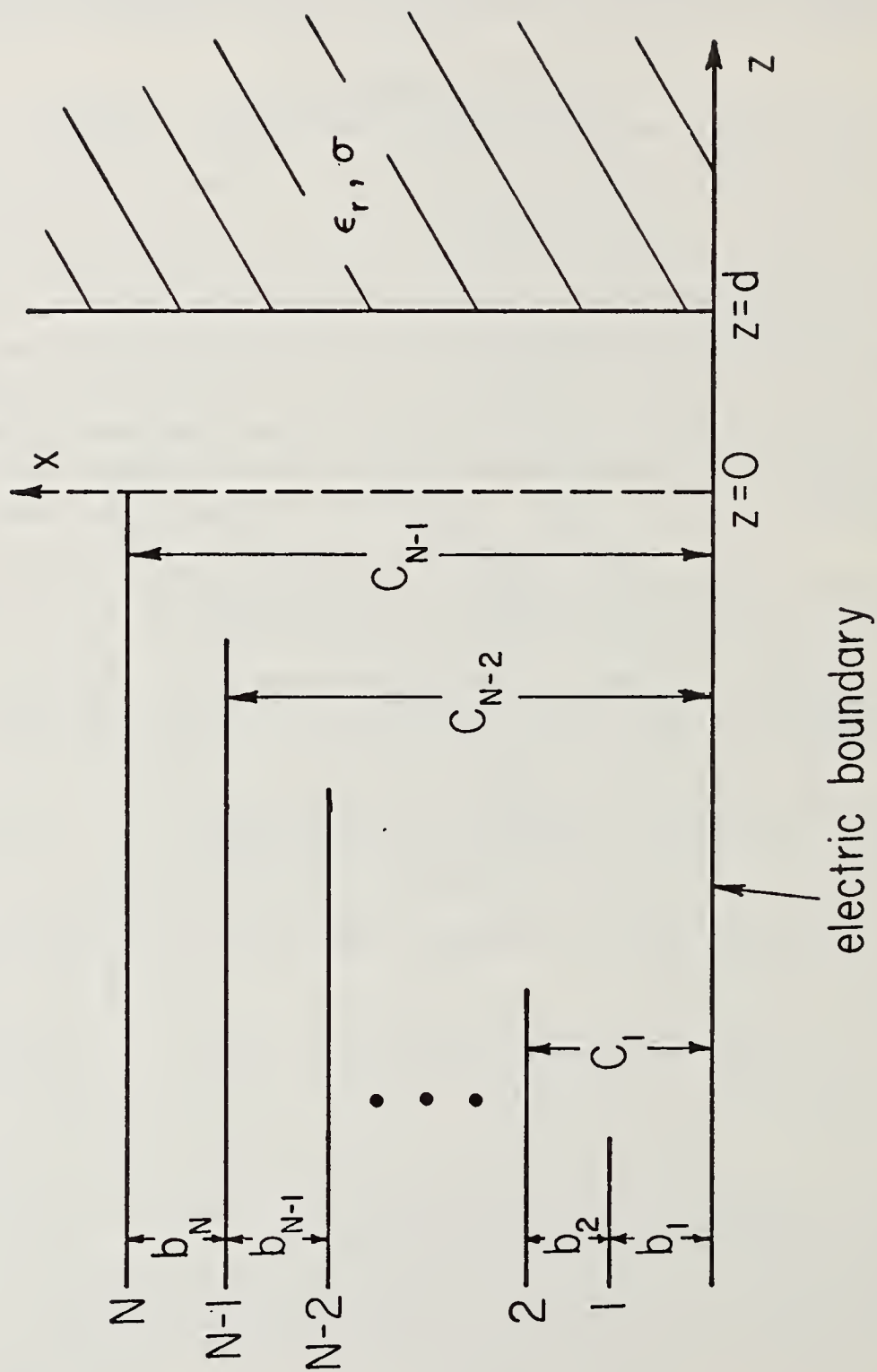$$A^o(\lambda) = R(\lambda) A(\lambda) \tag{2.2.5}$$

where

Fig. 11.2.2.1: Auxiliary Problem for Finite Array
Radiating into a Dielectric Half Space

$$R(\lambda) = \frac{\varepsilon\omega - \Gamma}{\varepsilon\omega + \Gamma} \, e^{-2\omega d}$$

where

$$\Gamma = \sqrt{\lambda^2 - \varepsilon k_o^2}$$

with the branch of Γ chosen such that $\mathrm{Re}(\Gamma) \geq 0$.

Using (2.2.2)-(2.2.5), we may arrive at the following

$$g^{(2)}(-\omega) = \frac{\sin \lambda c_{N-1}}{\pi} \, R(\lambda) \, e^{-j\lambda c_{N-1}} \, X^-(\omega) \left[\frac{K_o^N}{\omega - jk_o} + \sum_{n=1}^{\infty} \frac{g_n^{N,L}}{\omega - \gamma_{n,c_{N-1}}} \right.$$

$$\left. - \int_{L_1^-} \frac{g^{(2)}(-t) \, dt}{X(-t)(\omega + t)} \right] \qquad \omega\varepsilon L_1 \qquad (2.2.6)$$

Considering the change of variable

$$g^{(2)}(-\omega) = \frac{\sin \lambda c_{N-1}}{\pi} \, \frac{R(\lambda)}{(\omega - jk_o)} \, e^{-j\lambda c_{N-1}} \, X^-(\omega) \, G(\omega)$$

we transform (2.2.6) to

$$G(\omega) = K_o^N + (\omega - jk_o) \left[\sum_{n=1}^{\infty} \frac{g_n^{N,L}}{\omega - \gamma_{n,c_{N-1}}} + \int_{L_1^-} \frac{Q(t) \, G(t) \, dt}{t + \omega} \right], \qquad \omega\varepsilon L_1 \qquad (2.2.7)$$

where

$$Q(\omega) = - \frac{\sin \lambda c_{N-1} \, R(\lambda) \, e^{-j\lambda c_{N-1}} \, X^-(\omega)}{\pi(\omega - jk_o) \, X(-\omega)}$$

Equation (2.2.7) is the desired integral equation for $G(\omega)$.

We must also modify (2.2.8) of Chapter 10 to reflect the addition of the integral to $T_N(\omega)$. Hence,

$$T_N(-\gamma_{n,c_{N-1}}) = (-1)^n \gamma_{n,c_{N-1}} \, c_{M-1} [K_n^{N-1,R}]^{-1} \, g_n^{M-1,R}$$

$$= -X(-\gamma_{n,c_{N-1}}) \left[\frac{K_o^N}{\gamma_{n,c_{N-1}} + jk_o} + \sum_{m=1}^{\infty} \frac{g_n^{N,L}}{\gamma_{n,c_{N-1}} + \gamma_{m,c_{N-1}}} \right.$$

$$\left. + \int_{L_1^-} \frac{Q(t) \, G(t) \, dt}{t - \gamma_{n,c_{N-1}}} \right] \qquad (2.2.8)$$

where $n = 1,2,3, \ldots$. Equation (2.2.8) is also an integral equation for $G(\omega)$.

135

All other equations associated with the interior problem remain as given in Chapter 10.

For this particular problem, the TEM coefficients are known (ref. to (2.2.9)-(2.2.11) of Chapter 10). These equations all remain valid even in the presence of the half space.

In order to solve the integral and algebraic equations efficiently, we must consider the asymptotic behavior of the various perturbation coefficients. However, because the presence of the half space does not change or introduce any edge condition, all the asymptotic forms given in Chapter 10 ((2.2.12)-(2.2.13)) are still valid.

All remaining details of the analytical solution are the same as in Chapter 10 when using the new expression for $T_N(\omega)$.

2.3 The Magnetic Symmetry Case

Figure 11.2.3.1 illustrates the auxiliary problem of magnetic symmetry wall case. As in the case of the electric wall, only the exterior problem results need to be changed from the results of Chapter 10. Hence, we need to change only the Nth holomorphic function (i.e., (2.3.3) of Chapter 10). From Chapter 8, (2.3.12) we have that

$$T_N(\omega) = X(\omega) \left[\sum_{n=1}^{\infty} \frac{g_n^{N,L}}{\omega - \gamma_{2n-1,2c_{N-1}}} - \int_{L_2^+} \frac{g^{(2)}(t)\,dt}{X(t)\,(t-\omega)} \right] \qquad (2.3.1)$$

where $X(\omega)$ is the homogeneous solution for the magnetic wall case. Changing t to $-t$ in the integral we have

$$T_N(\omega) = X(\omega) \left[\sum_{n=1}^{\infty} \frac{g_n^{N,L}}{\omega - \gamma_{2n-1,2c_{N-1}}} - \int_{L_1^-} \frac{g^{(2)}(-t)\,dt}{X(-t)\,(t+\omega)} \right] \qquad (2.3.2)$$

We can arrive at an integral equation for $g^{(2)}(t)$ by recalling from Chapter 8 that

$$T_N^-(\omega) - T_N^+(\omega) = -2\pi j\, \omega \cos \lambda c_{N-1}\, A(\lambda), \qquad \omega \epsilon L_1 \qquad (2.3.3)$$

and

$$T_N^-(\omega) = -e^{j2\lambda c_{N-1}}\, T_N^+(\omega), \qquad \omega \epsilon L_1 \qquad (2.3.4)$$

Combining (2.3.3) and (2.3.4) yields,

$$T_N^-(\omega) = -j\pi\omega\, e^{j\lambda c_{N-1}}\, A(\lambda), \qquad \omega \epsilon L_1^- \qquad (2.3.5)$$

also from (2.3.13) of Chapter 8

$$g^{(2)}(\omega) = +\omega \cos \lambda c_{N-1}\, A^o(\lambda), \qquad \omega \epsilon L_2 \qquad (2.3.6)$$

But from the boundary condition at the half space we can relate $A(\lambda)$ and $A^o(\lambda)$

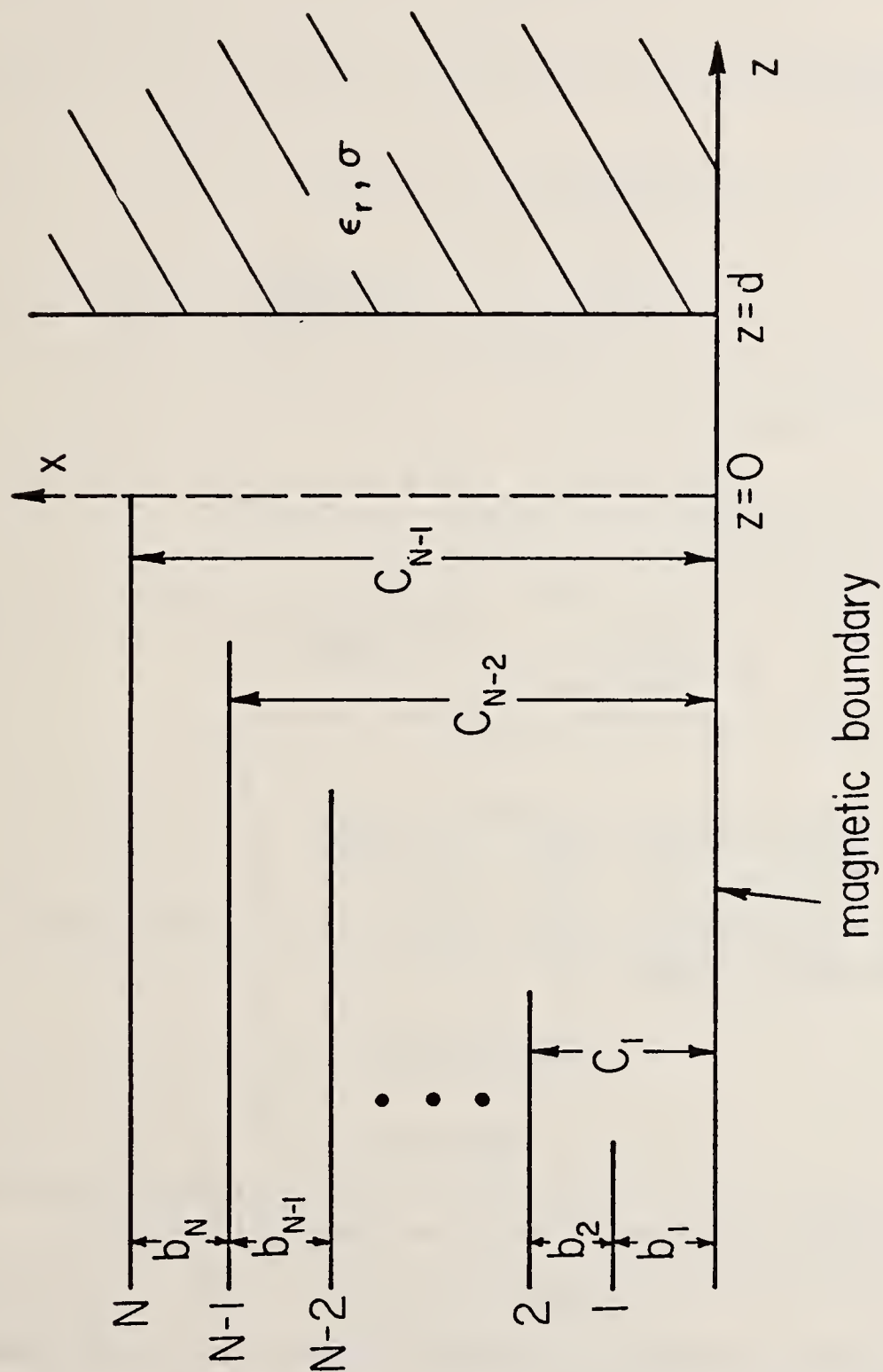$$A^o(\lambda) = R(\lambda)\, A(\lambda) \qquad (2.3.7)$$

Fig. 11.2.3.1: Auxiliary Problem for Finite Array
Radiating into a Dielectric Half Space

where

$$R(\lambda) = \frac{\varepsilon\omega - \Gamma}{\varepsilon\omega + \Gamma} \, e^{-2\omega d}$$

and where

$$\Gamma = \sqrt{\lambda^2 - \varepsilon k_o^2}$$

with ε being the complex permittivity of the half space. Using (2.3.5)-(2.3.7), we may arrive at the following

$$g^{(2)}(-\omega) = \frac{-j \cos \lambda c_{N-1}}{\pi} \, R(\lambda) \, e^{-j\lambda c_{N-1}} \, X^-(\omega).$$

$$\left(\sum_{n=1}^{\infty} \frac{g_n^{N,L}}{\omega - \gamma_{2n-1,2c_{N-1}}} - \int_{L_1^-} \frac{g^{(2)}(-t) \, dt}{X(-t)\,(t+\omega)} \right), \qquad \omega\varepsilon L_1^- \qquad (2.3.8)$$

Again a change of variable is made.

$$g^{(2)}(-\omega) = \frac{j \cos \lambda c_{N-1}}{\pi} \, R(\lambda) \, e^{-j\lambda c_{N-1}} \, X^-(\omega) \, G(\omega)$$

Thus we transform (2.3.8) to

$$G(\omega) = \sum_{n=1}^{\infty} \frac{g_n^{N,L}}{\omega - \gamma_{2n-1,2c_{N-1}}} - \int_{L_1^-} \frac{Q(t) \, G(t) \, dt}{t + \omega} \qquad (2.3.9)$$

where

$$Q(\omega) = j \cos \lambda c_{N-1} \, R(\lambda) \, e^{-j\lambda c_{N-1}} \, \frac{X^-(\omega)}{\pi \, X(-\omega)}$$

Equation (2.3.9) is the desired integral equation for $G(\omega)$. All other equations given in section 2.3 of Chapter 10 are valid.

3. Numerical Results

3.1 Introduction

The numerical solution of the integral equations derived in sections 2.2 and 2.3 was accomplished using Gaussian quadrature similar to that described in Chapter 9.

3.2 The Electric Wall Case

This section presents the results of two studies. The first study is an examination of how the closed region results of Chapters 3 and 4 converge to the open region results. The second study considers the convergence of the open region results as a function of the number of perturbation coefficients and truncation of the integral equation.

The evolution of closed region problems into open region problems is interesting due to two reasons: (1) It is interesting to examine a problem which can be solved both in the open and closed region cases to see which problem is "easier" to solve, and (2) It provides a check on the open region solution against previous closed region results.

Figures 11.3.2.1 (a)-(c) illustrate the variation of the dominant mode parameters for a dielectrically loaded trifurcated waveguide with $k_o b_2$ = 1.27046, $k_o b_1$ = 0.41417, and with $k_o b_o$ variable. Also, ε_r = 10, σ/k_o = 0.01, and $k_o d$ = 1.256. The open region data is shown for comparison. As in Chapter 10, the reflection coefficient for the smallest waveguide ($k_o b_1$ = 0.41417) converges fastest to the open region result. However, the reflection coefficient of the waveguide with $k_o b_2$ = 1.27046 and the coupling coefficient between the two guides both converge much slower to the open region solution. However, all of the data computed is observed to oscillate about the values computed using the open region analysis. It should be noted that the convergence to the open region solution is about the same as that shown in Chapter 10 where the dielectric half space is not present. The dielectric is quite lossy and $0.2\lambda_o$ away from the horn aperture. Hence, in order for the edge wall distance to become secondary, the distance to the half space must be an even smaller fraction of a wavelength than $0.2\lambda_o$.

Table 11.3.2.1 illustrates the convergence of some dominant mode parameters as a function of the number of intervals, N, along L_1 and the number of Gaussian quadrature points, M_n, within the nth interval for the case ε_r = 10, σ/k_o = 0.01, $k_o d$ = 1.256, $k_o b_1$ = 1.27046, $k_o b_2$ = 0.41417, and with $N^{2,L} = N^{1,R}$ = 5.

Table 11.3.2.1 Convergence of Open Region Solution

| N	M_1	M_2	M_3	M_4	M_5	$B_{o,1}$†		$B_{o,2}$†		T†	
2	16	8	--	--	--	0.19399	177.68°	0.87189	159.46°	0.50981	-57.44°
3	16	8	8	--	--	0.19385	177.66°	0.87150	159.39°	0.50993	-57.51°
4	16	8	8	8	--	0.19385	177.66°	0.87149	159.39°	0.40993	-57.51°
5	16	8	8	8	8	0.19385	177.66°	0.87149	159.39°	0.50993	-57.51°
3	16	16	8	--	--	0.19412	177.66°	0.87147	159.39°	0.51002	-57.52°
3	16	16	16	--	--	0.19413	177.67°	0.87148	159.39°	0.51002	-57.52°

†$B_{o,1}$ with $B_{o,1}^{(o)}$ = 1, $B_{o,2}^{(o)}$ = 0.

†$B_{o,2}$ with $B_{o,2}^{(o)}$ = 1, $B_{o,1}^{(o)}$ = 0.

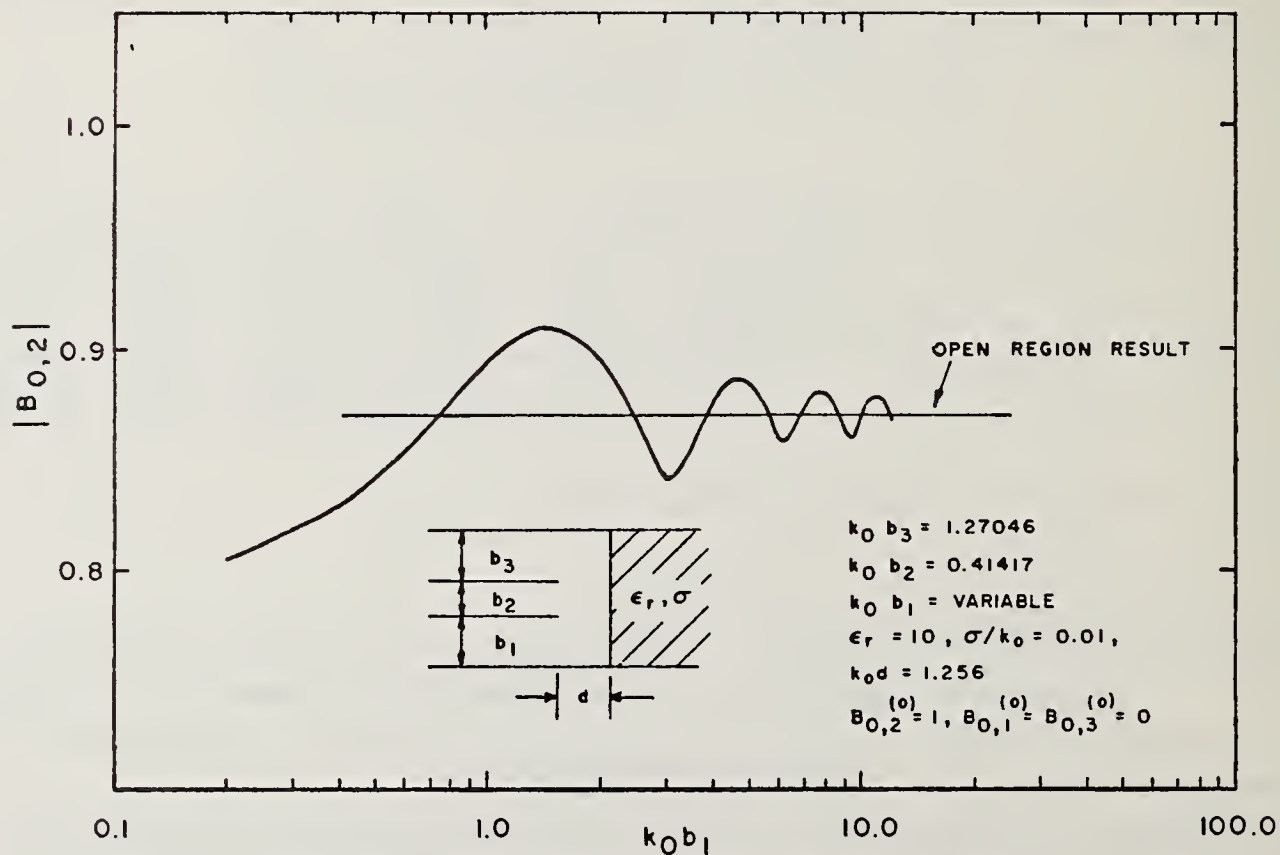†T = $B_{o,2}$ with $B_{o,1}^{(o)}$ = 1, $B_{o,2}^{(o)}$ = 0.

Essentially five place accuracy is achieved with as few as three matching intervals and 32 match points.

Table 11.3.2.2 illustrates the convergence of the same geometry considered in Table 11.2.3.1 except as a function of the number of perturbation coefficients, $N_p = N^{1,R} = N^{2,L}$ and with N = 2, M_1 = 16, M_2 = 8.
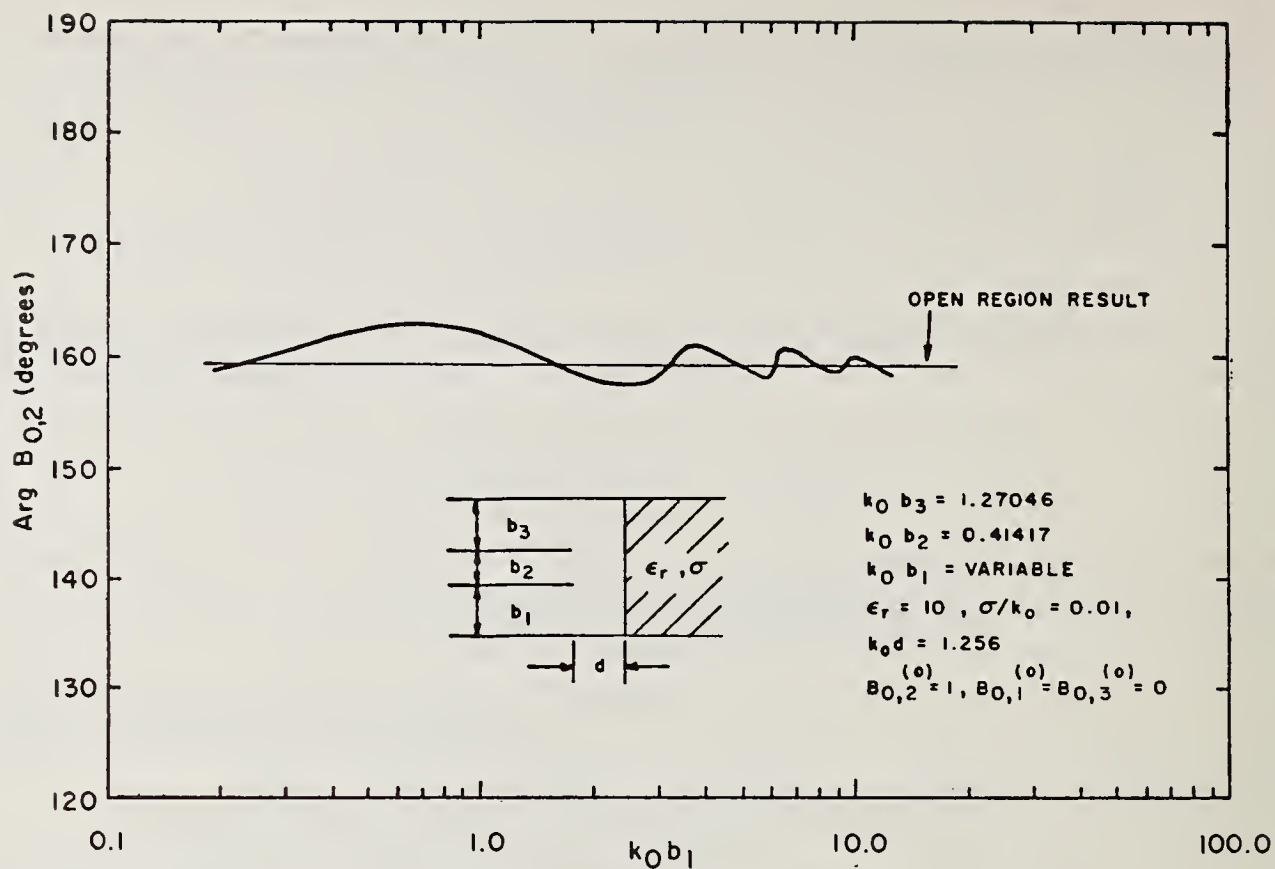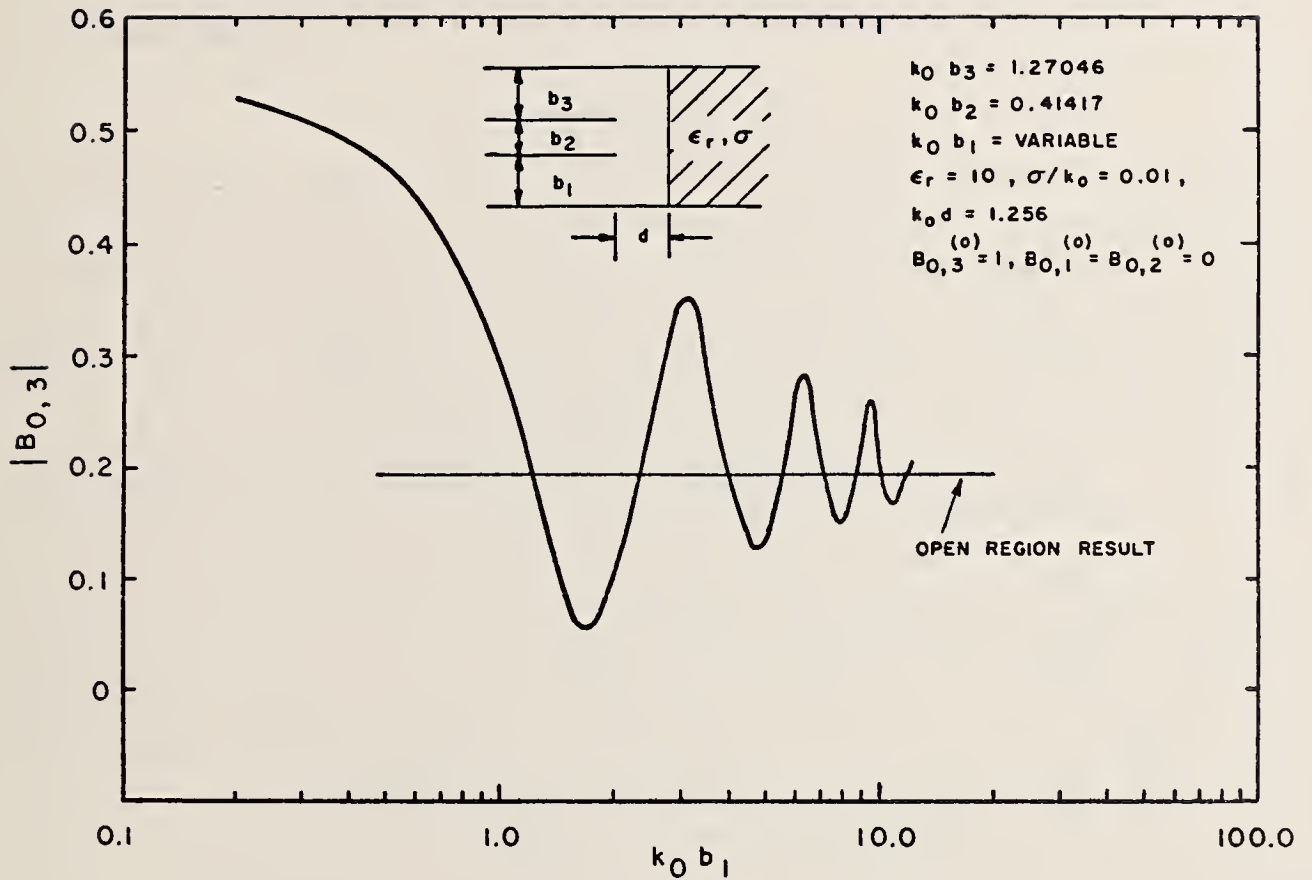
(a)   Phase of $B_{0,2}$

(b)   Magnitude of $B_{0,2}$

Fig. 11.3.2.1:   Scattering Parameters of Dielectrically
Loaded Waveguide as a Function of b_1

140

(c) Magnitude of $B_{0,3}$

Fig. 11.3.2.1: Scattering Parameters of Dielectrically Loaded Waveguide as a Function of b_1
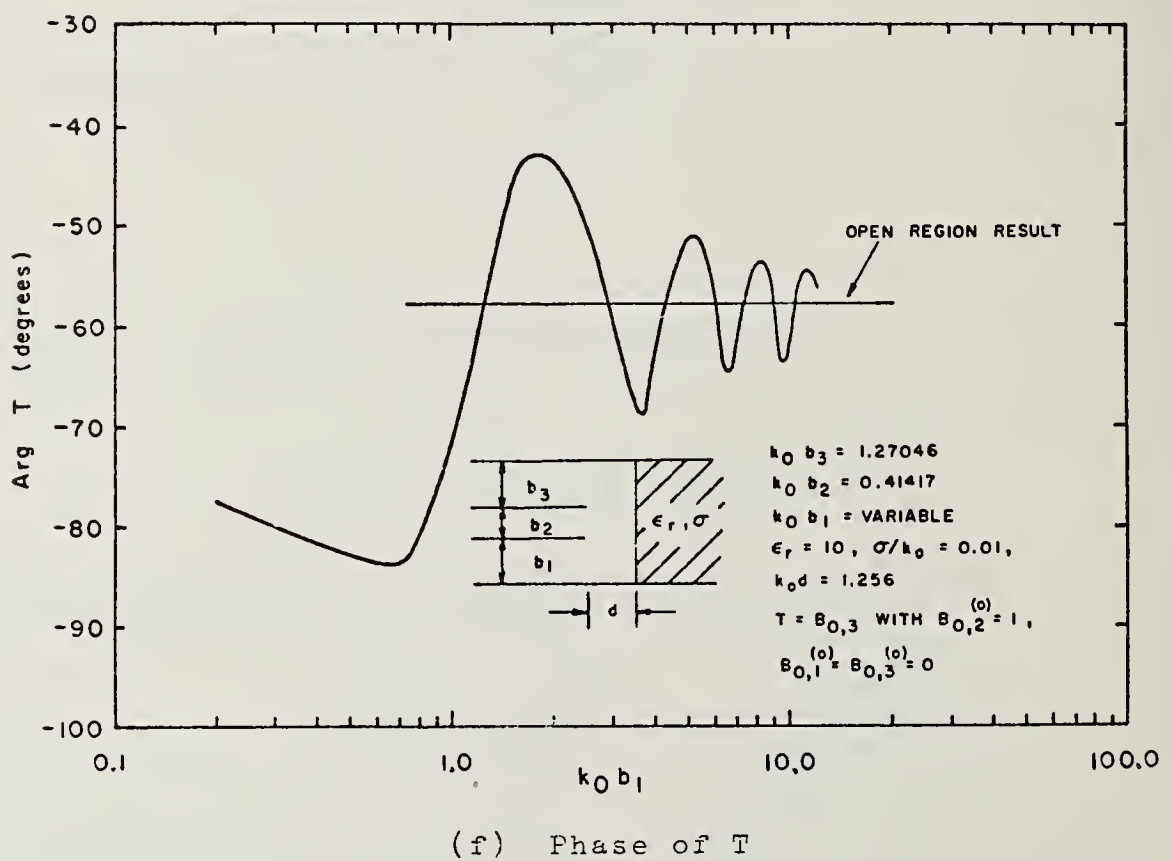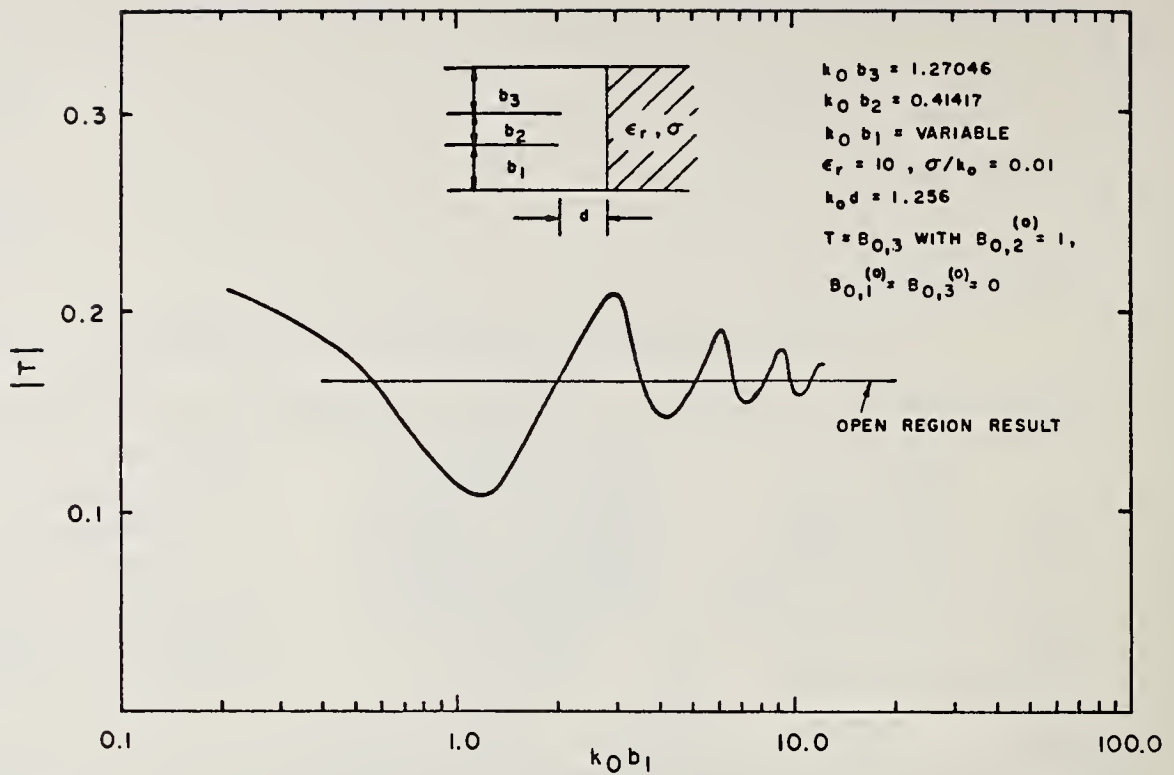
141

(e) Magnitude of T

(f) Phase of T

Fig. 11.3.2.1: Scattering Parameters of Dielectrically
Loaded Waveguide as a Function of b_1

142

Table 11.3.2.2 Convergence of Open Region Solution

N_p	$B_{o,1}$*		$B_{o,2}$*		T*	
5	0.19399	177.68°	0.87189	159.46°	0.50981	-57.44°
7	0.19400	177.68°	0.87188	159.46°	0.50896	-57.43°
9	0.19402	177.68°	0.87186	159.46°	0.50993	-57.43°

*Same as Table 11.3.2.1

This clearly illustrates that the convergence of the solution is quite good.

3.3 The Magnetic Wall Case

This section presents results similar to section 3.2, with one exception. No closed region data is presented since the problem of an N-furcated waveguide with dielectric loading and a magnetic symmetry wall was not implemented on the computer. However, an alternate check of the solution is available. Figure 11.3.3.1 illustrates the variation of the reflection coefficient of a truncated parallel plate waveguide parallel to a magnetic symmetry wall as a function of the distance from the waveguide aperture to a conducting half space. The reflection coefficient for the case of no dielectric is shown for comparison. One notes that the reflection coefficient for the case with the dielectric oscillates about the no dielectric case, symmetrically and with progressively smaller amplitude.

Table 11.3.3.1 shows the convergence of the dominant mode reflection coefficient for the following parameters: $\varepsilon_r = 10$, $\sigma/k_o - 0.01$, $k_o d = 1.256$, $k_o b_1 = 1.25046$, $k_o b_2 = 0.41417$ and $N^{1,R} = N^{2,L} = N_p$. N is the number of segments along L_1 and M_n is the number of matching points within the nth interval.

Table 11.3.3.1 Convergence of Open Region Solution

N_p	N	M_1	M_2	M_3	M_4	$B_{o,2}$	
7	3	4	4	4	--	0.74420	147.98°
7	3	6	6	6	--	0.75396	147.91°
7	3	8	8	8	--	0.75322	147.80°
7	3	10	10	10	--	0.75304	147.81°
7	3	12	12	12	--	0.74313	147.81°
7	4	12	12	12	12	0.75313	147.80°
7	3	16	8	16	--	0.75317	147.81°
5	3	16	8	16	--	0.75316	147.80°
9	3	16	8	16	--	0.75317	147.80°

Again, excellent convergence is observed, both with respect to approximation of the continuous as well as discrete parts of the problem.

3.4 Superposition of the Results

The title to this chapter suggests the use of waveguides to remotely sense the parameters of the earth. In this case, we are suggesting a locally plane approximation as well as a homogeneous half space.

143
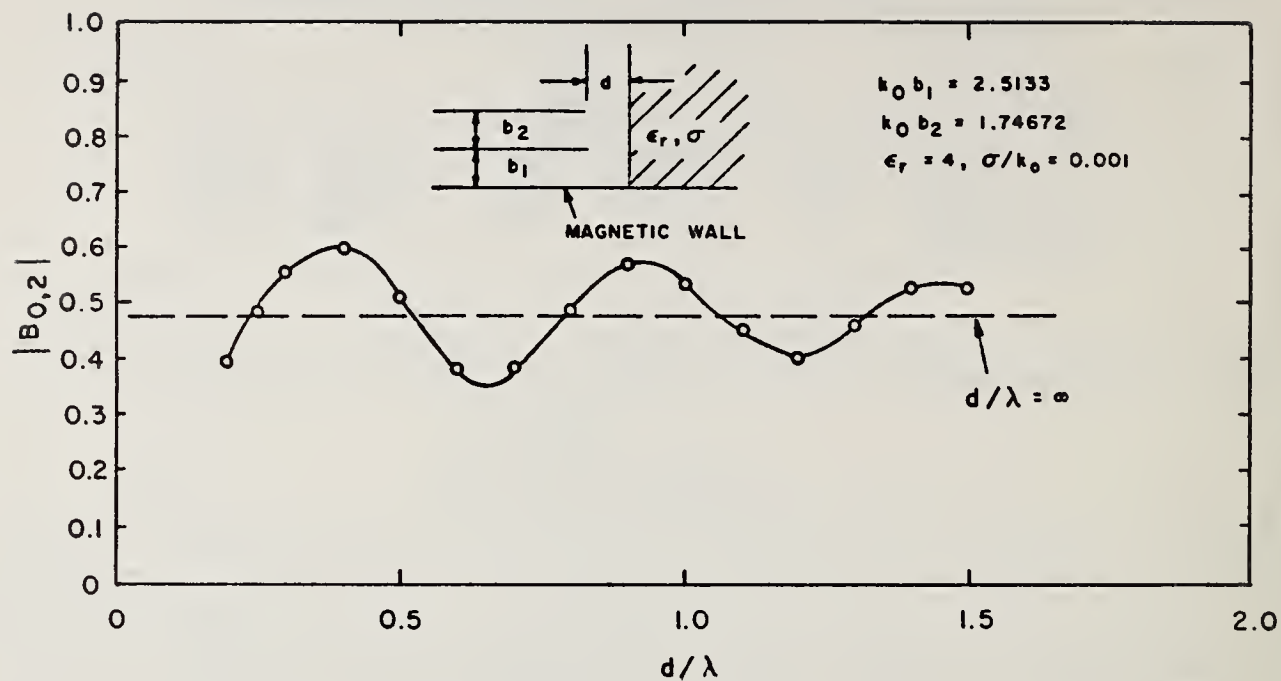
(a) Magnitude of Reflection Coefficient
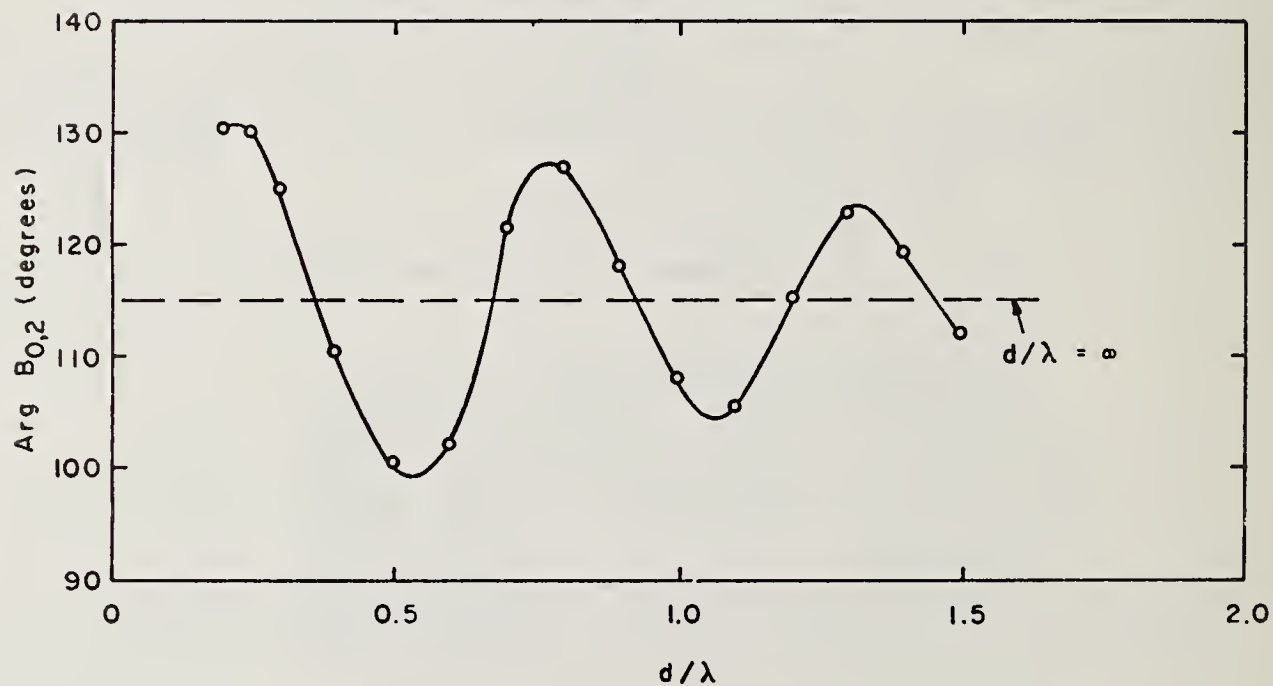
(b) Phase of Reflection Coefficient

Fig. 11.3.3.1: Variation of the Reflection Coefficient
of the Magnetic Wall Case as a Function
of Distance

144

Fig. 11.3.4.1: Reflection Coefficient of One Element
of a Two Element Parallel Plate Waveguide
Array Radiating into a Dielectric Half
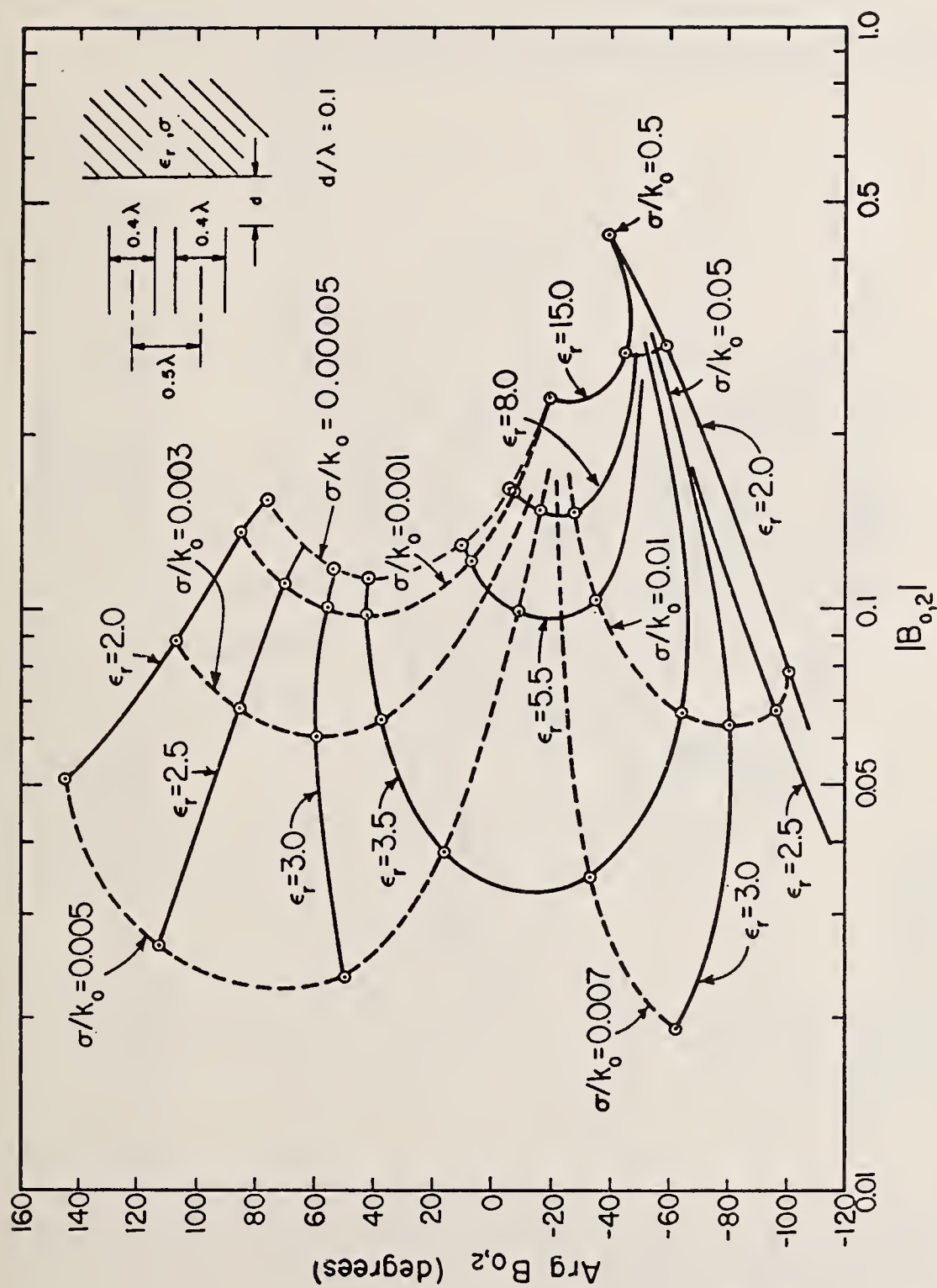Space as a Function of the Dielectric
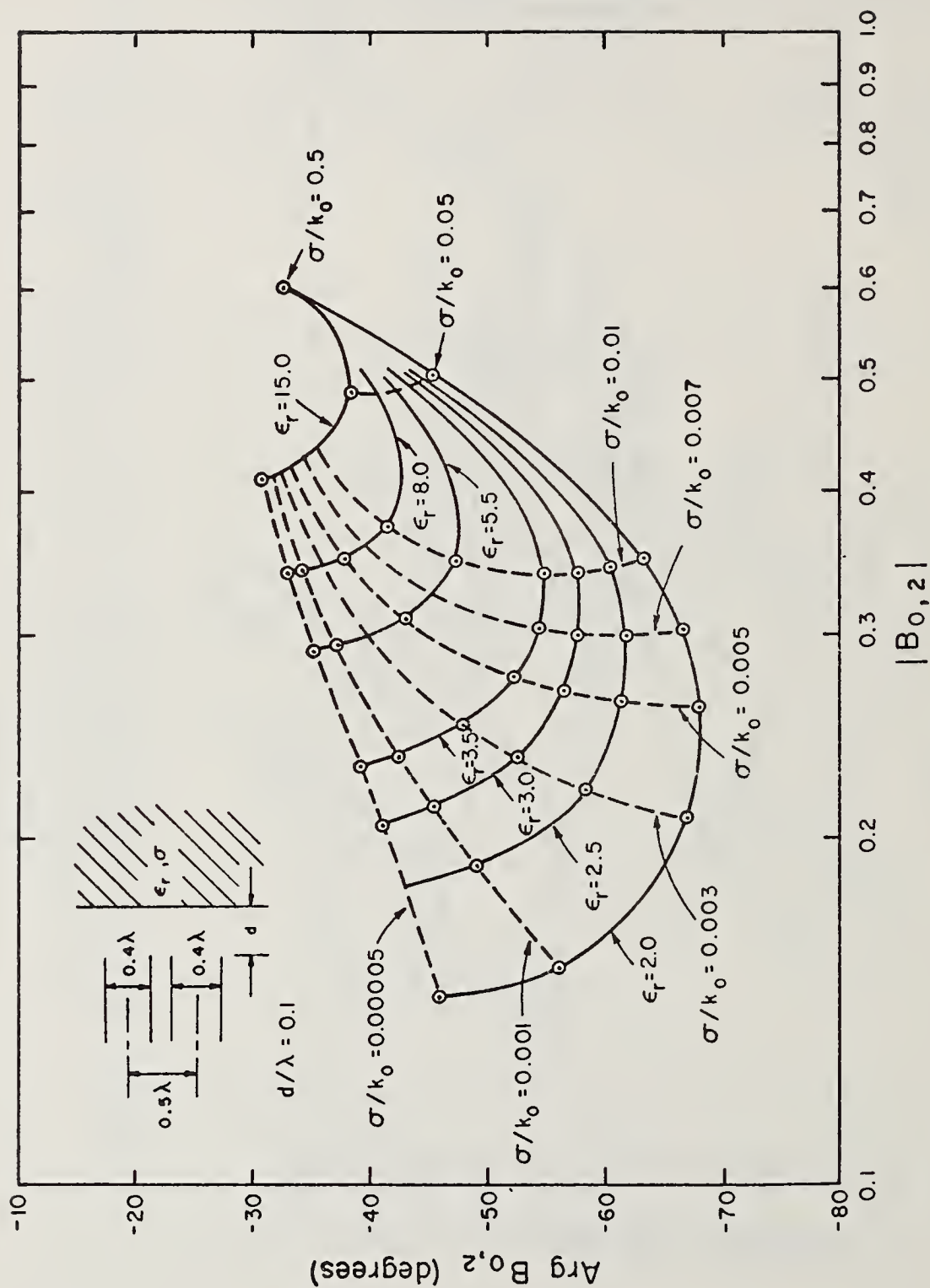Parameters

145

Fig. 11.3.4.2: Matched Reflection Coefficient of One
Element of a Two Element Parallel Plate
Waveguide Array Radiating into a Dielectric
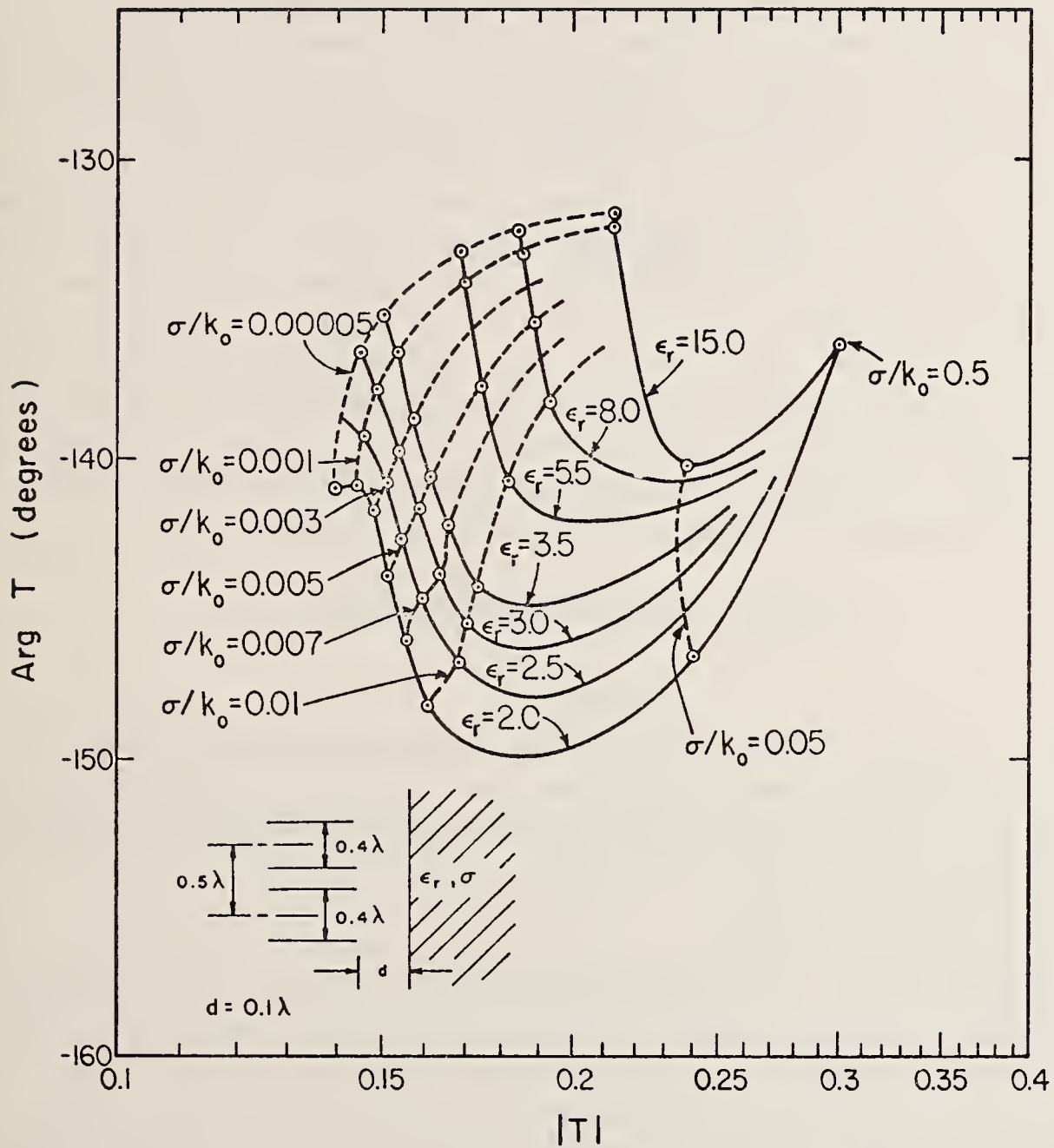Half Space as a Function of the Dielectric
Parameters

Fig. 11.3.4.3: Coupling Between Two Parallel Plate
Waveguides Radiating into a Dielectric
Half Space as a Function of the Dielectric
Parameters

Figure 11.3.4.1 illustrates reflection coefficient of one of two $0.4\lambda_o$ waveguides spaced $0.5\lambda_o$ apart with respect to their centers, at a distance of $0.1\lambda_o$ away from a half space. The variation of the permittivity and conductivity cause the reflection coefficient to change quite noticeably. In fact, the variation is quite similar to that of a single $0.4\lambda_o$ waveguide given in Chapter 9, in figure 9.4.3, as indeed it should be. Figure 11.3.4.2 illustrates this same data matched to the impedance of a single waveguide looking into free space. Again, this is quite similar to the data of Chapter 9, and resembles quite closely the normally incident Fresnel reflection coefficient. Figure 11.3.4.3 illustrates the the coupling coefficient between the two waveguides as a function of variation of the half space parameters. One should observe that the phase of the coupling coefficient varies over about 20° while the magnitude varies between about 0.15 to 0.3. This is to be compared with about 40° of change in the phase of the matched reflection coefficient and an amplitude of the matched reflection coefficient varying from about 0.15 to 0.6.

Hence, in this particular case it appears as if the pair of antennas is of little further help in solving the inverse problem of determining ϵ_r and σ, as compared with a single antenna. However, this is not to say that the coupling coefficient may not be useful in this determination. Additionally, the coupling coefficient might prove to be more sensitive to variation for such problems as layered earth models or buried dielectric anomalies.

CHAPTER 12. OTHER OPEN REGION PROBLEMS

1. Introduction

The purpose of this chapter is to illustrate the ease of application of the modified function theoretic technique to some additional open region problems. In particular the following problems are solved using the modified function theoretic technique: (1) a flanged waveguide radiating into half space, (2) scattering by a thick semi-infinite plane, and (3) radiation from a slot in a waveguide.

A flanged waveguide radiating into a grounded dielectric sheath has been solved by Wu (1969) using moment methods. Also Kostelnicek and Mittra (1969, 1971) discuss the solution of the problem of a flanged waveguide radiating into a dielectric slab using the modified function theoretic technique. In their 1971 paper they make the erroneous statement that the associated homogeneous Hilbert problem cannot be solved in closed form. Indeed the solution of this problem is quite straightforward using the techniques we have developed in chapter 8.

The scattering by a thick semi-infinite plane has been solved by Lee and Mittra (1968) using the generalized scattering matrix technique. The solution given in this chapter serves to illustrate the use of the modified function theoretic technique when the incident field is a plane wave.

Another problem of interest is the radiation from a slot in a waveguide wall. This problem is a simple extension of the problem of a waveguide radiating into a half space given in Chapter 9.

148

2. Flanged Waveguide Radiating into a Half Space

The geometry of this problem and its auxiliary problem are shown in Figure 12.2.1. From Chapter 8 we can clearly write the holomorphic function $T(\omega)$ as

$$T(\omega) = X(\omega)\left[\frac{K_o}{\omega-jk_o} + \int_{L_1^-} \frac{g^{(1)}(t)\ dt}{X^-(t)(t-\omega)} - \int_{L_2^+} \frac{g^{(2)}(t)\ dt}{X(t)(t-\omega)}\right] \tag{2.2}$$

where

$$X(\omega) = H_1(\omega)(\omega-jk_o)\Pi(\omega,\gamma_b)\exp\left\{\frac{b\sqrt{\omega^2+k_o^2}}{\pi}\left[\ln\left(\frac{\omega-\sqrt{\omega^2+k_o^2}}{k_o}\right) + \frac{j\pi}{2}\right]\right\}$$

where

$$H_1(\omega) = \exp\left\{\frac{\omega b}{\pi}\left[1-C_\ell-\ln\left(\frac{k_o b}{2\pi}\right)\right] - \frac{j\pi b}{2}\right\}$$

From Chapter 8 we have that

$$g^{(1)}(\omega) = -\omega \sin \lambda b\ e^{j\lambda b}\ C^o(\lambda), \quad \omega\varepsilon L_1 \tag{2.3a}$$

$$g^{(2)}(\omega) = \omega \sin \lambda b\ A^o(\lambda), \quad \omega\varepsilon L_2 \tag{2.3b}$$

Also we have

$$T^-(\omega)-T^+(\omega) = -2\pi j\ \omega \sin \lambda b\ A(\lambda), \quad \omega\varepsilon L_1 \tag{2.4}$$

and

$$T^+(-\omega)+T^-(-\omega) = 2\pi\omega[\cos \lambda b\ A^o(\lambda) - C(\lambda)], \quad \omega\varepsilon L_1 \tag{2.5}$$

However, the spectra are related at $z=d$ and at $z=-\delta$ by the following

$$C^o(\lambda) = R_C(\lambda)\ C(\lambda) \tag{2.6}$$

where

$$R_C(\lambda) = \frac{\varepsilon'\omega - \Gamma'}{\varepsilon'\omega + \Gamma'}\ e^{-2\omega\delta}$$

and
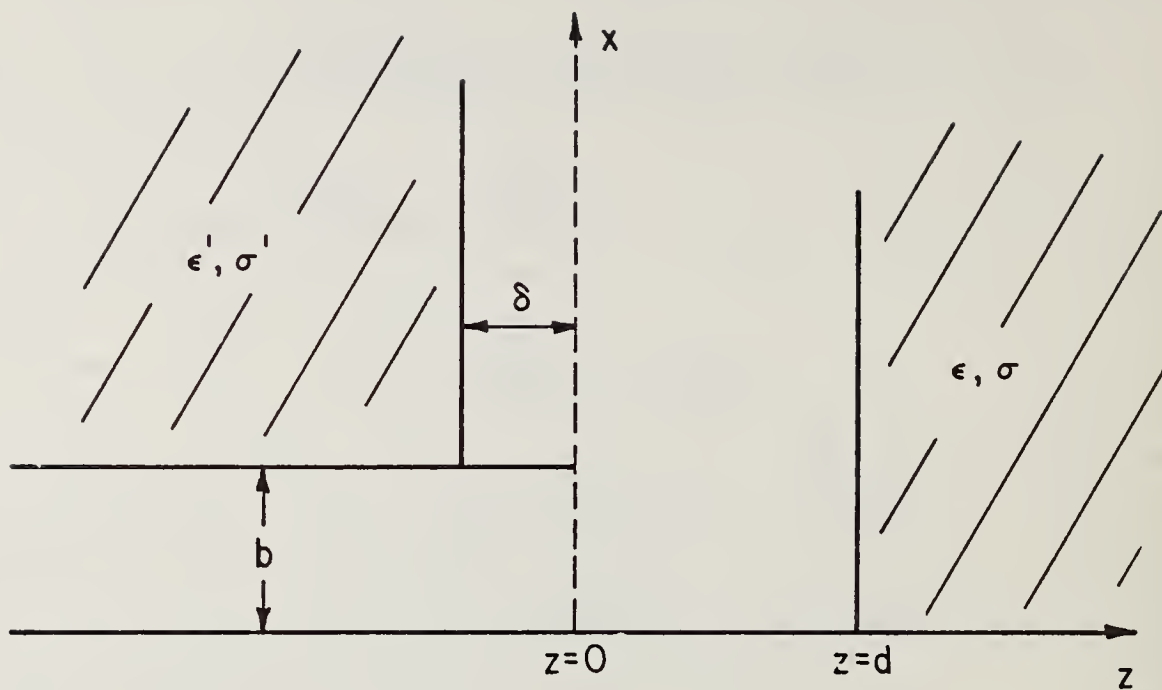
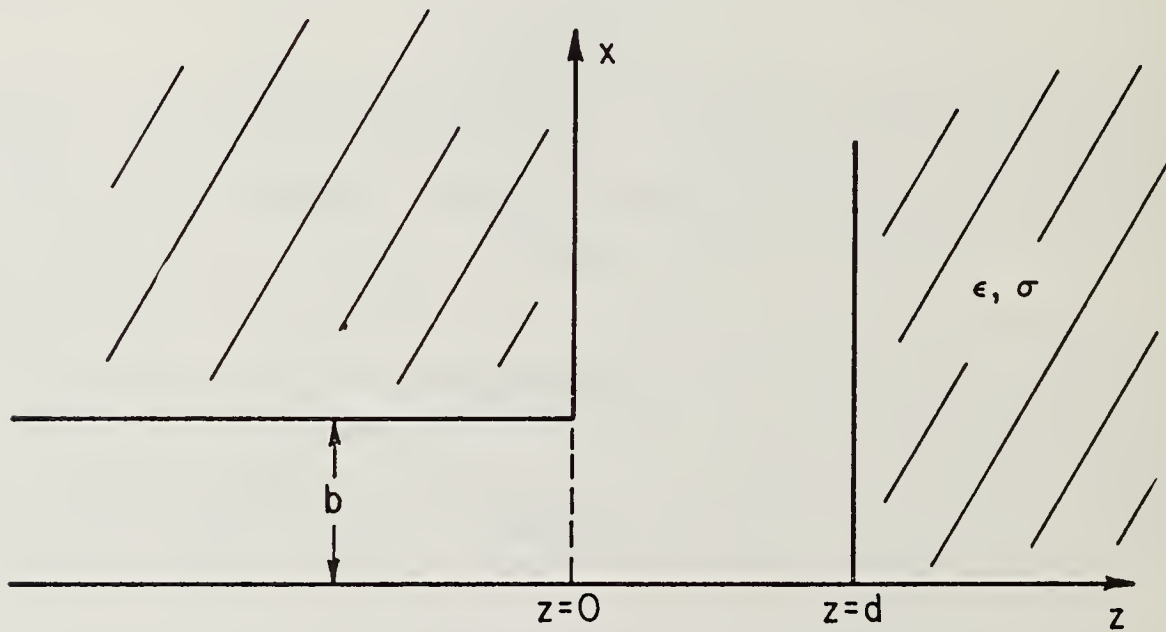$$A^o(\lambda) = R_A(\lambda)\ A(\lambda) \tag{2.7}$$

where

$$R_A(\lambda) = \frac{\varepsilon\omega - \Gamma}{\varepsilon\omega + \Gamma}\ e^{-2\omega d}$$

Using the property of $X(\omega)$ that

$$X^-(\omega) = X^+(\omega)e^{j2\lambda b}, \quad \omega\varepsilon L_1$$

(a) The Auxiliary Problem

(b). The Final Problem

Fig. 12.2.1: Flanged Waveguide Radiating into a Half
Space

we can immediately write (2.4) as

$$X^-(\omega)2je^{-j\lambda b}\sin\lambda b\left[\frac{K_o}{\omega-jk_o} + PV\int_{L_1^-}\frac{g^{(1)}(t)\,dt}{X^-(t)(t-\omega)} - \int_{L_2^+}\frac{g^{(2)}(t)\,dt}{X(t)(t-\omega)}\right]$$

$$+ 2\pi j\,g^{(1)}(\omega)e^{-j\lambda b}\cos\lambda b = -2\pi j\,\omega\sin\lambda b\,A(\lambda),\quad \omega\varepsilon L_1$$

The principal value of the integral associated with L_1^- has to be taken. Then using (2.7) and (2.3b) we arrive at the following integral equation

$$X^-(\omega)e^{-j\lambda b}\sin\lambda b\left[\frac{K_o}{\omega-jk_o} + PV\int_{L_1^-}\frac{g^{(1)}(t)\,dt}{X^-(t)(t-\omega)} - \int_{L_2^+}\frac{g^{(2)}(t)\,dt}{X(t)(t-\omega)}\right]$$

$$+ \pi\,g^{(1)}(\omega)e^{-j\lambda b}\cos\lambda b = \pi\,R_A^{-1}(\lambda)\,g^{(2)}(-\omega),\quad \omega\varepsilon L_1 \qquad (2.8)$$

Equation (2.8) is just the extension of equation (2.5) of Chapter 9.
   Similarly for $\omega\varepsilon L_2$ we know that

$$X^-(\omega) = X^+(\omega) = X(\omega)$$

hence we can write (2.5) explicitly as

$$X(\omega)\left[\frac{K_o}{\omega-jk_o} + \int_{L_1^-}\frac{g^{(1)}(t)\,dt}{X^-(t)(t-\omega)} - PV\int_{L_2^+}\frac{g^{(2)}(t)\,dt}{X(t)(t-\omega)}\right]$$

$$= \frac{-\pi}{\sin\lambda b}\left[\cos\lambda b\,g^{(2)}(\omega) - e^{-j\lambda b}\,R_C^{-1}(\lambda)g^{(1)}(-\omega)\right],\quad \omega\varepsilon L_2 \qquad (2.9)$$

Equation (2.9) is just the extension of equation (3.5) of Chapter 8.
   Equations (2.8) and (2.9) are simultaneous integral equations for the unknown functions $g^{(1)}(\omega)$ and $g^{(2)}(\omega)$. Note that in each equation we have a Cauchy principle value integral in contrast to the previous cases where the integrals existed in the usual Riemann sense. We will not give any numerical results here but we are in a position to discuss the asymptotic behavior of the unknowns. However, before doing this it is convenient to make a transformation of variables similar to those used for the flanged guide and the radiation into a half space. Thus consider

$$g^{(2)}(-\omega) = \frac{K_o\sin\lambda b\,R_A(\lambda)}{\pi(\omega-jk_o)}e^{-j\lambda b}\,X^-(\omega)G^{(2)}(\omega),\quad \omega\varepsilon L_1 \qquad (2.10)$$

and

$$g^{(1)}(\omega) = \frac{-K_o\sin\lambda b}{\pi(\omega+jk_o)}e^{j\lambda b}\,R_C(\lambda)X(-\omega)G^{(1)}(\omega),\quad \omega\varepsilon L_1 \qquad (2.11)$$

Using (2.10) and (2.11), (2.8) becomes

$$\left[\frac{1}{\omega-jk_o} + PV \int_{L_1^-} \frac{Q^{(1)}(t)G^{(1)}(t)\ dt}{t-\omega} + \int_{L_2^+} \frac{Q^{(2)}(t)G^{(2)}(-t)\ dt}{t-\omega}\right]$$

$$+ \pi \cot \lambda b\ Q^{(1)}(\omega)\ G^{(1)}(\omega) = \frac{G^{(2)}(\omega)}{\omega-jk_o}, \quad \omega\epsilon L_1 \tag{2.12}$$

where

$$Q^{(1)}(\omega) = \frac{-\sin \lambda b\ R_c(\lambda)e^{j\lambda b}\ X(-\omega)}{\pi(\omega+jk_o)\ X^-(\omega)}, \quad \omega\epsilon L_1$$

and

$$Q^{(2)}(\omega) = \frac{\sin \lambda b\ R_A(\lambda)e^{-j\lambda b}\ X^-(-\omega)}{\pi(\omega+jk_o)\ X(\omega)}, \quad \omega\epsilon L_2$$

Similarly, using (2.10) and (2.11), (2.9) becomes

$$\left[\frac{1}{\omega-jk_o} + \int_{L_1^-} \frac{Q^{(1)}(t)G^{(1)}(t)\ dt}{t-\omega} + PV \int_{L_2^+} \frac{Q^{(2)}(t)G^{(2)}(-t)\ dt}{t-\omega}\right]$$

$$= \pi \cot \lambda b\ Q^{(2)}(\omega)G^{(2)}(-\omega) + \frac{G^{(1)}(-\omega)}{\omega-jk_o}, \quad \omega\epsilon L_2 \tag{2.13}$$

Now from Chapters 8 and 9 we have already found that

$$Q^{(2)}(-\omega) = 0\left\{\frac{e^{-2\pi d}}{\omega}\right\} \quad |\omega| \to \infty,\ \omega\epsilon L_1$$

and

$$G^{(2)}(\omega) = 0(1), \quad |\omega| \to \infty,\ \omega\epsilon L_2$$

and we know that integrals involving $G^{(2)}(\omega)$ can be truncated because of the exponential decay of $Q^{(2)}(\omega)$. Also we have previously found that

$$Q^{(1)}(\omega) = 0(\omega^{-1}),\ |\omega| \to \infty,\ \omega\epsilon L_1$$

and

$$G^{(1)}(\omega) = 0(\omega^{-\Delta}),\ |\omega| \to \infty,\ \omega\epsilon L_2$$

152

where

$$\Delta = \frac{1}{\pi} \sin^{-1} \left[\frac{\epsilon'-1}{2(\epsilon'+1)} \right]$$

For the edge condition to be explicitly satisfied at $z = 0$, $x = b$, we can write

$$Q^{(1)}(\omega)G^{(1)}(\omega) = \overline{G} \, \omega^{-1-\Delta}, \quad \omega > \omega_0 \quad \omega \epsilon L_1 \tag{2.14}$$

In order to insure that the edge condition is explicitly satisfied we must insure that

$$\sin \lambda b \, A(\lambda) = 0(\lambda^{-3/2-\Delta}), \; |\lambda| \to \infty$$

Then from (2.4) or equivalently (2.12) we see that the following term must vanish in order that $G^{(2)}(\omega) = 0(\omega^{-\Delta})$.

$$1 + \int_{L_1^-} Q^{(1)}(t)G^{(1)}(t) \, dt + \int_{L_1^-} Q^{(2)}(-t)G^{(2)}(t) \, dt = 0$$

or

$$1 + \int_{L_1^-}^{(\omega_0)} Q^{(1)}(t)G^{(1)}(t) \, dt + \overline{G} \, \frac{\omega_0^{-\Delta}}{\Delta} + \int_{L_1^-} Q^{(2)}(-t)G^{(2)}(t) \, dt = 0 \tag{2.15}$$

Equation (2.15) is merely the extension of equation (3.13) of Chapter 8.

Before concluding this section, it is in order to briefly discuss the method of numerical solution that one might use in solving (2.12) and (2.13). Note that in contrast to the equations obtained in the solution of flanged waveguide and the solution of a waveguide radiating into a homogeneous half space that equations (2.12) and (2.13) require the evaluation of Cauchy principle value integrals. Hence any numerical approximation technique used for the solution of these equations must account for the principle value integrals. As noted by Kostelnicek and Mittra (1969, 1971) one possible alternative is to change the paths of integration. However, when doing this the new path of integration is rather arbitrary and may introduce more numerical difficulty than the original path.

3. Scattering by a Thick Semi-Infinite Plane

Figure 12.3.1 illustrates the geometry of the thick semi-infinite plane as well as the auxiliary problem. For simplicity we are only solving the electric boundary case. In general, incidence at an arbitrary angle requires that the magnetic symmetry problem be solved in addition to the electric case. However, the method is clearly illustrated from just the electric solution.

From Chapter 8 we see that the solution of the problem may be found from the holomorphic function

$$T(\omega) = X(\omega) \left[\sum_{n=0}^{\infty} \frac{g_n}{\omega - \gamma_{nb}} - \int_{L_2^+} \frac{g^{(2)}(t) \, dt}{X(t)(t-\omega)} \right] \tag{3.1}$$

153
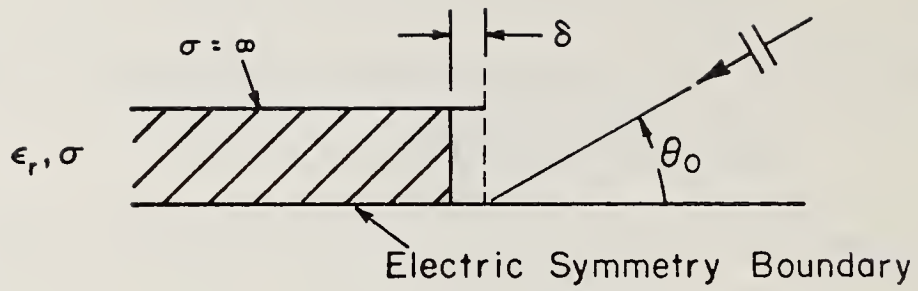
(a) Auxiliary Problem
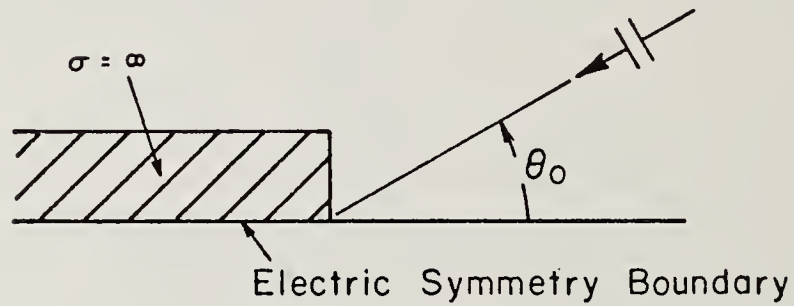
(b) Half Plane Geometry

Fig. 12.3.1: The Thick Half Plane

where $X(\omega)$ is the homogeneous solution. Since the incident field is a plane wave we have

$$A^o(\lambda) = A_o \delta(\omega - jk_o \cos \theta_o), \quad \omega \epsilon L_1$$

where $\delta(\cdot)$ is the Dirac delta function and hence

$$g^{(2)}(-\omega) = -\omega \sin \lambda b \, A_o \delta(\omega - jk_o \cos \theta_o), \quad \omega \epsilon L_1$$

Thus

$$\int_{L_2^+} \frac{g^{(2)}(t) \, dt}{X(t)(t-\omega)} = \int_{L_1^-} \frac{g^{(2)}(-t) \, dt}{X(-t)(t+\omega)} + \frac{-jk_o \cos \theta_o \, A_o \, \sin(k_o b \sin \theta_o)}{X(-jk_o \cos \theta_o)(\omega + jk_o \cos \theta_o)} \tag{3.2}$$

Note that in the limiting case as $\theta_o \to 0°$, that the electric solution furnishes the complete solution to the problem.

In order to find an equation for g_n we use the knowledge that $z = -\delta$ that

$$B_m^{(o)} = B_m R_m \tag{3.3}$$

where

$$R_m = \frac{\epsilon \gamma_{mb} - \Gamma_{mb}}{\epsilon \gamma_{mb} + \Gamma_{mb}} e^{-2\delta \gamma_{mb}}$$

where

$$\Gamma_{mb} = \left(\frac{m\pi}{b}\right)^2 - \epsilon k_o$$

Then using (v) of Chapter 8, section 2, we have

$$(-1)^{m+1} T(-\gamma_{mb}) = -\gamma_{mb} \, b \, \epsilon_m \, B_m$$

$$= -\gamma_{mb} \, b \, \epsilon_m \, R_m^{-1} \, B_m^{(o)} \tag{3.4}$$

but from (i) of Chapter 8, section 2, we have

$$(-1)^{m+1} T(\gamma_{mb}) = \gamma_{mb} \, b \, \epsilon_m \, B_m^{(o)}$$

$$= \begin{cases} (-1) \dfrac{X^{(m)}(\gamma_{mb})}{\gamma_{mb}} g_m & m > 0 \\[2mm] -X^{(o)}(jk_o) \, g_o & m = 0 \end{cases} \tag{3.5}$$

where $X^{(m)}(\gamma_{mb})$ indicates that the mth zero at γ_{mb} is to be omitted. Hence we can write in general

$$g_m = \lambda_m B_m^{(o)} \tag{3.6}$$

where λ_m is defined by (3.5). Using (3.6) in (3.4) we have

$$(-1)^{m+1} X(-\gamma_{mb}) \left[-\sum_{n=0}^{\infty} \frac{g_n}{\gamma_{mb}+\gamma_{nb}} + \frac{jk_o \cos\theta_o A_o \sin(k_o b \sin\theta_o)}{X(-jk_o \cos\theta_o)(jk_o \cos\theta_o - \gamma_{mb})} \right]$$

$$= -\gamma_{mb} b \, \varepsilon_m R_m^{-1} \lambda_m^{-1} g_m, \quad m = 0,1,2,\ldots \tag{3.7}$$

Equation (3.7) is an infinite matrix equation for g_m.

In order to truncate (3.7) efficiently, let us investigate the asymptotic behavior of g_m. We may follow a procedure similar to that used for the E-plane step in Chapter 2 and find that

$$g_n = 0(n^{-1-\Delta})$$

where

$$\Delta = \frac{1}{\pi} \sin^{-1}\left[\frac{(\varepsilon-1)}{2(\varepsilon+1)}\right]$$

Also if $g_m = \bar{g} \, m^{-1-\Delta}$ for $m > N$, then we can easily show that

$$\sum_{n=0}^{N} g_n + \bar{g} \sum_{n=N+1}^{\infty} n^{-1-\Delta} + \frac{jk_o \cos\theta_o A_o \sin(k_o b \sin\theta_o)}{X(-jk_o \cos\theta_o)} = 0 \tag{3.8}$$

From Chapter 10 we know that the far field for $z > 0$ is determined by

$$T(jk_o \cos\theta)e^{-jk_o b \sin\theta} \tag{3.9}$$

and thus upon solving for g_n and $\bar{g}$ we can easily find the far field scattering pattern.

One should note that as $\theta_o \to 0$ that the term involving A_o becomes singular and it would appear that we do not have a proper solution. However, for the case of $\theta_o = 0$, the waveguide walls are orthogonal to the incident electric field and the equations given in Chapter 8 are incomplete. In this case there will be an additional term

$$-2jk_o b \, A_o \, e^{jk_o z_o} \delta_{mo}$$

on the left hand side of (2.2.6) of Chapter 8 and an additional term will be present in (2.2.10) of Chapter 8. Thus we have that

$$(-1)^m T(-\gamma_{mb}) = \gamma_{mb} b \, \varepsilon_m B_m \, e^{\gamma_{mb} z_o} - 2jk_o b \, A_o \, e^{jk_o z_o} \delta_{mo} \tag{3.10}$$

156

In this case (3.7) must be modified to be

$$(-1)^m X(-\gamma_{mb}) \left(-\sum_{n=0}^{\infty} \frac{g_n}{\gamma_{mb}+\gamma_{nb}} \right) = \gamma_{mb} \, b \, \epsilon_m \, R_m^{-1} \, B_m^{(o)} - 2jk_o b \, A_o \, \delta_{mo} \qquad (3.11)$$

4. Radiation From a Slot in a Waveguide Wall

This section serves as a forum for presenting some results using the theory of Chapter 9. In particular, if one considers the case of a waveguide radiating into a half space, a slot in the waveguide wall can be simulated by superposition of the case where the half space is allowed to become either a perfect electric or magnetic conductor.

For TEM excitation this type of slot is known as a series slot, because the equivalent circuit is just a series admittance.

Figure 12.4.1 shows the series conductance and susceptance as a function of slot width for the case of $(2b/\lambda) = 0.278$. For this particular case the slot is resonant at a slot width of about 0.2 wavelengths.

CHAPTER 13. CONCLUSIONS (PART II)

This part of the monograph has presented the MRCT and MFTT solution of a new class of open region problems. The approach has been to solve a canonical problem of a semi-infinite parallel plate waveguide with known incident fields. The solution of composite problems is readily found from the associated auxiliary problem. Many of the problems solved in this part were combined open and closed region problems for which the results of part I of this monograph were also applicable. An example is the finite phased array. The auxiliary problem may be recognized to be composed of an N-furcated waveguide and a semi-infinite parallel plate waveguide.

This particular problem is essentially the open region analogue of the N-furcated waveguide and its modifications as given in part I of this monograph.

The convergence of the solutions is rapid and only requires a small number of perturbation coefficients or a limited representation of a continuous perturbation spectrum.

Several physically interesting problems were solved. Among these were the problem of radiation of a waveguide into a homogeneous half space. This solution indicates that remote sensing of the earth is quite feasible even when the earth is in the near field of the waveguide aperture. Even in the near field, one is able to relate the reflection coefficient to the normally incident Fresnel reflection coefficient. The primary difference is that the argand diagram is rotated. This same problem was also solved for the case of two waveguides. For the case of a homogeneous earth, no particular advantage of measuring the coupling coefficient was observed. However, this may not hold true for such problems as the remote sensing of dielectric anomalies or in layered media.

Another problem of physical interest is the problem of a finite phased array without a ground plane. The analysis to date has assumed an infinite ground plane (or some approximation
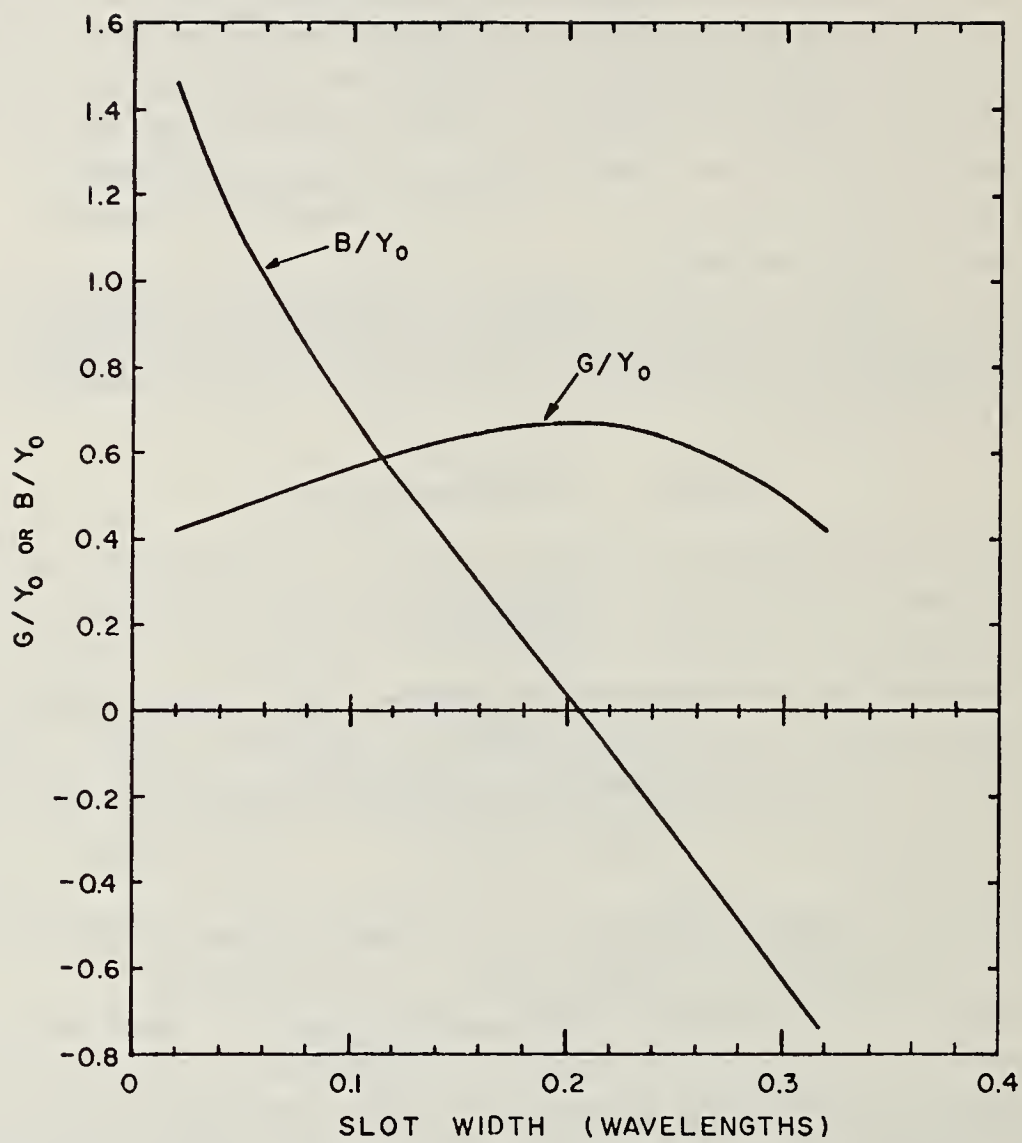
Fig. 12.4.1: Series Slot Admittance

to it) in order to simplify the analysis. This is a good approximation if one is only interested in the array patterns near broadside. However, for wide angle scanning arrays the correlation is increasingly bad because of ground plane effects. It should also be noted that this analysis can be easily extended to the case of a finite ground plane.

Solutions are also indicated for more complicated problems such as a flanged waveguide radiating into a layered media.

CHAPTER 14. COMMENTS AND FINAL SUMMARY

This monograph has endeavored to fill the gaps that existed in the modified residue calculus and modified function theoretic techniques. The key to this realization has been the identification of certain canonical problems. In part I, the canonical problem was the bifurcated waveguide filled with homogeneous media. For part II, the canonical problem was the semi-infinite parallel plate waveguide. These choices of canonical problems were made because of the cartesian nature of problems were to be solved. This choice of canonical problems is by no means an implied limitation of the MRCT and MFTT. For example, a wide range of problems dealing with the modification of semi-infinite circular or coaxial waveguide can be solved in the same manner. For example, one can solve the problem of a non-contacting coaxial short by recognizing that it is a modification of the coaxial bifurcated junction. Such a solution would involve the construction of two holomorphic functions, one with a single modification and the other with a double modification.

One can also solve a wide class of modified semi-infinite circular and coaxial open region waveguide problems. The primary difficulty in this case compared to the closed region is that the solution of the associated homogeneous Hilbert problem must be obtained numerically. However, efficient techniques for this factorization may be found in Weinstein (1969) as well as Mittra and Lee (1971). This canonical problem admits the possibility of solving such problems as a flanged circular waveguide radiating into a homogeneous half space. Also the problem of a flanged (or un-flanged) coaxial waveguide radiating into free space or a layered half space can be solved using the techniques.

Other canonical problems which offer interesting possibilities are the open and closed region problems concerned with the excitation of surface wave on a grounded dielectric slab by a semi-infinitely long parallel-plate waveguide filled with the same dielectric. This problem cannot be solved in closed form, but Bates and Mittra (1968) have given efficient numerical schemes for the factorization. This canonical problem allows one to solve two interesting problems. The first is the diffraction and scattering of waves from a dielectric step in a waveguide. This problem was solved by Royer and Mittra (1971) and is also discussed in Chapter 5 of this monograph. The open region canonical problem allows one to solve the open region analogue of the dielectric step, the semi-infinite dielectric waveguide. This problem has not yet received a satisfactory analytical solution. One cannot, however, solve the coaxial and circular analogue of these parallel plate problems because the hybrid nature of the mode structure does not permit a solution of this form.

One area which was not explored in this monograph was the ultimate use of asymptotics. Most of the numerical solutions given displayed several place accuracy with only a few perturbational terms or only a few sample points of a continuous perturbational spectrum.

The logical course one can follow from this is to solve problems using the MRCT and the MFTT using <u>only</u> the asymptotic terms. Such solutions should easily have two place accuracy and be quite sufficient for many engineering tasks. This technique might be comparible to say the geometrical theory of diffraction where nominally two place accuracy is obtained (Yee, Felson, and Keller, 1968). In fact, an investigation into the connection between these two techniques might prove very fruitful.

Yet another area of investigation appears to be the very nature of the solutions themselves. In essence, both the MRCT and the MFTT seek solutions by expanding the spectral representations of the fields using their singularities. In this case the singularities are either simple poles or branch points. This is very similar to the singularity expansion method (SEM) expounded by Baum (1973) for solving electromagnetic transient problems. This leads one to ask the question if more complicated problems which do not have Wiener-Hopf type canonical problems can be solved using the same basic technique. One would then depend on a numerical technique such as the method of moments to solve the canonical problem.

Both the MRCT and the MFTT have their foundation in the generalized scattering matrix technique (GSMT). As an alternative to the development of the MRCT and the MFTT one might also consider extending the GSMT to include asymptotic terms. Such terms would compensate for the major weakness of the GSMT: the failure to <u>change</u> the edge condition to conform with the known asymptotic solution. In fact, this particular technique might prove to be more powerful than either the MRCT or the MFTT since it is not limited to problems which are basically two dimensional in nature.

In is hoped that these comments will be useful to the researcher interested in the extension of these techniques.

ACKNOWLEDGMENT

BIBLIOGRAPHY

Abramowitz, M. and I.A. Stegun (1965), <u>Handbook of Mathematical Functions</u>, Dover Publications, New York, New York, pp. 231-233, p. 17, & p. 67.

Amitay, N., V. Galindo, and C.P. Wu (1972), <u>Theory and Analysis of Phased Array Antennas</u>, Wiley-Interscience, New York.

Bates, C.P. and R. Mittra (1968), "Waveguide Excitation of Dielectric and Plasma Slabs," Radio Science, <u>3</u>, pp. 251-266.

Baum, C. (1973), "Introduction to SEM," 1973 G-AP International Symposium Digest, Boulder, CO, pp. 459-462.

Chang, D.C. (1971), "Characteristics of a Horizontal Loop Antenna Over a Dissipative Half Space," Tech. Report No. 4, University of Colorado, Boulder.

Davis, H.T. (1962), <u>The Summation of Series</u>, Principia Press of Trinity University, San Antonio, Texas, Chapter 2.

Dybdal, R.B., R.C. Rudduck, and L.L. Tsai (1966), "Mutual Coupling Between TEM and TE_{01} Parallel Plate Waveguide Apertures," IEEE Trans., <u>AP-14</u>, pp. 574-580.

Erdelyi, A. et al. (1964), <u>Higher Transcendental Functions</u>, McGraw-Hill, New York.

Evgrafov, M.A. (1961), <u>Asymptotic Estimates and Entire Functions</u>, Gordon and Breach, New York, New York.

Gel'fand, I.M. and G.E. Shilov (1964), <u>Generalized Functions</u>, Academic Press, New York, New York.

Gradshteyn, I.S. and J.M. Ryzhik (1965), <u>Table of Integrals, Series, and Products</u>, Academic Press, New York, New York, p. 284.

Heins, A.E. (1948), "Systems of Wiener-Hopf Integral Equations and Their Applications to Some Boundary Value Problems in Electromagnetic Theory," Proc. Symposia, Appl. Math., <u>2</u>, Amer. Math. Soc., New York, New York, pp. 76-81.

Igarashi, Q. (1964), "Simultaneous Wiener-Hopf Equations and Their Application to Diffraction Problems in Electromagnetic Theory," J. Phys. Soc., Japan, <u>19</u>, No. 7, pp. 1213-1221.

Itoh, T. and R. Mittra (1971), "A New Method of Solution for Radiation from a Flanged Waveguide," Proc. IEEE, <u>59</u>, pp. 1131-1133.

Kostelnicek, R.J. and R. Mittra (1969), "Radiation from an Open Ended Waveguide Into an Inhomogeneously Filled Space," Scientific Report No. 12, University of Illinois, Urbana.

Kostelnicek, R.J. and R. Mittra (1971), "Radiation From a Parallel Plate Waveguide Into a Dielectric or Plasma Layer," Radio Science, <u>6</u>, No. 11, pp. 981-990.

Lee, S.W. (1967), "Radiation from the Infinite Aperiodic Array of Parallel Plate Waveguides," IEEE Trans., <u>AP-15</u>, pp. 598-606.

Lee, S.W. and R. Mittra (1968), "Diffraction by Thick Conducting Half-Plane and a Dielectric-Loaded Waveguide," IEEE Trans., <u>AP-16</u>, pp. 454-461.

Marcuvitz, N. (1964), <u>Waveguide Handbook</u>, Dover Publications, New York, New York.

Mittra, R. and S.W. Lee (1970), "On the Solution of a Generalized Wiener-Hopf Equation," J. of Math. Phys., <u>2</u>, No. 3, pp. 775-783.

Mittra, R. and S.W. Lee (1971), _Analytical Techniques in the Theory of Guided Waves_, The MacMillan Company, New York, New York.

Mittra, R. and J.L. Richardson (1970), "A Numerical Technique for Solving a Class of Open Region Radiation and Scattering Problems," Proc. IEEE, $\underline{58}$, No. 2, pp. 276-278.

Mittra, R., S.W. Lee and G.F. VanBlaricum, Jr. (1968), "A Modified Residue Calculus Technique," Intern. J. Eng. Sci., $\underline{6}$, No. 7, pp. 395-408.

Montgomery, J.P. (1971), "On the Complete Eigenvalue Solution of Ridged Waveguide," IEEE Trans., $\underline{MTT-14}$, pp. 547-555.

Montgomery, J.P. (1973), "Comments on Radiation From a Parallel Plate Waveguide Into a Dielectric or Plasma Layer," Radio Science, to be published in October.

Muskhelishvili, N.I. (1953), _Singular Integral Equations_, P. Noordhoff N.V., Groningerr, Holland.

Pace, J. and R. Mittra (1964), "Generalized Scattering Matrix Analysis of Waveguide Discontinuity Problems," _Quasi-Optics_, XIV, Polytechnic Institute of Brooklyn Press, New York, pp. 177-197.

Pace, J. and R. Mittra (1966), "The Trifurcated Waveguide," Radio Science, $\underline{1}$, pp. 117-121.

Royer, E.G. and R. Mittra (1972), "The Diffraction of Electromagnetic Waves by Dielectric Steps in Waveguides," IEEE Trans., $\underline{MTT-20}$, pp. 273-279.

Rudduck, R.C., L.L. Tsai, and W.D. Burnside (1969), "Reflection Coefficient of a Parallel Plate Waveguide Illuminating a Conducting Sheet," IEEE Trans., $\underline{AP-17}$, pp. 175-179.

Ward, S.H. (1967), _Mining Geophysics_, Vol. 2, Chap. 2, Pts. A and C, Society of Exploration Geophysicists, Tulsa, Oklahoma.

Weinstein, L.A. (1969), The Theory _of Diffraction and the Factorization Method_, Golem Press, Boulder, CO.

Wu, C.P. (1969), "Integral Equation Solutions for the Radiation From a Waveguide Through a Dielectric Slab," IEEE Trans., $\underline{AP-17}$, No. 6, pp. 733-739.

Yee, H.Y., L.B. Felson, and J.B. Keller (1968), "Ray Theory of Reflection from the Open End of a Waveguide," SIAM J. Appl. Math., $\underline{16}$, pp. 268-300.

Appendix A: The Edge Condition and the
Asymptotic Behavior of $T(\omega)$

From Mittra and Lee (1971) it is easy to show that E_x must behave as $|x-x_1|^{-1/2}$ as $x \to x_1$ with $z = z_0$. Similarly, E_z must behave as $|z-z_0|^{-1/2}$ as $z \to z_0$ and $x = x_1$. Thus, according to the field expression given in section 2.2, chapter 2 of part I, we have

$$\lim_{x \to x_1} \sum_{n=1}^{\infty} n B_n e^{\gamma_{nb} z_0} \cos \frac{n\pi}{b}(x-x_0) \; \alpha \; (x_1-x)^{-1/2} \tag{A.1}$$

$$\lim_{x \to x_1} \sum_{n=1}^{\infty} n C_n e^{\gamma_{nc} z_0} \cos \frac{n\pi}{c}(x-x_1) \; \alpha \; (x-x_1)^{-1/2} \tag{A.2}$$

$$\lim_{g \to z_0} \sum_{n=1}^{\infty} n A_n e^{-\gamma_{na} z_0} \sin \frac{n\pi}{a}(x_1-x_0) e^{-(z-z_0)n\pi/a} \; \alpha \; (z-z_0)^{-1/2} \tag{A.3}$$

In order to find the asymptotic behavior of A_n, B_n and C_n, one only needs to realize that the following two summations;

$$\sum_{n=1}^{\infty} n^{-1/2} \cos \delta n \qquad \text{and} \qquad \sum_{n=1}^{\infty} n^{-1/2} e^{-\delta n}$$

can be approximated for small δ, by integrals of the form

$$\int_1^{\infty} n^{-1/2} \cos \delta n \; dn \qquad \text{and} \qquad \int_1^{\infty} n^{-1/2} e^{-\delta n} \; dn$$

which are known immediately as $(\pi\delta/2)^{-1/2}$ and $(\pi\delta)^{-1/2}$ when $\delta \to 0$. Thus, by setting $\delta = x_1-x$ in (A.1), $\delta = (x-x_1)$ in (A.2) and $\delta = (z-z_0)$ in (A.3), we find

$$B_n e^{nb z_0} = 0[(-1)^n n^{-3/2}] \; , \tag{A.4}$$

$$C_n e^{nc z_0} = 0[n^{-3/2}] \; , \tag{A.5}$$

$$A_n e^{-\gamma_{na} z_0} \sin \frac{n\pi b}{a} = 0[n^{-3/2}] \; , \tag{A.6}$$

Now since $\sin^2(n\pi b/a) = 0(1)$, we obtain by multiplying $\sin(n\pi b/a)$ on both sides of (A.6), an alternative form

$$A_n e^{-\gamma_{na} z_0} = 0[n^{-3/2} \sin(n\pi b/a)] \; . \tag{A.7}$$

Using property (vii) of section 2 and (A.4) we see that

$$T(\omega) = O(\omega^{-1/2}) \tag{A.8}$$

for $\omega = -\gamma_{mb}$, $m \to \infty$. Using property (vi) of section 2, Chapter 2 and (A.5), (A.8) is true for $\omega = -\gamma_{mc}$, $m \to \infty$. Similarly using property (ii) of section 2 and (A.7), we have

$$RES[T, \gamma_{na}] = O(n^{-1/2} \sin^2 \frac{n\pi b}{a})$$

for $n \to \infty$. This is equivalent to saying (A.8) holds as $\omega \to \gamma_{na}$, $n \to \infty$ (see Royer and Mittra, 1972). Hence we have that

$$T(\omega) = O(\omega^{-1/2}) \qquad |\omega| \to \infty \tag{A.9}$$

Appendix B: Asymptotic Behavior of the Perturbation

Sum for the E-Plane Step

Consider

$$S = \sum_{n=N+1}^{\infty} \frac{n^{-1-\Delta}}{\omega - n} \tag{B.2}$$

In order to examine this sum for $|\omega| \to \infty$ we follow Evgrafov (1961) and examine the contour integral

$$S^1 = \frac{1}{2j} \int_{\Sigma} \frac{\alpha^{-1-}\cot \alpha\pi \, d\alpha}{\omega - \alpha} \tag{B.2}$$

where the contour is shown in Figure B-1.

Following Evgrafov (1961) we first evaluate the integral by residues

$$S^1 = \sum_{n=N+1}^{\infty} \frac{n^{-1-\Delta}}{\omega - n} + \pi \, \omega^{-1-\Delta} \cot \omega\pi \tag{B.3}$$

for $R \to \infty$ and Re $\omega > \theta$. But let us now seek an alternate representation of (B.2). Note that

$$\cot \alpha\pi \to -j \, \text{sign} \, (\alpha_{imag}), \quad |\alpha_{imag}| \to \infty \tag{B.3}$$

and hence let us examine

$$S^1 = \frac{-1}{2j} \int_{C_{\theta}^{+}} \frac{\alpha^{-1-\Delta}(\cot \alpha\pi + j)d\alpha}{\omega - \alpha} + \frac{1}{2} \int_{C_{\theta}^{+}} \frac{\alpha^{-1-\Delta} \, d\alpha}{\omega - \alpha}$$

$$+ \frac{1}{2j} \int_{C_{\theta}^{-}} \frac{\alpha^{-1-\Delta}(\cot \alpha\pi - j)d\alpha}{\omega - \alpha} + \frac{1}{2} \int_{C_{\theta}^{-}} \frac{\alpha^{-1-\Delta} d\alpha}{\omega - \alpha}$$

where C_{θ}^{+} is the contour $(\theta, \theta+iR, \infty+iR)$ and C_{θ}^{-} is $(\theta, \theta-iR, \infty-iR)$ as $R \to \infty$

$$\cot \alpha\pi \pm j = 0(e^{-2\pi R})$$

and thus

$$S^1 = \frac{-1}{2j} \int_{\theta}^{\theta+j\infty} \frac{\alpha^{-1-\Delta}(\cot \alpha\pi + j)d\alpha}{\omega - \alpha} + \frac{1}{2j} \int_{\theta}^{\theta-j\infty} \frac{\alpha^{-1-\Delta}(\cot \alpha\pi - j)d\alpha}{\omega - \alpha}$$

$$+ \frac{1}{2} \int_{C_{\theta}^{+}} \frac{\alpha^{-1-\Delta} d\alpha}{\omega - \alpha} + \frac{1}{2} \int_{C_{\theta}^{-}} \frac{\alpha^{-1-\Delta} d\alpha}{\omega - \alpha}$$

165

Fig. B-1: Contour of Integration for Asymptotic
Evaluation of Sum.

Now consider deforming the contours, C_θ^+, C_θ^- to $(\theta \pm i\varepsilon, \infty \pm i\varepsilon)$ as $\varepsilon \to 0$. If $\mathrm{Im}\ \omega > 0$ then

$$\frac{1}{2} \int_{C_\theta^+} \frac{\alpha^{-1-\Delta} d\alpha}{\omega - \alpha} = \frac{1}{2} \int_\theta^\infty \frac{\alpha^{-1-\Delta} d\alpha}{\omega - \alpha} - \pi j\ \omega^{-1-\Delta}$$

$$\frac{1}{2} \int_{C_\theta^-} \frac{\alpha^{-1-\Delta} d\alpha}{\omega - \alpha} = \frac{1}{2} \int_\theta^\infty \frac{\alpha^{-1-\Delta} d\alpha}{\omega - \alpha}$$

If $\mathrm{Im}\ \omega < 0$

$$\frac{1}{2} \int_{C_\theta^+} \frac{\alpha^{-1-\Delta} d\alpha}{\omega - \alpha} = \frac{1}{2} \int_\theta^\infty \frac{\alpha^{-1-\Delta} d\alpha}{\omega - \alpha}$$

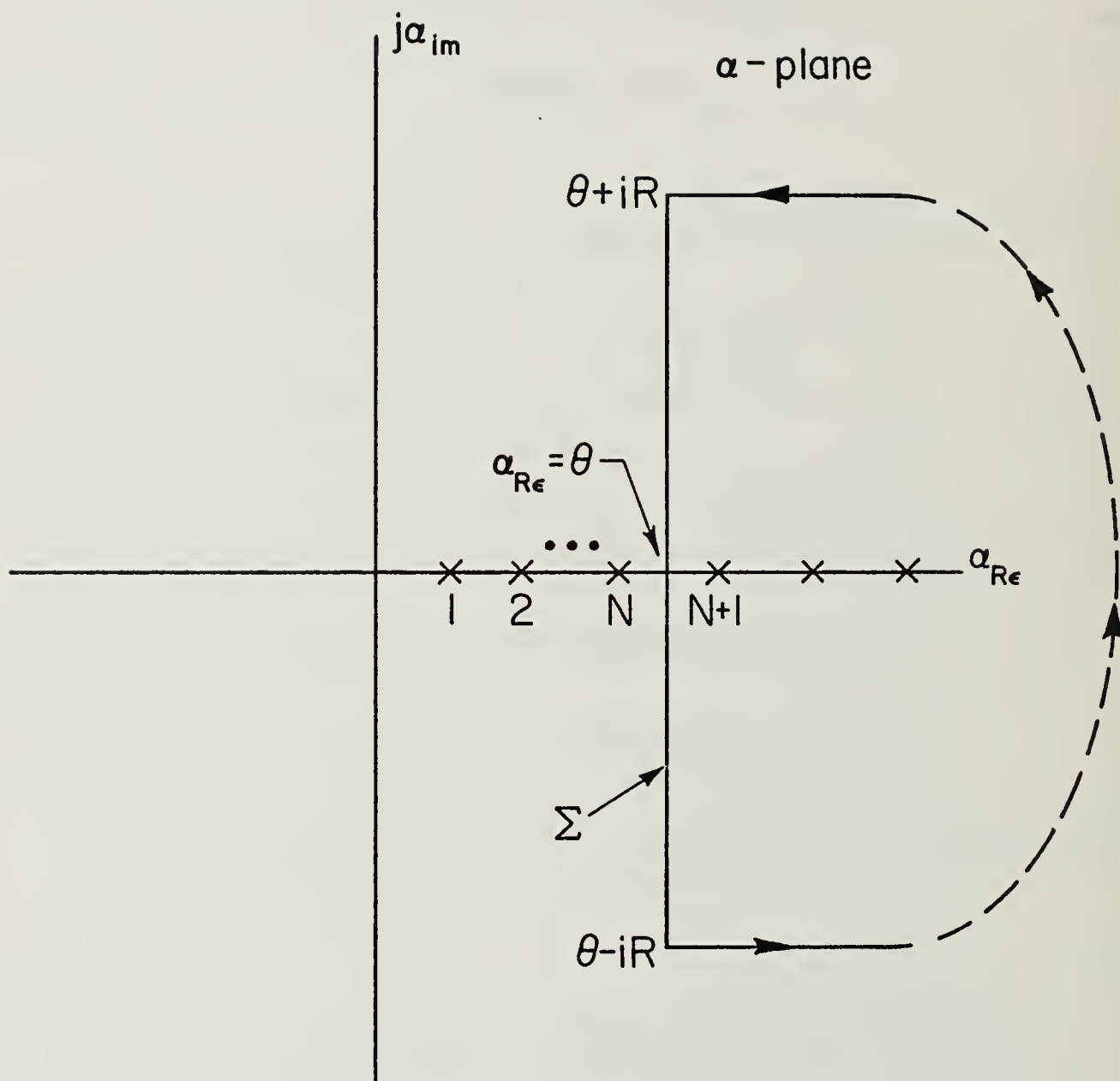$$\frac{1}{2} \int_{C_\theta^-} \frac{\alpha^{-1-\Delta} d\alpha}{\omega - \alpha} = \frac{1}{2} \int_\theta^\infty \frac{\alpha^{-1-\Delta} d\alpha}{\omega - \alpha} + \pi j\ \omega^{-1-\Delta}$$

and if $\mathrm{Im}\ \omega = 0$

$$\frac{1}{2} \int_{C_\theta^+} \frac{\alpha^{-1-\Delta} d\alpha}{\omega - \alpha} + \frac{1}{2} \int_{C_\theta^-} \frac{\alpha^{-1-\Delta} d\alpha}{\omega - \alpha} = PV \int_\theta^\infty \frac{\alpha^{-1-\Delta} d\alpha}{\omega - \alpha}$$

For our purposes it is sufficient to consider two cases: (1) $\mathrm{Re}\ \omega > \theta$, and (2) $\mathrm{Re}\ \omega < \theta$. For $\mathrm{Re}\ \omega > \theta$ we have

$$S^1 = \sum_{n=N+1}^\infty \frac{n^{-1-\Delta}}{\omega - n} + \pi \omega^{-1-\Delta} \cot \omega\pi$$

$$= PV \int_\theta^\infty \frac{\alpha^{-1-\Delta} d\alpha}{\omega - \alpha} - \frac{1}{2j} \int_\theta^{\theta+j\infty} \frac{\alpha^{-1-\Delta}(\cot \alpha\pi + j) d\alpha}{\omega - \alpha}$$

$$+ \frac{1}{2j} \int_\theta^{\theta-j\infty} \frac{\alpha^{-1-\Delta}(\cot \alpha\pi - j) d\alpha}{\omega - \alpha}$$

$$= PV \int_\theta^\infty \frac{\alpha^{-1-\Delta} d\alpha}{\omega - \alpha} - \int_\theta^{\theta+j\infty} \frac{\alpha^{-1-\Delta} d\alpha}{(\omega - \alpha)(1 - e^{-2j\alpha\pi})}$$

$$+ \int_\theta^{\theta-j\infty} \frac{\alpha^{-1-\Delta} d\alpha}{(\omega - \alpha)(e^{j2\alpha\pi} - 1)} \tag{B.4}$$

as $\omega \to \infty$ we use the residue term at $\alpha = \omega$ and the principle value integral as the leading terms.

$$S = 0(\omega^{-1}) + 0(\omega^{-1-\Delta}) \tag{B.5}$$

For arg $\omega = \pi$, we have

$$S^1 = \sum_{n=N+1}^{\infty} \frac{n^{-1-\Delta}}{\omega - n}$$

$$= \int_{\theta}^{\infty} \frac{\alpha^{-1-\Delta} d\alpha}{\omega - \alpha} - \int_{\theta}^{\theta+j\infty} \frac{\alpha^{-1-\Delta} d\alpha}{(\omega-\alpha)(1-e^{-2j\alpha\pi})}$$

$$+ \int_{\theta}^{\theta-j} \frac{\alpha^{-1-\Delta} d\alpha}{(\omega-\alpha)(e^{j2\alpha\pi}-1)} \qquad (B.6)$$

as $\omega \to \infty$, we use the first integral as the leading term. By changing variables we recognize the integral to be a hypergeometric function (Gradshteyn and Ryzhik, 1965). From the hypergeometric function, it is easy to show that again we have (B.5).

Hence (3.11) is justified.

Appendix C: Asymptotic Behavior of the Perturbation
Sum for the Trifurcated Waveguide

Consider

$$S = \sum_{n=N}^{\infty} \frac{n^{-1} \sin n\theta}{n - \omega} \tag{C.1}$$

In order to examine this sum for $|\omega| \to \infty$ we follow Evgrafox (1961) and examine the contour integral

$$S^1 = \frac{1}{2j} \int_{\Sigma} \frac{\sin \alpha\theta \cot \alpha\pi \, d\alpha}{\alpha(\alpha - \omega)} \tag{C.2}$$

where Σ is shown in Figure B-1 (replace θ by θ_o to eliminate confusion). Evaluating the integral by residues

$$S^1 = \sum_{n=N}^{\infty} \frac{\sin n\theta}{n(n-\omega)} + \frac{\pi \sin \omega\theta \cot \omega\pi}{\omega} \tag{C.3}$$

for $R \to \infty$ and $\mathrm{Re} \, \omega > \theta_o$. In a similar manner to Appendix B we can find the following alternate representation of (C.2).

$$S^1 = \mathrm{PV} \int_{\theta_o}^{\infty} \frac{\sin \alpha\theta \, d\alpha}{\alpha(\alpha - \omega)} + \int_{\theta_o}^{\theta_o+j\infty} \cdots + \int_{\theta_o}^{\theta_o-j\infty} \cdots \tag{C.4}$$

for $\arg \omega = 0$ and where the second and third integrals are similar to those given in Appendix B and are not given since only the leading terms of the asymptotic expansion of S are desired.

Let us examine the integral and the residue term as the leading terms

$$\mathrm{PV} \int_{\theta_o}^{\infty} \frac{\sin \alpha\theta \, d\alpha}{\alpha(\alpha - \omega)} = \frac{-1}{\omega} \int_{\theta_o}^{\infty} \frac{\sin \alpha\theta \, d\alpha}{\alpha} + \frac{1}{\omega} \mathrm{PV} \int_{\theta_o}^{\infty} \frac{\sin \alpha\theta \, d\alpha}{\alpha - \omega}$$

The first term is order ω^{-1}. The second integral can be evaluated asymptotically by changing variables and using asymptotic expansions of the sine and cosine integrals given in Abramowitz and Stegun (1965). This yields

$$\mathrm{PV} \int_{\theta_o}^{\infty} \frac{\sin \alpha\theta \, d\alpha}{\alpha - \omega} \simeq \pi \cos \omega\theta$$

Thus

$$S = 0(\omega^{-1}) + 0\left[\pi \frac{\sin \omega(\pi-\theta)}{\omega \sin \omega\pi}\right] \tag{C.5}$$

as $\omega \to \infty$. It should be noted that the second term on the right in expression (C.5) vanishes if $\arg \omega = \pi$ in (C.1).

The result presented here is applicable to the electric wall case. A similar result, applicable to the magnetic wall case, is given by

$$\frac{1}{2j} \int_\Sigma \frac{\sin \alpha\theta \ \tan \alpha\pi}{\alpha(\alpha-\omega)} \ d\alpha = \frac{\pi \ \sin \omega\theta \ \tan \omega\pi}{\omega} - \sum_{m=n}^\infty \frac{(m-1/2)^{-1} \ \sin(m+1/2)\theta}{m - \omega - 1/2}$$

$$= - \text{ P.V.} \ \frac{1}{\omega} \int_{\theta_o -\omega}^\infty \frac{\sin(t+)\theta}{t} + \frac{1}{\omega} \int_{\theta_o}^\infty \frac{\sin \alpha\theta}{\alpha} \ d\alpha$$

$$+ \frac{1}{2} \int_{\theta_o}^{\theta_o+j\infty} \cdots + \frac{1}{2} \int_{\theta_o}^{\theta_o-j\infty} \cdots \qquad\qquad (C.6)$$

Retaining the principal value integral and the residue term once again as the leading terms, we obtain

$$\sum_{m=n}^\infty \frac{(m-1/2)^{-1} \ \sin(m+1/2)\theta}{m - \omega - 1/2} = O(\omega^{-1}) + O \ \frac{\pi \ \cos \omega(\pi-\theta)}{\omega \ \cos \omega\pi} \qquad\qquad (C.7)$$

Again, the second term on the right disappears for arg $\omega = \pi$.

170

Consider the product

$$P(\omega) = \prod_{n=1}^{\infty} \frac{(1-\omega/\gamma_{nb})(1-\omega/\gamma_{nc})}{(1-\omega/\gamma_{na})} \tag{D.1}$$

This can be written as

$$P(\omega) = \prod_{n=1}^{N-1} \frac{(1-\omega/\gamma_{nb})(1-\omega/\gamma_{nc})}{(1-\omega/\gamma_{na})} R_N(\omega) \tag{D.2}$$

where $R_N(\omega)$ is the remainder. Following a procedure similar to Kostelnicek and Mittra (1961) we have

$$R_N(\omega) = \exp\left\{ \sum_{n=N}^{\infty} \left[\ln\left(1-\frac{\omega}{\gamma_{nb}}\right) + \ln\left(1-\frac{\omega}{\gamma_{nc}}\right) \right.\right.$$
$$\left.\left. - \ln\left(1-\frac{\omega}{\gamma_{na}}\right) \right] \right\} \tag{D.3}$$

for $|\omega/\gamma_{nb}|$, $|\omega/\gamma_{nc}|$, $|\omega/\gamma_{na}| < 1$ we can expand the logarithmic terms

$$R_N(\omega) = \exp\left\{ -\sum_{n=N}^{\infty} \sum_{m=1}^{\infty} \frac{\omega^m}{m}\left(\frac{1}{\gamma_{nb}^m} + \frac{1}{\gamma_{nc}^m} - \frac{1}{\gamma_{na}^m} \right) \right\} \tag{D.4}$$

Now consider the expansion

$$\frac{1}{\gamma_{nb}^m} = \left(\frac{b}{n\pi}\right)^m \left[1 + \frac{m}{2}\left(\frac{b}{n\pi}\right)^2 + \frac{(m/2+1)m/2}{2!}\left(\frac{b}{n\pi}\right)^4 \right.$$

$$+ \frac{(m/2+2)(m/2+1)m/2}{3!}\left(\frac{b}{n\pi}\right)^6 + \cdots$$

$$= \left(\frac{b}{n\pi}\right)^m \sum_{p=1}^{\infty} C_p^{(m)}\left(\frac{b}{n\pi}\right)^{2p-2} \tag{D.5}$$

where $k_o = 1$ is convenient.

Thus

$$R_N(\omega) = \exp\left\{ -\sum_{n=N}^{\infty} \sum_{m=1}^{\infty} \frac{\omega^m}{m} \sum_{p=1}^{\infty} C_p^{(m)}\left[\left(\frac{b}{n\pi}\right)^{2p-2+m} \right.\right.$$

$$\left.\left. + \left(\frac{c}{n\pi}\right)^{2p-2+m} - \left(\frac{a}{n\pi}\right)^{2p-2+m} \right] \right\} \tag{D.6}$$

Using Davis (1962) we find that we can evaluate sums of reciprocal powers of integers using polygamma functions.

$$\sum_{n=N}^{\infty} \frac{1}{n^m} = \frac{(-1)^m}{(m-1)!} \psi^{(m-1)}(N) \tag{D.7}$$

N is chosen large enough that an asymptotic expansion of ψ is used. Only two or three terms of this series are generally needed to find the polygamma function. Reversing orders of summation of (D.6) we have

$$R_N(\omega) = \exp\left\{-\sum_{m=2}^{\infty} \frac{\omega^m}{m} \sum_{p=1}^{\infty} c_p^{(m)} \left[\left(\frac{b}{\pi}\right)^{2p-2+m} + \left(\frac{c}{\pi}\right)^{2p-2+m}\right.\right.$$

$$\left.\left. - \left(\frac{a}{\pi}\right)^{2p-2+m}\right] \sum_{n=N}^{\infty} \frac{1}{n^{2p-2+m}} - \omega \sum_{n=N}^{\infty} \left[\frac{1}{\gamma_{nb}} + \frac{1}{\gamma_{nc}} - \frac{1}{\gamma_{na}}\right]\right\} \tag{D.8}$$

Note that the linear term of ω is isolated. Let us consider this last term for a finite upper limit and use (D.5)

$$\sum_{n=N}^{M} \left[\frac{1}{\gamma_{nb}} + \frac{1}{\gamma_{nc}} - \frac{1}{\gamma_{na}}\right] = \sum_{n=N}^{M} \left[\left(\frac{b}{n\pi}\right) \sum_{p=1}^{\infty} c_p^{(1)} \left(\frac{b}{n\pi}\right)^{2p-2}\right.$$

$$\left. + \left(\frac{c}{n\pi}\right) \sum_{p=1}^{\infty} c_p^{(1)} \left(\frac{c}{n\pi}\right)^{2p-2} - \left(\frac{a}{n\pi}\right) \sum_{p=1}^{\infty} c_p^{(1)} \left(\frac{a}{n\pi}\right)^{2p-2}\right]$$

but $b + c = a$ thus as $M \to \infty$.

$$\sum_{n=N}^{\infty} \left[\frac{1}{\gamma_{nb}} + \frac{1}{\gamma_{nc}} - \frac{1}{\gamma_{na}}\right] = \sum_{p=2}^{\infty} \left\{c_p^{(1)} \left[\left(\frac{b}{\pi}\right)^{2p-1} + \left(\frac{c}{\pi}\right)^{2p-1}\right.\right.$$

$$\left.\left. - \left(\frac{a}{\pi}\right)^{2p-1}\right] \sum_{n=N}^{\infty} \frac{1}{n^{2p-1}}\right\} \tag{D.9}$$

The summation over p and n are fastly convergent. In order to determine how many powers of ω are necessary the remainder term (of ω) can be approximated by using a procedure similar to Kostelnicek (1969). Using the approximation $\gamma_{nh} \simeq n\pi/h$ in the sum

$$S_M = -\sum_{m=M}^{\infty} \frac{\omega^m}{m} \sum_{n=N}^{\infty} \left[\frac{1}{\gamma_{nb}^m} + \frac{1}{\gamma_{nc}^m} - \frac{1}{\gamma_{na}^m}\right] \tag{D.10}$$

172

we find

$$S_M \simeq -N \left\{ g_M \left(\frac{\omega b}{N \pi} \right) + g_M \left(\frac{\omega c}{N \pi} \right) - g_M \left(\frac{\omega a}{N \pi} \right) \right\} \qquad \text{(D.11)}$$

where

$$g_M(t) = \sum_{m=M}^{\infty} \frac{t^m}{m(m-1)}$$

This enables the remaining sum to be truncated accurately.

Consider Figure 2.2.1, except let the boundary at $x=x_o$ be a magnetic wall. We can find the TM fields from $\phi = H_y$ where

$$\phi_A = \sum_{n=1}^{\infty} [A_n^{(o)} e^{\gamma_{2n-1,2a}z} + A_n e^{-\gamma_{2n-1,2a}z}]\sin k_{na}(x-x_o) \tag{E.1}$$

$$\theta_B = \sum_{n=1}^{\infty} [B_n^{(o)} e^{-\gamma_{2n-1,2b}z} + B_n e^{\gamma_{2n-1,2b}z}]\sin k_{nb}(x-x_o) \tag{E.2}$$

$$\theta_C = \sum_{n=0}^{\infty} [C_n^{(o)} e^{-\gamma_{nc}z} + C_n e^{\gamma_{nc}z}]\cos \frac{n\pi}{c} (x-x_1) \tag{E.3}$$

where

$$k_{na} = \frac{(2n-1)\pi}{2a}, \quad k_{nb} = \frac{(2n-1)\pi}{2b}$$

Note that regions A and B cannot support a TEM mode.

We proceed in an identical manner as section 2 and find that the solution may be found from a meromorphic function $T(\omega)$ which has the properties:

(i) $\quad RES[T,\gamma_{2n-1,2a}] = k_{na} \cos k_{na}b\, A_n e^{-\gamma_{2n-1,2a}z_o}$

$\quad\quad n = 1,2,\cdots$

(ii) $\quad RES[T,-\gamma_{2n-1,2a}] = k_{na} \cos k_{na}b\, A_n^{(o)} e^{\gamma_{2n-1,2a}z_o}$

$\quad\quad n = 1,2,\cdots$

(iii) $\quad T(\gamma_{nc}) = -\gamma_{nc}\, c\, C_n^{(o)} e^{-\gamma_{nc}z_o} \quad n = 1,2,\cdots$

(iv) $\quad T(jk_o) = -2jk_o\, c\, C_n^{(o)} e^{-jk_oz_o}$

(v) $\quad (-1)^{n+1}T(\gamma_{2n-1,2b}) = \gamma_{2n-1,2b}\, b\, B_n^{(o)} e^{-\gamma_{2n-1,2b}z_o} \quad n = 1,2,\cdots$

(vi) $\quad T(-\gamma_{nc}) = \gamma_{nc}\, c\, C_n\, e^{+\gamma_{nc}z_o} \quad n = 1,2,\cdots$

(vii) $\quad T(-jk_o) = 2jk_o\, c\, C_o\, e^{jk_oz_o}$

(viii) $\quad (-1)^{n+1}T(-\gamma_{2n-1,2b}) = -\gamma_{2n-1,2b}\, b\, B_n e^{\gamma_{2n-1,2b}z_o} \quad n = 1,2,\cdots$

(ix) $\quad T(\omega) = 0(\omega^{-1/2}) \quad\quad |\omega| \to \infty$

$T(\omega)$ can be constructed as follows:

$$T(\omega) = H(\omega)F(\omega)\left[K_o + (\omega - jk_o)\left\{\sum_{n=1}^{\infty} \frac{g_n^{(c)}}{\omega - \gamma_{nc}}\right.\right.$$

$$\left.\left. + \sum_{n=1}^{\infty} \frac{g_n^{(b)}}{\omega - \gamma_{2n-1,2b}} + \sum_{n=1}^{\infty} \frac{g_n^{(a)}}{\omega + \gamma_{2n-1,2a}}\right\}\right] \tag{E.4}$$

where

$$H(\omega) = \exp\left\{\frac{-\omega}{\pi}\left[b \ln \frac{b}{a} + c \ln \frac{c}{a}\right]\right\} \tag{E.5}$$

and

$$F(\omega) = \prod_{n=1}^{\infty} \frac{(1 - \omega/\gamma_{2n-1,2b})(1 - \omega/\gamma_{nc})}{(1 - \omega/\gamma_{2n-1,2a})} \tag{E.6}$$

k_o, $g_n^{(c)}$, $g_n^{(b)}$, $g_n^{(a)}$ are related to the incident fields by (iv), (iii), (v) and (ii).

175

Appendix F: The Trifurcated Waveguide with a Magnetic Wall

Figure F-1 illustrates the magnetic wall trifurcated waveguide and the auxiliary problem.

The solution is obtained by constructing two mermorphic functions.

$$T_1(\omega) = H_1(\omega)F_1(\omega)\left[K_0^{(1)} + (\omega - jk_0)\sum_{n=1}^{\infty}\frac{g_n^{(1)}g_{m,n}}{\omega + \gamma_{2n-1,2c}}\right] \tag{F.1}$$

$$T_2(\omega) = H_2(\omega)F_2(\omega)\left[K_0^{(2)} + (\omega - jk_0)\sum_{n=1}^{\infty}\frac{g_n^{(2)}}{\omega - \gamma_{2n-1,2c}}\right] \tag{F.2}$$

where $T_1(\omega)$ is identified with the junction at $z = 0$ and $T_2(\omega)$ is identified with the junction $z = \Delta$. $H_1(\omega)$, $H_2(\omega)$, $F_1(\omega)$, $F_2(\omega)$, $K_0^{(1)}$, and $K_0^{(2)}$ are given by (E.4)--(E.6) with only a change of geometrical factors necessary.

We can derive two infinite equations for $g_n^{(1)}$ and $g_n^{(2)}$ by requiring that the expressions for the modal coefficients in the coupling region be consistent.

$$\text{RES}[T_1, \gamma_{2n-1,2c}] = g_n^{(2)}[K_n^{(2)}]^{-1}k_{nc}\cos k_{nc}b_0 \tag{F.3}$$

$$(-1)^{n+1}T_2(-\gamma_{2n-1,2c}) = -\gamma_{2n-1,2c}\, c\, g_n^{(1)}[K_n^{(1)}]^{-1} \tag{F.4}$$

where

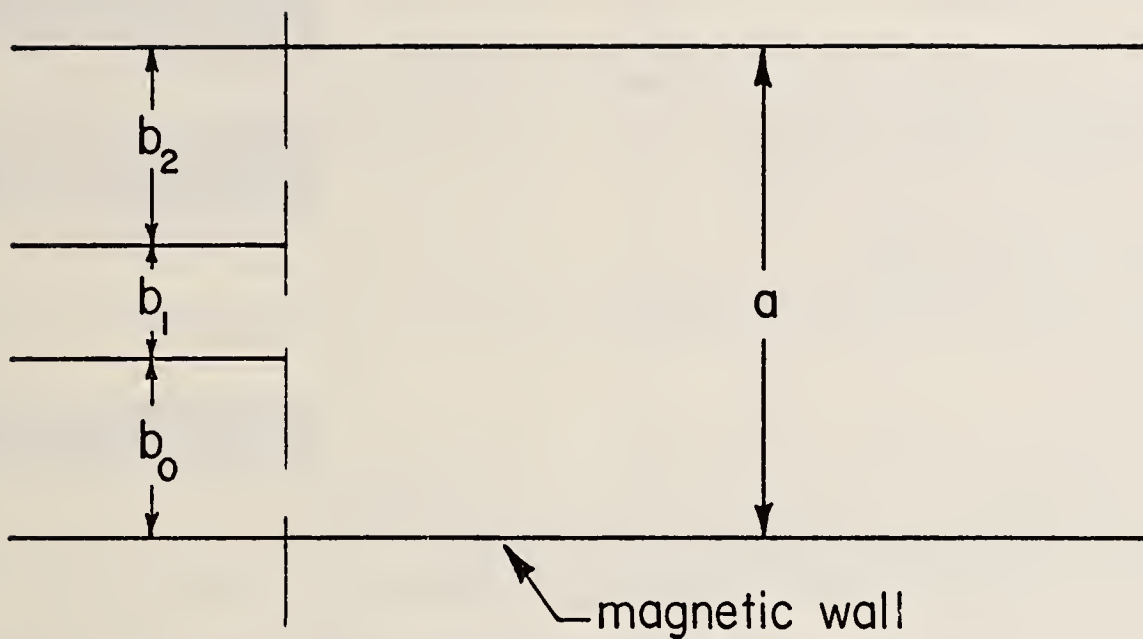$$g_n^{(1)} = K_n^{(1)}\, c_n^- \tag{F.5}$$

$$g_n^{(2)} = K_n^{(2)}\, c_n^+ \tag{F.6}$$

and $K_n^{(1)}$ and $K_n^{(2)}$ are found from properties (ii) and (v) of Appendix E.
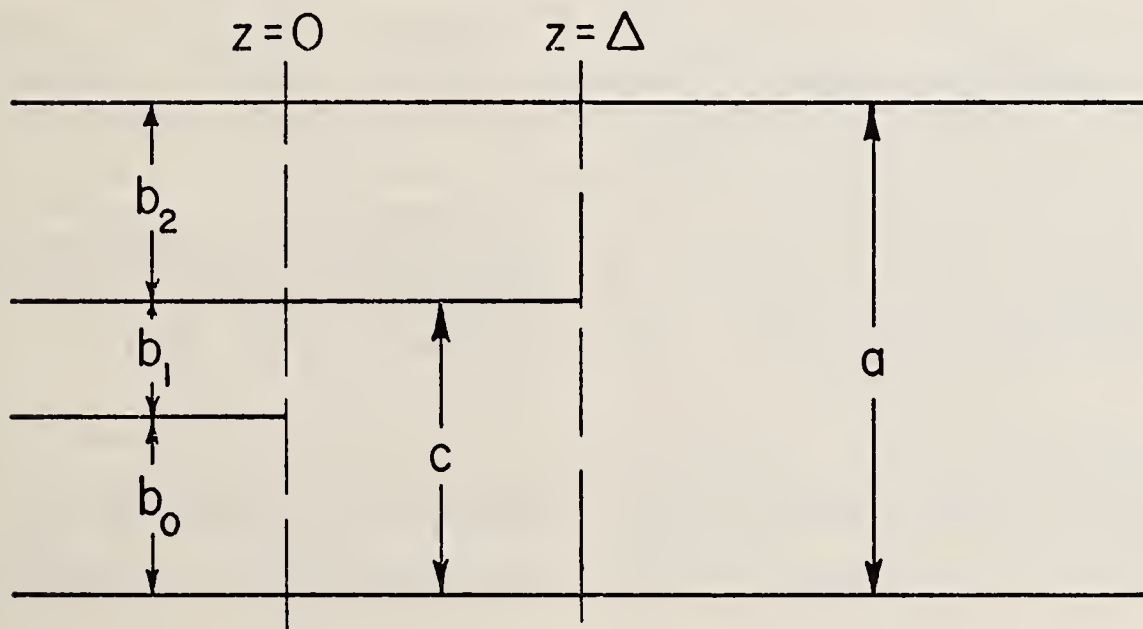
In order to truncate equations (F.3) and (F.4) we find the asymptotic behavior of $g_n^{(1)}$ and $g_n^{(2)}$. From (F.5) and (F.6) we can find

$$g_n^{(1)}, g_n^{(2)} = 0(n^{-1}(-1)^n\cos k_{n,c}b_0) \tag{F.7}$$

This choice allows the efficient solution of equations.

(a) The Trifurcated Waveguide

(b) Auxiliary Geometry

Fig. F-1: The Trifurcated Waveguide (with a Magnetic Symmetry Wall) and the Auxiliary Problem.

| 4. TITLE AND SUBTITLE
Electromagnetic Boundary-Value Problems Based Upon a Modification of Residue Calculus and Function Theoretic Techniques | | 5. Publication Date
June 1979 |
| | | 6. Performing Organization Code |

| 7. AUTHOR(S)
James Patrick Montgomery and David C. Chang | 8. Performing Organ. Report No. |

| 9. PERFORMING ORGANIZATION NAME AND ADDRESS

National Bureau of Standards
Department of Commerce
Boulder, Colorado 80302 | 10. Project/Task/Work Unit No.
7203900 |
| | 11. Contract/Grant No. |

| 12. SPONSORING ORGANIZATION NAME AND COMPLETE ADDRESS *(Street, City, State, ZIP)*

Same as No. 9. | 13. Type of Report & Period Covered |
| | 14. Sponsoring Agency Code |

16. ABSTRACT *(A 200-word or less factual summary of most significant information. If document includes a significant bibliography or literature survey, mention it here.)*

The solution of a number of electromagnetic problems, in both closed and open systems, using the modified residue calculus and functional theoretic techniques is presented.

The solutions start with known closed region problems and then are extended to new closed region problems and finally to several open region problems.

Specific problems considered for the closed region are: 1) the trifurcated waveguide; 2) the dielectrically loaded trifurcated waveguide; 3) the N-furcated waveguide; 4) the dielectrically loaded N-furcated waveguide; 5) determination of the Eigenvalues of ridged; waveguide; and 6) scattering by a dielectric step.

Open region problems considered are: 1) a parallel plate radiating into a homogeneous half-space; 2) a finite phased array; 3) remote sensing of the earth using parallel plate waveguides; 4) a flanged waveguide radiating into a half-space; 5) scattering by a thick semi-infinite plane; and 6) radiation from a slot in a waveguide wall.

Some suggested extension of the techniques to other types of problems is also included.

17. KEY WORDS *(six to twelve entries; alphabetical order; capitalize only the first letter of the first key word unless a proper name; separated by semicolons)*

Closed systems; electromagnetic problems; functional theoretic techniques; modified residue calculus; open systems; remote sensing.

18. AVAILABILITY ☒ Unlimited	19. SECURITY CLASS (THIS REPORT)	21. NO. OF PRINTED PAGES
☐ For Official Distribution. Do Not Release to NTIS	UNCLASSIFIED	183
☒ Order From Sup. of Doc., U.S. Government Printing Office, Washington, DC 20402, SD Stock No. SN003–003–02075–3	20. SECURITY CLASS (THIS PAGE)	22. Price
☐ Order From National Technical Information Service (NTIS), Springfield, VA. 22161	UNCLASSIFIED	$5.00

NBS TECHNICAL PUBLICATIONS

PERIODICALS

JOURNAL OF RESEARCH—The Journal of Research of the National Bureau of Standards reports NBS research and development in those disciplines of the physical and engineering sciences in which the Bureau is active. These include physics, chemistry, engineering, mathematics, and computer sciences. Papers cover a broad range of subjects, with major emphasis on measurement methodology, and the basic technology underlying standardization. Also included from time to time are survey articles on topics closely related to the Bureau's technical and scientific programs. As a special service to subscribers each issue contains complete citations to all recent NBS publications in NBS and non-NBS media. Issued six times a year. Annual subscription: domestic $17.00; foreign $21.25. Single copy, $3.00 domestic; $3.75 foreign.

Note: The Journal was formerly published in two sections: Section A "Physics and Chemistry" and Section B "Mathematical Sciences."

DIMENSIONS/NBS

This monthly magazine is published to inform scientists, engineers, businessmen, industry, teachers, students, and consumers of the latest advances in science and technology, with primary emphasis on the work at NBS. The magazine highlights and reviews such issues as energy research, fire protection, building technology, metric conversion, pollution abatement, health and safety, and consumer product performance. In addition, it reports the results of Bureau programs in measurement standards and techniques, properties of matter and materials, engineering standards and services, instrumentation, and automatic data processing.

Annual subscription: Domestic, $11.00; Foreign $13.75

NONPERIODICALS

Monographs—Major contributions to the technical literature on various subjects related to the Bureau's scientific and technical activities.

Handbooks—Recommended codes of engineering and industrial practice (including safety codes) developed in cooperation with interested industries, professional organizations, and regulatory bodies.

Special Publications—Include proceedings of conferences sponsored by NBS, NBS annual reports, and other special publications appropriate to this grouping such as wall charts, pocket cards, and bibliographies.

Applied Mathematics Series—Mathematical tables, manuals, and studies of special interest to physicists, engineers, chemists, biologists, mathematicians, computer programmers, and others engaged in scientific and technical work.

National Standard Reference Data Series—Provides quantitative data on the physical and chemical properties of materials, compiled from the world's literature and critically evaluated. Developed under a world-wide program coordinated by NBS. Program under authority of National Standard Data Act (Public Law 90-396).

NOTE: At present the principal publication outlet for these data is the Journal of Physical and Chemical Reference Data (JPCRD) published quarterly for NBS by the American Chemical Society (ACS) and the American Institute of Physics (AIP). Subscriptions, reprints, and supplements available from ACS, 1155 Sixteenth St. N.W., Wash., D.C. 20056.

Building Science Series—Disseminates technical information developed at the Bureau on building materials, components, systems, and whole structures. The series presents research results, test methods, and performance criteria related to the structural and environmental functions and the durability and safety characteristics of building elements and systems.

Technical Notes—Studies or reports which are complete in themselves but restrictive in their treatment of a subject. Analogous to monographs but not so comprehensive in scope or definitive in treatment of the subject area. Often serve as a vehicle for final reports of work performed at NBS under the sponsorship of other government agencies.

Voluntary Product Standards—Developed under procedures published by the Department of Commerce in Part 10, Title 15, of the Code of Federal Regulations. The purpose of the standards is to establish nationally recognized requirements for products, and to provide all concerned interests with a basis for common understanding of the characteristics of the products. NBS administers this program as a supplement to the activities of the private sector standardizing organizations.

Consumer Information Series—Practical information, based on NBS research and experience, covering areas of interest to the consumer. Easily understandable language and illustrations provide useful background knowledge for shopping in today's technological marketplace.

Order above NBS publications from: Superintendent of Documents, Government Printing Office, Washington, D.C. 20402.

Order following NBS publications—NBSIR's and FIPS from the National Technical Information Services, Springfield, Va. 22161.

Federal Information Processing Standards Publications (FIPS PUB)—Publications in this series collectively constitute the Federal Information Processing Standards Register. Register serves as the official source of information in the Federal Government regarding standards issued by NBS pursuant to the Federal Property and Administrative Services Act of 1949 as amended, Public Law 89-306 (79 Stat. 1127), and as implemented by Executive Order 11717 (38 FR 12315, dated May 11, 1973) and Part 6 of Title 15 CFR (Code of Federal Regulations).

NBS Interagency Reports (NBSIR)—A special series of interim or final reports on work performed by NBS for outside sponsors (both government and non-government). In general, initial distribution is handled by the sponsor; public distribution is by the National Technical Information Services (Springfield, Va. 22161) in paper copy or microfiche form.

BIBLIOGRAPHIC SUBSCRIPTION SERVICES

The following current-awareness and literature-survey bibliographies are issued periodically by the Bureau:

Cryogenic Data Center Current Awareness Service. A literature survey issued biweekly. Annual subscription: Domestic, $25.00; Foreign, $30.00.

Liquified Natural Gas. A literature survey issued quarterly. Annual subscription: $20.00.

Superconducting Devices and Materials. A literature survey issued quarterly. Annual subscription: $30.00. Send subscription orders and remittances for the preceding bibliographic services to National Bureau of Standards, Cryogenic Data Center (275.02) Boulder, Colorado 80302.